ISSN 1881-7815 Online ISSN 1881-7823

BST BioScience Trends

Volume 19, Number 4
August 2025

IRCA BSSA

IACMHR

www.biosciencetrends.com

BST
BioScience Trends

ISSN: 1881-7815
Online ISSN: 1881-7823
CODEN: BTIRCZ
Issues/Year: 6
Language: English
Publisher: IACMHR Co., Ltd.

BioScience Trends is one of a series of peer-reviewed journals of the International Research and Cooperation Association for Bio & Socio-Sciences Advancement (IRCA-BSSA) Group. It is published bimonthly by the International Advancement Center for Medicine & Health Research Co., Ltd. (IACMHR Co., Ltd.) and supported by the IRCA-BSSA.

BioScience Trends devotes to publishing the latest and most exciting advances in scientific research. Articles cover fields of life science such as biochemistry, molecular biology, clinical research, public health, medical care system, and social science in order to encourage cooperation and exchange among scientists and clinical researchers.

BioScience Trends publishes Original Articles, Brief Reports, Reviews, Policy Forum articles, Communications, Editorials, News, and Letters on all aspects of the field of life science. All contributions should seek to promote international collaboration.

Editorial Board

Editorial and Head Office

Pearl City Koishikawa 603,
2-4-5 Kasuga, Bunkyo-ku, Tokyo 112-0003, Japan
E-mail: office@biosciencetrends.com

BioScience Trends

Editorial and Head Office

Pearl City Koishikawa 603, 2-4-5 Kasuga, Bunkyo-ku,
Tokyo 112-0003, Japan

E-mail: office@biosciencetrends.com
URL: www.biosciencetrends.com

Editorial Board Members

CONTENTS

Volume 19, Number 4, 2025

Editorial

368-373 **From dengue to chikungunya: Guangdong as a sentinel for arboviral threats in East Asia.**
Yong Feng, Fangfang Chang, Yang Yang, Hongzhou Lu

374-378 **Anatomical study of the caudate lobe of the liver on hepatic casts and the dawn of isolated caudate lobectomy.**
Yoshihiro Sakamoto, Masaharu Kogure, Satoru Seo, Masamitsu Kumon

Consensus

379-403 **Chinese multicenter expert consensus on the diagnosis and treatment of hilar cholangiocarcinoma: 2025 edition.**
Sulai Liu, Jinqiong Jiang, Qian Jian, Yingbin Liu, Zhiyong Huang, Yongjun Chen, Chihua Fang, Zhaohui Tang, Lu Wang, Deyu Li, Fuyu Li, Shaoqiang Li, Xuemin Liu, Cuncai Zhou, Yamin Zheng, Heguang Huang, Chen Chen, Xu Chen, Bo Sun, Weimin Yi, Bingzhang Tian, Liansheng Gong, Wei Liu, Feizhou Huang, Jia Luo, Dongde Wu, Shuke Fei, Lixin Xiong, Caixi Tang, Shaojie Li, Yi Yu, Jushi Li, Biao Tang, Yongqing Yang, Xuzhao Gao, Xingguo Tan, Yu Liu, Wei Tang, Bo Jiang, Zhiming Wang, Huihuan Tang, Jinshu Wu, Chuang Peng

Review

404-409 **Chikungunya's global rebound and Asia's growing vulnerability: Implications for integrated vector control and pandemic preparedness.**
Jing Ni, Zhifang Li, Xiaowei Hu, Hui Zhou, Zhenyu Gong

410-420 **A technological convergence in hepatobiliary oncology: Evolving roles of smart surgical systems.**
Xuanci Bai, Runze Huang, Qinyu Liu, Xin Jin, Lu Wang, Wei Tang, Kenji Karako, Weiping Zhu

Original Article

421-431 **Survival benefit of adjuvant chemotherapy and individualized prognosis in resected cHCC-CCA.**
Bo Sun, Yimeng Wang, Ruyu Han, Yuren Xia, Meng Zhao, Liyu Sun, Xiaochen Ma, Tianqiang Song, Xiangdong Tian, Wenchen Gong, Lu Chen

432-444 **Conversion therapy followed by surgery and adjuvant therapy improves survival in Barcelona C stage hepatocellular carcinoma — A propensity score-matched analysis.**
Yinbiao Cao, Liru Pan, Zikun Ran, Wenwen Zhang, Junfeng Li, Xuerui Li, Tianyu Jiao, Zhe Liu, Tao Wan, Haowen Tang, Shichun Lu

445-455 **Textbook outcome and survival following laparoscopic versus open right hemihepatectomy for hepatocellular carcinoma: A propensity score-matched study.**
Jun Ji, Ding Hu, Jiaao Wang, Ziqi Hou, Zhihong Zhang, Haichuan Wang, Jiwei Huang

456-467 **A new strategy of laparoscopic anatomical right hemihepatectomy via a hepatic parenchymal transection-first approach guided by the middle hepatic vein.**
Nan You, Yongkun Li, Qifan Zhang, Chaoqun Wang, Ke Wu, Zheng Wang, Qian Ren, Jing Li, Lu Zheng

468-478 **Radiotherapy enhances triple therapy for conversion and survival in patients with unresectable hepatocellular carcinoma with portal vein tumor thrombus.**
Ying Zhou, Minghong Yao, Tianfu Wen, Chuan Li

Editorial

DOI: 10.5582/bst.2025.01228

From dengue to chikungunya: Guangdong as a sentinel for arboviral threats in East Asia

Yong Feng[1,2,§], Fangfang Chang[1,2,§], Yang Yang[1,2,*], Hongzhou Lu[1,2,*]

[1] Shenzhen Third People's Hospital, Second Hospital Affiliated with the School of Medicine, Southern University of Science and Technology, Shenzhen, China;
[2] National Clinical Research Center for Infectious Disease, Shenzhen, China.

SUMMARY: Chikungunya virus (CHIKV), an emerging mosquito-borne alphavirus, poses an escalating global public health threat due to its rapid geographic expansion and increasing outbreak frequency. While most infections present with acute fever and severe polyarthralgia, a significant proportion of patients develop chronic, disabling joint symptoms. Recent local transmission in subtropical urban regions of China, and particularly Guangdong Province, where over 4,800 cases were reported in Foshan alone by July 2025, highlights the virus's adaptability to new environments. Globally, over 220,000 cases and 80 deaths were reported in the first half of 2025 across 14 countries, with Brazil accounting for the majority of the reported cases. Climate factors, viral evolution, and human mobility are major drivers of the virus' spread. Despite the growing threat, no specific antiviral treatment or licensed vaccine is currently available. An effective response requires integrated strategies combining vaccine development, vector control, early warning systems, and climate-adaptive public health planning to mitigate further transmission and its health and socioeconomic impact.

Keywords: chikungunya virus (CHIKV), mosquito-borne disease, Guangdong outbreak, climate change, public health response

1. Introduction

Chikungunya virus (CHIKV) is a mosquito-borne alphavirus from the Togaviridae family, which causes chikungunya fever (CHIKF) and poses a growing global public health threat. CHIKF typically presents as acute fever accompanied by severe polyarthritis and myalgia (*1*). Although CHIKF is mostly self-limiting, chronic arthritis-like symptoms can persist for months or even years in some patients, leading to functional disability and severely affecting quality of life. This is particularly problematic in resource-poor regions, where it causes a significant socio-economic burden (*2*).

In recent years, CHIKV has expanded beyond traditional tropical areas, emerging as a major concern for global health security. Since 2010, multiple local outbreaks have occurred in China, indicating the virus' ability to sustain transmission in subtropical urban environments (*3*). By July 26, 2025, Foshan has reported a total of 4,824 confirmed cases, with the outbreak spreading to other cities in the Pearl River Delta, such as Guangzhou, Zhongshan, and Dongguan (Figure 1) (*4*). The outbreak was triggered by imported cases, with climate factors such as high temperature and humidity after typhoons, which promote mosquito breeding and enhanced viral strain transmissibility, being identified as key driving factors (*5*).

The spread of CHIKV extends far beyond China. In the first half of 2025, 14 countries and regions reported 220,000 cases and 80 deaths globally (*6*). The majority of cases were in the Americas (mainly Brazil, accounting for 64%), followed by Asia with over 33,000 cases, and ongoing outbreaks in Africa. Although Europe has not reported local transmission, its overseas territories, such as Réunion Island (with over 51,000 cases and an ongoing ORSEC Level 4 public health emergency response) and Mayotte Island, have entered an epidemic phase (Figure 2) (*6,7*). The World Health Organization (WHO) has designated CHIKV as a priority pathogen for global vaccine development and control (*8*). On July 4, 2025, WHO issued the "WHO guidelines for clinical management of arboviral diseases: Dengue, Chikungunya, Zika and Yellow Fever," warning of the trends in the widespread transmission of vector-borne diseases (*9*). Despite the growing health threat from CHIKV, there is currently no specific antiviral treatment, and a vaccine is still in clinical development. Since 2017, the Coalition for Epidemic Preparedness Innovations

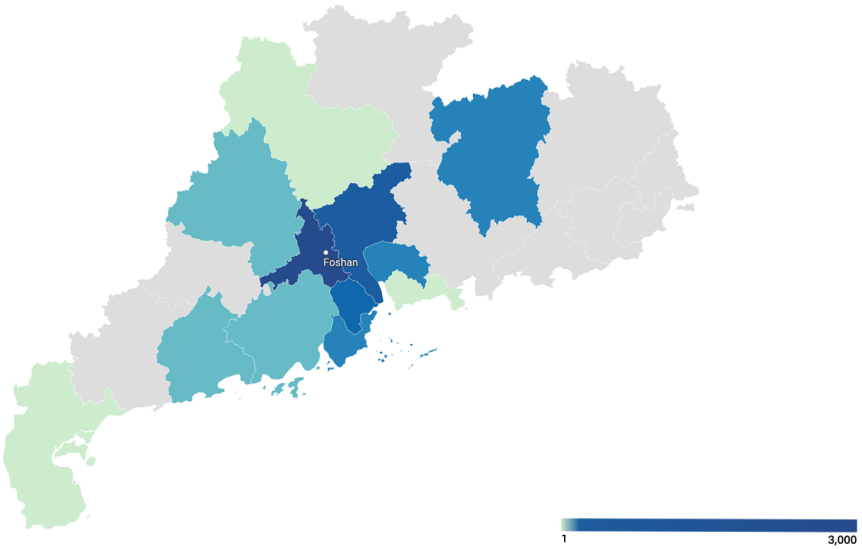

Figure 1. Locally acquired Chikungunya cases reported in Guangdong Province from July 20 to July 26, 2025.

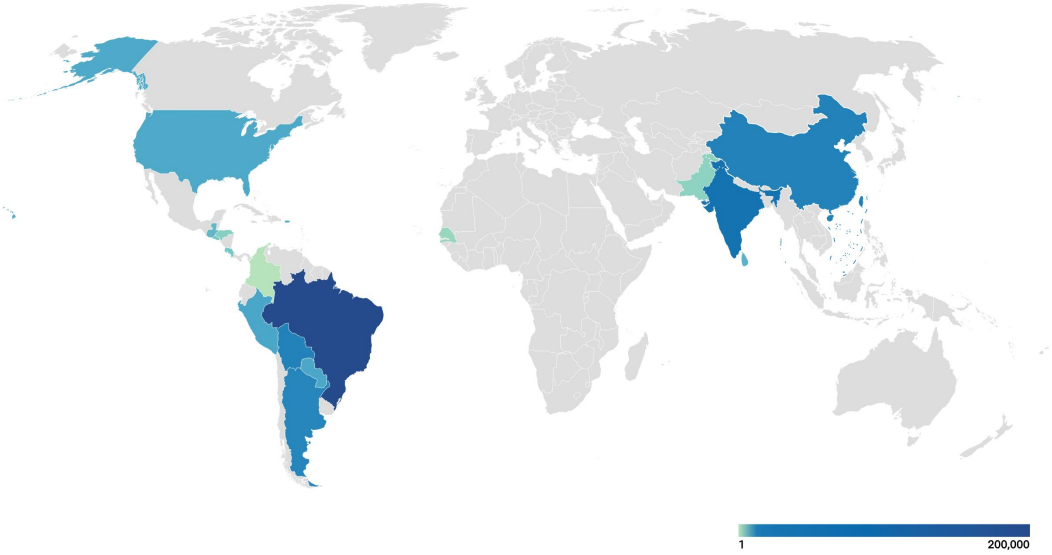

Figure 2. CHIKV disease case notification rate per 200,000 population, March 2025 - July 2025. The data represent reported cases of CHIKV infection from March to July 2025. Case counts were compiled from both official public health authorities and non-official sources, including news media. Depending on the data source, both autochthonous (locally acquired) and non-autochthonous (imported) cases may be included.

(CEPI) has included CHIKV in its list of priority pathogens for vaccine development, but a vaccine is still some years away. Therefore, vector control remains the main line of defense (*10*). A multi-layered response strategy integrating vaccine development, precise vector control, and community engagement is essential to addressing the spread of CHIKV (*11,12*).

Global warming not only expands the geographical range and prolongs the season suitable for mosquito breeding but it also increases the efficiency of virus transmission. Additionally, dense human populations act as "high-speed pathways" for cross-regional virus spread. Previous prevention and control strategies face significant challenges. The urgent need is for vector surveillance, early warning systems, cross-border collaborative defense mechanisms, and climate-adaptive public health strategies to be at the heart of health defense systems in the future.

2. Environmental and epidemiological context

Guangdong is located in a subtropical monsoon climate zone with an average annual temperature of 22-25°C and annual precipitation exceeding 1,800 mm. High

temperature and humidity provide ideal breeding conditions for Aedes aegypti and Ae. albopictus. Studies show that the larvae of these two mosquito species develop most rapidly at water temperatures between 25-30°C, and higher humidity increases the frequency of blood-feeding in adult mosquitoes, which in turn enhances virus transmission efficiency (*13,14*). Guangdong's hot and humid climate is a key ecological factor driver of local mosquito-borne viruses transmission.

At the same time, rapid urbanization, increased population density, and complex infrastructure further amplify the risk of mosquito-borne disease transmission. In the core area of the Pearl River Delta, the population density exceeds 7,000 people per square kilometer, leading to "frequent human–mosquito interactions" that significantly increase individual exposure risk (*15*). During urban development, artificial water sources such as puddles at construction sites, flowerpot trays, discarded containers, and poorly maintained urban water systems become major breeding grounds for mosquitoes, allowing mosquito populations to breed on a large scale (*16*). As a key national transportation hub and a major destination for migrant workers, Guangdong receives about 23% of the country's incoming travelers annually (*17*), and the frequent international movement of people significantly increases the likelihood of imported cases triggering local transmission.

An important point worth noting is that CHIKV, like dengue virus (DENV) and Zika virus (ZIKV), has adapted from a forest transmission cycle to an urban transmission cycle, no longer requiring non-human primates to maintain its transmission chain. In densely populated urban areas where mosquitos are active, CHIKV can sustain low-level transmission in the population, and once conditions are favorable, it can lead to large-scale outbreaks (*11*).

According to an epidemiological study of dengue fever released by the Chinese Center for Disease Control and Prevention (CCDC) on October 11, 2024, a total of 117,892 dengue cases were reported nationwide from 2005 to 2023, with Guangdong accounting for over half of the cases, totaling 68,070 (57.74% of the total cases) (*18*). In 2024, Guangdong experienced another dengue outbreak, with more than 10,000 reported cases by the time of the report (*19*). This outbreak provides important empirical data on the local transmission risk of mosquito-borne viruses. The outbreak not only demonstrates that densely populated urban areas with high mosquito densities provide an ideal platform for virus transmission but also underscores the importance of a rapid response and effective vector control in reducing the risk of virus spread.

Of particular note, CHIKV shares the same mosquito hosts — Ae. albopictus and Ae. aegypti — with DENV. This biological similarity means that prevention and control measures for CHIKV can directly draw on those used for dengue, particularly in addressing the "imported cases + high mosquito density + delayed response" risk framework in the early stages of an outbreak. This framework underscores the fact that timely and effective vector control is crucial to interrupting the virus transmission chain. In fact, past dengue outbreaks have shown that failure to take timely control measures after imported cases often leads to uncontrolled local transmission, resulting in large-scale outbreaks.

Based on current trends and historical data, priority must thus be given to early vector surveillance, rapid identification of sources of viral importation, and the swift initiation of response mechanisms in CHIKV prevention. This is not only a necessary measure for dealing with CHIKV outbreaks but also an important safeguard to enhance overall mosquito-borne virus control capacity.

3. Public health challenges exposed

The recent CHIKV outbreak in Foshan, Guangdong, has highlighted the significant challenges faced by the grassroots epidemic monitoring system. As an example, there was a 7-day delay between the discovery of the first case (July 8) and the initial report (July 15), far exceeding the typical CHIKV transmission cycle of 3–4 days (*20,21*). This delay highlights deficiencies in timely detection within the early warning system. In the absence of effective preventive interventions, epidemic control relies entirely on passive monitoring and vector control. This dual disadvantage — delayed monitoring and a lack of population immunity — significantly lowers the outbreak threshold.

Clinically, primary healthcare facilities face diagnostic challenges when identifying CHIKV's non-specific acute symptoms (such as fever and rash), leading to a high rate of misdiagnosis and confusion with dengue fever in particular (*22*). Vector control also suffers from systemic flaws, with chemical insecticide spraying mostly occurring only after an outbreak has occurred. Seasonal mosquito control efforts are inconsistent and insufficient. The extent of breeding site elimination remains inadequate, and especially in areas with limited environmental management, such as ponds and wetlands. Additionally, mosquitoes have developed a high level of resistance to commonly used pyrethroid insecticides (*23,24*). The compounded errors of inaccurate clinical diagnosis and delayed control measures have caused critical windows for interrupting the transmission chain to be repeatedly missed.

At the community level, confusion over the recognition of CHIKV is a major obstacle to effective prevention. Residents often misinterpret the disease's characteristic joint pain as strain or ordinary arthritis, leading to delays in seeking medical attention and missing the intervention window during the viremia phase. Moreover, the difficulty in distinguishing between

CHIKV and DENV results in significantly lower protective behavior among the public (*22*). Gaps persist in the existing health education and communication systems, and standardized prevention information does not adequately reach areas with highly fluid populations. Furthermore, the current one-way communication model has failed to translate into practical protective behaviors, leading to a disconnect between knowledge dissemination and action. The "cognitive gap — behavioral inertia — failed intervention" feedback loop continues to weaken the community-level protective barrier (*25*).

4. Strategic recommendations

To overcome the current bottlenecks in mosquito-borne disease control, the urgent necessity is to formulate a multi-layered, enhanced prevention and control strategy. First, a comprehensive digital mosquito-borne disease monitoring network should be established, integrating pathogen screening at sentinel hospitals, dynamic vector density assessments, and real-time meteorological data analysis to establish a multidimensional early warning system capable of detecting emerging risks (*26*). This network would not only allow for real-time monitoring of virus transmission dynamics but also enable adjustments to control strategies based on real-time data, significantly improving the efficiency and accuracy of emergency responses.

Additionally, the rapid development of tropical virus laboratory capabilities is crucial, and especially the capacity for high-throughput testing and genotyping of multiple pathogens, including CHIKV, DENV, and ZIKV (*27*). Building such laboratories will facilitate accurate tracing and provide scientific data with which to predict viral mutations and epidemic trends.

Building on that step, a key task is to create a routine provincial-level response mechanism, incorporating mosquito control threshold-based responses into routine public health operations. When, for example, the Breteau Index remains above 10, emergency insecticide measures should be implemented (*28*). Moreover, community mobilization plans should be formulated to normalize prevention and control efforts, shifting from a reactive approach during outbreaks to a proactive defense model. This mechanism would enable year-round surveillance and vector control, preventing epidemic spread due to a delayed response.

At the regional cooperation level, a real-time cross-border case information reporting platform needs to be created under the Guangdong-Hong Kong-Macao Greater Bay Area health integration framework. This platform would cross administrative boundaries, enabling real-time sharing and coordinated control of case data throughout the region, significantly enhancing coordinated response capacity (*29*). At the same time, unified vector control technical standards should be devised and joint emergency drill mechanisms should be created to address fragmented cross-regional prevention and control.

Finally, a widely available vaccine does not yet exist, so accelerating local vaccine clinical trials should be prioritized in light of the current vaccine gap (*30*). Additionally, exploring vaccine pre-purchase agreements and reserve pathways would provide strategic reserves for future vaccine interventions. This strategy aims to ensure a quick response in the event of an outbreak and achieve effective vaccination coverage. By integrating multiple dimensions such as early warning systems, standardized response mechanisms, regional collaboration, and technical reserves, this framework should create a resilient and responsive mosquito-borne disease prevention and control ecosystem (Figure 3).

5. Broader implications for global health

Guangdong, as a key observation point for the interaction between climate change and emerging infectious diseases in China and East Asia, offers valuable insights for understanding and addressing global climate-sensitive diseases due to its unique geography, climate,

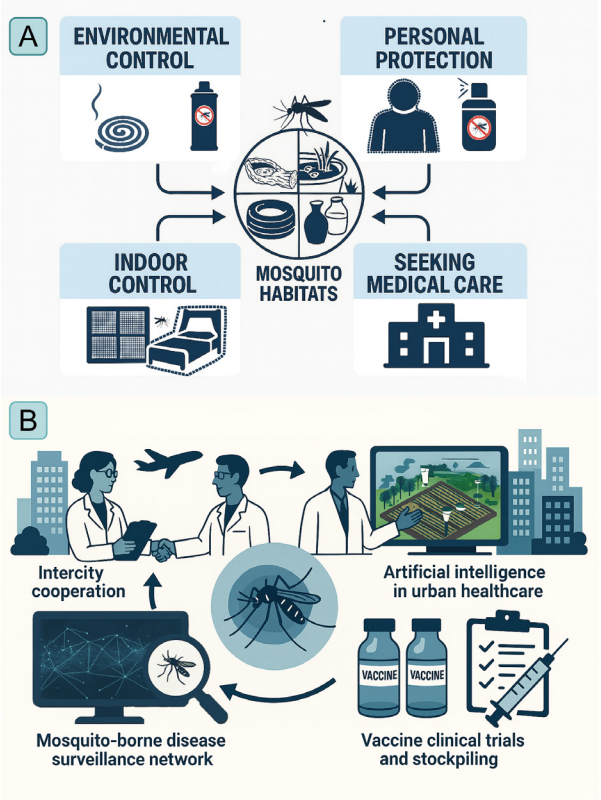

Figure 3. The integrated ecological framework for mosquito-borne disease prevention. (A) Personal and community protection are necessary measures. The first line of defense against mosquito-borne diseases is afforded by personal protection measures such as insect repellents, mosquito nets, and long-sleeved clothing. **(B)** Broader community and environmental interventions have evolved from individual-level protection. The synergy between micro- and macro-level strategies in interrupting transmission cycles and controlling mosquito populations in subtropical urban settings is underscored by this layered framework.

and population characteristics. The region's subtropical hot and humid climate is intensifying due to global warming. When this is combined with the population dynamics of its megacities and its role as an international transportation hub, it means that Guangdong is a natural laboratory for studying how climate change intensifies the transmission dynamics of mosquito-borne viruses (*31*). This combination of ecological and social risks makes Guangdong highly representative in the study and intervention of emerging viruses (such as DENV, CHIKV, and ZIKV) (*32*).

More importantly, Guangdong has established an adaptive comprehensive mosquito-borne virus governance system amidst rapid urbanization. Driven by the recurrent outbreaks of diseases like dengue, the province has gradually built an integrated model of "monitoring–response–community mobilization," which includes AI-driven real-time mosquito risk warnings, cross-border regional defense mechanisms, environmental management in high-risk areas like informal urban settlements (i.e., "urban villages"), and public health education strategies involving community participation (*33,34*). This governance experience not only proves the feasibility of interrupting vector transmission pathways in high-density urban environments but also provides a policy and practice template for developing countries similarly facing the dual pressures of urbanization and infectious diseases.

Therefore, experiences adapting to health risks should be shared among countries in the Global South under the "South-South Cooperation" framework. Against the backdrop of intensifying climate change, developing countries need to jointly create early warning and response networks to deal with climate-sensitive diseases, collaborate to innovate vector control technologies, and enhance disease monitoring and intervention at lower levels. At the same time, climate health risks should be integrated into urban planning, infrastructure development, and social governance systems, shifting from reactive emergency responses to proactive collective resilience (*35,36*). Only by turning regional governance models into collective multinational action can countries in the Global South effectively combat the growing threat from infectious diseases amidst climate change.

Funding: This work was supported by grants from the Shenzhen Clinical Research Center for Emerging Infectious Diseases (No. LCYSSQ20220823091203007) and the Sanming Project of Medicine in Shenzhen (SZSM202311033).

Conflict of Interest: The authors have no conflicts of interest to disclose.

References

1. Chikungunya. *https://www.who.int/zh/news-room/fact-sheets/detail/chikungunya* (accessed July 25, 2025). (in Chinese)
2. Suhrbier A. Rheumatic manifestations of chikungunya: Emerging concepts and interventions. Nat Rev Rheumatol. 2019; 15:597-611.
3. Chikungunya epidemiology update. *https://www.who.int/publications/m/item/chikungunya-epidemiology-update-june-2025* (accessed July 25, 2025)
4. Guangdong Center for Disease Control and Prevention. *https://cdcp.gd.gov.cn/ywdt/tfggwssj/content/post_4750007.html* (accessed July 25, 2025). (in Chinese)
5. Wu YR, Wang XW, Zhao L, Lu B, Yu JF, Liu ZH, Sun Y, Liang WN, Huang CR. Combination patterns of precipitation and its concentration degree determining the risk of dengue outbreaks in China. Adv Clim Change Res. 2023; 14:768-777.
6. Chikungunya virus disease worldwide overview. 3 March 2025. *https://www.ecdc.europa.eu/en/chikungunya-monthly* (accessed July 25, 2025)
7. Ribeiro dos Santos G, Jawed F, Mukandavire C, *et al*. Global burden of chikungunya virus infections and the potential benefit of vaccination campaigns. Nat Med. 2025; 31:2342-2349.
8. Mehand MS, Al-Shorbaji F, Millett P, Murgue B. The WHO R&D Blueprint: 2018 review of emerging infectious diseases requiring urgent research and development efforts. Antiviral Res. 2018; 159:63-67.
9. Bartholomeeusen K, Daniel M, LaBeaud DA, Gasque P, Peeling RW, Stephenson KE, Ng LFP, Ariën KK. Chikungunya fever. Nat Rev Dis Primer. 2023; 9:17.
10. CEPI. Priority diseases. *https://cepi.net/priority-diseases/* (accessed July 25, 2025)
11. De Lima Cavalcanti TYV, Pereira MR, De Paula SO, Franca RFDO. A review on chikungunya virus epidemiology, pathogenesis and current vaccine development. Viruses. 2022; 14:969.
12. Silva LA, Dermody TS. Chikungunya virus: Epidemiology, replication, disease mechanisms, and prospective intervention strategies. J Clin Invest. 2017; 127: 737-749.
13. Vega-Rúa A, Marconcini M, Madec Y, Manni M, Carraretto D, Gomulski LM, Gasperi G, Failloux AB, Malacrida AR. Vector competence of Aedes albopictus populations for chikungunya virus is shaped by their demographic history. Commun Biol. 2020; 3:326.
14. Kraemer MUG, Reiner RC, Brady OJ, *et al*. Past and future spread of the arbovirus vectors Aedes aegypti and Aedes albopictus. Nat Microbiol. 2019; 4:854-863.
15. Kolimenakis A, Heinz S, Wilson ML, Winkler V, Yakob L, Michaelakis A, Papachristos D, Richardson C, Horstick O. The role of urbanisation in the spread of Aedes mosquitoes and the diseases they transmit — A systematic review. PLoS Negl Trop Dis. 2021; 15:e0009631.
16. Wilke ABB, Caban-Martinez AJ, Ajelli M, Vasquez C, Petrie W, Beier JC. Mosquito adaptation to the extreme habitats of urban construction sites. Trends Parasitol. 2019; 35:607-614.
17. National Bureau of Statistics of China. China Statistical Yearbook 2023. 2023. *https://www.stats.gov.cn/sj/ndsj/2023/indexeh.htm* (accessed July 25, 2025)
18. Li Z, Huang X, Li A, Du S, He G, Li J. Epidemiological characteristics of dengue fever — China, 2005–2023. China CDC Wkly. 2024; 6:1045-1048.
19. Guangdong Center for Disease Control and Prevention. *https://cdcp.gd.gov.cn/zwgk/sjfb/index_4.html* (accessed July 25, 2025). (in Chinese)
20. Guangdong Center for Disease Control and Prevention.

https://cdcp.gd.gov.cn/ywdt/zdzt/yfjkkyr/yqxx/content/post_4747600.html (accessed July 25, 2025). (in Chinese)
21. Burt FJ, Rolph MS, Rulli NE, Mahalingam S, Heise MT. Chikungunya: A re-emerging virus. The Lancet. 2012; 379:662-671.
22. Wahid B, Ali A, Rafique S, Idrees M. Global expansion of chikungunya virus: Mapping the 64-year history. Int J Infect Dis. 2017; 58:69-76.
23. Su X, Guo Y, Deng J, Xu J, Zhou G, Zhou T, Li Y, Zhong D, Kong L, Wang X, Liu M, Wu K, Yan G, Chen XG. Fast emerging insecticide resistance in Aedes albopictus in Guangzhou, China: Alarm to the dengue epidemic. PLoS Negl Trop Dis. 2019; 13:e0007665.
24. Gan SJ, Leong YQ, Bin Barhanuddin MFH, Wong ST, Wong SF, Mak JW, Ahmad RB. Dengue fever and insecticide resistance in Aedes mosquitoes in Southeast Asia: A review. Parasit Vectors. 2021; 14:315.
25. Feng X, Jiang N, Zheng J, *et al*. Advancing knowledge of One Health in China: Lessons for One Health from China's dengue control and prevention programs. Sci One Health. 2024; 3:100087.
26. Caputo B, Manica M. Mosquito surveillance and disease outbreak risk models to inform mosquito-control operations in Europe. Curr Opin Insect Sci. 2020; 39:101-108.
27. Cardona-Trujillo MC, Ocampo-Cárdenas T, Tabares-Villa FA, Zuluaga-Vélez A, Sepúlveda-Arias JC. Recent molecular techniques for the diagnosis of Zika and Chikungunya infections: A systematic review. Heliyon. 2022; 8:e10225.
28. Institute of Medicine (US) Forum on Microbial Threats. Vector-borne diseases: Understanding the environmental, human health, and ecological connections. Washington (DC): National Academies Press (US); 2008. *https://www.ncbi.nlm.nih.gov/books/NBK52948/* (accessed July 25, 2025).
29. Wu W. China's health service collaboration in the Guangdong-Hong Kong-Macao Greater Bay Area: Barriers and next steps. Front Public Health. 2025; 13:1442328.
30. Huang Z, Zhang Y, Li H, Zhu J, Song W, Chen K, Zhang Y, Lou Y. Vaccine development for mosquito-borne viral diseases. Front Immunol. 2023; 14:1161149.
31. Yao-Dong D, Xian-Wei W, Xiao-Feng Y, Wen-Jun M, Hui A, Xiao-Xuan W. Impacts of climate change on human health and adaptation strategies in South China. Adv Clim Change Res. 2013; 4:208-214.
32. Khan M, Pedersen M, Zhu M, Zhang H, Zhang L. Dengue transmission under future climate and human population changes in mainland China. Appl Math Model. 2023; 114:785-798.
33. Xu L, Stige LC, Chan KS, *et al*. Climate variation drives dengue dynamics. Proc Natl Acad Sci. 2017; 114:113-118.
34. Lin H, Liu T, Song T, Lin L, Xiao J, Lin J, He J, Zhong H, Hu W, Deng A, Peng Z, Ma W, Zhang Y. Community involvement in dengue outbreak control: An integrated rigorous intervention strategy. PLoS Negl Trop Dis. 2016; 10:e0004919.
35. Ebi KL, Hess JJ. Health risks due to climate change: Inequity in causes And consequences: Study examines health risks due to climate change. Health Aff (Millwood). 2020; 39:2056-2062.
36. Integrating health in urban and territorial planning: A sourcebook. *https://www.who.int/publications/i/item/9789240003170* (accessed July 25, 2025).

Received July 26, 2025; Accepted August 1, 2025.

[§]These authors contributed equally to this work.
**Address correspondence to:*
Hongzhou Lu and Yang Yang, Second Affiliated Hospital, Affiliated with the School of Medicine, Southern University of Science and Technology, Shenzhen, China.
E-Mail: luhongzhou@fudan.edu.cn (Lu HZ); young@mail.sustech.edu.cn (Yang Y)

Released online in J-STAGE as advance publication August 2, 2025.

Editorial

DOI: 10.5582/bst.2025.01246

Anatomical study of the caudate lobe of the liver on hepatic casts and the dawn of isolated caudate lobectomy

Yoshihiro Sakamoto[1,*], Masaharu Kogure[1], Satoru Seo[2], Masamitsu Kumon[3]

[1] Department of Hepato-Biliary-Pancreatic Surgery, Kyorin University Hospital, Tokyo, Japan;
[2] Department of Surgery, Kochi Medical School, Kochi, Japan;
[3] Noichi Central Hospital, Kochi, Japan.

SUMMARY: Surgical resection of the caudate lobe of the liver remains the final hurdle for liver surgeons, not only in open hepatectomy but also in recent minimally invasive hepatectomy. In the dawn of liver surgery, Prof. Kumon made hepatic casts and showed the anatomy of the caudate lobe of the liver based on the portal segmentation in the National Cancer Center Hospital, Tokyo. Meanwhile, liver surgeons in the center successfully performed isolated caudate lobectomy of the liver for liver cancers one after another. Prof. Kumon is still dissecting hepatic casts to demonstrate the right border of the paracaval portion of the caudate lobe against segment VIII of the liver. An approach to right hemihepatectomy preserving the paracaval portion of the caudate lobe was developed thanks to the detailed anatomical knowledge of the liver based on hepatic casts.

Keywords: liver, cast, caudate lobe, paracaval portion, caudate lobectomy

1. Introduction

Surgical resection of the caudate lobe of the liver remains the final hurdle for liver surgeons not only in open hepatectomy (*1-3*) but also in recent minimally invasive hepatectomy (*4,5*). This is because the caudate lobe of the liver, *i.e.*, segment I in Couinaud's classification, is located deep in the liver, surrounded by the major hepatic vein, the inferior vena cava (IVC), and the hepatic hilum (*6*). One cannot see this lobe of until full mobilization of the whole liver from the IVC. Surgical resection of the caudate lobe is associated with bleeding from the short hepatic veins branching from the IVC in a minute surgical field. Thus, caudate lobe resection has been challenging for liver surgeons, since the late of 1980s, the dawn of safe liver surgery in Japan.

2. The dawn of liver surgery

In the 1980s, in the National Cancer Center Hospital, Tokyo, Prof. Hasegawa, Yamazaki, and Makuuchi started a new liver surgery for liver cancer using intraoperative ultrasonography (IOUS). They were pioneers of anatomical subsegmentectomy of the liver, exposing the landmark major hepatic veins on the transactional surface of the liver.

However, the precise location of the caudate lobe of the liver was unclear at the time. Prof. Hasegawa asked Dr. Masamitsu Kumon, a resident, to make hepatic casts to reveal the anatomy of the caudate lobe. He made 75 hepatic casts injecting colored epoxy resin, Mercox resin, silicon and so other chemicals into the portal vein (blue), hepatic artery (red) and the bile duct (yellow) of the whole liver between 1981 and 1990. The liver tissue was corroded completely using potassium hydroxide.

The completed liver cast was so exquisite (Figure 1A). Dr. Kumon dissected the tiny branches of the cast liver to reveal the anatomy of the caudate lobe. The epoxy resin was hard and fragile; therefore, meticulous dissection was necessary to excavate the caudate lobe preserving the surrounding other segments (Figure 2). Finally, he classified the caudate branches into three; the Spiegel branch, the paracaval (PC) branch and the caudate process branch. He defined the caudate branch as the dorsal branch from the main trunk of the portal vein or the first-order branch of the portal vein (Figure 1B). His first classification of the caudate lobe was published in 1985 in Japanese (*7*), and later republished in English with color photos (*8*).

3. Initial experiences of caudate lobectomy

Liver surgeons in the National Cancer Center Hospital challenged isolated total caudate lobectomy in patients

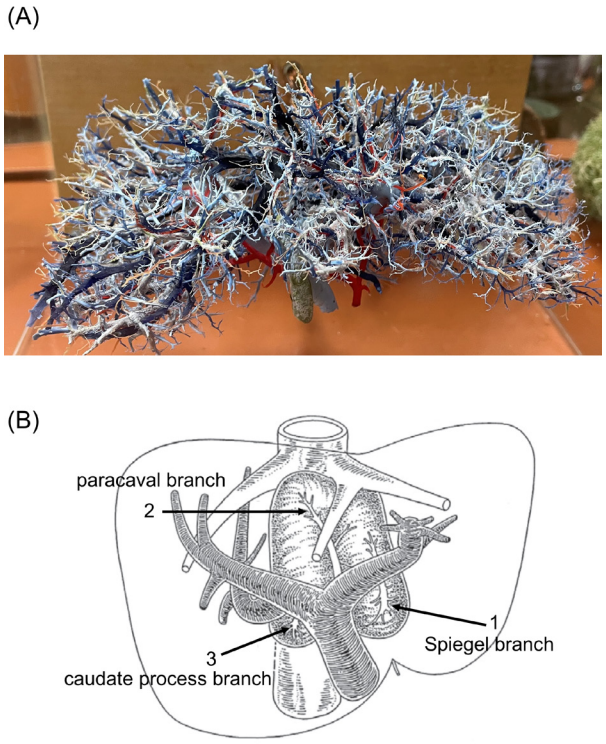

Figure 1. (A), Anterior view of the whole liver cast. (B), Definition of the three portions of the caudate lobe of the liver. (1), The Spiegel branch; (2), The paracaval branch; (3), The caudate process branch. Figure (B) adapted with modifications from *Ref. (7,8)*.

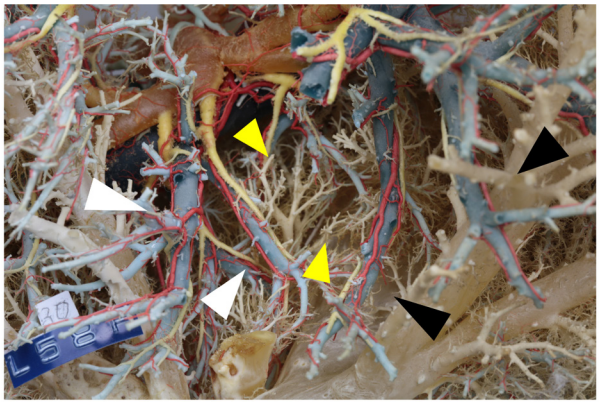

Figure 2. Cranial view of the liver cast focusing on the boundary between the paracaval portion and the segment VIII of the liver. White arrowheads indicate the portal venous branches in the paracaval portion of the caudate lobe. Black arrowheads indicate the venous branches in segment VIII. Yellow arrowheads indicate short hepatic veins between the two hepatic segments.

with hepatocellular carcinoma (HCC) in the 1990s (*1-3,9*) (Table 1). As most patients with HCC were associated with cirrhotic liver caused by the hepatitis C virus, isolated caudate lobectomy was required to prevent posthepatectomy liver failure. They successfully performed isolated caudate lobectomy using the transhepatic (*1,3,9*) or high dorsal approaches (*2*).

Sakamoto compared the short-term and long-term outcomes of surgical resection for HCC in the National Cancer Center Hospital (*10*). No survival difference was found between patients with HCC in the caudate lobe (n = 46) and in those with HCC at other sites (n = 737) of the liver. However, the resection of the paracaval portion (n = 27) was associated with longer surgical procedures (p = 0.002), more intraoperative blood loss (p = 0.02), and shorter surgical margins (p < 0.001) than the resection of the Spiegel lobe (n = 10) or caudate process (n = 19).

4. Where is the right boundary of the caudate lobe of the liver?

Prof. Kumon was born in Kochi in 1948 and went to the National Cancer Center Hospital as a surgical resident in 1979. He still dissects his hepatic casts in his laboratory. His recent primary focus is the right border of the caudate lobe of the liver because it is clinically important and has remained a mystery for a long time.

Prof. Couinaud in Paris, defined the hepatic eight segments of the liver (from segment I to VIII); however, he suffered from the definition of segment I (Figure 3) (*11*). He divided segment I into two subsegments, Ir and Il and further classified subsegment Ir into b, c, and d portions in 1989 (*12*). He reclassified subsegment Ir into segment IX in 1994 (13) and then divided segment IX into subsegments IXb and IXd in 1998 (*14*). He reclassified subsegments IXb and IXd into subsegments IX_L and IL_R in 2000 (*15*). He mentioned that segments I and IX are crossed by overlapping branches from the left and right sectors, and thus the entire dorsal liver is more correctly termed a single portal segment that has three subsegments: the Spiegel lobe, the PC portion, and the caudate process, as proposed by Kumon (*16*). Therefore, Prof. Couinaud gave the rights over the definition of the caudate lobe to Dr. Kumon.

Table 1. Reports on surgical resection of caudate lobe from National Cancer Center Hospital

Author	Year	Journal	Disease	Approaches	Number
Yamamoto J	1992	World J Surg	HCC	Transhepatic isolated caudate lobectomy	1
Takayama T	1994	J Am Coll Surg	HCC	High dorsal resection	1
Kosuge T	1994	Arch Surg	HCC	Transhepatic isolated caudate lobectomy	1
Yamamoto J	1999	World J Surg	HCC, meta	Transhepatic isolated caudate lobectomy	5
Sakamoto Y	2011	Surgery	HCC	Anatomical or non-anatomical resections	46

HCC, hepatocellular carcinoma; meta, colorectal liver metastasis.

In the original article published in 1985, Dr. Kumon found several branches from the anterior sector toward the paracaval portion, named them "PV^{8}C," and excluded them from caudate lobe branches (Figure 4A) (*7,8*). However, it is sometimes difficult to distinguish the PC branches from PV^{8}C on computed tomography (CT) images, because PC branches and PV^{8}C branches can be visualized on CT images in 33% and 45% of case, respectively (unpublished data).

Dr. Kumon found tiny, short hepatic veins toward IVC located at the boundary between the PC portion and segment VIII (Figure 4B) (*11*). He also divided the hepatic cast along the Rex-Cantlie's line and demonstrated the PC portal and biliary branches at the boundary of the PC portion of the caudate lobe and segment VIII (*17*). He found accessory branches along the IVC beside the PC branches. They were from the posterior portal vein; thus, they should be included in the posterior section.

Furthermore, he found venous plexuses in the PC and also in segment VIII of the liver. The venous plexuses joined the IVC and middle hepatic vein, while the plexuses in segment VIII joined the right hepatic vein and IVC (Figure 5) (*18*) So far, it has not been possible to reveal these venous plexuses on CT images

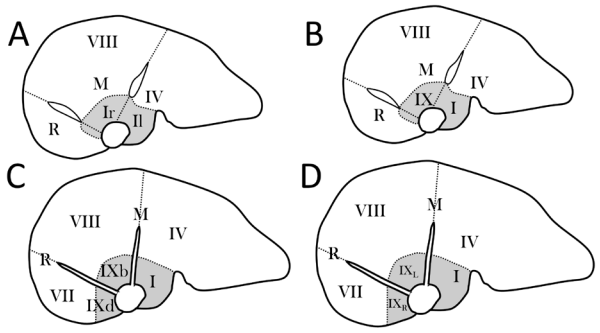

Figure 3. Serial change of the definition of the dorsal liver by Prof. Couinaud. Prof. Couinaud changed his definition on the caudate lobe of the liver in 1989 **(A)**, 1994 **(B)**, 1998 **(C)**, and 2000 **(D)**.

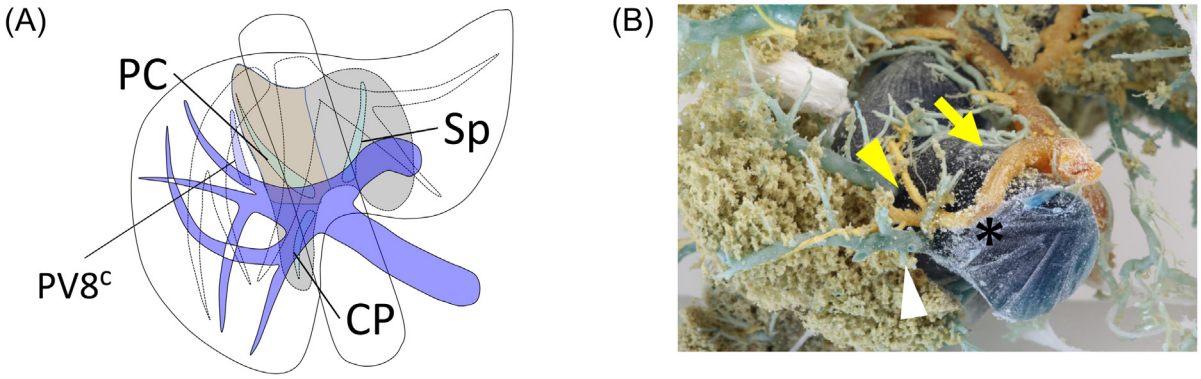

Figure 4. (A), Paracaval branch of the caudate lobe and PV8^{c}. The root of the paracaval portal branch is the right branch of the portal vein, while the root of PV8^{c} is the anterior portal vein. PC, paracaval portion; Sp, Spiegel portion; CP, caudate process. **(B), The right border of the paracaval portion of the liver.** The yellow arrow indicates the posterior bile duct, and the yellow arrowhead indicates the paracaval branch of the bile duct. The white arrowhead indicates the paracaval branch of the portal vein. The posterior bile duct is divided at the point of the asterisk.

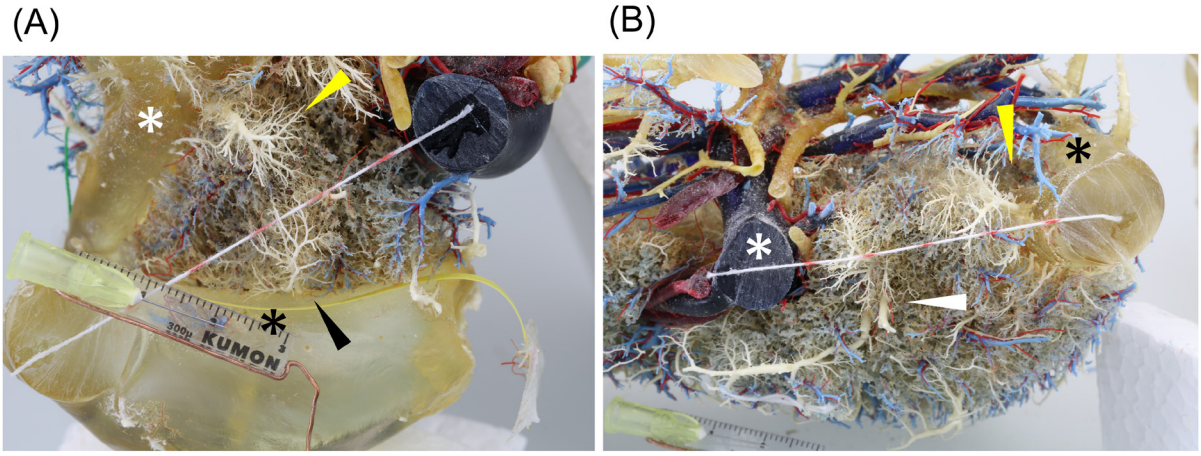

Figure 5. (A), The right border of the paracaval portion of the caudate lobe. One venous plexus (yellow arrowhead) joins the middle hepatic vein (white asterisk), whereas another venous plexus (black arrowhead) joins the inferior vena cava (black asterisk). **(B), The left border of the right liver.** Two venous plexuses are seen: one plexus (yellow arrowhead) joins the right hepatic vein (black asterisk) and the other plexus (white arrowhead) joins the inferior vena cava that has been divided at the root of the short hepatic vein.

Figure 6. Photos of the second meeting of the caudate lobe of the liver held in Kochi on July 12, 2025. Prof. Kumon (center) brought his hepatic casts to the meeting and the participants found that the casts are so fragile and the dissection of tiny branches is not easy.

or to detect them during hepatectomy. To the best of our knowledge, this study will be the first to reveal these plexuses in the PC and segment VIII.

5. Clinical application of anatomical knowledge on the caudate lobe

How can we translate the above anatomical knowledge to real-world liver surgery? Kogure *et al* first performed right hemihepatectomy preserving the PC of the caudate lobe completely (*19*). The patient was a man in his 40s with a metastatic mass from colorectal cancer measuring 24 × 10 cm in the right lobe of the liver. Preoperative CT volumetry revealed that the left hemiliver and the caudate lobe constituted 55% and 5.3%, respectively, of the total liver volume.

To preserve the future liver remnant volume, he decided to preserve the PC portion of the caudate lobe. He injected a mixture of indigo carmine and indocyanine green solution into the PC portal branch under IOUS guidance. During right hemihepatectomy, the PC portion was visualized fluorescently using a near-infrared image system. The fluorescently visible PC portion was preserved with the left hemiliver, and right hemihepatectomy was completed. To the best of our knowledge, this is the first report of isolated fluorescent visualization and preservation of the PC of the caudate lobe during right hemihepatectomy. The patient had enough functional reserve of the liver; however, this technique might be useful in patents with deteriorated hepatic function, in whom the liver parenchyma should be preserved as much as possible.

Comments

The anatomy of the liver does not change; however, the required anatomical knowledge changes with the advancement of surgical technology. Recent three-dimensional analyses of CT images do not always visualize tiny hepatic branches, which can be clearly demonstrated on the hepatic casts produced in the 1980s. We must reconsider the anatomy of the liver with the advancement of surgical techniques.

Appendix

In honor of the anatomical study of the caudate lobe on hepatic casts, the second meeting of the caudate lobe of the liver was held in Kochi, Japan on July 12, 2025. This meeting was planned by Prof. Sakamoto Y, and managed by Prof. Satoru Seo of the Department of Surgery, Kochi Medical School. The clinical and anatomical importance of the caudate lobe of the liver was discussed around Prof. Masamitsu Kumon (Figure 6).

Funding: None.

Conflict of Interest: The authors have no conflicts of interest to disclose.

References

1. Yamamoto J, Takayama T, Kosuge T, Yoshida J, Shimada K, Yamasaki S, Hasegawa H. An isolated caudate lobectomy by the transhepatic approach for hepatocellular carcinoma in cirrhotic liver. Surgery. 1992; 111:699-702.
2. Kosuge T, Yamamoto J, Takayama T, Shimada K, Yamasaki S, Makuuchi M, Hasegawa H. An isolated, complete resection of the caudate lobe, including the paracaval portion, for hepatocellular carcinoma. Arch Surg. 1994; 129:280-284.
3. Takayama T, Tanaka T, Higaki T, Katou K, Teshima Y, Makuuchi M. High dorsal resection of the liver. J Am Coll Surg. 1994; 179:72-75.
4. Liu F, Wei Y, Li B. Laparoscopic isolated total caudate lobectomy for hepatocellular carcinoma located in the paracaval portion of the cirrhotic liver. Ann Surg Oncol. 2019; 26:2980.
5. Zhao ZM, Yin ZZ, Pan LC, Jiang N, Tan XL, Chen X, Liu R. Robotic anatomic isolated complete caudate lobectomy: left-side approach and techniques. Asian J Surg. 2021; 44:269-274.
6. Couinaud C. Lobes et segments hepatiques, Notes sur l'architecture anatomique et chirurgicale du foie. La Press

Medicale 5. 1954; 62:709-12. (in French)
7. Kumon M. Anatomy of the caudate lobe with special reference to portal vein and bile duct. Acta Hepatol Jpn. 1985; 26:1193-1199. (in Japanese)
8. Kumon M. Anatomical study of the caudate lobe with special reference to portal venous and biliary branches using corrosion liver casts and clinical application. Liver Cancer. 2017; 6:161-170.
9. Yamamoto J, Kosuge T, Shimada K, Yamasaki S, Takayama T, Makuuchi M. Anterior transhepatic approach for isolated resection of the caudate lobe of the liver. World J Surg. 1999; 23:97-101.
10. Sakamoto Y, Nara S, Hata S, Yamamoto Y, Esaki M, Shimada K, Kosuge T. Prognosis of patients undergoing hepatectomy for solitary hepatocellular carcinoma originating in the caudate lobe. Surgery. 2011; 150:959-967.
11. Kumon M, Kumon T, Tsutsui E *et al*. Definition of the caudate lobe of the liver based on portal segmentation. Glob Health Med. 2020; 2:328-336.
12. Couinaud C. Surgical anatomy of the liver revisited. 130-2, Acheve Dimprimer Sur Les Presses, Paris, France, 1989.
13. Couinaud C. The paracaval segments of the liver. J Hepatobiliary Pancreat Surg. 1994; 2:145-151.
14. Couinaud C. Dorsal sector of the Liver. Chirurgie. 1998; 123:8-15.
15. Filipponi F, Romagnoli P, Mosca F, Couinaud C. The dorsal sector of human liver: embryological, anatomical and clinical relevance. Hepatogastroenterology. 2000; 47:1726-1731.
16. Abdalla EK, Vauthey JN, Couinaud C. The caudate lobe of the liver. Implications of embryology and anatomy for surgery. Surg Oncol Clin N Am. 2002; 11:835-848.
17. Kumon M, Kumon T, Sakamoto Y. Demonstration of the right-side boundary of the caudate lobe in a liver cast. Glob Health Med. 2022; 28:52-56.
18. Kumon M, Kumon T, Kogure M, Seo S, Sakamoto Y. Hepatic venous plexuses on the right border of the caudate lobe against the right liver in a liver cast. Glob Health Med. 2025; 7:324-328.
19. Kogure M, Kumon M, Matski R, Suzuki Y, Sakamoto Y. Right hemihepatectomy preserving the fluorescently visible paracaval portion of the caudate lobe. Glob Health Med. 2023; 5:377-380.

Received July 25, 2025; Accepted August 15, 2025.

**Address correspondence to:*
Yoshihiro Sakamoto, Department of Hepato-Biliary-Pancreatic Surgery, Kyorin University Hospital, 6-20-2 Shinkawa, Mitaka, Tokyo 186-8611, Japan.
E-mail: yosakamo@ks.kyorin-u.ac.jp

Released online in J-STAGE as advance publication August 17, 2025.

Consensus

DOI: 10.5582/bst.2025.01233

Chinese multicenter expert consensus on the diagnosis and treatment of hilar cholangiocarcinoma: 2025 edition

Sulai Liu[1,§], Jinqiong Jiang[1,§], Qian Jian[1], Yingbin Liu[2], Zhiyong Huang[3], Yongjun Chen[3], Chihua Fang[4], Zhaohui Tang[5], Lu Wang[6], Deyu Li[7], Fuyu Li[8], Shaoqiang Li[9], Xuemin Liu[10], Cuncai Zhou[11], Yamin Zheng[12], Heguang Huang[13], Chen Chen[1], Xu Chen[1], Bo Sun[1], Weimin Yi[1], Bingzhang Tian[1], Liansheng Gong[14], Wei Liu[15], Feizhou Huang[16], Jia Luo[17], Dongde Wu[18], Shuke Fei[19], Lixin Xiong[20], Caixi Tang[21], Shaojie Li[22], Yi Yu[23], Jushi Li[24], Biao Tang[25], Yongqing Yang[26], Xuzhao Gao[27], Xingguo Tan[28], Yu Liu[29], Wei Tang[30], Bo Jiang[1], Zhiming Wang[14], Huihuan Tang[14], Jinshu Wu[1], Chuang Peng[1,*]

[1] Hunan Provincial People's Hospital/The First Affiliated Hospital of Hunan Normal University, Changsha, Hunan, China;
[2] Renji Hospital, School of Medicine, Shanghai Jiao Tong University, Shanghai, China;
[3] Tongji Hospital, Tongji Medical College, Huazhong University of Science and Technology, Wuhan, Hubei, China;
[4] Zhujiang Hospital of Southern Medical University, Guangzhou, Guangdong, China;
[5] Xinhua Hospital Affiliated to Shanghai Jiao Tong University School of Medicine, Shanghai, China;
[6] Fudan University Shanghai Cancer Center, Shanghai, China
[7] Henan Provincial People's Hospital, Zhengzhou, Henan, China;
[8] West China Hospital, Sichuan University, Chengdu, Sichuan, China;
[9] The First Affiliated Hospital of Sun Yat-sen University, Guangzhou, Guangdong, China;
[10] The First Affiliated Hospital of Xi'an Jiaotong University, Xi'an, Shanxi, China;
[11] Jiangxi Cancer Hospital, Nanchang, Jiangxi, China;
[12] Xuanwu Hospital, Capital Medical University, Beijing, China;
[13] Fujian Medical University Union Hospital, Fuzhou, Fujian, China;
[14] Xiangya Hospital, Central South University, Changsha, Hunan, China;
[15] The Second Xiangya Hospital, Central South University, Changsha, Hunan, China;
[16] The Third Xiangya Hospital, Central South University, Changsha, Hunan, China;
[17] Cancer Hospital of Xiangya School of Medicine, Central South University/Hunan Cancer Hospital, Changsha, Hunan, China;
[18] Affiliated Cancer Hospital of Tongji Medical College, Huazhong University of Science and Technology/Hubei Cancer Hospital, Wuhan, Hubei, China;
[19] The Second Affiliated Hospital of University of South China, Hengyang, Hunan, China;
[20] Changsha Hospital Affiliated to Xiangya School of Medicine, Central South University/Changsha First Hospital, Changsha, Hunan, China;
[21] Zhuzhou Hospital Affiliated to Xiangya School of Medicine, Central South University/Zhuzhou Central Hospital, Zhuzhou, Hunan, China;
[22] Xiangtan First People's Hospital, Xiangtan, Hunan, China;
[23] Chenzhou First People's Hospital, Chenzhou, Hunan, China;
[24] Shaoyang Central Hospital, Shaoyang, Hunan, China;
[25] Yongzhou Central Hospital, Yongzhou, Hunan, China;
[26] Loudi Central Hospital, Loudi, Hunan, China;
[27] Zhangjiajie People's Hospital, Zhangjiajie, Hunan, China;
[28] Yueyang People's Hospital, Yueyang, Hunan, China;
[29] Yueyang Central Hospital, Yueyang, Hunan, China;
[30] Department of Surgery, Graduate School of Medicine, The University of Tokyo, Tokyo, Japan.

SUMMARY: Hilar cholangiocarcinoma (hCCA) is a malignant tumor originating from the epithelial cells of the bile ducts, and it is characterized by an aggressive nature, complex surgical management, high mortality, and poor prognosis. Despite recent advances in surgical techniques, medical devices, and related technologies, there remains a pressing need to standardize diagnostic and therapeutic pathways to improve treatment outcomes and extend long-term patient survival. To better integrate and refine these standards, this consensus was reached through a national conference held in Changsha, Hunan Province, involving multidisciplinary experts from various regions across China. This collaborative effort, drawing from various medical facilities and academic organizations nationwide, resulted in the reaching of the "Chinese Multicenter Expert Consensus on the Diagnosis and Treatment of Hilar Cholangiocarcinoma: 2025 Edition" based on current clinical studies and over 40 years of clinical practice experience in managing hCCA. The consensus provides a comprehensive overview of hCCA, including its epidemiological characteristics, diagnostic and screening methods, pathological features, staging and classification systems, and various treatment modalities, while offering specific and actionable recommendations for clinical practice that highlight well-defined indications for surgical, local, and systemic therapies and that emphasize the importance of multidisciplinary approaches to both diagnostic and therapeutic workflows.

Keywords: hilar cholangiocarcinoma, diagnosis and treatment consensus, multidisciplinary approach, surgical management, biliary tract cancer

1. Introduction

Hilar cholangiocarcinoma (hCCA), also known as proximal cholangiocarcinoma, refers to cholangiocarcinoma arising from the bile duct epithelium between the confluence of the cystic duct and the common bile duct and the second-order bile ducts. It predominantly involves the left and right hepatic ducts, the bifurcation of the common hepatic duct, and the common hepatic duct itself. As the most prevalent biliary tract malignancy (accounting for approximately 40-60% of cases) (*1,2*), hCCA presents major therapeutic challenges due to its predilection for invading critical hilar structures, including blood vessels, neural plexuses, lymphatic tissues, and adjacent hepatic parenchyma (*3*). Curative-intent resection with microscopically negative margins (R0) remains the only potentially curative modality; however, approximately two-thirds of patients present with unresectable disease at initial diagnosis or surgical exploration (*4*). Comprehensive preoperative assessment and multidisciplinary treatment are critical to achieving optimal outcomes in patients with hCCA.

2. Methods

The Hepatobiliary Surgery Professional Committee of the Hunan Medical Association, the Hunan Provincial Clinical Research Center for the Prevention and Treatment of Biliary Diseases, the Hunan Provincial Key Laboratory for the Prevention and Treatment of Biliary Diseases, the Hunan Provincial Engineering Research Center for Digital Hepatobiliary Medicine, the Hepatobiliary Surgery Professional Committee of the Hunan International Medical Exchange and Promotion Association, the Hunan Alliance of Hepatobiliary and Pancreatic Surgery, the Hunan Alliance for the Diagnosis and Treatment of Malignant Biliary Tumors, and the Hepatopancreatobiliary Disease Research Center of the Furong Laboratory assembled multidisciplinary experts to systematically compile the latest evidence on hCCA diagnosis and treatment, incorporating over 40 years of clinical practice to draft the "Chinese Multicenter Expert Consensus on the Diagnosis and Treatment of Hilar Cholangiocarcinoma: 2025 Edition". This consensus emphasizes precise preoperative evaluation and the formulation of individualized treatment plans, while also highlighting the need for meticulous intraoperative techniques to enhance surgical quality and improve overall prognosis.

The consensus drafting process was initiated in early March 2024. From May to June 2024, the draft underwent rigorous review and discussion by an expert audit panel, with multiple revisions implemented during this period. On November 1, 2024, all members of the consensus committee convened in Changsha for the finalization meeting, where voting was conducted to establish consensus recommendations and their respective evidence grades, culminating in the finalized document. To systematically review recent advances in hCCA, the consensus committee implemented a comprehensive literature search strategy across multiple databases: PubMed, MEDLINE, EMBASE, Cochrane Library, Chinese Biomedical Literature Database (CBM), China National Knowledge Infrastructure (CNKI), and Wanfang Database. Search terms included: Hilar Cholangiocarcinoma, Epidemiology, Diagnosis, Pathology, Staging, Multidisciplinary Treatment, Surgery, Local Therapy and Systemic Therapy. Eligible studies encompassed systematic reviews, meta-analyses, randomized controlled trials (RCTs), cohort studies, and case-control studies addressing hCCA epidemiology, diagnostic approaches, therapeutic

Table 1. Levels of evidence quality

Level	Content
1++	High-quality meta-analyses, systematic reviews of RCTs, or RCTs with very low risk of bias.
1+	Well-conducted meta-analyses, systematic reviews, or RCTs with low risk of bias.
1-	Meta-analyses, systematic reviews, or RCTs with a high risk of bias.
2++	High-quality systematic reviews of case-control or cohort studies. High-quality case-control or cohort studies demonstrating minimal confounding or bias risk and a high likelihood of causality.
2+	Well-conducted case-control or cohort studies demonstrating minimal confounding or bias risk and a moderate likelihood of causality.
2-	Case-control or cohort studies with a high risk of confounding or bias and a significant risk of no causal relationship.
3	Non-analytical studies, such as case reports or case series.
4	Expert opinions

Table 2. Levels of recommendation

Level	Definition
A	At least one meta-analysis, systematic review, or RCT rated as 1++, directly applicable to the target population; or evidence primarily from studies rated as 1+, directly applicable to the target population, demonstrating overall consistency in results.
B	Evidence includes studies rated as 2++, directly applicable to the target population; or studies rated as 2+, directly applicable to the target population and demonstrating overall consistency in results; or evidence extrapolated from studies rated as 1++ or 1+.
0	Evidence of level 3 or 4; or evidence extrapolated from studies rated as 2++ or 2+.
GPP	Good Practice Points (GPP): Best practices recommended by the guideline development group based on clinical experience.

interventions (surgical, local, and systemic), pathological characteristics, staging systems, and multidisciplinary treatment. Exclusions comprised basic research, brief communications, conference abstracts, and other low-evidence-level publications. The consensus adopted the Scottish Intercollegiate Guidelines Network (SIGN) (*5*) framework for evidence classification (Table 1). Recommendations were categorized into four levels (A, B, 0, and GPP) based on evidence quality (Table 2). A formal voting system was implemented to determine consensus levels: strong consensus, consensus, indeterminate opinion, and no consensus. An expert consensus was established if the ratio of a strong consensus and a consensus was ≥ 75% (Table 3).

Table 3. Classification of consensus strength

Level	Content
Strong consensus	> 90% of participants agree.
Consensus	75-90% of participants agree.
Indeterminate opinion	50-75% of participants agree.
No consensus	< 50% of participants agree.

Consensus Text

3. Epidemiology of and risk factors for hCCA

hCCA primarily occurs in individuals ages 50 to 70 years, with a male-to-female ratio of approximately 1.4:1 (*6-8*). The incidence of hCCA exhibits significant geographic heterogeneity. In Europe, the United States, and Australia, incidence ranges from 0.35/100,000 to 2/100,000. In contrast, regions where hepatobiliary flukes are endemic, such as Thailand, China, and South Korea, have a particularly high incidence, reaching 85/100,000 in Northeastern Thailand. The geographic heterogeneity of incidence probably reflects different underlying risk factors. In Western countries, primary sclerosing cholangitis (PSC) is the most prevalent risk factor for hCCA, while in Southeast Asia, hepatobiliary fluke infections predominate (*7*). Other established risk factors include congenital bile duct dilatation, hepatolithiasis, choledocholithiasis, liver cirrhosis, and chronic hepatitis B and C virus infections (*9,10*). A common characteristic of these risk factors is that they are associated with chronic inflammation of the biliary epithelium and cholestasis (*10*).

4. Screening and diagnosis of hCCA

4.1. Clinical manifestations

Patients with hCCA are usually asymptomatic in the early stages and may be incidentally detected during liver function tests or imaging studies performed for other reasons. Obstructive jaundice is the most frequent symptom of advanced disease, occurring in up to 90% of patients, and is characterized by progressive skin and sclera icterus, clay-colored stools, dark tea-colored urine, and pruritus. Other symptoms of advanced disease include abdominal pain, malaise, asthenia, anorexia, and weight loss. Approximately 10% of patients may develop concurrent biliary tract infection, presenting with right upper abdominal pain, fever, and jaundice (*11-13*).

4.2. Laboratory results

In cases of obstructive jaundice, liver function tests typically reveal elevated direct bilirubin levels. Alkaline phosphatase and gamma-glutamyl transferase levels usually rise in conjunction with bilirubin levels. In addition, some patients may also have elevated transaminases levels (*2*). Additional blood tests can be used to detect evidence of infection, particularly in cases of biliary obstruction (*e.g.*, elevated white blood cell count, neutrophilia, elevated C-reactive protein, and positive blood or bile cultures) (*12*).

Carbohydrate antigen 19-9 (CA19-9) is the most commonly used tumor marker for hCCA, with elevated levels observed in up to 85% of patients. Approximately 10% of patients lack the Lewis antigen and do not secrete CA19-9 (*14*). Elevated CA19-9 levels can also occur in biliary obstruction, pancreatitis, cirrhosis, hepatocellular carcinoma, and pancreatic cancer, resulting in a low positive predictive value (16–40%) (*13,14*). Despite these limitations, CA19-9 remains an important auxiliary diagnostic marker for hCCA. Persistent elevation after effective biliary drainage strongly suggests malignancy. Moreover, elevated serum CA19-9 levels in patients after radical surgery serve as an independent prognostic factor for disease recurrence and poor outcome (*15,16*). Carcinoembryonic antigen (CEA) is also a commonly used tumor marker for hCCA. Combining CA19-9 and CEA for screening in high-risk populations is recommended (*17*). Notably, approximately 15% of patients undergoing surgery for suspected hCCA are ultimately diagnosed with benign lesions, such as autoimmune cholangiopathy (*18,19*). IgG4-related sclerosing cholangitis, characterized by bile duct wall thickening, bile duct stricture, and obstructive jaundice, represents a critical differential diagnosis. Serum IgG4 levels are useful for distinguishing IgG4-related sclerosing cholangitis from hCCA (*20*).

Recommendation 1:

Liver function tests, CA19-9, CEA and IgG4 are recommended as baseline evaluations for suspected hCCA.

(1) While CA19-9 lacks specificity for hCCA and may be elevated due to obstructive jaundice, persistent elevation after effective biliary drainage strongly suggests malignancy.

(2) Combined detection of IgG4 aids in differentiating hCCA from IgG4-related sclerosing cholangitis. [Evidence Level: 1-, Recommendation Grade: A]

5. Imaging studies

Imaging studies play a pivotal role in the screening, diagnosis, staging, resectability evaluation, treatment assessment and follow-up of hCCA. Imaging assessments should include the extent of tumor axial spread along the bile duct tree, radial invasion beyond the bile duct wall, the relationship between the tumor and the portal vein and hepatic artery, regional lymph node metastasis, neural plexus infiltration, as well as intrahepatic and distant metastasis (*21*). The two primary pieces of radiological evidence for hCCA diagnosis are biliary obstruction and tumor mass.

Currently, the imaging modalities commonly used to reveal hCCA include non-invasive techniques such as ultrasonography, computed tomography (CT), magnetic resonance imaging (MRI), magnetic resonance cholangiopancreatography (MRCP), and positron emission tomography-computed tomography (PET/CT). In addition, there are invasive diagnostic approaches such as endoscopic retrograde cholangiopancreatography (ERCP), percutaneous transhepatic cholangiography (PTC), cholangioscopy, and endoscopic ultrasonography (EUS). Performing CT or MRI before biliary decompression or an endoscopy is recommended to avoid secondary inflammation, stents, or other procedural factors that may affect the accurate assessment of the tumor (*22*). The diagnostic algorithm for hCCA is shown in Figure 1.

5.1. Ultrasound

Ultrasound is the preferred initial screening method for hCCA and is characterized by its convenience, speed, cost-effectiveness and non-invasiveness. Sonographic findings typically include intrahepatic bile duct dilation with abrupt truncation at the hilum, occasionally demonstrating intraluminal tumor echoes. Doppler ultrasound provides additional value in evaluating hepatic artery and portal vein involvement. However, ultrasonography has limitations in determining the location of obstruction, differentiating benign from malignant lesions, and evaluating the extent of tumor involvement. Enhanced CT and MRI need to be combined for further confirmation of the diagnosis (*23*). The diagnostic accuracy of ultrasonography may be compromised by technical factors such as abdominal wall adiposity or bowel gas interference, so its principal clinical utility thus lies in initial screening. Additionally, ultrasound can be used to guide percutaneous biopsy or biliary drainage procedures.

5.2. CT

CT is routinely used as the standard imaging modality with which to initially identify hCCA, and the scan includes the chest, abdomen, and pelvis. Its main advantage is the excellent spatial resolution, providing comprehensive assessment of the primary tumor, its local vascular relationships, and overall resectability. It also allows detection of local lymph adenopathy and metastatic disease, although it is less sensitive than PET/CT (*24-26*). A meta-analysis including 448 patients from

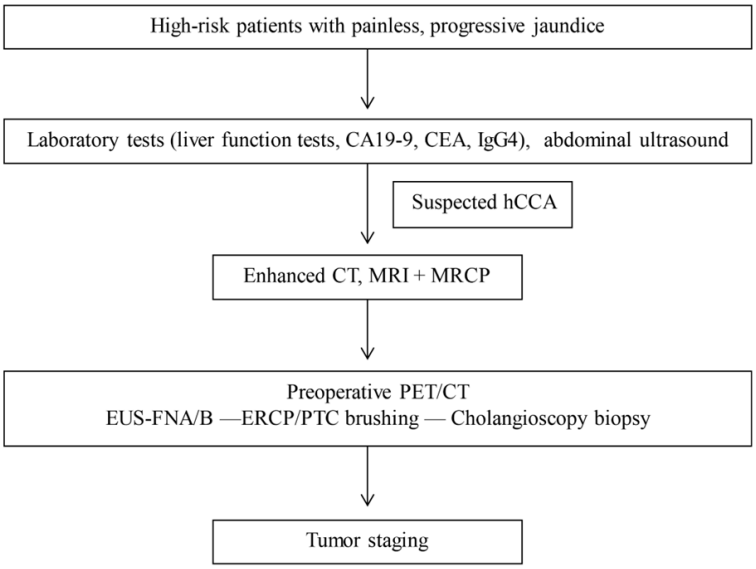

Figure 1. Diagnostic workflow for hCCA.

16 studies revealed that CT had a sensitivity of 89% and specificity of 92% for assessing portal vein involvement and a sensitivity of 83% and specificity of 93% for assessing hepatic artery involvement (*27*). In comparison, CT had a relatively lower accuracy in identifying lymph node metastasis (a sensitivity of 61%, a specificity of 88%) and distant metastasis (a sensitivity of 67%, a specificity of 94%). In contrast, PET/CT is superior at detecting distant metastasis, achieving a detection rate as high as 100% (*28*). Assessment of the extent of biliary involvement can also be difficult with CT, and particularly the proximal extent of perihilar tumors. Related studies have demonstrated that three-dimensional reconstruction of the bile ducts can improve the accuracy in evaluating the extent of bile duct involvement (*24,29*). Typical CT manifestations of hCCA include strictures at the major ductal confluence, accompanied by irregular wall thickening. CT generally displays progressive delayed enhancement and dilation of the upstream bile ducts (*30*).

5.3. MRI

MRI has advantages such as no radiation exposure, superior soft tissue resolution, and multi-parametric imaging. Moreover, hepatocyte-specific contrast agents can enhance the sensitivity of detecting intrahepatic micrometastases (*31*). MRCP provides unique diagnostic value for the biliary system, clearly displaying the biliary tree and depicting hilar obstruction and upstream biliary dilation. Abdominal contrast-enhanced MRI combined with MRCP can accurately show the primary tumor, biliary obstruction, vascular invasion, as well as regional lymph node metastasis and intrahepatic metastasis (*22*). hCCA lesions typically present with slight hyperintensity on T2-weighted imaging (T2WI), hypointensity on T1-weighted imaging (T1WI), hyperintensity on diffusion-weighted imaging (DWI), and progressive enhancement during contrast-enhanced scanning (*32*). Integrating MRI with MR angiography enables non-invasive vascular assessment comparable to conventional angiography (*33*). The available literature has indicated that the accuracy of contrast-enhanced MRI in association with MRCP is comparable to that of direct cholangiography *via* ERCP or PTC in differentiating benign from malignant obstruction, as well as the degree of extension. The presence of a long stenotic segment with thick and irregular margins, asymmetric narrowing, lumen irregularity, enhancement during the portal phase, a mass of periductal soft tissue, and nodal enlargement is suggestive of hCCA (*34*).

5.4. PET/CT

PET/CT is a functional imaging modality that has been found to play an important role in preoperative lymph node staging (N staging) and evaluation of distant metastasis (M staging) in hCCA. A prospective study found that PET/CT demonstrated superior N-stage accuracy (76%) compared to conventional CT alone (60%)(*35*). Another study revealed that PET/CT was able to detect occult metastatic lesions, leading to treatment strategy modifications in 30% (11 of 36) of patients (*36*). Nevertheless, PET/CT exhibits reduced sensitivity for small masses or periductal infiltrating hCCA. False-positive results may occur in non-malignant conditions such as primary sclerosing cholangitis (PSC), biliary infections, or granulomatous diseases. Considering the high cost, as well as its limitations, PET/CT is not recommended as a routine imaging modality for the initial diagnosis of hCCA.

Current clinical uses of PET/CT primarily focus on metastatic surveillance, recurrence assessment, and comprehensive lymph node evaluation.

5.5. Invasive examinations

Invasive examinations encompass ERCP, PTC, cholangioscopy, and EUS. Direct cholangiography, including ERCP and PTC, provides clear visualization of the obstruction site, the extent of involvement, and the morphology of upstream bile ducts. It is commonly used in patients with unresectable hCCA to obtain cytology or tissue for pathological diagnosis and to manage obstructive jaundice (*17*). Due to the risk of bleeding and infection, direct cholangiography is not recommended as a routine diagnostic method. Cholangioscopy provides direct visualization and allows biopsy of strictured segments. By inserting the SpyScope through the working channel of a duodenoscope and utilizing SpyBite, specimens can be obtained with a sensitivity of 64%, and especially in cases where ERCP sampling is insufficient or biliary strictures are indeterminate (*27*). Anatomically, the extrahepatic bile ducts are located close to the duodenum. Thus, EUS enables detailed observation of the extrahepatic bile duct tree and its adjacent structures. A study has shown that EUS can detect metastatic lymph nodes not identified on conventional cross-sectional imaging, with a detection rate of 15–20% (*37*). Nevertheless, endosonographic morphology and echogenic characteristics cannot reliably predict malignant lymph node involvement, necessitating endoscopic ultrasound-guided fine-needle aspiration/biopsy (EUS-FNA/B) (*35*). A point worth noting is that EUS-FNA/B may increase the risk of tumor seeding. Therefore, it should be avoided when liver transplantation is considered a treatment option (*27,38*).

Recommendation 2:

For patients with suspected hCCA, enhanced chest, abdominal, and pelvic CT and/or enhanced MRI + MRCP are recommended to assess the primary tumor, its local vascular relationships, distant metastases, and overall resectability. [Evidence Level: 2+, Recommendation Grade: B]

Recommendation 3:

If biliary drainage is required, imaging should be performed before endoscopic nasobiliary drainage (ENBD), endoscopic retrograde biliary drainage (ERBD), or percutaneous transhepatic cholangial drainage (PTCD) to obtain high-quality imaging for tumor evaluation and to avoid inflammation or artifacts caused by interventions such as catheters or stents. [Evidence Level: 1-, Recommendation Grade: A]

Recommendation 4:

PET/CT is recommended for evaluating distant metastases, disease recurrence, lymph node metastases, and differential diagnosis when routine imaging is inconclusive for hCCA. PET/CT is not recommended as a routine imaging method for initial diagnosis. [Evidence Level: 2++, Recommendation Grade: A]

Recommendation 5:

Invasive procedures such as PTC, ERCP, cholangioscopy, and EUS can be utilized for pathological diagnosis in unresectable hCCA. Additionally, they can serve as complementary methods to other imaging techniques. Despite their potential therapeutic applications, such as in biliary drainage, these invasive procedures are nevertheless not recommended as routine diagnostic tools for suspected cases of hCCA. [Evidence Level: 2+, Recommendation Grade: B]

6. Pathological characteristics of hCCA

6.1. Methods of pathological diagnostic

Histopathological and/or cytological examination is the gold standard for diagnosing hCCA. For unresectable hCCA, pathological diagnosis is required to guide subsequent treatment and predict prognosis (*19,37*). For patients scheduled to undergo surgical resection, preoperative biopsy may be avoided due to its low sensitivity and risk of tumor dissemination (*17*). Most hCCAs are periductal-infiltrating carcinomas, so percutaneous biopsy is less often used to obtain tissue samples. ERCP, PTC, cholangioscopy, and EUS can provide channels for cytological brushing and biopsy (*39*). Due to the high fibrous stromal content of tumors, the cellular yield from brushing is limited, resulting in a low sensitivity for cytological brushing of approximately 30–60% (*39,40*). Therefore, combining cytological brushing with tissue biopsy is recommended to improve diagnostic sensitivity (*37*).

Current ERCP-guided sampling techniques require X-ray assistance. The procedure involves continuous cholangiography to visualize the operational pathway and location, without direct visualization of the biliary tract. Cholangioscopy systems enable transoral direct visualization of the biliary tract, enabling the assessment of biliary strictures and characterization of lesions. Studies have shown that the sensitivity, specificity, and accuracy of cholangioscopy in diagnosing malignant biliary strictures are 86.7-100%, 71.2-95%, and 77.2-95.1%, respectively (*41-43*). The SpyBite biopsy forceps, specifically designed for use with cholangioscopy, can be used to perform targeted biopsies under direct visualization, with a sensitivity of 63.6-86% and a specificity of as high as 100% (*41,43,44*). A study of 16 patients who underwent transabdominal fine-needle aspiration indicated that among six patients with adenocarcinoma confirmed by histological examination, five had peritoneal metastases

during surgery (*38*). When liver transplantation is considered as a treatment option, EUS-FNA/B should be avoided. Therefore, EUS-FNA/B and percutaneous puncture methods for biopsy are not recommended as initial diagnostic approaches for patients with malignant hilar strictures. Intraluminal sampling using multiple techniques (*e.g.*, brushing, biopsy forceps, and biopsy guided by a cholangioscope) during ERCP is preferred (*45*). EUS-FNA/B can be used to obtain biopsies of regional lymphadenopathy or for biopsy of the tumor site when ERCP or PTC-guided biopsies are negative or inconclusive (*13,19*). The optimal sampling method for patients should be selected based on the location and extent of the biliary stricture, the size of the mass, and the skills and experience of the operator, along with the method of biliary drainage and the risk of tumor dissemination.

Recommendation 6:

Given that approximately 15% of resected hilar specimens are benign (such as autoimmune cholangiopathy), histological or cytological confirmation is mandatory before initiating chemoradiotherapy for unresectable hCCA. Preoperative biopsy may not be necessary for resectable hCCA. In cases of unresectable lesions with multiple negative sampling results, the treatment plan should be determined through multidisciplinary team discussion. For potentially resectable hCCA, the decision to perform a biopsy should be made through multidisciplinary team discussion. [Evidence Level: 2+, Recommendation Grade: B]

6.2. Pathological subtypes

Most hCCAs originate from columnar mucinous cholangiocytes or peribiliary glands (*10*). Tumor grading should be based on the least differentiated component within the neoplasm, rather than the proportion of glandular components. According to glandular differentiation, mucin production, mitotic activity, and nuclear features, hCCA can be classified as well-differentiated, moderately differentiated, or poorly differentiated adenocarcinoma. In cases of histological heterogeneity, the worst grade should be reported (*46*). hCCA can also be classified into distinct morphologic subtypes termed by the Liver Cancer Study Group of Japan as periductal infiltrating, mass-forming, intraductal growing, and mixed subtypes. The periductal infiltrating type is the most common and is characterized by irregular thickening of the bile duct (*47*).

6.3. Immunophenotype and molecular features

hCCA shares similar pathological and molecular characteristics with large duct intrahepatic cholangiocarcinoma (iCCA) (*48,49*). Immunohistochemically, hCCA is typically positive for CK7 and CK19. Subtyping markers, including MUC5AC, MUC6, and S100P, are also frequently positive. The molecular landscape of hCCA is characterized by rare IDH mutations and FGFR fusions; a high frequency of KRAS and TP53 mutations, though the KRAS G12C mutation occurs in only about 1% patients, and frequent Her-2 amplification and SMAD4 loss of expression (*10,48,50*). Advances in precision medicine and genetic testing have identified more therapeutic targets. For unresectable or metastatic hCCA, relevant therapeutic targets should be tested for, such as HER2 overexpression or amplification, IDH1/2 mutations, FGFR2 fusions, BRAF V600E mutation, NTRK fusions, RET fusions, KRAS mutations, microsatellite instability (MSI), and PD-L1 expression (*17*).

Recommendation 7:

For patients with unresectable or metastatic hCCA, molecular testing should be conducted based on therapeutic needs, such as identification of HER2 overexpression or amplification, IDH1/2 mutations, FGFR2 fusions, BRAF V600E mutation, NTRK fusions, RET fusions, KRAS mutations, MSI, and PD-L1. [Evidence Level: 2-, Recommendation Grade: 0]

6.4. Key Points in pathological diagnosis

The most common type of hCCA is the periductal infiltrating type. For the periductal infiltrating and intraductal growing types, specimens should be obtained by longitudinal sectioning along the bile duct axis. These specimens should encompass the tumor, the adjacent liver tissue, and the bile duct wall. Measuring the length of the affected bile ducts, the thickness of the wall, and the shortest distance between the tumor and the margin is essential. Sampling should be performed at the junctions between the affected duct walls and the surrounding liver parenchyma, as well as at the ductal margins. For mass-forming hCCA, specimens should be collected following "7-point" baseline sampling (*51*). According to the International Collaboration on Cancer Reporting (ICCR) standards, pathology reports should include detailed descriptions of gross specimens, tumor location and number, size, length and thickness of the affected bile ducts, tumor type, histological grade, extent of local invasion, perineural and vascular invasion, lymph node status, margin status, precancerous lesions, and other associated conditions (*46*).

Recommendation 8:

Standardized pathological sampling should be performed. For the periductal infiltrating and intraductal growing types of hCCA, specimens should be obtained by sectioning along the long axis of the bile duct, including the tumor and adjacent liver tissue. For mass-forming hCCA, "7-point" baseline sampling should be used. Pathology reports should conform to ICCR standards to

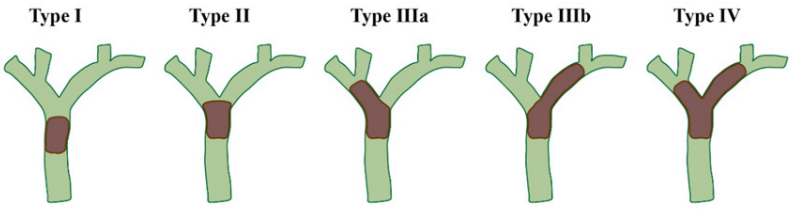

Figure 2. Bismuth-Corlette Classification of hCCA.

improve diagnostic consistency and uniformity. [Evidence Level: 3, Recommendation Grade: GPP]

7. Classification and staging of hCCA

Classification and staging of hCCA are crucial to guiding surgery and predicting prognosis. Currently, three widely used international classification/staging systems are available. However, due to the complex location and infiltrative nature of hCCA, these systems have certain limitations.

7.1. Bismuth-corlette classification

This classification was first proposed by Bismuth *et al*. in 1975 and, after several revisions, evolved into the widely used Bismuth-Corlette classification system in 1992 (Figure 2, Table 4). This classification is based on the location and extent of tumor involvement in the bile duct tree. It is simple and provides significant guidance for surgical planning. Though its efficacy has been proven, its limitation is its inability to predict the presence of distant metastases, lymph nodal and vascular involvement, and consequent lobar atrophy, and subsequently, patient survival (*52*).

Table 4. Bismuth-Corlette Classification of hCCA

Classification	Tumor Characteristics
Type I	Tumor in common hepatic duct
Type II	Tumor with confluence involvement
Type IIIa	Tumor with the confluence and right hepatic duct involvement
Type IIIb	Tumor with the confluence and left hepatic duct involvement
Type IV	Tumor invasion of bilateral intrahepatic secondary bile ducts

7.2. MSKCC staging system

The MSKCC (Memorial Sloan-Kettering Cancer Center) staging system (Table 5) evaluates hCCA based on tumor extent, portal vein invasion, and the presence of liver lobe atrophy. Its main purpose is to evaluate resectability. Since it incorporates two additional evaluation factors, namely portal vein invasion and liver lobe atrophy, it is superior to the Bismuth-Corlette classification in determining resectability. However, MSKCC staging does not take into account factors such as hepatic artery involvement, lymph node status, and distant metastasis, making its assessment less comprehensive (*53*).

7.3. American Joint Committee on Cancer (AJCC)/Union for International Cancer Control (UICC) TNM staging system

The TNM staging system (Table 6) aims to standardize staging with other malignancies. This classification system considers the size of the primary tumor (T), the number of regional lymph node metastases (N), and the size and extent of distant metastases (M). It is currently the most widely used clinical staging system and serves as a standard for evaluating prognosis. However, it primarily relies on pathological histological criteria, which are often difficult to determine preoperatively (*54*).

Recommendation 9:

The three commonly used international classification/staging systems for hCCA each have distinct advantages while also having certain limitations. The Bismuth-Corlette classification focuses on describing the anatomical location of the tumor, incorporating vascular and lymph node involvement to guide surgical planning. MSKCC staging evaluates resectability. The AJCC/UICC TNM staging system serves to guide postoperative treatment and assess prognosis. [Evidence Level: 3, Recommendation Grade: GPP]

8. Multidisciplinary treatment (MDT)

hCCA demonstrates aggressive biological behavior. It is frequently diagnosed in advanced stages and has a dismal prognosis. Patients are categorized into those with resectable, potentially resectable, or unresectable hCCA. For early-stage hCCA, surgery is preferred, aiming for an R0 resection. Potentially resectable hCCA cases where an R0 resection cannot be ensured have the following imaging features: (1) metastatic lymph nodes in the hepatoduodenal ligament or retroperitoneum; (2) involvement of the portal vein and/or hepatic artery, hepatic vein, or inferior vena cava, requiring vascular resection. For advanced or late-stage unresectable

Table 5. MSKCC staging system for hCCA

Classification	Tumor Characteristics
T1	Tumor involving biliary confluence +/- Unilateral extension to secondary bile duct root.
T2	Tumor involving biliary confluence +/- Unilateral extension to secondary bile duct root and ipsilateral portal vein involvement +/- ipsilateral liver lobe atrophy.
T3	Tumor involving biliary confluence + Bilateral extension to secondary bile duct roots/unilateral extension to secondary bile duct root and contralateral portal vein/unilateral extension to secondary bile duct root with contralateral hepatic lobe atrophy; Main portal vein or bilateral portal vein involvement.

Table 6. AJCC 8th TNM staging system for hCCA

Primary tumor (T)	Tx: The primary tumor cannot be evaluated. T0: No evidence of primary tumor. Tis: Carcinoma in situ. T1: Limited to bile ducts, reaching muscularis or fibrous tissue. T2a: Beyond the bile duct wall to the surrounding adipose tissue. T2b: Invasion of adjacent liver parenchyma. T3: Invasion of one branch of the portal vein or hepatic artery. T4: Invasion of the main portal vein or its bilateral branches, or common hepatic artery; or tumor invasion of one secondary bile duct into the contralateral portal vein or hepatic artery
Regional lymph nodes (N)	Nx: Regional lymph nodes cannot be determined. N0: No regional lymph node metastasis. N1: 1–3 regional lymph nodes involved. (Regional lymph nodes are defined as those distributed along the hepatic hilum, cystic duct, common bile duct, hepatic artery, portal vein, and posterior to the pancreaticoduodenal region). N2: ≥ 4 regional lymph nodes involved.
Distant metastasis (M)	M0: No distant metastasis. M1: Distant metastasis present (includes non-regional lymph nodes metastasis).
Staging	0 TisN0M0 I T1N0M0 II T2a-2bN0M0 IIIA T3N0M0 IIIB T4N0M0 IIIC any TN1M0 IVA any TN2M0 IVB any T any NM1

hCCA, the mainstay of management is systemic therapy, which includes chemotherapy, targeted therapy, and immunotherapy. These are often combined with localized treatments such as radiotherapy and interventional procedures. Given the limited efficacy of single-treatment modalities, the rational combination and sequential use of multiple therapeutic approaches are required. The MDT-based diagnostic and therapeutic model has become an essential strategy for prolonging survival in patients with complex hCCA. After completing imaging studies, MDT meetings should integrate the patient's medical history, clinical presentation, laboratory results, and imaging results to perform a comprehensive evaluation, determine disease staging, and formulate a rational treatment plan. The MDT expert consensus recommends the participation of specialties such as hepatobiliary surgery, medical oncology, radiology, interventional medicine, gastroenterology, radiotherapy, ultrasound, and pathology (*55*). The goal of MDT is to incorporate the latest advances in various specialties and the comprehensive patient profile, including disease stage, treatment needs, financial capacity, and psychological tolerance, to devise a more scientific, rational, and standardized therapeutic strategy. Additionally, it also supervises treatment implementation, regularly evaluates efficacy, and adjusts the strategy to maximize patient benefits (*56*).

Recommendation 10:

The MDT model has become an important strategy for prolonging survival in hCCA patients. An early MDT approach for complex hCCA cases is recommended to determine disease stage and potential treatment strategies. A rational combination and sequential use of multiple treatments are advised. [Evidence Level: 4, Recommendation Grade: GPP]

9. Surgery for hCCA

Currently, surgery is the only potentially curative treatment for hCCA, with the primary goal of achieving an R0 resection (*57*). However, the rate of non-R0 resections remains high. Adequate preoperative preparation

and standardized surgical planning are essential to accomplishing high-quality curative resections. Enhanced preoperative evaluations, including detailed disease stage and comprehensive assessment of physical condition, are recommended to improve surgical success rates and reduce postoperative complications. Postoperative follow-up should be conducted regularly based on pathological findings and recovery status, with additional therapies used as necessary.

9.1. Preoperative biliary drainage (PBD)

PBD is a critical component of the perioperative management strategy for hCCA patients. Jaundice is known to have detrimental effects on mitochondrial function, diminish immunity, impair intestinal barrier function, and increase the risk of bacterial translocation (*58*). The aim of PBD is to relieve obstructive jaundice, improve liver function, and prepare for curative surgery. Studies have demonstrated that PBD can reduce post-hepatectomy complications and promotes liver regeneration. However, it may also pose risks such as tumor seeding, prolonged hospitalization, morbidities, and infection(*59*). PBD is not recommended for all patients. Instead, it should be selectively considered under specific conditions: (1) presence of cholangitis; (2) preoperative preparation for portal vein embolization (PVE); (3) total serum bilirubin >200 μmol/L; (4) planned extensive hepatectomy with a future liver remnant (FLR) < 40%; (5) planned preoperative neoadjuvant/conversion therapy; and (6) poor physical condition or hepatic/renal insufficiency (*39,58,60-62*).

The associated controversies are the optimum level of bilirubin to be achieved, the duration of the drainage, and methods of drainage. The optimal level of serum bilirubin differs in various studies, with levels of 50 μmol/L and 85 μmol/L being the most common (*4*). The optimal duration of PBD remains unclear because of the risk of drain malfunction, inflammation surrounding the surgical field with subsequent increased anastomotic leaks, and tumor progression in the event of longer waiting times. In previous studies, the waiting period has ranged from 10 to 32 days, with complete normalization typically occurring around 4 to 8 weeks (*63*). There are three main methods of biliary drainage for hCCA: percutaneous transhepatic biliary drainage (PTBD), ERBD, and ENBD. However, no randomized trials have compared them. They all possess distinct advantages and drawbacks. At present, selection of the optimal method of drainage remains a subject of contention. Insufficient data exist to reach a universal consensus. A medical center can determine the method of drainage by performing a comprehensive multidisciplinary evaluation tailored to the patient's specific condition. Prior to decision-making, several key factors need to be taken into account, including the anatomical site of the obstruction, the intended goal of drainage, the availability of equipment at the medical center, the operator's experience and local skills, as well as the patient's preferences.

PBD is recommended in Western countries, and yet the precise method of drainage has yet to be clearly defined (*37*). The guideline suggests that hCCA patients scheduled for extensive hepatectomy should undergo PBD, with ENBD being the first choice and that preoperative serum bilirubin should be less than 50 μmol/L in Japan (*64*). Li *et al*. developed a short-cycle biliary drainage protocol (within 3 to 4 weeks) for performing PTBD on the planned residual liver lobe (*65*). This protocol adopts the criterion that the preoperative total serum bilirubin level of ≤ 85 μmol/L serves as an indication that liver reserve function can endure extensive hepatectomy. Moreover, it places significant emphasis on bile reinfusion. Within a relatively shorter period of drainage, PTBD does not elevate the risk of tumor seeding. This protocol has proven beneficial in shortening the preoperative preparation period and lowering the risk of cholangitis (*66*).

Recommendation 11:

Routine PBD is not recommended. Instead, PBD should be considered under the following specific conditions: (1) presence of cholangitis; (2) preoperative preparation for PVE; (3) total serum bilirubin >200 μmol/L; (4) planned extensive hepatectomy (FLR <40%); (5) planned preoperative neoadjuvant/conversion therapy; (6) poor physical condition or hepatic/renal insufficiency. [Evidence Level: 2+, Recommendation Grade: B]

9.2. PVE

The future liver remnant (FLR) is a critical factor in assessing tumor resectability and the risk of postoperative liver failure. Patients who fail to meet the required FLR threshold face a significantly increased risk of postoperative liver failure and mortality (*67,68*). Generally, an FLR of at least 20% is required for a normal liver, 30% for patients receiving chemotherapy, and 40% for cirrhotic patients (*69*). A study has indicated that the critical threshold of the future liver remnant volume-to-body weight ratio (FLRV/BW) for predicting postoperative complications, mortality, and liver failure is 0.5%. Patients with a FLRV/BW < 0.5% face significantly higher risks of these outcomes (*68*). Methods commonly used to induce FLR hypertrophy include PVE and associating liver partition and portal vein ligation for staged hepatectomy (ALPPS).

PVE achieves FLR hypertrophy by embolizing the portal vein of the liver segment planned for resection, redirecting blood flow. It is indicated for patients with an insufficient FLR for surgery. PVE reduces surgical risks and provides an opportunity for patients with an insufficient FLR to undergo surgery, making it an effective preoperative strategy (*70,71*). PVE enables

the planned residual liver lobe to pre-adapt to the hemodynamic alterations in blood supply before surgery. By doing so, it mitigates the risk of liver failure caused by the sudden changes in portal venous blood supply and pressure within the residual liver lobe following extensive hepatectomy. A clinical study conducted in the Netherlands revealed that three weeks after PVE, the FLR not only grew, but liver function was also markedly enhanced. Moreover, the rate at which liver function improved exceeded the rate of the increase in liver volume (*72*). In healthy livers, FLR growth can typically be observed within 2 to 4 weeks following PVE. A study has indicated that the FLR increases by an average of 8% to 27% after PVE treatment (*73*). ALPPS can induce FLR hypertrophy. Nevertheless, complications such as postoperative infections and bleeding caused by the first-stage operation, as well as the impact of the second operation within a short period of time, lead to a persistently high incidence of complications and a high mortality rate among patients (*74,75*). In a case-control analysis of an international ALPPS registry, the mortality rate in the ALPPS group was twice that of the matched patients who received standard hepatectomy (48% *vs.* 24%) (*58*). Therefore, PVE can be regarded as the preferred approach for FLR hypertrophy.

There is no definitive criterion for when preoperative PVE is indicated for hCCA. The guideline recommends PVE for cases where the planned hepatectomy volume/liver total volume ratio is ≥50%–60% in Japan (*64*). The early expert consensus on hCCA in China suggests that PVE should be performed for patients undergoing extended hepatectomy (≥ 5 liver segments) (*76*). The consensus also recommends performing biliary drainage first to reduce serum total bilirubin levels below 85 μmol/L before proceeding with PVE.

<u>Recommendation 12:</u>

PVE is recommended for patients with anticipated FLR <30% before major liver resection, along with indocyanine green clearance (ICG) testing. FLR should be re-evaluated 2–4 weeks after PVE to enhance the likelihood of safe resection. [Evidence Level: 1-, Recommendation Grade: A]

9.3. Definition of radical resection

Radical resection of hCCA is defined as a pathologically negative margin (pR0) for all surgical specimens, including the bile duct, adjacent liver tissue, blood vessels, and soft tissues. Therefore, evaluating whether radical resection is achieved should not only rely on tumor-free bile duct margins but also include comprehensive dissection of soft tissue from the hepatoduodenal ligament to the hepatic hilum, achieving skeletonization of the portal vein and hepatic artery. Pathological analysis of surgical specimens must follow standardized sampling and processing protocols to enhance diagnostic accuracy (*77*).

ICCR recommends defining an R0 resection as having no cancer cell infiltration within 1 mm of the surgical margin, although evidence regarding its prognostic significance remains limited (*46*). Unlike most intrahepatic tumors with well-defined margins, accurately determining the tumor margins with the naked eye is sometimes difficult due to the growth characteristics of hCCA. Therefore, performing rapid intraoperative pathology to ascertain the nature of the bile duct resection margin is of great importance (*78*). A Japanese study found no significant difference in disease-free or overall survival (OS) between patients whose initial pR1 bile duct margins were converted to pR0 through re-resection and those whose margins remained pR1, both faring worse than patients with primary pR0 margins. Negative bile duct margins (pR0) should be achieved in a single attempt whenever possible (*79*). According to the literature, patients with an R1 resection have better survival than those with an R2 resection or those who are deemed inoperable. Therefore, palliative resection is recommended over conservative treatment for hCCA cases where an R1 resection is achievable (*80-82*).

<u>Recommendation 13:</u>

Maintaining the integrity of bile duct tumor resection is crucial for prognosis. Achieving negative margins (pR0) in a single attempt is recommended. According to the literature, an R1 resection offers better survival than an R2 resection or inoperability. For hCCA cases where an R1 resection is achievable, palliative resection is recommended over conservative management. [Evidence Level: 2+, Recommendation Grade: B]

9.4. Extent of hepatectomy

hCCA often presents with occult symptoms, and most cases are diagnosed in an advanced stage, requiring extended hemihepatectomy for curative surgery (*29*). The goal of surgery is an R0 resection, while preserving a sufficient FLR is a crucial preoperative consideration. Surgical approaches for Bismuth-Corlette type I and II hCCA are a subject of debate, particularly regarding whether to perform simple extrahepatic bile duct resection or to combine it with hepatic resection (*83*). Currently, the mainstream view holds that for Bismuth-Corlette type I and II tumors without vascular invasion, bile duct tumor resection with regional lymphadenectomy is sufficient for patients with Bismuth–Corlette type I and that it should be combined with caudate lobectomy for patients with Bismuth–Corlette type II. The rationale behind caudate lobe resection is that its duct drains near the hepatic confluence, which increases the risk of tumor involvement. Ruling out tumor involvement of the caudate lobe bile duct branch based solely on non-dilated imaging findings is difficult, and its resection improves

the rate of an R0 resection (*4,21,65,66,76*).

For Bismuth type III and IV hCCA, surgical strategies involve hemihepatectomy, central hepatectomy, or more extensive liver resection. For Bismuth IIIa hCCA, right hemihepatectomy combined with caudate lobe resection is recommended. For Bismuth IIIb hCCA, left hemihepatectomy combined with caudate lobe resection is advised (*4,13*). Bismuth type IV hCCA was once considered unresectable; however, recent advances allow curative resection in some patients through extended hemihepatectomy or trisegmentectomy combined with caudate lobe resection and vascular reconstruction (*84,85*). For type IV hCCA where the tumor on the right side spreads to the left side and invades the root of the bile duct of the left medial segment (S4), extended right trisegmentectomy combined with caudate lobe resection can be performed. For type IV hCCA where the tumor on the left side invades the right and involves the root of the bile duct of the right anterior lobe, extended left trisegmentectomy combined with caudate lobe resection can be performed.

For centrally located tumors, both extended right and left hepatectomy are viable treatments. The literature suggests similar survival and recurrence rates for both approaches; however, surgeons tend to prefer right hepatectomy due to various anatomical considerations, like the longer extrahepatic course of the left duct, the right-sided lie of the bile duct confluence, the right hepatic artery running behind the common duct with the risk of tumor involvement, and anatomical variations being more likely on the right side, which may preclude a safe left hepatectomy. Right-sided resections have a higher incidence of posthepatectomy liver failure in comparison to the left-sided resections. However, the 5-year survival and recurrence free survival were similar in both groups (*4,86,87*). In addition, in long-term clinical practice the Consensus Committee has found that after right hemihepatectomy combined with caudate lobe resection, the remaining left liver may grow, with the liver hilum rotating towards the right. This can lead to compression of the biliary-enteric anastomosis and impaired drainage, thereby increasing the risk of cholangitis and biliary calculi in the remnant liver. Moreover, for Bismuth-Corlette type III and IV cases where extensive hepatectomy cannot be tolerated, surgical plans such as tumor resection combined with segment S4b and S5 resection or combined resection of the central liver lobes (segments S4, 5, 8, 1, 9, or segments S4, 1, 9) can be used for radical treatment and to achieve damage control.

<u>*Recommendation 14*</u>:

Individualized surgical plans should be based on the patient's condition. The goal is to achieve an R0 resection, and preserving a sufficient functional FLR is essential. Definitively excluding tumor invasion of the caudate lobe bile ducts is challenging based solely on imaging findings that show no evidence of bile duct dilation. For Bismuth type I cases without vascular invasion, tumor and extrahepatic bile duct resection with regional lymphadenectomy is recommended. For type II cases, caudate lobe resection should be added. Type III and IV hCCA necessitate hemihepatectomy, central lobectomy, or more extensive resection. [Evidence Level: 2+, Recommendation Grade: B]

9.5. Combined vascular resection and reconstruction

The liver's unique vascular anatomy, characterized by the bile duct, artery, and portal vein being encapsulated within Glisson's capsule, combined with axial spread and radial infiltration, makes vascular involvement a common feature in hCCA. Specifically, the right hepatic artery, which traverses behind the common hepatic duct and lies close to the origin of the right hepatic duct, is more susceptible to tumor invasion than the left hepatic artery.

Recent literature, consensus, and clinical guidelines agree on the clinical value of combined segmental portal vein resection and reconstruction for hCCA with portal vein involvement. The widely accepted view is that segmental portal vein resection and reconstruction do not increase postoperative complications. Instead, they improve the rate of an R0 resection and OS (*4,21,65,88*). The length of portal vein resection depends on the extent of tumor invasion, and the complexity of reconstruction is determined by its location. Therefore, a sufficient portal vein length after right liver resection allows for simple resection, repair, or anastomosis, whereas left liver resection often necessitates more complex techniques such as patching or vein grafting for reconstruction. Additionally, whether there are any variations in the bifurcation of the portal vein needs to be determined (*89*).

Combined hepatic artery resection also increases the rate of an R0 resection and benefits some previously inoperable patients but provides significantly less prognostic improvement compared to portal vein resection and reconstruction. Hepatic artery reconstruction is technically challenging, with low long-term patency rates and a high incidence of complications such as bleeding, thrombosis, and aneurysm, as well as increased mortality. These factors limit its widespread clinical acceptance (*72,90*). When imaging studies show tumor invasion of the hepatic artery, the morphological characteristics of the hepatic arterial system should be carefully analyzed preoperatively, and different surgical plans should be weighed. The key considerations are as follows: (1) whether the remaining liver can retain the blood supply from branches of the hepatic artery or phrenic artery, (2) whether high-quality arterial reconstruction can be performed in the remaining liver (including the use of the uninvolved hepatic artery on the affected side, the gastroduodenal artery, or the splenic artery), (3) if imaging suggests tumor invasion of bilateral

hepatic artery branches or the proper hepatic artery, mobilization of the remaining liver needs to be avoided and the vascular branches within the perihilar ligaments need to be protected, (4) if arterial reconstruction cannot be carried out after resection of the invaded artery, the potential for liver abscess after surgery needs to be monitored and preventive measures need to be taken as early as possible, (5) if the tumor is found to only invade the arterial sheath without penetrating the adventitia, intrasheath dissection and tumor stripping along the plane of the adventitia can be performed, and (6) the risk of intrasheath dissection lies in the potential for excessive traction, which may injure the arterial intima, leading to the formation of postoperative pseudoaneurysms and bleeding. This procedure should be performed with caution in elderly patients or those with atherosclerosis (*72*).

Recommendation 15:

Portal vein resection enables a better R0 resection with improved OS and acceptable complications. It should be considered for patients with portal vein invasion. The role of hepatic artery resection is controversial. It is associated with high morbidity and mortality and should be performed in selected patients at experienced centers. [Evidence Level: 2+, Recommendation Grade: B]

9.6. Lymph node dissection

According to Kitagawa *et al*., the most commonly involved lymph nodes in hCCA are around the common bile duct (42.7%), followed by those around the portal vein (30.9%), the hepatic artery (27.3%), and the posterior pancreaticoduodenal nodes (14.5%) (*91*). The 8th edition of the TNM staging system removed recommendations on the total number of lymph nodes for dissection and did not define the extent of lymphadenectomy for hCCA. It only recommends dissecting at least six lymph nodes to accurately assess lymph node metastasis. Regional lymph nodes are defined as those located along the hepatic hilum, cystic duct, common bile duct, hepatic artery, posterior pancreaticoduodenal region, and portal vein, while positive nodes outside these areas are classified as M1 disease (*72*). pN0 is defined as no metastasis in regional lymph nodes. Cases with negative regional nodes but fewer than six examined are still classified as pN0. pN1 is defined as 1-3 regional lymph node metastases. pN2 is defined as ≥ 4 regional lymph node metastases (*54*). The JSBS staging system specifies that lymphadenectomy for hCCA should include lymph nodes in the hepatoduodenal ligament (Station 12), around the hepatic artery (Station 8), and posterior-superior pancreatic head nodes (Station 13a), without specifying the number of nodes to dissect (*92*).

Radical resection begins with the clearance of Station 8 lymph nodes. It involves carefully exposing and suspending the common hepatic artery and then dissecting to the left, to the right, and upward. This approach facilitates the en bloc resection of the specimen. Subsequently, Station 9, 12, and 13a lymph nodes should be cleared. If no enlarged lymph nodes are found, the extent of dissection should not be expanded to stations 16 and13b.

Recommendation 16:

Standard lymphadenectomy for hCCA should include lymph nodes within the hepatoduodenal ligament (Station 12), those along the hepatic artery (Station 8), and posterior-superior pancreaticoduodenal nodes (Station 13a). Dissecting Station 9 facilitates en bloc resection. If no enlarged nodes are found, dissection should not be extended to stations 16 and 13b. [Evidence Level: 2+, Recommendation Grade: B]

9.7. Liver transplantation

The Mayo Clinic proposed a liver transplantation protocol following neoadjuvant chemoradiotherapy. Diagnosis of hCCA had to be established with brush cytology or biopsy or with CA19-9 greater than 100 ng/mL in the presence of a radiographically malignant stricture in the absence of cholangitis. In addition, the tumor had to be deemed unresectable by experienced hepatobiliary surgeons in the absence of PSC. Patients with PSC are eligible even if the tumor is resectable. The size of the tumor must be less than 3 cm. Patients with intrahepatic metastases, evidence of extrahepatic disease (including lymph nodal metastases), uncontrolled infections, prior surgery, prior radiation/chemotherapy, or percutaneous biopsy are excluded from this protocol. The protocol includes external beam radiation therapy (a dose of 45Gy in 30 fractions) with 5-fluorouracil (5-FU) administered during the first three days of radiation. Two to three weeks after external beam radiation, brachytherapy with Ir-192 (a dose of 20–30Gy) is initiated. Concurrently, a continuous infusion of 5-FU is maintained until the liver transplantation procedure. Capecitabine may be administered during the waiting period. All patients underwent staged laparotomy before liver transplantation. Preliminary results from 11 patients were published in 2000, showing promising outcomes. The final study results, published in 2005, reported a 5-year survival rate of 82% (*93-95*). Subsequently, multicenter clinical studies were initiated in line with the Mayo criteria.

Numerous studies have demonstrated that neoadjuvant chemoradiotherapy followed by liver transplantation can offer long-term survival for carefully selected patients with unresectable hCCA, and particularly those with PSC-related hCCA (*96,97*). For patients with resectable hCCA, whether they can benefit from liver transplantation remains a question. A study by Croome *et al*. suggested that radical surgical resection remains the recommended approach for resectable hCCA patients,

as there is currently no high-level evidence supporting the superiority of liver transplantation over surgical resection (*98*). Additionally, the scarcity of donor organs and the complexity of liver transplantation techniques must be considered. Currently, radical resection surgery remains the standard treatment for hCCA according to major guidelines. Most guidelines advise participation in clinical trials or, in strictly selected patients with chronic liver diseases such as PSC, consideration of liver transplantation (*17,19,39*). As the "ultimate weapon" for treating end-stage liver disease, liver transplantation can not only achieve an R0 resection of the tumor but also restore liver function in carefully selected hCCA patients with PSC.

Recommendation 17:

Due to the scarcity of donor organs and the lack of PSC background in most domestic patients, a radical cure can be achieved in the majority of patients meeting the Mayo transplant criteria through surgical resection. Liver transplantation should only be considered for those who are no longer able to undergo surgery and who exhibit no lymph node or distant metastasis. [Evidence Level: 2+, Recommendation Grade: B]

9.8. Minimally invasive techniques

Laparoscopic techniques were initially used in hCCA for intraoperative exploration and tumor staging (*99, 100*). Laparoscopic exploration for hCCA should begin with a thorough examination of the liver, peritoneum, and lymph nodes outside the hepatic hilum to determine the feasibility of regional resection. If Station 16 lymph nodes are enlarged, intraoperative rapid pathology should be performed, and positive biopsy results should lead to abandoning radical surgery in favor of systemic therapy.

Laparoscopic techniques have gradually been used for radical hCCA surgery. A 2020 systematic review that examined the state of laparoscopic radical surgery for hCCA in China included 13 studies and 189 patients. Results indicated that the average operating time was 354 minutes, the average intraoperative blood loss was 324 milliliters, the rate of an R0 resection was 95.2%, the average number of lymph nodes dissected was 9.5, the conversion rate to open surgery was 2.6%, the complication rate was 21.2%, and the 1-year OS rate for patients was 84.5% (*101*). A 2023 multicenter real-world study by Chinese researchers compared the efficacy of laparoscopic and open surgery for hCCA and revealed equivalent short-term and long-term outcomes (*102*). According to the expert consensus, laparoscopic radical resection of hCCA is indicated for patients with Bismuth-Corlette type I and II hCCA, as well as selected cases of Bismuth-Corlette type III and IV hCCA without vascular invasion (*103*). Vascular invasion in the hepatic hilum significantly increases the technical difficulty of laparoscopic surgery due to the limited operative space and complexity of the procedure. Although laparoscopic hepatic artery resection and reconstruction has been reported, the procedure is technically challenging, so it is not recommended routinely (*104*). Portal vein invasion is relatively easier to resect and reconstruct, with some experienced hepatobiliary surgical centers reporting successful cases. Robotic surgery is an emerging minimally invasive approach for radical hCCA treatment, but current studies, both domestic and international, are mostly case reports lacking an analysis of large samples.

Due to the anatomical complexity and biological characteristics of hCCA, radical surgery typically involves combined liver segment and caudate lobe resection, biliary-enteric anastomosis, regional lymph node dissection, and vascular resection and reconstruction. Both laparoscopic and robotic surgeries present significant technical challenges and require advanced surgical skills. Currently, most of the relevant studies are limited to case reports and small-sample studies (*105,106*). Minimally invasive laparoscopic surgery is a promising field, but further RCTs are needed to prove its advantages over traditional open surgery and to develop standardized surgical procedures. Therefore, laparoscopic and robotic radical resection for hCCA should be performed at experienced hepatobiliary surgery centers with extensive expertise in minimally invasive procedures, and only after careful selection of suitable hCCA patients.

Recommendation 18:

For patients with hCCA who are preparing to undergo surgery, undergoing laparoscopic exploration first is recommended to determine the feasibility of radical resection. Laparoscopic and robotic radical resection of hCCA is recommended at hepatobiliary surgery centers with extensive experience in minimally invasive surgery and for carefully selected hCCA cases. [Evidence Level: 2++, Recommendation Grade: A]

10. Local treatment

10.1. Biliary drainage

The majority of hCCA cases also involve malignant obstructive jaundice. In recent years, the benefits of PBD have been increasingly recognized. For palliative care patients, biliary drainage not only allows them to benefit from systemic treatment but also aids in the prevention and treatment of cholangitis, thereby relieving symptoms. The most frequently used techniques are PTBD and ERCP.

There remains controversy over whether PTBD or ERCP should be the preferred method of biliary drainage (*107*). Advantages of PTBD include precise catheter placement to maximize bile drainage, quicker achievement of a satisfactory reduction in bilirubin compared to ERCP, and a lower risk of biliary infection. However, PTBD is invasive and may increase the risk of

tumor seeding and dissemination (*108,109*). Prolonged PTBD exceeding 60 days is an independent risk factor for tumor dissemination and reduced postoperative survival (*110*). ERCP, in contrast, is less invasive but more technically challenging, with a potential for higher rates of biliary infection. Chinese researchers tend to favor PTBD, whereas Japanese researchers lean towards ERCP (*64,65*). The British Society of Gastroenterology guidelines for cholangiocarcinoma recommend selecting methods of drainage based on specific conditions. For instance, ERCP is preferred for patients requiring biopsy or brush cytology, whereas PTBD is more suitable for complex hCCA cases, such as Bismuth type IV, where ERCP has a high failure rate (*39*).

Recently, EUS-guided biliary drainage (EUS-BD) has garnered increasing attention in clinical practice. Given its technical complexity, EUS-BD requires highly skilled operators, and further research is needed to confirm its clinical efficacy and long-term prognosis. EUS-BD may be used for patients where ERCP fails. EUS-BD combined with hepatogastrostomy can be a valuable option for patients with an unresectable malignant hilar bile duct obstruction and left hepatic duct dilatation, when ERCP and/or PTBD are inadequate (*111*). The choice of optimal biliary drainage for hCCA patients should follow an individualized approach, taking into account the anatomical location of the obstruction, the goals of drainage, the availability of equipment, the operator's skill level, and the patient's status.

10.2. Endoscopic biliary stent placement

The primary debates regarding stent placement for malignant hilar biliary obstruction concern the type of stent (plastic *vs.* metal) and the extent of drainage (unilateral *vs.* bilateral). A plastic stent (PS) is easy to replace and does not interfere with other therapeutic efforts, such as local ablation or surgery. Thus, a PS is recommended for PBD. However, due to its smaller diameter, a PS has a higher failure rate and requires frequent replacement, potentially reducing quality of life and increasing costs. A self-expandable metal stent (SEMS), with its larger diameter, provides longer patency and is easier to pass through stenotic segments (*112*). Studies comparing SEMSes and PSes have indicated that SEMSes result in higher technical and clinical success rates, less need for re-intervention, and greater cost-effectiveness due to extended stent patency (*113,114*). Therefore, SEMSes are mainly used for palliative biliary drainage. For hCCA with a predicted survival of <3 months, a PS or an uncovered SEMS is recommended. For those with a predicted survival > 3 months, an SEMS is preferred over a PS (*27*). If the future treatment strategy is uncertain, SEMS insertion should be avoided (*115*).

There is no consensus yet regarding unilateral versus bilateral stents. Increasingly, experts believe that the goal of stent placement for hilar strictures is to drain >50% of the liver volume. When a single stent cannot achieve this, bilateral drainage should be considered for better clinical outcomes (*45*).

Recommendation 19:

For PBD, use of a PS is recommended. An SEMS is primarily for palliative biliary drainage. For hCCA with a predicted survival of <3 months, a PS or an uncovered SEMS is recommended. For hCCA with a predicted survival of >3 months, an SEMS is preferred over a PS. If the treatment strategy remains uncertain, SEMS insertion should be avoided. For patients with hilar stricture, the goal of stent placement should be to drain >50% of the liver volume. [Evidence Level: 2+, Recommendation Grade: B]

10.3. Intraluminal therapy

Most patients with unresectable hCCA experience malignant obstructive jaundice requiring biliary drainage. Biliary stenting improves quality of life, and intraluminal therapies can be used concurrently with drainage. Research has indicated that combining chemotherapy with intraluminal therapy improves survival and quality of life in unresectable hCCA by controlling local tumor growth and extending stent patency (*116-118*). Intraluminal therapeutic techniques include radiofrequency ablation (RFA), photodynamic therapy (PDT), and intraluminal brachytherapy (ILBT).

Intraluminal RFA:RFA uses high-frequency electric currents to generate heat, causing cellular dehydration, coagulation, and necrosis, ultimately killing tumor cells (*112*). RFA is primarily used for palliative treatment of unresectable hCCA, improving survival and quality of life compared to stenting alone (*119*). Two small-scale studies indicated that combining RFA with stents extended patient survival and stent patency compared to stenting alone, without increasing adverse event rates (*120,121*). Moreover, RFA combined with systemic chemotherapy improved efficacy in treating unresectable hCCA, further prolonging survival (*122,123*). For patients with malignant biliary obstruction, stent occlusion and tumor regrowth are major concerns. Intraluminal RFA can help unclog stents blocked by tumor growth, and combining RFA with stents may enhance stent patency rates (*119,124*).

PDT: PDT uses photosensitizers that selectively accumulate in proliferating tumor cells and that are cytotoxic when subjected to specific laser wavelengths. PDT is minimally invasive, precise, and repeatable, making it suitable for palliative treatment of unresectable hCCA (*125*). A 2022 meta-analysis indicated that PDT combined with biliary stents improved survival in patients with unresectable hCCA without increasing adverse events (*126*). PDT also extended stent patency (*127*). Studies have shown that PDT and chemotherapy

have a synergistic effect; they are often administered sequentially, with PDT preceding chemotherapy (*117,118,128*). PDT can be repeated at approximately three-month intervals (*129*). Some studies are currently exploring the potential of PDT as a neoadjuvant therapy for hCCA, with ongoing clinical trials such as NCT04824742 investigating its efficacy and safety. Due to its minimally invasive and precise nature, PDT holds significant promise as a palliative treatment option for hCCA.

ILBT: ILBT offers the advantages of a small radiation radius, long half-life, sustained tumor cell killing, and minimal damage to adjacent tissues (*130*). A meta-analysis of 981 patients with malignant biliary obstruction found that ILBT combined with stenting reduced the risk of stent obstruction, improved survival, and did not increase complications compared to stenting alone (*131*). However, the clinical use of ILBT is limited due to its complexity, challenges managing radioactive materials, and potential late complications such as duodenal stricture and gastrointestinal bleeding (*130*). Recent advances include biliary stents combined with iodine-125 seeds. A study has indicated that such combinations extend stent patency and improve survival (*132*). A small-scale retrospective study conducted at the Sun Yat-sen University Cancer Center reported encouraging outcomes for patients treated with stents and iodine-125 seeds, followed by systemic therapies such as lenvatinib and PD-1 inhibitors. Results indicated a median survival of 6.1 months, with significant bilirubin reduction within four weeks. ILBT remains a palliative option for patients with advanced disease, with potential for further clinical exploration and research.

Recommendation 20:

Intraluminal therapies (RFA, PDT, and ILBT) currently lack high-quality clinical evidence. Therefore, they are not recommended as standard first-line palliative treatments for hCCA. Discussions of MDT should carefully evaluate potential benefits and risks before administering these therapies. [Evidence Level: 2-, Recommendation Grade: 0]

10.4. Radiotherapy

Neoadjuvant radiotherapy: The clinical value of neoadjuvant radiotherapy for hCCA remains under evaluation, and participation in clinical trials is encouraged. Small-scale studies suggest that preoperative radiotherapy may increase resectability, reduce recurrence, and potentially improve survival rates (*133,134*). The Mayo Clinic's neoadjuvant chemoradiotherapy protocol serves as a bridge for liver transplantation. This protocol includes external beam radiation therapy (45Gy/30 fractions) followed by brachytherapy with iridium-192 (20-30Gy) administered 2-3 weeks later (*95*).

Adjuvant radiotherapy: The data supporting adjuvant radiotherapy or chemoradiotherapy are limited and mostly come from retrospective studies. Postoperative recurrence rates for hCCA are high (60-70%), indicating that surgery alone provides limited improvement in prognosis (*135*). SWOG S0809, a phase II single-arm trial, enrolled 79 patients with extrahepatic cholangiocarcinoma and gallbladder cancer (38 with hCCA) who underwent curative resection. Eligible patients (T2-T4, N1, or positive margins) received four cycles of gemcitabine-capecitabine followed by chemoradiotherapy (45Gy for regional lymph nodes; 54-59.4Gy for the tumor bed) with capecitabine as a sensitizer. The study's primary endpoint (2-year survival > 45%) was achieved, with a 2-year survival rate of 65% and median overall survival (mOS) of 35 months (*136*). Further analysis indicated that patients with nodal involvement (N1) had a 2-year disease-free survival (DFS) rate of 49.8%, better than the historical control of 29.7%. However, high rates of distant failure (42.2%) persisted among these patients (*136,137*). A meta-analysis of 21 retrospective studies, encompassing over 1,400 patients with extrahepatic cholangiocarcinoma and gallbladder cancer, demonstrated that adjuvant radiotherapy improved 5-year OS, and especially in patients with nodal positivity or an R1 resection. Local recurrence rates were reduced, although distant metastasis rates were unchanged (*138*). Another meta-analysis included 21 studies with 6,712 patients with cholangiocarcinoma and gallbladder cancer. Results indicated that adjuvant therapy provided the greatest benefit in patients with lymph node positivity (OR = 0.49, $p = 0.004$) and an R1 resection (OR = 0.36, $p = 0.002$) (*139*). ASCO, ESMO, NCCN, and CSCO guidelines all recommend adjuvant radiotherapy for R1-resected hCCA (*17,19,62,140*). Patients with an R0 resection and nodal involvement may also benefit from adjuvant radiotherapy, which is a level II recommendation in the CSCO guidelines (*62*). The management of patients with an R2 resection is the same as that for those with unresectable hCCA. Currently, a phase III prospective randomized trial is ongoing (NCT02798510), and its results are highly anticipated.

Palliative radiotherapy: For unresectable locally advanced hCCA, clinical trial participation is encouraged. Small-sample retrospective studies suggest that chemoradiotherapy improves survival and local control rates compared to chemotherapy alone in patients with good performance status. A study of 2,996 patients with unresectable extrahepatic cholangiocarcinoma by the National Cancer Database in the United States found that, compared to the group receiving chemotherapy alone, the mOS of patients in the chemoradiotherapy group was extended from 12.6 months to 14.5 months ($p < 0.001$) (*141*). The optimal radiation dose remains uncertain, with standard recommendations around 45-50 Gy within five weeks. An increased dose may improve local control but is limited by the proximity of the

hCCA to radiation-sensitive organs like the duodenum (*64*). Several small-scale studies have indicated that metal stent placement combined with palliative external radiotherapy and/or brachytherapy may improve local tumor control, extend stent patency, and prolong survival (*142,143*). In cases of distant metastases, and particularly those involving bone or brain, palliative radiotherapy may be considered to relieve symptoms.

Recommendation 21:

Neoadjuvant chemoradiotherapy plays a pivotal role in the management of patients awaiting liver transplantation. For resectable hCCA, however, the current evidence base is limited by the absence of randomized phase III trials. Thus, eligible patients are advised to participate in clinical trials. For unresectable locally advanced hCCA, chemoradiotherapy may be considered for patients with good performance status. [Evidence Level: 2++, Recommendation Grade: A]

Recommendation 22:

Postoperative recurrence rates of 60-70% highlight the limited benefit of surgery alone. Patients with R1-resected and R0-resected node-positive hCCA should receive adjuvant chemoradiotherapy. Management of R2-resected hCCA should align with that of unresectable hCCA. [Evidence Level: 2++, Recommendation Grade: A]

11. Systemic treatment

11.1. Adjuvant chemotherapy

The BILCAP phase III multicenter RCT in the UK included 447 patients who underwent radical surgery for cholangiocarcinoma and gallbladder cancer. In the intention-to-treat analysis, the mOS was 51.1 months in the capecitabine group and 36.4 months in the observation group, so there were no significant differences in the mOS ($p = 0.097$). In the prespecified per-protocol analysis, however, the mOS was 53 months for the capecitabine group compared to 36 months for the observation group, so the mOS differed significantly ($p = 0.028$) (*144,145*). Despite limitations in the BILCAP study's results, international guidelines recommend adjuvant capecitabine treatment for six months following radical resection of hCCA as the current standard therapy (*17,19,140*).

The use of adjuvant therapy has been further supported by the Japanese JCOG1202: ASCOT phase III RCT trial, which demonstrated that adjuvant therapy with S1 (tegafur-gimeracil-oteracil, an orally acting fluoropyrimidine) prolonged OS compared to surgery alone. The 3-year OS rates for the S1 group and the observation group were 77.1% and 67.6% respectively ($p = 0.008$) (*146*). Therefore, S1 can also be considered for adjuvant chemotherapy after hCCA surgery. The Asian BCAT trial and the French PRODIGE 12 randomized trial failed to respectively demonstrate that the gemcitabine and GEMOX (gemcitabine-oxaliplatin) regimens improved recurrence-free survival and OS compared to the observation group (*147,148*). The prospective, randomized phase II STAMP study in South Korea enrolled patients with extrahepatic cholangiocarcinoma and positive lymph nodes. Adjuvant therapy with the GC (gemcitabine-cisplatin) regimen was compared to capecitabine. Results indicated that there was no significant improvement in the 2-year DFS rate and the 2-year OS rate (*149*). Other adjuvant chemotherapy regimens, primarily based on gemcitabine or 5-FU, include the GC regimen, gemcitabine-capecitabine, capecitabine-oxaliplatin, 5-FU-oxaliplatin, and 5-FU monotherapy. These primarily come from small-sample or retrospective studies.

11.2. Neoadjuvant chemotherapy

Neoadjuvant chemoradiotherapy plays a pivotal role for hCCA patients scheduled for liver transplantation. However, there is currently a lack of randomized controlled phase III clinical trials to prove the benefits of a neoadjuvant treatment strategy in routine surgical resection. Participation of eligible patients in clinical trials is recommended.

11.3. First-line treatment for unresectable or advanced hCCA

Two-drug combination chemotherapy regimens: The ABC-02 phase III RCT demonstrated that the gemcitabine-cisplatin doublet significantly extended OS in patients with advanced cholangiocarcinoma from 8.1 months (gemcitabine monotherapy) to 11.7 months ($p < 0.001$) (*150*). This established gemcitabine-cisplatin as the first-line treatment for advanced hCCA. The phase III JCOG1113/FUGA-BT non-inferiority study indicated that gemcitabine-S1 achieved an OS of 15.1 months, comparable to gemcitabine-cisplatin (13.4 months), making it an alternative first-line therapy for advanced cholangiocarcinoma (*151*).

Immunotherapy-based chemotherapy regimens: The TOPAZ-1 phase III RCT indicated that durvalumab combined with gemcitabine-cisplatin as first-line therapy for advanced cholangiocarcinoma improved mOS from 11.3 months (gemcitabine-cisplatin alone) to 12.9 months, and median progression-free survival (mPFS) from 5.7 months to 7.2 months (*152*). The KEYNOTE-966 phase III RCT found that pembrolizumab combined with gemcitabine-cisplatin as first-line therapy for advanced cholangiocarcinoma increased mOS from 10.9 months (chemotherapy alone) to 12.7 months, with no significant increase in toxicity (*153*). Therefore, durvalumab or pembrolizumab combined with gemcitabine-cisplatin is recommended as a first-line therapy for advanced cholangiocarcinoma.

Triple-drug chemotherapy regimens: The KHBO1401 phase III RCT in Japan demonstrated that the gemcitabine-cisplatin-S1 combination achieved an OS of 13.5 months, superior to 12.6 months for gemcitabine-cisplatin alone (p = 0.046) (*154*). Thus, for hCCA patients with a good performance status, the gemcitabine-cisplatin-S1 triple regimen can also be considered a first-line therapy.

11.4. Second-line Treatment for Advanced hCCA

Chemotherapy: The ABC-06 phase III study enrolled patients with advanced cholangiocarcinoma that progressed after first-line gemcitabine-cisplatin treatment. Results indicated that the mFOLFOX group had a survival advantage (OS: 6.2 months *vs.* 5.3 months, p = 0.031) over active symptom control (ASC) (*155*). Thus, mFOLFOX is recommended as a second-line treatment regimen for advanced cholangiocarcinoma. The FOLFIRI and irinotecan-capecitabine (XELIRI) regimens have demonstrated favorable survival benefits and tolerability in the second-line treatment of advanced cholangiocarcinoma, making them viable options (*156,157*). The phase IIb NIFTY study revealed that liposomal irinotecan combined with fluorouracil and leucovorin achieved a progression-free survival (PFS) of 7.1 months, compared to 1.4 months for fluorouracil and leucovorin alone in advanced cholangiocarcinoma (*158*). Chemotherapy for hCCA patients primarily involves gemcitabine- or fluorouracil-based regimens. Second-line chemotherapy options may include other unused first-line recommended regimens, according to the individual patient's treatment history, as well as institutional experience.

Targeted therapy and immunotherapy: Patients with advanced or progressive disease should undergo comprehensive genetic testing, including that for HER2 overexpression or amplification, IDH1/2 mutations, FGFR2 fusions, BRAF V600E mutations, NTRK fusions, RET fusions, and microsatellite instability, to guide targeted therapy and immunotherapy (*17,159*). This approach enables personalized treatment strategies based on the molecular profile of the tumor, potentially improving therapeutic outcomes. Ivosidenib for IDH1 mutations and pemigatinib for FGFR2 fusions have been approved for second-line treatment of advanced cholangiocarcinoma. However, IDH mutations and FGFR fusions are rare in hCCA patients. HER2 is a noteworthy target in hCCA patients. The MyPathway study enrolled 39 patients with HER2-positive cholangiocarcinoma, and trastuzumab-pertuzumab achieved an objective response rate (ORR) of 23%, mPFS of 4 months, and mOS of 10.9 months (*160*). The HERB study, a multicenter, single-arm phase II trial, included 30 patients with HER2-positive or low-expression cholangiocarcinoma refractory to gemcitabine, and trastuzumab deruxtecan achieved an ORR of 36.4% and a disease control rate (DCR) of 81.8% (*161,162*). Other therapeutic targets include BRAF V600E mutations, NTRK fusions, and RET fusions. Dabrafenib-trametinib achieved an ORR of 51%, mPFS of 9 months, and mOS of 14 months in patients with advanced cholangiocarcinoma with BRAF V600E mutations (*163*). Pembrolizumab immunotherapy can be considered for patients with MSI-H tumors (*164*). Entrectinib and larotrectinib, inhibitors targeting NTRK fusions, have been approved for treating advanced solid tumors with NTRK fusion positivity. Pralsetinib or selpercatinib may be considered for treatment of RET fusion-positive patients (*17,62*).

There are no precision targets in the majority of hCCA patients. Multi-target drugs such as lenvatinib, anlotinib, and sulfatinib are used in clinical practice. However, high-level clinical evidence for these drugs still needs to be compiled. A single-arm study involving 41 patients with advanced cholangiocarcinoma who underwent at least one systemic therapy reported an ORR of 12%, mPFS of 3.8 months, and mOS of 11.4 months with lenvatinib monotherapy until disease progression (*165*). A real-world study involving 57 patients with advanced cholangiocarcinoma (9 with extrahepatic cholangiocarcinoma) treated with lenvatinib combined with a PD-1/PD-L1 inhibitor and the GEMOX regimen indicated an mPFS of 9.27 months and mOS of 13.4 months (*166*). A phase Ib study of 66 patients with advanced cholangiocarcinoma who failed to respond to first-line treatment reported an ORR of 21.21%, DCR of 72.73%, and mOS and mPFS of 15.77 months and 6.24 months, respectively, using anlotinib combined with benmelstobart (*167*). A phase II study involving 20 patients with advanced cholangiocarcinoma that progressed after first-line chemotherapy indicated an ORR of 30%, DCR of 90%, and mOS and mPFS of 12.3 months and 6.5 months, respectively, with anlotinib and sintilimab (*168*). Another phase II single-arm study of 39 patients with advanced cholangiocarcinoma undergoing second-line therapy reported a 16-week PFS rate of 46.33% with surufatinib (*169*).

Recommendation 23:

(1) After radical resection, capecitabine adjuvant chemotherapy for 6 months is recommended. [Evidence level: 1-, Recommendation grade: A]

(2) First-line treatment: The GC regimen, GS (gemcitabine-S1) regimen, GC combined with durvalumab, or GC combined with pembrolizumab is recommended. [Evidence level: 2++, Recommendation grade: A]. For patients with a good performance status, the three-drug combination regimen (GC plus S1) is recommended as first-line treatment. [Evidence level: 2++, Recommendation grade: A]

(3) Second-line treatment: The FOLFOX regimen is recommended. [Evidence level: 2++, Recommendation grade: A]. Irinotecan-based combination regimens,

such as FOLFIRI or XELIRI, may also be considered. [Evidence level: 2++, Recommendation grade: A]

(4) Molecular analysis is recommended to guide second-line treatment: ① For IDH1 mutations, ivosidenib is recommended; ② For patients positive for FGFR2 fusions, pemigatinib is recommended; ③ For BRAF V600E mutations, the combination of dabrafenib and trametinib is recommended; ④ For patients positive for NTRK fusions, entrectinib or larotrectinib is recommended; ⑤ For HER2 amplification, trastuzumab plus pertuzumab or trastuzumab deruxtecan is recommended; ⑥ For those with MSI-H, pembrolizumab immunotherapy is recommended. [Evidence level: 2+, Recommendation grade: B]

12. Conclusion

hCCA is characterized by high malignancy and presents significant challenges in surgical resection, which contribute to its dismal prognosis. Proactive screening and early diagnosis are crucial to identifying hCCA and improving early detection rates. Selecting appropriate treatment strategies and surgical techniques ensures complete tumor resection while preserving residual liver function and minimizing postoperative complications. Moreover, multidisciplinary comprehensive care, along with standardized local and systemic treatments, allows for full-cycle management of hCCA patients. This holistic approach is pivotal to improving treatment outcomes and overall prognosis.

Acknowledgements

The authors wish to thank the Hepatobiliary Surgery Professional Committee of the Hunan Medical Association, the Hunan Provincial Clinical Research Center for the Prevention and Treatment of Biliary Diseases, the Hunan Provincial Key Laboratory for the Prevention and Treatment of Biliary Diseases, the Hunan Provincial Engineering Research Center for Digital Hepatobiliary Medicine, the Hepatobiliary Surgery Professional Committee of the Hunan International Medical Exchange and Promotion Association, the Hunan Alliance of Hepatobiliary and Pancreatic Surgery, the Hunan Alliance for the Diagnosis and Treatment of Malignant Biliary Tumors, and the Hepatopancreatobiliary Disease Research Center of the Furong Laboratory, as well as multidisciplinary experts from various regions across China, for their invaluable contributions to the reaching of this consensus.

Funding: This work was supported by grants from the Hunan Provincial Science and Technology Innovation Leading Talent Fund (2024RC1051); the Huxiang Young Talent Fund (2024RC3232); the Natural Science Fund for Outstanding Young Scholars of Hunan Province (2024JJ2037); Key Projects Sponsored by the Hunan Provincial People's Hospital Benevolence Fund (KCT202404, RS2022A07); and Projects of the Hunan Provincial Health Commission of China (Z2023031).

Conflict of Interest: The authors have no conflicts of interest to disclose.

References

1. DeOliveira ML, Cunningham SC, Cameron JL, Kamangar F, Winter JM, Lillemoe KD, Choti MA, Yeo CJ, Schulick RD. Cholangiocarcinoma: Thirty-one-year experience with 564 patients at a single institution. Ann Surg. 2007; 245:755-762.
2. Dar FS, Abbas Z, Ahmed I, *et al*. National guidelines for the diagnosis and treatment of hilar cholangiocarcinoma. World J Gastroenterol. 2024; 30:1018-1042.
3. Zhang L, Zhu J, Yang G, Li J. Features of lymph node metastasis and nerve plexus invasion in hilar cholangiocarcinoma and key points for dissection. J Clin Hepatol. 2023; 39:2045-2048. (in Chinese)
4. Jena SS, Mehta NN, Nundy S. Surgical management of hilar cholangiocarcinoma: Controversies and recommendations. Ann Hepatobiliary Pancreat Surg. 2023; 27:227-240.
5. Healthcare Improvement Scotland. Scottish Intercollegiate Guidelines Network (SIGN). *https://www.healthcareimprovementscotland.scot/clinical-guidance-for-professionals/scottish-intercollegiate-guidelines-network-sign* (accessed July 23, 2025)
6. Sarcognato S, Sacchi D, Fassan M, Fabris L, Cadamuro M, Zanus G, Cataldo I, Capelli P, Baciorri F, Cacciatore M, Guido M. Cholangiocarcinoma. Pathologica. 2021; 113:158-169.
7. Pascale A, Rosmorduc O, Duclos-Vallee JC. New epidemiologic trends in cholangiocarcinoma. Clin Res Hepatol Gastroenterol. 2023; 47:102223.
8. Qurashi M, Vithayathil M, Khan SA. Epidemiology of cholangiocarcinoma. Eur J Surg Oncol. 2023; 107064.
9. Clements O, Eliahoo J, Kim JU, Taylor-Robinson SD, Khan SA. Risk factors for intrahepatic and extrahepatic cholangiocarcinoma: A systematic review and meta-analysis. J Hepatol. 2020; 72:95-103.
10. Banales JM, Marin JJG, Lamarca A, *et al*. Cholangiocarcinoma 2020: The next horizon in mechanisms and management. Nat Rev Gastroenterol Hepatol. 2020; 17:557-588.
11. Blechacz B, Komuta M, Roskams T, Gores GJ. Clinical diagnosis and staging of cholangiocarcinoma. Nat Rev Gastroenterol Hepatol. 2011; 8:512-522.
12. Valle JW, Kelley RK, Nervi B, Oh DY, Zhu AX. Biliary tract cancer. Lancet. 2021; 397:428-444.
13. Dondossola D, Ghidini M, Grossi F, Rossi G, Foschi D. Practical review for diagnosis and clinical management of perihilar cholangiocarcinoma. World J Gastroenterol. 2020; 26:3542-3561.
14. Malik AK, Davidson BR, Manas DM. Surgical management, including the role of transplantation, for intrahepatic and peri-hilar cholangiocarcinoma. Eur J Surg Oncol. 2025; 51:108248.
15. Lee JW, Lee JH, Park Y, Kwon J, Lee W, Song KB, Hwang DW, Kim SC. Prognostic impact of perioperative CA19-9 levels in patients with resected perihilar cholangiocarcinoma. J Clin Med. 2021; 10.

16. Wang JK, Hu HJ, Shrestha A, Ma WJ, Yang Q, Liu F, Cheng NS, Li FY. Can preoperative and postoperative CA19-9 levels predict survival and early recurrence in patients with resectable hilar cholangiocarcinoma? Oncotarget. 2017; 8:45335-45344.
17. Benson AB, D'Angelica MI, Abrams T, *et al*. NCCN Guidelines: Biliary Tract Cancers, Version 3. 2023.
18. Roos E, Hubers LM, Coelen RJS, Doorenspleet ME, de Vries N, Verheij J, Beuers U, van Gulik TM. IgG4-associated cholangitis in patients resected for presumed perihilar cholangiocarcinoma: A 30-year tertiary care experience. Am J Gastroenterol. 2018; 113:765-772.
19. Vogel A, Bridgewater J, Edeline J, Kelley RK, Klumpen HJ, Malka D, Primrose JN, Rimassa L, Stenzinger A, Valle JW, Ducreux M, clinicalguidelines@esmo.org EGCEa. Biliary tract cancer: ESMO Clinical Practice Guideline for diagnosis, treatment and follow-up. Ann Oncol. 2023; 34:127-140.
20. Hori Y, Chari ST, Tsuji Y, Takahashi N, Inoue D, Hart PA, Uehara T, Horibe M, Yamamoto S, Satou A, Zhang L, Notohara K, Naitoh I, Nakazawa T. Diagnosing biliary strictures: Distinguishing IgG4-related sclerosing cholangitis from cholangiocarcinoma and primary sclerosing cholangitis. Mayo Clin Proc Innov Qual Outcomes. 2021; 5:535-541.
21. Group of Biliary Surgery of Society of Surgery of Chinese Medical Association , Special Committee of Hepatobiliary Surgery of PLA Army. Guidelines for diagnosis and treatment of hilar cholangiocarcinoma (2013 edition). Chin J Surg. 2013; 51:865-871. (in Chinese)
22. Kim DW, Kim SY, Yoo C, Hwang DW. Update on biliary cancer imaging. Radiol Clin North Am. 2022; 60:825-842.
23. Shin DW, Moon SH, Kim JH. Diagnosis of cholangiocarcinoma. Diagnostics (Basel). 2023; 13.
24. Ni Q, Wang H, Zhang Y, Qian L, Chi J, Liang X, Chen T, Wang J. MDCT assessment of resectability in hilar cholangiocarcinoma. Abdom Radiol (NY). 2017; 42:851-860.
25. Cao J, Srinivas-Rao S, Mroueh N, Anand R, Kongboonvijit S, Sertic M, Shenoy-Bhangle AS, Kambadakone A. Cholangiocarcinoma imaging: From diagnosis to response assessment. Abdom Radiol (NY). 2024.
26. Lamarca A, Barriuso J, Chander A, McNamara MG, Hubner RA, D OR, Manoharan P, Valle JW. ^{18}F-fluorodeoxyglucose positron emission tomography (^{18}FDG-PET) for patients with biliary tract cancer: Systematic review and meta-analysis. J Hepatol. 2019; 71:115-129.
27. Ruys AT, van Beem BE, Engelbrecht MR, Bipat S, Stoker J, Van Gulik TM. Radiological staging in patients with hilar cholangiocarcinoma: A systematic review and meta-analysis. Br J Radiol. 2012; 85:1255-1262.
28. Caragut RL, Ilie M, Cabel T, Gunsahin D, Panaitescu A, Pavel C, Plotogea OM, Rinja EM, Constantinescu G, Sandru V. Updates in diagnosis and endoscopic management of cholangiocarcinoma. Diagnostics (Basel). 2024; 14.
29. Seo H, Lee JM, Kim IH, Han JK, Kim SH, Jang JY, Kim SW, Choi BI. Evaluation of the gross type and longitudinal extent of extrahepatic cholangiocarcinomas on contrast-enhanced multidetector row computed tomography. J Comput Assist Tomogr. 2009; 33:376-382.
30. Joo I, Lee JM, Yoon JH. Imaging diagnosis of intrahepatic and perihilar cholangiocarcinoma: Recent advances and challenges. Radiology. 2018; 288:7-13.
31. Hammerstingl R, Huppertz A, Breuer J, *et al*. Diagnostic efficacy of gadoxetic acid (Primovist)-enhanced MRI and spiral CT for a therapeutic strategy: Comparison with intraoperative and histopathologic findings in focal liver lesions. Eur Radiol. 2008; 18:457-467.
32. Masselli G, Gualdi G. Hilar cholangiocarcinoma: MRI/MRCP in staging and treatment planning. Abdom Imaging. 2008; 33:444-451.
33. Lee MG, Park KB, Shin YM, Yoon HK, Sung KB, Kim MH, Lee SG, Kang EM. Preoperative evaluation of hilar cholangiocarcinoma with contrast-enhanced three-dimensional fast imaging with steady-state precession magnetic resonance angiography: Comparison with intraarterial digital subtraction angiography. World J Surg. 2003; 27:278-283.
34. Cholangiocarcinoma Working G. Italian Clinical Practice Guidelines on Cholangiocarcinoma - Part I: Classification, diagnosis and staging. Dig Liver Dis. 2020; 52:1282-1293.
35. Kim JY, Kim MH, Lee TY, Hwang CY, Kim JS, Yun SC, Lee SS, Seo DW, Lee SK. Clinical role of 18F-FDG PET-CT in suspected and potentially operable cholangiocarcinoma: A prospective study compared with conventional imaging. Am J Gastroenterol. 2008; 103:1145-1151.
36. Anderson CD, Rice MH, Pinson CW, Chapman WC, Chari RS, Delbeke D. Fluorodeoxyglucose PET imaging in the evaluation of gallbladder carcinoma and cholangiocarcinoma. J Gastrointest Surg. 2004; 8:90-97.
37. Fong ZV, Brownlee SA, Qadan M, Tanabe KK. The clinical management of cholangiocarcinoma in the United States and Europe: A comprehensive and evidence-based comparison of guidelines. Ann Surg Oncol. 2021; 28:2660-2674.
38. Heimbach JK, Sanchez W, Rosen CB, Gores GJ. Trans-peritoneal fine needle aspiration biopsy of hilar cholangiocarcinoma is associated with disease dissemination. HPB (Oxford). 2011; 13:356-360.
39. Rushbrook SM, Kendall TJ, Zen Y, *et al*. British Society of Gastroenterology guidelines for the diagnosis and management of cholangiocarcinoma. Gut. 2023; 73:16-46.
40. Yoon SB, Moon SH, Ko SW, Lim H, Kang HS, Kim JH. Brush cytology, forceps biopsy, or endoscopic ultrasound-guided sampling for diagnosis of bile duct cancer: A meta-analysis. Dig Dis Sci. 2022; 67:3284-3297.
41. Pereira P, Santos S, Morais R, Gaspar R, Rodrigues-Pinto E, Vilas-Boas F, Macedo G. Role of peroral cholangioscopy for diagnosis and staging of biliary tumors. Dig Dis. 2020; 38:431-440.
42. de Oliveira P, de Moura DTH, Ribeiro IB, Bazarbashi AN, Franzini TAP, Dos Santos MEL, Bernardo WM, de Moura EGH. Efficacy of digital single-operator cholangioscopy in the visual interpretation of indeterminate biliary strictures: A systematic review and meta-analysis. Surg Endosc. 2020; 34:3321-3329.
43. Almadi MA, Itoi T, Moon JH, *et al*. Using single-operator cholangioscopy for endoscopic evaluation of indeterminate biliary strictures: results from a large multinational registry. Endoscopy. 2020; 52:574-582.
44. Urban O, Vanek P, Zoundjiekpon V, Falt P. Endoscopic perspective in cholangiocarcinoma diagnostic process. Gastroenterol Res Pract. 2019; 2019:9704870.
45. Elmunzer BJ, Maranki JL, Gomez V, Tavakkoli A, Sauer BG, Limketkai BN, Brennan EA, Attridge EM, Brigham TJ, Wang AY. ACG Clinical Guideline: Diagnosis and Management of Biliary Strictures. Am J Gastroenterol.

2023; 118:405-426.
46. Burt A, Alves V, Coulston A. Intrahepatic cholangiocarcinoma, perihilar cholangiocarcinoma and hepatocellular carcinoma histopathology reporting guide. 2nd ed. Sydney, Australia: International Collaboration on Cancer Reporting, 2020.
47. Engelbrecht MR, Katz SS, van Gulik TM, Lameris JS, van Delden OM. Imaging of perihilar cholangiocarcinoma. AJR Am J Roentgenol. 2015; 204:782-791.
48. Guedj N. Pathology of cholangiocarcinomas. Curr Oncol. 2022; 30:370-380.
49. Akita M, Sofue K, Fujikura K, Otani K, Itoh T, Ajiki T, Fukumoto T, Zen Y. Histological and molecular characterization of intrahepatic bile duct cancers suggests an expanded definition of perihilar cholangiocarcinoma. HPB (Oxford). 2019; 21:226-234.
50. Brown ZJ, Patwardhan S, Bean J, Pawlik TM. Molecular diagnostics and biomarkers in cholangiocarcinoma. Surg Oncol. 2022; 44:101851.
51. Wang H, Chen J, Zhang X, Sheng X. Expert consensus on pathological diagnosis of intrahepatic cholangiocarcinoma (2022 version). Chin J Pathol. 2022; 51:819-827. (in Chinese)
52. Bismuth H, Nakache R, Diamond T. Management strategies in resection for hilar cholangiocarcinoma. Ann Surg. 1992; 215:31-38.
53. Jarnagin WR, Fong Y, DeMatteo RP, Gonen M, Burke EC, Bodniewicz BJ, Youssef BM, Klimstra D, Blumgart LH. Staging, resectability, and outcome in 225 patients with hilar cholangiocarcinoma. Ann Surg. 2001; 234:507-517; discussion 517-509.
54. Amin MB, Edge S, Greene FL, *et al*. AJCC Cancer Staging Manual. 8th ed. 2017.
55. Casadio M, Cardinale V, Klumpen HJ, Morement H, Lacasta A, Koerkamp BG, Banales J, Alvaro D, Valle JW, Lamarca A. Setup of multidisciplinary team discussions for patients with cholangiocarcinoma: Current practice and recommendations from the European Network for the Study of Cholangiocarcinoma (ENS-CCA). ESMO Open. 2022; 7:100377.
56. Precision Medicine and Tumor MDT Committee of the Chinese Research Hospital Association. Expert consensus on multidisciplinary comprehensive treatment of biliary tract cancer. J Multidisciplinary Cancer Mgmt: Electronic Version. 2023; 9:57-68. (in Chinese)
57. Zhang Y, Wang H, Zheng W. Controversies and advances in surgical treatment of hilar cholangiocarcinoma. Chin J Gen Surg. 2024; 33:257-264. (in Chinese)
58. Lauterio A, De Carlis R, Centonze L, Buscemi V, Incarbone N, Vella I, De Carlis L. Current surgical management of peri-hilar and intra-hepatic cholangiocarcinoma. Cancers (Basel). 2021; 13.
59. Teng F, Tang YY, Dai JL, Li Y, Chen ZY. The effect and safety of preoperative biliary drainage in patients with hilar cholangiocarcinoma: An updated meta-analysis. World J Surg Oncol. 2020; 18:174.
60. Mansour JC, Aloia TA, Crane CH, Heimbach JK, Nagino M, Vauthey JN. Hilar cholangiocarcinoma: Expert consensus statement. HPB (Oxford). 2015; 17:691-699.
61. Cholangiocarcinoma Working G. Italian Clinical Practice Guidelines on Cholangiocarcinoma - Part II: Treatment. Dig Liver Dis. 2020; 52:1430-1442.
62. Guidelines Working Committee of the Chinese Society of Clinical Oncology. Guidelines of Chinese Society of Clinical Oncology (CSCO) of biliary tract cancer 2023. People's Medical Publishing House, Beijing, 2023, China. (in Chinese)
63. Paik WH, Loganathan N, Hwang JH. Preoperative biliary drainage in hilar cholangiocarcinoma: When and how? World J Gastrointest Endosc. 2014; 6:68-73.
64. Nagino M, Hirano S, Yoshitomi H, *et al*. Clinical practice guidelines for the management of biliary tract cancers 2019: The 3rd English edition. J Hepatobiliary Pancreat Sci. 2021; 28:26-54.
65. Li B, Jiang X. Key technical criteria and evaluation for radical resection of hilar cholangiocarcinoma. Chin J Practical Surg. 2024; 44:55-60. (in Chinese)
66. Li B, Li Z, Qiu Z, Qin Y, Gao Q, Ao J, Ma W, Jiang X. Surgical treatment of hilar cholangiocarcinoma: Retrospective analysis. BJS Open. 2023; 7.
67. Watanabe Y, Kuboki S, Shimizu H, Ohtsuka M, Yoshitomi H, Furukawa K, Miyazaki M. A new proposal of criteria for the future remnant liver volume in older patients undergoing major hepatectomy for biliary tract cancer. Ann Surg. 2018; 267:338-345.
68. Lee JW, Lee JH, Park Y, Lee W, Kwon J, Song KB, Hwang DW, Kim SC. Risk factors of posthepatectomy liver failure for perihilar cholangiocarcinoma: Risk score and significance of future liver remnant volume-to-body weight ratio. J Surg Oncol. 2020; 122:469-479.
69. Thirunavukarasu P, Aloia TA. Preoperative assessment and optimization of the future liver remnant. Surg Clin North Am. 2016; 96:197-205.
70. Glantzounis GK, Tokidis E, Basourakos SP, Ntzani EE, Lianos GD, Pentheroudakis G. The role of portal vein embolization in the surgical management of primary hepatobiliary cancers. A systematic review. Eur J Surg Oncol. 2017; 43:32-41.
71. Olthof PB, Wiggers JK, Groot Koerkamp B, Coelen RJ, Allen PJ, Besselink MG, Busch OR, D'Angelica MI, DeMatteo RP, Kingham TP, van Lienden KP, Jarnagin WR, van Gulik TM. Postoperative liver failure risk score: Identifying patients with resectable perihilar cholangiocarcinoma who can benefit from portal vein embolization. J Am Coll Surg. 2017; 225:387-394.
72. Rassam F, Olthof PB, van Lienden KP, Bennink RJ, Besselink MG, Busch OR, van Gulik TM. Functional and volumetric assessment of liver segments after portal vein embolization: Differences in hypertrophy response. Surgery. 2019; 165:686-695.
73. Abulkhir A, Limongelli P, Healey AJ, Damrah O, Tait P, Jackson J, Habib N, Jiao LR. Preoperative portal vein embolization for major liver resection: A meta-analysis. Ann Surg. 2008; 247:49-57.
74. Lang H, de Santibanes E, Schlitt HJ, *et al*. 10th Anniversary of ALPPS-Lessons learned and quo vadis. Ann Surg. 2019; 269:114-119.
75. Olthof PB, Coelen RJS, Wiggers JK, Groot Koerkamp B, Malago M, Hernandez-Alejandro R, Topp SA, Vivarelli M, Aldrighetti LA, Robles Campos R, Oldhafer KJ, Jarnagin WR, van Gulik TM. High mortality after ALPPS for perihilar cholangiocarcinoma: Case-control analysis including the first series from the international ALPPS registry. HPB (Oxford). 2017; 19:381-387.
76. Chinese Anti-Cancer Association. Expert consensus on diagnosis and treatment of hilar cholangiocarcinoma (2015 edition). Chin J Hepatobiliary Surg. 2015; 21:505-511. (in Chinese)
77. D'Souza MA, Al-Saffar HA, Fernandez Moro C, Shtembari S, Danielsson O, Sparrelid E, Sturesson C.

Redefining resection margins and dissection planes in perihilar cholangiocarcinoma-radical resection is a rare event. Virchows Arch. 2022; 480:557-564.
78. Zhang XF, Squires MH, 3rd, Bagante F, *et al*. The impact of intraoperative re-resection of a positive bile duct margin on clinical outcomes for hilar cholangiocarcinoma. Ann Surg Oncol. 2018; 25:1140-1149.
79. Kawano F, Ito H, Oba A, Ono Y, Sato T, Inoue Y, Mise Y, Saiura A, Takahashi Y. Role of intraoperative assessment of proximal bile duct margin status and additional resection of perihilar cholangiocarcinoma: Can local clearance trump tumor biology? A retrospective cohort study. Ann Surg Oncol. 2023; 30:3348-3359.
80. van Keulen AM, Buettner S, Olthof PB, *et al*. Comparing survival of perihilar cholangiocarcinoma after R1 resection versus palliative chemotherapy for unresected localized disease. Ann Surg Oncol. 2024; 31:6495-6503.
81. Ni Q, Wang J. Interpretation of guideline for diagnosis and treatment of hilar cholangiocarcinoma (2013 edition). J Hepatopancreatobil Surg. 2015; 27:450-454. (in Chinese)
82. Xu L, Liu J. Surgical treatment and prognostic factors analysis of hilar cholangiocarcinoma. Chin J Hepatobil Surg. 2011; 17:829-832. (in Chinese)
83. Yang J, Ye L, Yang Y. Advances in surgical treatment of hilar cholangiocarcinoma. Chin J General Surg. 2023; 32:1264-1270. (in Chinese)
84. Bae J, Shin DW, Cho KB, Ahn KS, Kim TS, Kim YH, Kang KJ. Survival outcome of surgical resection compared to non-resection for Bismuth type IV perihilar cholangiocarcinoma. Langenbecks Arch Surg. 2023; 408:229.
85. Ersan V, Usta S, Aydin C, Carr BI, Karatoprak S, Yilmaz S. Critical overview of resection for Bismuth-Corlette type IV perihilar cholangiocarcinoma. Acta Chir Belg. 2023; 123:489-496.
86. Hartog H, Ijzermans JN, van Gulik TM, Groot Koerkamp B. Resection of perihilar cholangiocarcinoma. Surg Clin North Am. 2016; 96:247-267.
87. Jo HS, Kim DS, Yu YD, Kang WH, Yoon KC. Right-side versus left-side hepatectomy for the treatment of hilar cholangiocarcinoma: A comparative study. World J Surg Oncol. 2020; 18:3.
88. Mizuno T, Ebata T, Nagino M. Advanced hilar cholangiocarcinoma: An aggressive surgical approach for the treatment of advanced hilar cholangiocarcinoma: Perioperative management, extended procedures, and multidisciplinary approaches. Surg Oncol. 2020; 33:201-206.
89. Chen Z, Y. Y. Technical points of combined vascular resection and reconstruction in radical resection of hilar cholangiocarcinoma. Chin J Hepatobil Surg. 2022; 28:862-865. (in Chinese)
90. Serrablo A, Serrablo L, Alikhanov R, Tejedor L. Vascular resection in perihilar cholangiocarcinoma. Cancers (Basel). 2021; 13:5278.
91. Kitagawa Y, Nagino M, Kamiya J, Uesaka K, Sano T, Yamamoto H, Hayakawa N, Nimura Y. Lymph node metastasis from hilar cholangiocarcinoma: Audit of 110 patients who underwent regional and paraaortic node dissection. Ann Surg. 2001; 233:385-392.
92. Miyazaki M, Ohtsuka M, Miyakawa S, *et al*. Classification of biliary tract cancers established by the Japanese Society of Hepato-Biliary-Pancreatic Surgery: 3(rd) English edition. J Hepatobiliary Pancreat Sci. 2015; 22:181-196.
93. De Vreede I, Steers JL, Burch PA, Rosen CB, Gunderson LL, Haddock MG, Burgart L, Gores GJ. Prolonged disease-free survival after orthotopic liver transplantation plus adjuvant chemoirradiation for cholangiocarcinoma. Liver Transpl. 2000; 6:309-316.
94. Rea DJ, Heimbach JK, Rosen CB, Haddock MG, Alberts SR, Kremers WK, Gores GJ, Nagorney DM. Liver transplantation with neoadjuvant chemoradiation is more effective than resection for hilar cholangiocarcinoma. Ann Surg. 2005; 242:451-458; discussion 458-461.
95. Heimbach JK, Gores GJ, Haddock MG, Alberts SR, Nyberg SL, Ishitani MB, Rosen CB. Liver transplantation for unresectable perihilar cholangiocarcinoma. Semin Liver Dis. 2004; 24:201-207.
96. Tan EK, Taner T, Heimbach JK, Gores GJ, Rosen CB. Liver transplantation for peri-hilar cholangiocarcinoma. J Gastrointest Surg. 2020; 24:2679-2685.
97. Giovinazzo F, Pascale MM, Cardella F, Picarelli M, Molica S, Zotta F, Martullo A, Clarke G, Frongillo F, Grieco A, Agnes S. Current perspectives in liver transplantation for perihilar cholangiocarcinoma. Curr Oncol. 2023; 30:2942-2953.
98. Croome KP, Rosen CB, Heimbach JK, Nagorney DM. Is liver transplantation appropriate for patients with potentially resectable de novo hilar cholangiocarcinoma? J Am Coll Surg. 2015; 221:130-139.
99. Coelen RJ, Ruys AT, Besselink MG, Busch OR, van Gulik TM. Diagnostic accuracy of staging laparoscopy for detecting metastasized or locally advanced perihilar cholangiocarcinoma: A systematic review and meta-analysis. Surg Endosc. 2016; 30:4163-4173.
100. Bird N, Elmasry M, Jones R, Elniel M, Kelly M, Palmer D, Fenwick S, Poston G, Malik H. Role of staging laparoscopy in the stratification of patients with perihilar cholangiocarcinoma. Br J Surg. 2017; 104:418-425.
101. Chen Y, Xu Y, Zhang Y. Current status of laparoscopic radical hilar cholangiocarcinoma in Mainland China. Biosci Trends. 2020; 14:168-173.
102. Qin T, Wang M, Zhang H, *et al*. The long-term outcome of laparoscopic resection for perihilar cholangiocarcinoma compared with the open approach: A real-world multicentric analysis. Ann Surg Oncol. 2023; 30:1366-1378.
103. Xiong Y, Jingdong L, Zhaohui T, Lau J. A Consensus Meeting on Expert Recommendations on Operating Specifications for Laparoscopic Radical Resection of Hilar Cholangiocarcinoma. Front Surg. 2021; 8:731448.
104. Li W, Li J. Technical key points and difficulties of laparoscopic radical resection for hilar cholangiocarcinoma. Chin J Hepatic Surg. 2021; 10:348-351. (in Chinese)
105. Liu S, Liu X, Li X, Li O, Yi W, Khan J, Yang P, Guo C, Peng C, Jiang B. Application of laparoscopic radical resection for type III and IV hilar cholangiocarcinoma treatment. Gastroenterol Res Pract. 2020; 2020:1506275.
106. Wu J, Wang L, Yu F. Efficacy of laparoscopic versus open radical resection in the treatment of hilar cholangiocarcinoma: A meta-analysis. Chin J General Surg. 2024; 33:1206-1219. (in Chinese)
107. Moll CF, de Moura DTH, Ribeiro IB, Proenca IM, do Monte Junior ES, Sanchez-Luna SA, Merchan MFS, Intriago JMV, Bernardo WM, de Moura EGH. Endoscopic biliary darinage (EBD) versus percutaneous transhepatic biliary drainage (PTBD) for biliary drainage in patients with perihilar cholangiocarcinoma (PCCA): A systematic review and meta-analysis. Clinics (Sao Paulo). 2023; 78:100163.
108. Ba Y, Yue P, Leung JW, Wang H, Lin Y, Bai B, Zhu X,

Zhang L, Zhu K, Wang W, Meng W, Zhou W, Liu Y, Li X. Percutaneous transhepatic biliary drainage may be the preferred preoperative drainage method in hilar cholangiocarcinoma. Endosc Int Open. 2020; 8:E203-E210.
109. Komaya K, Ebata T, Yokoyama Y, Igami T, Sugawara G, Mizuno T, Yamaguchi J, Nagino M. Verification of the oncologic inferiority of percutaneous biliary drainage to endoscopic drainage: A propensity score matching analysis of resectable perihilar cholangiocarcinoma. Surgery. 2017; 161:394-404.
110. Mocan T, Horhat A, Mois E, Graur F, Tefas C, Craciun R, Nenu I, Sparchez M, Sparchez Z. Endoscopic or percutaneous biliary drainage in hilar cholangiocarcinoma: When and how? World J Gastrointest Oncol. 2021; 13:2050-2063.
111. van der Merwe SW, van Wanrooij RLJ, Bronswijk M, *et al*. Therapeutic endoscopic ultrasound: European Society of Gastrointestinal Endoscopy (ESGE) Guideline. Endoscopy. 2022; 54:185-205.
112. Takenaka M, Lee TH. Role of radiofrequency ablation in advanced malignant hilar biliary obstruction. Clin Endosc. 2023; 56:155-163.
113. Sawas T, Al Halabi S, Parsi MA, Vargo JJ. Self-expandable metal stents versus plastic stents for malignant biliary obstruction: A meta-analysis. Gastrointest Endosc. 2015; 82:256-267 e257.
114. Xia MX, Cai XB, Pan YL, Wu J, Gao DJ, Ye X, Wang TT, Hu B. Optimal stent placement strategy for malignant hilar biliary obstruction: A large multicenter parallel study. Gastrointest Endosc. 2020; 91:1117-1128 e1119.
115. Qumseya BJ, Jamil LH, Elmunzer BJ, *et al*. ASGE guideline on the role of endoscopy in the management of malignant hilar obstruction. Gastrointest Endosc. 2021; 94:222-234 e222.
116. Weismuller TJ. Role of intraductal RFA: A novel tool in the palliative care of perihilar cholangiocarcinoma. Visc Med. 2021; 37:39-47.
117. Wu L, Merath K, Farooq A, Hyer JM, Tsilimigras DI, Paredes AZ, Mehta R, Sahara K, Shen F, Pawlik TM. Photodynamic therapy may provide a benefit over systemic chemotherapy among non-surgically managed patients with extrahepatic cholangiocarcinoma. J Surg Oncol. 2020; 121:286-293.
118. Yu Y, Wang N, Wang Y, Shi Q, Yu R, Gu B, Maswikiti EP, Chen H. Photodynamic therapy combined with systemic chemotherapy for unresectable extrahepatic cholangiocarcinoma: A systematic review and meta-analysis. Photodiagnosis Photodyn Ther. 2023; 41:103318.
119. de Oliveira Veras M, de Moura DTH, McCarty TR, de Oliveira GHP, Gomes RSA, Landim DL, Nunes FG, Franzini TAP, Lera Dos Santos ME, Bernardo WM, de Moura EGH. Intraductal radiofrequency ablation plus biliary stent versus stent alone for malignant biliary obstruction: A systematic review and meta-analysis. Endosc Int Open. 2024; 12:E23-E33.
120. Yang J, Wang J, Zhou H, Zhou Y, Wang Y, Jin H, Lou Q, Zhang X. Efficacy and safety of endoscopic radiofrequency ablation for unresectable extrahepatic cholangiocarcinoma: A randomized trial. Endoscopy. 2018; 50:751-760.
121. Gao DJ, Yang JF, Ma SR, Wu J, Wang TT, Jin HB, Xia MX, Zhang YC, Shen HZ, Ye X, Zhang XF, Hu B. Endoscopic radiofrequency ablation plus plastic stent placement versus stent placement alone for unresectable extrahepatic biliary cancer: A multicenter randomized controlled trial. Gastrointest Endosc. 2021; 94:91-100 e102.
122. Yang J, Wang J, Zhou H, Wang Y, Huang H, Jin H, Lou Q, Shah RJ, Zhang X. Endoscopic radiofrequency ablation plus a novel oral 5-fluorouracil compound versus radiofrequency ablation alone for unresectable extrahepatic cholangiocarcinoma. Gastrointest Endosc. 2020; 92:1204-1212 e1201.
123. Xia M, Qin W, Hu B. Endobiliary radiofrequency ablation for unresectable malignant biliary strictures: Survival benefit perspective. Dig Endosc. 2023; 35:584-591.
124. Chinese Society of Digestive Endoscopy, Digestive Endoscopy Professional Committee of Endoscopy Branch of Chinese Medical Doctor Association, National Clinical Research Center for Digestive Diseases. Expert consensus on endoscopic radiofrequency ablation for malignant bile duct stenosis. Chin J Dig Endosc. 2023; 40:673-682. (in Chinese)
125. Li Y, Li Y, Song Y, Liu S. Advances in research and application of photodynamic therapy in cholangiocarcinoma (Review). Oncol Rep. 2024; 51.
126. Chen P, Yang T, Shi P, Shen J, Feng Q, Su J. Benefits and safety of photodynamic therapy in patients with hilar cholangiocarcinoma: A meta-analysis. Photodiagnosis Photodynamic Ther. 2022; 37.
127. Lee TY, Cheon YK, Shim CS, Cho YD. Photodynamic therapy prolongs metal stent patency in patients with unresectable hilar cholangiocarcinoma. World J Gastroenterol. 2012; 18:5589-5594.
128. Park DH, Lee SS, Park SE, Lee JL, Choi JH, Choi HJ, Jang JW, Kim HJ, Eum JB, Seo DW, Lee SK, Kim MH, Lee JB. Randomised phase II trial of photodynamic therapy plus oral fluoropyrimidine, S-1, versus photodynamic therapy alone for unresectable hilar cholangiocarcinoma. Eur J Cancer. 2014; 50:1259-1268.
129. Surgical Operation Group of Chinese Surgical Society, Biliary Surgery Group of Chinese Surgical Society, Chinese Committee of Biliary Surgeons. Expert consensus on technical specifications for clinical application of photodynamic therapy for cholangiocarcinoma. Chin J General Surg. 2023; 32:265-276. (in Chinese)
130. Di Girolamo E, Belli A, Ottaiano A, *et al*. Impact of endobiliary radiofrequency ablation on survival of patients with unresectable cholangiocarcinoma: A narrative review. Front Oncol. 2023; 13:1077794.
131. Xu X, Li J, Wu J, Zhu R, Ji W. A systematic review and meta-analysis of intraluminal brachytherapy versus stent alone in the treatment of malignant obstructive jaundice. Cardiovasc Intervent Radiol. 2018; 41:206-217.
132. Sheng Y, Fu X, Wang G, Mu M, Jiang W, Chen Z, Qi H, Gao F. Safety and efficacy of self-expandable metallic stent combined with (125)I brachytherapy for the treatment of malignant obstructive jaundice. Cancer Imaging. 2023; 23:33.
133. Sumiyoshi T, Shima Y, Okabayashi T, Negoro Y, Shimada Y, Iwata J, Matsumoto M, Hata Y, Noda Y, Sui K, Sueda T. Chemoradiotherapy for initially unresectable locally advanced cholangiocarcinoma. World J Surg. 2018; 42:2910-2918.
134. Frosio F, Mocchegiani F, Conte G, Bona ED, Vecchi A, Nicolini D, Vivarelli M. Neoadjuvant therapy in the treatment of hilar cholangiocarcinoma: Review of the literature. World J Gastrointest Surg. 2019; 11:279-286.
135. Groot Koerkamp B, Wiggers JK, Allen PJ, Besselink MG, Blumgart LH, Busch OR, Coelen RJ, D'Angelica MI,

DeMatteo RP, Gouma DJ, Kingham TP, Jarnagin WR, van Gulik TM. Recurrence rate and pattern of perihilar cholangiocarcinoma after curative intent resection. J Am Coll Surg. 2015; 221:1041-1049.
136. Ben-Josef E, Guthrie KA, El-Khoueiry AB, Corless CL, Zalupski MM, Lowy AM, Thomas CR, Jr., Alberts SR, Dawson LA, Micetich KC, Thomas MB, Siegel AB, Blanke CD. SWOG S0809: A phase II intergroup trial of adjuvant capecitabine and gemcitabine followed by radiotherapy and concurrent capecitabine in extrahepatic cholangiocarcinoma and gallbladder carcinoma. J Clin Oncol. 2015; 33:2617-2622.
137. Gholami S, Colby S, Horowitz DP, Guthrie KA, Ben-Josef E, El-Khoueiry AB, Blanke CD, Philip PA, Kachnic LA, Ahmad SA, Rocha FG. Adjuvant chemoradiation in patients with lymph node-positive biliary tract cancers: Secondary analysis of a single-arm clinical trial (SWOG 0809). Ann Surg Oncol. 2023; 30:1354-1363.
138. Ren B, Guo Q, Yang Y, Liu L, Wei S, Chen W, Tian Y. A meta-analysis of the efficacy of postoperative adjuvant radiotherapy versus no radiotherapy for extrahepatic cholangiocarcinoma and gallbladder carcinoma. Radiat Oncol. 2020; 15:15.
139. Horgan AM, Amir E, Walter T, Knox JJ. Adjuvant therapy in the treatment of biliary tract cancer: A systematic review and meta-analysis. J Clin Oncol. 2012; 30:1934-1940.
140. Shroff RT, Kennedy EB, Bachini M, Bekaii-Saab T, Crane C, Edeline J, El-Khoueiry A, Feng M, Katz MHG, Primrose J, Soares HP, Valle J, Maithel SK. Adjuvant therapy for resected biliary tract cancer: ASCO Clinical Practice Guideline. J Clin Oncol. 2019; 37:1015-1027.
141. Torgeson A, Lloyd S, Boothe D, Cannon G, Garrido-Laguna I, Whisenant J, Lewis M, Kim R, Scaife C, Tao R. Chemoradiation therapy for unresected extrahepatic cholangiocarcinoma: A propensity score-matched analysis. Ann Surg Oncol. 2017; 24:4001-4008.
142. Chigurupalli K, Vashistha A. Role of intraluminal brachytherapy as a palliative treatment modality in unresectable cholangiocarcinomas. J Cancer Res Ther. 2021; 17:10-12.
143. Sahai P, Kumar S. External radiotherapy and brachytherapy in the management of extrahepatic and intrahepatic cholangiocarcinoma: Available evidence. Br J Radiol. 2017; 90:20170061.
144. Primrose JN, Fox RP, Palmer DH, *et al*. Capecitabine compared with observation in resected biliary tract cancer (BILCAP): A randomised, controlled, multicentre, phase 3 study. Lancet Oncol. 2019; 20:663-673.
145. Bridgewater J, Fletcher P, Palmer DH, *et al*. Long-term outcomes and exploratory analyses of the randomized phase III BILCAP study. J Clin Oncol. 2022; 40:2048-2057.
146. Nakachi K, Ikeda M, Konishi M, *et al*. Adjuvant S-1 compared with observation in resected biliary tract cancer (JCOG1202, ASCOT): A multicentre, open-label, randomised, controlled, phase 3 trial. Lancet. 2023; 401:195-203.
147. Ebata T, Hirano S, Konishi M, *et al*. Randomized clinical trial of adjuvant gemcitabine chemotherapy versus observation in resected bile duct cancer. Br J Surg. 2018; 105:192-202.
148. Edeline J, Benabdelghani M, Bertaut A, *et al*. Gemcitabine and oxaliplatin chemotherapy or surveillance in resected biliary tract cancer (PRODIGE 12-ACCORD 18-UNICANCER GI): A randomized phase III study. J Clin Oncol. 2019; 37:658-667.
149. Jeong H, Kim KP, Jeong JH, Hwang DW, Lee JH, Kim KH, Moon DB, Lee MA, Park SJ, Chon HJ, Park JH, Lee JS, Ryoo BY, Yoo C. Adjuvant gemcitabine plus cisplatin versus capecitabine in node-positive extrahepatic cholangiocarcinoma: The STAMP randomized trial. Hepatology. 2023; 77:1540-1549.
150. Valle J, Wasan H, Palmer DH, Cunningham D, Anthoney A, Maraveyas A, Madhusudan S, Iveson T, Hughes S, Pereira SP, Roughton M, Bridgewater J, Investigators ABCT. Cisplatin plus gemcitabine versus gemcitabine for biliary tract cancer. N Engl J Med. 2010; 362:1273-1281.
151. Morizane C, Okusaka T, Mizusawa J, *et al*. Combination gemcitabine plus S-1 versus gemcitabine plus cisplatin for advanced/recurrent biliary tract cancer: The FUGA-BT (JCOG1113) randomized phase III clinical trial. Ann Oncol. 2019; 30:1950-1958.
152. Oh DY, He AR, Bouattour M, *et al*. Durvalumab or placebo plus gemcitabine and cisplatin in participants with advanced biliary tract cancer (TOPAZ-1): Updated overall survival from a randomised phase 3 study. Lancet Gastroenterol Hepatol. 2024; 9:694-704.
153. Kelley RK, Ueno M, Yoo C, *et al*. Pembrolizumab in combination with gemcitabine and cisplatin compared with gemcitabine and cisplatin alone for patients with advanced biliary tract cancer (KEYNOTE-966): A randomised, double-blind, placebo-controlled, phase 3 trial. Lancet. 2023; 401:1853-1865.
154. Ioka T, Kanai M, Kobayashi S, *et al*. Randomized phase III study of gemcitabine, cisplatin plus S-1 versus gemcitabine, cisplatin for advanced biliary tract cancer (KHBO1401-MITSUBA). J Hepatobiliary Pancreat Sci. 2023; 30:102-110.
155. Lamarca A, Palmer DH, Wasan HS, *et al*. Second-line FOLFOX chemotherapy versus active symptom control for advanced biliary tract cancer (ABC-06): A phase 3, open-label, randomised, controlled trial. Lancet Oncol. 2021; 22:690-701.
156. Choi IS, Kim KH, Lee JH, Suh KJ, Kim JW, Park JH, Kim YJ, Kim JS, Kim JH, Kim JW. A randomised phase II study of oxaliplatin/5-FU (mFOLFOX) versus irinotecan/5-FU (mFOLFIRI) chemotherapy in locally advanced or metastatic biliary tract cancer refractory to first-line gemcitabine/cisplatin chemotherapy. Eur J Cancer. 2021; 154:288-295.
157. Zheng Y, Tu X, Zhao P, Jiang W, Liu L, Tong Z, Zhang H, Yan C, Fang W, Wang W. A randomised phase II study of second-line XELIRI regimen versus irinotecan monotherapy in advanced biliary tract cancer patients progressed on gemcitabine and cisplatin. Br J Cancer. 2018; 119:291-295.
158. Yoo C, Kim KP, Jeong JH, Kim I, Kang MJ, Cheon J, Kang BW, Ryu H, Lee JS, Kim KW, Abou-Alfa GK, Ryoo BY. Liposomal irinotecan plus fluorouracil and leucovorin versus fluorouracil and leucovorin for metastatic biliary tract cancer after progression on gemcitabine plus cisplatin (NIFTY): A multicentre, open-label, randomised, phase 2b study. Lancet Oncol. 2021; 22:1560-1572.
159. Li Y, Yu J, Zhang Y, Peng C, Song Y, Liu S. Advances in targeted therapy of cholangiocarcinoma. Ann Med. 2024; 56:2310196.
160. Javle M, Borad MJ, Azad NS, *et al*. Pertuzumab and trastuzumab for HER2-positive, metastatic biliary tract cancer (MyPathway): a multicentre, open-label, phase 2a, multiple basket study. Lancet Oncol. 2021; 22:1290-1300.
161. Ohba A, Morizane C, Ueno M, *et al*. Multicenter phase

II trial of trastuzumab deruxtecan for HER2-positive unresectable or recurrent biliary tract cancer: HERB trial. Future Oncol. 2022; 18:2351-2360.
162. Ohba A, Morizane C, Kawamoto Y, *et al*. Trastuzumab deruxtecan in human epidermal growth factor receptor 2-expressing biliary tract cancer (HERB; NCCH1805): A multicenter, single-arm, phase II trial. J Clin Oncol. 2024; 42:3207-3217.
163. Subbiah V, Lassen U, Elez E, *et al*. Dabrafenib plus trametinib in patients with BRAF(V600E)-mutated biliary tract cancer (ROAR): A phase 2, open-label, single-arm, multicentre basket trial. Lancet Oncol. 2020; 21:1234-1243.
164. Marabelle A, Le DT, Ascierto PA, *et al*. Efficacy of pembrolizumab in patients with noncolorectal high microsatellite instability/mismatch repair-deficient cancer: Results from the phase II KEYNOTE-158 study. J Clin Oncol. 2020; 38:1-10.
165. Wang Y, Yang X, Wang D, Yang X, Wang Y, Long J, Zhou J, Lu Z, Mao Y, Sang X, Guan M, Zhao H. Lenvatinib beyond first-line therapy in patients with advanced biliary tract carcinoma. Front Oncol. 2022; 12:785535.
166. Zhu C, Xue J, Wang Y, Wang S, Zhang N, Wang Y, Zhang L, Yang X, Long J, Yang X, Sang X, Zhao H. Efficacy and safety of lenvatinib combined with PD-1/PD-L1 inhibitors plus Gemox chemotherapy in advanced biliary tract cancer. Front Immunol. 2023; 14:1109292.
167. Zhou J, Sun Y, Zhang W, Yuan J, Peng Z, Wang W, Gong J, Yang L, Cao Y, Zhao H, Chen C, Wang W, Shen L, Zhou A. Phase Ib study of anlotinib combined with TQB2450 in pretreated advanced biliary tract cancer and biomarker analysis. Hepatology. 2023; 77:65-76.
168. Jin S, Zhao R, Zhou C, *et al*. Feasibility and tolerability of sintilimab plus anlotinib as the second-line therapy for patients with advanced biliary tract cancers: An open-label, single-arm, phase II clinical trial. Int J Cancer. 2023; 152:1648-1658.
169. Xu J, Bai Y, Sun H, Bai C, Jia R, Li Y, Zhang W, Liu L, Huang C, Guan M, Zhou J, Su W. A single-arm, multicenter, open-label phase 2 trial of surufatinib in patients with unresectable or metastatic biliary tract cancer. Cancer. 2021; 127:3975-3984.

Received May 25, 2025; Revised August 1, 2025; Accepted August 9, 2025.

[§]These authors contributed equally to this work.
**Address correspondence to:*
Chuang Peng, Department of Hepatobiliary Surgery, Hunan Provincial People's Hospital (The First Affiliated Hospital of Hunan Normal University), Changsha, Hunan 410005, China.
E-mail: pengchuangcn@163.com

Released online in J-STAGE as advance publication August 14, 2025.

Review

DOI: 10.5582/bst.2025.01239

Chikungunya's global rebound and Asia's growing vulnerability: Implications for integrated vector control and pandemic preparedness

Jing Ni[1,§], Zhifang Li[2,§], Xiaowei Hu[3,§], Hui Zhou[4], Zhenyu Gong[5,*]

[1] School of Public Health, Hangzhou Medical College, Hangzhou, China;
[2] Tonglu Centre for Disease Control and Prevention, Hangzhou, China;
[3] Hangzhou West Lake District Center for Disease Control and Prevention, Hangzhou, China;
[4] Longyou Centre for Disease Control and Prevention, Quzhou, China;
[5] Department of Communicable Disease Control and Prevention, Zhejiang Provincial Center for Disease Control and Prevention, Hangzhou, China.

SUMMARY: Chikungunya fever is a mosquito-borne disease caused by an RNA virus of the Alphavirus genus and is characterized by fever and severe joint pain. The disease is primarily transmitted by Aedes aegypti and Ae. albopictus mosquitoes. Since its re-emergence in 2005, chikungunya has spread extensively, affecting more than 2.8 billion people across 119 countries worldwide. This article reviews the global epidemiological features of chikungunya, with a focus on its transmission dynamics, the characteristics of the virus and its vectors, as well as the influence of ecological and climatic factors. The article also discusses public health response measures, including the Wolbachia strategy, vaccine development, and integrated vector management. Despite China being a non-epidemic area, imported cases have led to localized outbreaks, prompting the implementation of the 'Four Pests-free Village' initiative to reduce mosquito density and improve public health. Notably, as of July 31, 2025, Guangdong Province in China has reported over 5,158 chikungunya cases and has initiated a Level 3 emergency response in the City of Foshan. In the face of global challenges such as climate change and the spread of invasive species, establishing a normalized rapid response system and enhancing monitoring, early warning, and inter-departmental collaboration are crucial to controlling the spread of mosquito-borne diseases and protecting public health.

Keywords: chikungunya, mosquito-borne disease, Four Pests-free Village, Asia, vector-borne disease, vaccine, One Health

1. Introduction

Chikungunya fever is a mosquito-borne viral disease that can cause fever and severe joint pain. It is caused by a ribonucleic acid (RNA) virus belonging to the genus Alphavirus in the family Togaviridae (*1*). The Chikungunya virus (CHIKV) is transmitted by day-biting Aedes aegypti and Ae. albopictus females; after 2–12 days, patients develop an abrupt fever, severe joint pain, muscle aches, headaches, nausea, fatigue, and a rash — symptoms last days to years, but are rarely fatal (*2*). Since its re-emergence in the Indian Ocean region in 2005, CHIKV has nearly spread to all major regions inhabited by its primary vectors, the Ae. aegypti and Ae. albopictus mosquitoes (*3*). An estimated 119 countries have experienced the transmission of CHIKV, affecting 2.8 billion people (Figure 1). In epidemic settings, the average duration between two outbreaks is 6.2 years, with 8.4% of the susceptible population infected during each outbreak. There are approximately 35 million infections globally each year, primarily occurring in Southeast Asia, Africa, and the Americas (*4*).

The dense areas of Ae. aegypti and Ae. albopictus are mainly located in southern China (*5*). China is a non-endemic area for CHIKV, with most cases imported and confirmed in Guangdong and Zhejiang provinces (*6*).The provinces of Guangzhou in 2010, Zhejiang in 2017, and Yunnan in 2019 reported local outbreaks of chikungunya fever (*7*). Zhejiang Province, located in the southeastern coastal region of China, is economically active, has the highest social mobility and population density, and is thus vulnerable to infectious diseases, and particularly those related to travel-related imported diseases (*8*). A point worth noting is that in 2025, there will be another chikungunya epidemic in Guangdong Province (*9*). The epidemic was triggered by imported cases, and the climate conditions of a high temperature and high humidity after a typhoon promoted mosquito reproduction and virus transmission. Based on the epidemiological data and characteristics of

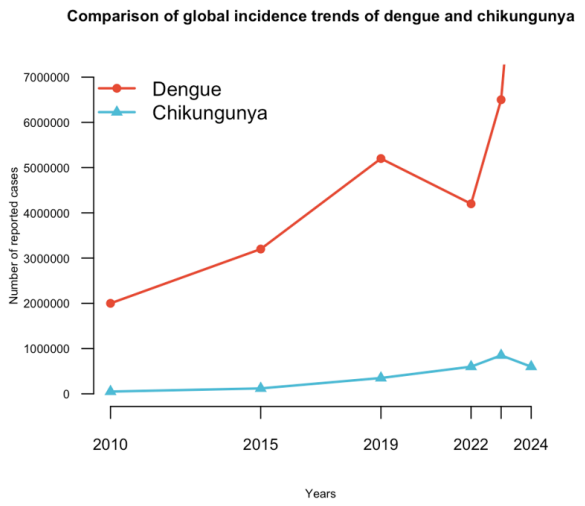

Figure 1. Comparison of global trends in the incidence of dengue and chikungunya.

chikungunya's vector ecology, this review presents the public health response measures of various countries and systematically proposes precise prevention and control strategies.

2. Viral and vector foundations

CHIKV originated in Africa over 500 years ago and was subsequently introduced to Asia. Preliminary genetic analysis of the common African lineage of CHIKV showed that the virus was divided into three genotypes, West Africa (WA), Eastern/Central/South Africa (ECSA), and Asia. ECSA can be further classified into Indian Ocean lineage (IOL) subfamilies (*2*). These genotypes are now distributed around the world, with ECSA and Asian genotypes being the main genotypes found (*10*). Ae. aegypti and Ae. albopictus are potent vectors of several arboviruses, including dengue fever (DEN), yellow fever (YF), chikungunya fever (CHIK), and Zika virus, which have significant implications for human health (*11*). Ae. aegypti mosquitoes prefer urban artificial containers, with a radius of ≈ 200 m; Ae. albopictus can breed in urban, suburban, rural, and forest environments, and it is highly adaptable to a variety of small waterlogged containers (*12*). Ae. albopictus is more ecologically adaptable and has expanded globally in 30–40 years, spreading about 13.3 times faster than Ae. aegypti (*13*). Both mosquitoes are the main vectors of dengue, Zika, and chikungunya viruses, but Ae. aegypti is more efficient at transmitting the virus, and Ae. albopictus is generally a secondary or maintenance vector (*14*).The efficiency with which Ae. aegypti mosquitoes transmit DENV and ZIKV is significantly higher than that for Ae. albopictus. The latter is highly transmissible only under specific genotypes or environmental conditions, as is the case in the Americas (*14*).

3. Epidemiological profile of chikungunya globally

Since the outbreak of CHIK around the world, there have been tens of millions of confirmed cases: Between 2015 and 2023, 909 suspected deaths due to CHIKV were reported in Brazil, where the northeastern region (such as Ceará) was a hot spot (*15*). India, Brazil, Sudan, and Thailand were countries with a sustained high incidence from 2011 to 2022, while Latin America and the Caribbean have historically had a high incidence (*16*). Over the past decade, chikungunya has broken through its traditional tropical-subtropical range and spread to Mediterranean Europe and the southern United States (*17*). Deaths mostly occur due to multi-organ infections (the brain, lungs, liver, and kidneys), central nervous system injury, and hemodynamic disorders. Survivors had fever and joint pain, while 21.9% of those who died had neurological symptoms (*e.g.*, confusion or syncope) (*15*). RT-PCR is the gold standard for diagnosis in the acute phase (within 7 days of symptom onset) and can detect viral RNA. IgM/IgG ELISA is used for convalescent diagnosis, and double serum (7–14 days apart) is required to confirm a 4-fold increase in the antibody titer. Virus isolation is time-consuming and complex due to the need for a BSL-3 laboratory and is only used for research. Rapid diagnostic tests (RDTs) have developed 43 antibody RDTs and 2 antigen RDTs worldwide, but the sensitivity varies greatly (20–100%); 23 are approved by ANVISA in Brazil but are not registered with the FDA/EMA (*18*). As of July 31, 2025, more than 5,158 cases of CHIK (Figures 2 and 3) have been confirmed in Guangdong Province, China, and a level III response has been launched in Foshan (*19,20*). The chikungunya outbreak in the region in 2025 had a faster rate of community transmission compared to dengue outbreaks in previous years in Guangdong, indicating a higher baseline vector density or earlier silent transmission. In addition, It is expected that the epidemic in Guangdong will continue for 1-2 months (Figure 4).

4. Ecological and climate factors

Air temperature determines the spread of dengue/chikungunya by affecting mosquito lifespan, bite rate, and virus replication (*21*). There is a significant spatial regression relationship between air temperature and mosquito vector density, and temperature changes can significantly affect the distribution and density of mosquito vectors, which in turn affect the transmission risk of dengue/chikungunya (*22*). WorldClim data provides high-resolution climate data on a global scale, which are valuable for studying the impact of climate factors such as temperature and precipitation on mosquito-borne diseases (*22*). The simulation results of the CMIP6 model suggest that future climate change will lead to higher temperatures and changes

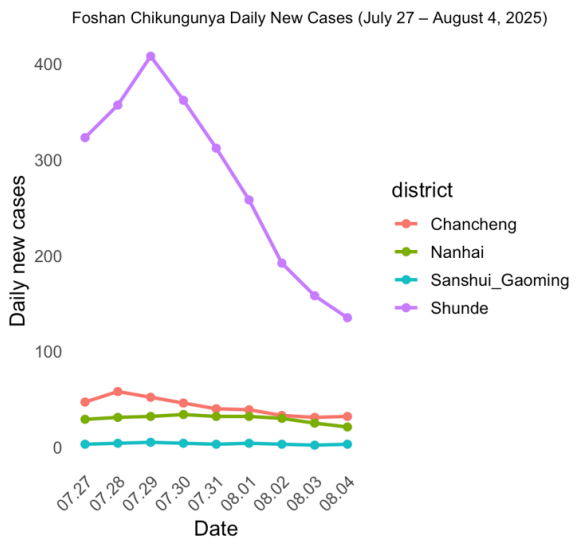

Figure 2. New chikungunya cases daily in Foshan (Jul 27– Aug 3, 2025).

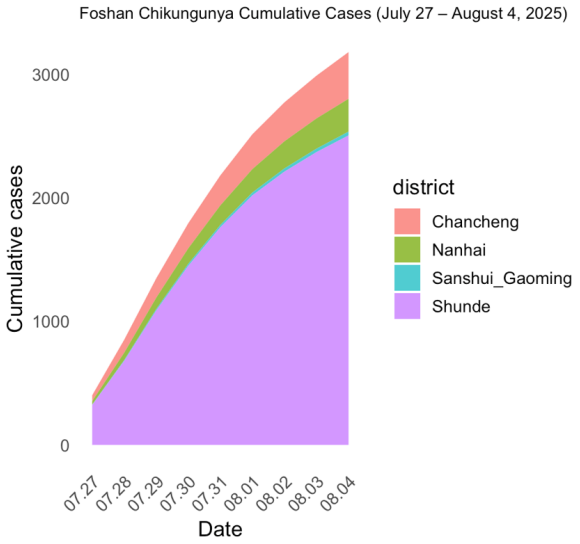

Figure 3. Cumulative chikungunya cases in Foshan (Jul 27– Aug 3, 2025).

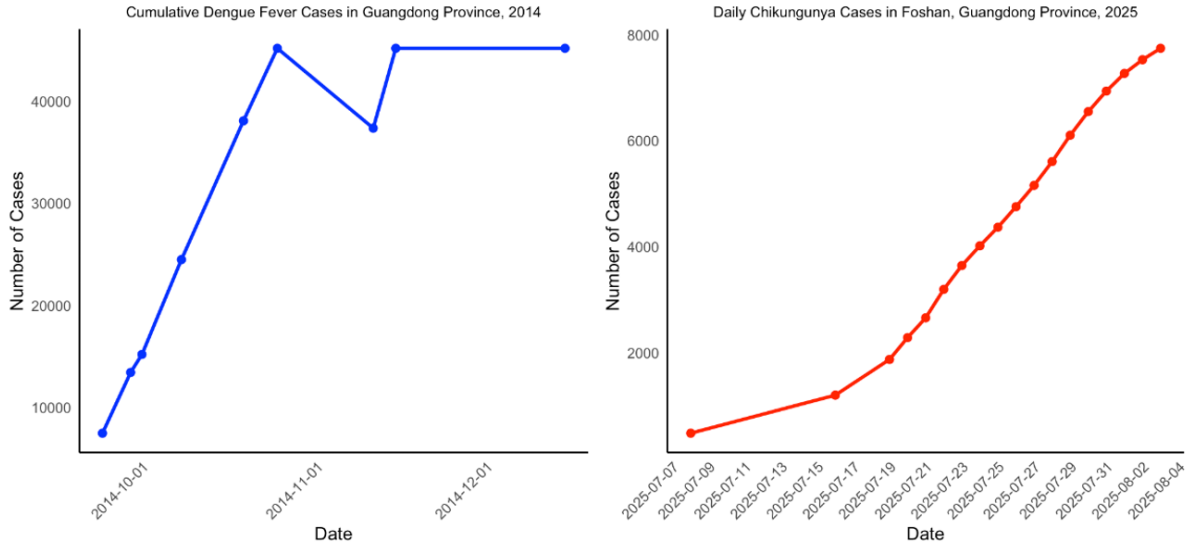

Figure 4. Comparison of the trends in the dengue fever epidemic in Guangdong in 2014 and the trends in the chikungunya epidemic in the City of Foshan, Guangdong Province in 2025.

in precipitation patterns, which may further expand the spread of mosquito-borne diseases such as dengue/chikungunya (*23*). Using the climate prediction model under the SSP5-8.5 scenario of CMIP6, researchers predict that by 2045, South China will be suitable for year-round CHIKV transmission, with an average annual increase of 1.3 times. The daily temperature difference (DTR) is more influential than the average air temperature in determining the transmission potential of dengue/chikungunya (*24,25*). The urban heat island effect can allow the virus to establish transmission in otherwise unsuitable areas, such as Europe (*24*). Indoor water containers become a breeding ground for Ae. aegypti mosquito larvae (*26*). International travel and air transport are the main drivers of cross-border transmission of mosquito-borne diseases such as chikungunya (*24*). Human communication patterns affect not only the spread of pathogens, but also daytime exposure to vectors (*27*).

5. Public health response

The Wolbachia strategy offers a promising solution to this public health challenge as a biological adaptation approach that can reduce mosquito populations and transmission capacity (*28*).There are currently no approved chikungunya or Zika vaccines, and strategic consideration is needed to develop chikungunya vaccines

Table 1. Progress of research on vaccines for major mosquito-borne diseases

Disease	Vaccine Name	Country/Institution	Current status	Key milestone
Dengue (DFV)	Qdenga (TAK-003)	Takeda, Japan	Marketed (EU, Indonesia, Brazil, *etc*.)	EU approval for ≥ 4 y, 2023
	Dengvaxia (CYD-TDV)	Sanofi-Pasteur, France	Marketed	/
	Butantan-DV	Butantan Institute & NIAID	Regulatory review Phase I/II ongoing	Phase III completed in 2023; approval anticipated in 2025
	mRNA vaccines	China, USA, Europe		First-in-human trials started in 2024
Chikungunya (CHIKV)	Vimkunya (inactivated)	Valneva, France/EU	Marketed	EU approval granted early in 2025
Zika (ZIKV)	DNA vaccine (GLS-5700)	Inovio, USA	Phase II (on hold)	First-in-human trial in Q3 2016
	mRNA vaccine (NIAID)	NIH, USA	Phase I ongoing	Trial initiated in 2019
Rift Valley Fever (RVFV)	mRNA vaccine (Afrigen)	Afrigen, South Africa & CEPI	Transition from pre-clinical to Phase I	Phase I started in 2025

(Table 1) and ensure equitable access in countries with limited resources (*29*). In November 2023, the US Food and Drug Administration (FDA) approved the VLA1553 live attenuated vaccine (brand name: IXCHIQ) for use in adults ≥ the age of 18 at risk of exposure to chikungunya (*30*). Based on 100% seroconversion and antibody levels over 12 months in a Phase 1 trial, VLA1553 proceed directly to the Phase 3 development phase (*31*). PXVX0317 (formerly VRC-CHKVLP059-00-VP) has completed Phase 1, 2, and 3 trials with a seroprotection rate of 98% in adults (*30,32*). In terms of epidemic surveillance, the association between international travel restrictions and declines in mosquito borne-disease can be assessed through epidemiological and viral genomic data. At the same time, targeted testing and monitoring of arrivals from high-risk areas can help guide public health strategies (*33*). Enhancing public health education is one of the priorities for future mosquito-borne disease prevention, addressing concerns, building trust, and ensuring that interventions are tailored to local needs through community engagement and dialogue (*34*). At present, there are some issues with this initiative, mainly because mobilizing and coordinating across departments and fields is difficult, and lack of leadership in one word. Surveillance of and research on vector-borne diseases, such as integrated vector management (IVM), should be enhanced (*34*). Since 2016, Zhejiang has promoted Four Pests-free Villages based on the "2017-2030 Global Vector Control Response" and integrated vector management, along with the One Health (OH) concept (*35-37*), which has significantly reduced the local mosquito density and thus reduced the incidence of mosquito-borne diseases (*38-40*). At the same time, China has issued a series of action guidelines for mosquito-borne diseases, aiming to provide action guidelines for high-incidence areas (*41*).

6. Conclusion

At present, the world is facing the "quadruple pressure" of climate change, the surge of people across borders, an increase in pesticide resistance, and a lag in vaccine research and development, and mosquito-borne diseases have become the latest problem with International Health Regulations. A model has predicted that the exposed population will jump from 4 billion to 5 billion by 2050. In light of this trend, China has taken the initiative to connect with the "2017-2030 Global Vector Control Response" at the international level, exported the dual-mode digital tool of the "Four Pests-free Village," and established a cross-border joint monitoring network. It continues to follow up on the WHO pre-certified live chikungunya vaccine and Wolbachia-infected mosquito release technology, and incorporate them into the national emergency technology reserve to provide a replicable and generalizable "Chinese plan" for the world.

In line with the OH concept and IVM, China has extensively integrated Zhejiang's "Four Pests-free Village" initiative with Guangdong's "sub-national sentinel framework response" experience. Zhejiang has achieved a 78% reduction in mosquito larvae density and a 90% reduction in adult mosquito density in Yuhang, Ningbo, and other places with environmental transformation. AI mosquito traps, UAV ultra-low-capacity spraying, Guangdong launched grid governance in Shunde, Foshan, subdivided 26 villages into 1,873 responsibility grids, and completed the first round of full-coverage household investigation within 4 days; the Brett index dropped from 12 to 3 within 5 days. Guangdong pioneered a joint team to ensure "disease control-housing construction-urban management-public security," inspecting 12,000 water containers per day. The experience of these two places jointly supports the "one-click start" of the national mosquito vector

rapid response system. Meteorology, customs, disease control, and agriculture four-dimensional real-time data are integrating to create a national big data platform for mosquito vectors. The cross-departmental "Minimum Common Task Package for Mosquito Vector Prevention and Control" has been issued to include responsibilities as part of the appraisal if government performance. Through the dual-track mobilization of the "Digital Sentinel" applet and the grassroots grid, 24-hour direct community reporting of risks has been achieved. The network's central feature will be its ability to institute an emergency response to a cross-border imported epidemic within 7 days, providing a Chinese paradigm for ecological, technological and governance innovation to facilitate global mosquito vector prevention and control.

Acknowledgements

The authors wish to express their sincere gratitude to everyone who provided various forms of assistance during the course of preparing this review.

Funding: None.

Conflict of Interest: The authors have no conflicts of interest to disclose.

References

1. WHO. Chikungunya. *https://www.who.int/health-topics/chikungunya/#tab=tab_1* (accessed August 5, 2025)
2. de Lima Cavalcanti TYV, Pereira MR, de Paula SO, Franca RFO. A review on chikungunya virus epidemiology, pathogenesis and current vaccine development. Viruses. 2022; 14:969.
3. Roques P, Fritzer A, Dereuddre-Bosquet N, Wressnigg N, Hochreiter R, Bossevot L, Pascal Q, Guehenneux F, Bitzer A, Corbic Ramljak I, Le Grand R, Lundberg U, Meinke A. Effectiveness of CHIKV vaccine VLA1553 demonstrated by passive transfer of human sera. JCI Insight. 2022; 7:e160173.
4. Ribeiro Dos Santos G, Jawed F, Mukandavire C, *et al*. Global burden of chikungunya virus infections and the potential benefit of vaccination campaigns. Nat Med. 2025; 31:2342-9.
5. Wang G, Zhang H, Gao J, Ma Z, Du Y, Liu Q, Liu Y, Xing D, Guo X, Zhao T, Jiang Y, Li C, Zhao T. Insecticide resistance status of Aedes aegypti in border areas of Yunnan Province. Pest Manag Sci. 2024; 80:2905-2919.
6. Qiu S, Guo J, Li P, *et al*. Source-tracking of the Chinese Chikungunya viruses suggests that Indian subcontinent and Southeast Asia act as major hubs for the recent global spread of Chikungunya virus. Virol J. 2021; 18:203.
7. Ren J, Chen Z, Ling F, Liu Y, Chen E, Shi X, Guo S, Zhang R, Wang Z, Sun J. The epidemiology of Aedes-borne arboviral diseases in Zhejiang, Southeast China: A 20 years population-based surveillance study. Front Public Health. 2023; 11:1270781.
8. Wu Y, Ling F, Hou J, Guo S, Wang J, Gong Z. Will integrated surveillance systems for vectors and vector-borne diseases be the future of controlling vector-borne diseases? A practical example from China. Epidemiol Infect. 2016; 144:1895-903.
9. YiH Li SJ, Meng Z, Yan Li, JianF He, ZeF Yang, XiQ Huang, QiH Guan, ZhuF Li, Qun Lin HL, WingS Li, YuenS Lam, Lei Zhou, Min Kang. An outbreak of chikungunya fever in China — Foshan City, Guangdong Province, China, July 2025. China CDC Wkly. 2025; dio:10.46234/ccdcw2025.172.
10. Wahid B, Ali A, Rafique S, Idrees M. Global expansion of chikungunya virus: Mapping the 64-year history. Int J Infect Dis. 2017; 58:69-76.
11. Lepore L, Vanlerberghe V, Verdonck K, Metelo E, Diallo M, Van Bortel W. Vector control for Aedes aegypti and Aedes albopictus mosquitoes implemented in the field in sub-Saharan Africa: A scoping review. PLoS Negl Trop Dis. 2025; 19:e0013203.
12. Gómez M, Martinez D, Muñoz M, Ramírez JD. Aedes aegypti and Ae. albopictus microbiome/virome: New strategies for controlling arboviral transmission? Parasit Vectors. 2022; 15:287.
13. Nie P, Feng J. Niche and range shifts of Aedes aegypti and Ae. albopictus suggest that the latecomer shows a greater invasiveness. Insects. 2023; 14:810.
14. Parry R, James ME, Asgari S. Uncovering the worldwide diversity and evolution of the virome of the mosquitoes *Aedes aegypti* and *Aedes albopictus*. Microorganisms. 2021; 9:1653.
15. de Souza WM, Fumagalli MJ, de Lima STS, *et al*. Pathophysiology of chikungunya virus infection associated with fatal outcomes. Cell Host Microbe. 2024; 32:606-622.e8.
16. Grabenstein JD, Tomar AS. Global geotemporal distribution of chikungunya disease, 2011-2022. Travel Med Infect Dis. 2023; 54:102603.
17. Lim A, Shearer FM, Sewalk K, *et al.* The overlapping global distribution of dengue, chikungunya, Zika and yellow fever. Nat Commun. 2025; 16:3418.
18. Moreira J, Brasil P, Dittrich S, Siqueira AM. Mapping the global landscape of chikungunya rapid diagnostic tests: A scoping review. PLoS Negl Trop Dis. 2022; 16:e0010067.
19. Gong ZY, WZ. A wake-up call triggered by chikungunya: The urgency of applying a One Health approach to the control of Aedes-borne diseases. Chin J Infectious Diseases. 2025; doi:10.3760/cma.j.cn311365 -20250729-00251 (in Chinese)
20. Feng Y CF, Yang Y, Lu HZ. From dengue to chikungunya: Guangdong as a sentinel for arboviral threats in East Asia. BioSci Trends. 2025: 19:368-373.
21. Caldwell JM, LaBeaud AD, Lambin EF, *et al*. Climate predicts geographic and temporal variation in mosquito-borne disease dynamics on two continents. Nat Commun. 2021; 12:1233.
22. Panagos P, Ballabio C, Meusburger K, Spinoni J, Alewell C, Borrelli P. Towards estimates of future rainfall erosivity in Europe based on REDES and WorldClim datasets. J Hydrol (Amst). 2017; 548:251-262.
23. Shakeel M, Abbas H, Ali Z, Tariq A, Almazroui M, Kader S. A novel framework for future drought characterization under ranked-based subset selection and weighted aggregative multi-modal ensemble of global climate models. J Environ Manage. 2025; 392:126692.
24. Tozan Y, Sjödin H, Muñoz Á G, Rocklöv J. Transmission

dynamics of dengue and chikungunya in a changing climate: Do we understand the eco-evolutionary response? Expert Rev Anti Infect Ther. 2020; 18:1187-1193.
25. Jian XY, Jiang YT, Wang M, Jia N, Cai T, Xing D, Li CX, Zhao TY, Guo XX, Wu JH. Effects of constant temperature and daily fluctuating temperature on the transovarial transmission and life cycle of Aedes albopictus infected with Zika virus. Front Microbiol. 2022; 13:1075362.
26. Turner EA, Clark SD, Peña-García VH, Christofferson RC. Investigating the effects of microclimate on arboviral kinetics in Aedes aegypti. Pathogens. 2024; 13:1105.
27. Knoblauch S, Heidecke J, de ARAA, *et al*. Modeling Intraday Aedes-human exposure dynamics enhances dengue risk prediction. Sci Rep. 2025; 15:7994.
28. Branda F, Cella E, Scarpa F, Slavov SN, Bevivino A, Moretti R, Degafu AL, Pecchia L, Rizzo A, Defilippo F, Moreno A, Ceccarelli G, Alcantara LCJ, Ferreira A, Ciccozzi M, Giovanetti M. Wolbachia-based approaches to controlling mosquito-borne viral threats: Innovations, AI integration, and future directions in the context of climate change. Viruses. 2024; 16:1868
29. Lee D, Kim K. A practical approach to multifaceted perspectives for sustainable international collaboration on mosquito-borne diseases in Southeast Asia. Acta Trop. 2024; 260:107481.
30. Weber WC, Streblow DN, Coffey LL. Chikungunya virus vaccines: A review of IXCHIQ and PXVX0317 from pre-clinical evaluation to licensure. BioDrugs. 2024; 38:727-742.
31. Chen LH, Fritzer A, Hochreiter R, Dubischar K, Meyer S. From bench to clinic: The development of VLA1553/IXCHIQ, a live-attenuated chikungunya vaccine. J Travel Med. 2024; 31:taae123.
32. Rosso A, Flacco ME, Cioni G, Tiseo M, Imperiali G, Bianconi A, Fiore M, Calò GL, Orazi V, Troia A, Manzoli L. Immunogenicity and safety of chikungunya vaccines: A systematic review and meta-analysis. Vaccines (Basel). 2024; 12:969.
33. Li N, Feng Y, Vrancken B, Chen Y, Dong L, Yang Q, Kraemer MUG, Pybus OG, Zhang H, Brady OJ, Tian H. Assessing the impact of COVID-19 border restrictions on dengue transmission in Yunnan Province, China: An observational epidemiological and phylogenetic analysis. Lancet Reg Health West Pac. 2021; 14:100259.
34. Kulkarni MA, Duguay C, Ost K. Charting the evidence for climate change impacts on the global spread of malaria and dengue and adaptive responses: A scoping review of reviews. Global Health. 2022; 18:1.
35. Winkler AS, Brux CM, Carabin H, *et al*. The Lancet One Health Commission: Harnessing our interconnectedness for equitable, sustainable, and healthy socioecological systems. Lancet. 2025; 406:501-570
36. Zhang W, Wang J, Liu Q, Gong Z. A review of pathogens transmitted by the container-inhabiting mosquitoes, Aedes Albopictus, A global public health threat. China CDC Wkly. 2023; 5:984-990.
37. Dantas-Torres F, Chomel BB, Otranto D. Ticks and tick-borne diseases: A One Health perspective. Trends Parasitol. 2012; 28:437-446.
38. Ni J, Wang J, Zhang W, Chen E, Gao Y, Sun J, Huang W, Xia J, Zeng W, Guo J, Gong Z. Sustainable control and integrated management through a One Health approach to mitigate vector-borne disease. One Health. 2025; 20:101018.
39. Ni J, Wang J, Fang C, Zhang W, Gong Z. A review of the latest control strategies for mosquito-borne diseases. China CDC Wkly. 2024; 6:852-856.
40. Gong ZY W, Li YF, Sun JM, Ni J, Gao Y, Xia J, Guo JX. Study on strategies of "four-pests free village"countryside sustainable vector management under the "One Health" in Zhejiang Province, China. Disease Surveillance. 2025; 40:1-6. (in Chinese)
41. Xinhua. China unveils 2025-2030 plan to promote healthy environments 2025 *https://govt.chinadaily.com.cn/s/202508/05/WS6891b3b0498edec913cdff15/china-unveils-2025-2030-plan-to-promote-healthy-environments.html*. (accessed August 5, 2025)

Received July 23, 2025; Revised August 5, 2025; Accepted August 7, 2025.

[§]These authors contributed equally to this work.
**Address correspondence to:*
Zhenyu Gong, Department of Communicable Disease Control and Prevention, Zhejiang Provincial Center for Disease Control and Prevention, Hangzhou 310051, China.
E-mail: zhygong@cdc.zj.cn

Released online in J-STAGE as advance publication August 8, 2025.

Review

DOI: 10.5582/bst.2025.01047

A technological convergence in hepatobiliary oncology: Evolving roles of smart surgical systems

Xuanci Bai[1,2,§], Runze Huang[1,2,§], Qinyu Liu[1,2], Xin Jin[1,2], Lu Wang[1,2], Wei Tang[3,4], Kenji Karako[4,*], Weiping Zhu[1,2,*]

[1] Department of Hepatic Surgery, Fudan University Shanghai Cancer Center, Shanghai Medical College, Fudan University, Shanghai, China;
[2] Department of Oncology, Shanghai Medical College Fudan University, Shanghai, China;
[3] National Center for Global Health and Medicine, Japan Institute for Health Security, Tokyo, Japan.
[4] Hepato-Biliary-Pancreatic Surgery Division, Department of Surgery, Graduate School of Medicine, The University of Tokyo, Tokyo, Japan.

SUMMARY: Cancer remains a major threat to human health, with the incidence of hepatobiliary tumors consistently high. Treatment methods for hepatobiliary tumors include surgical intervention, ablation, embolization, and pharmacological treatments, with surgery being a critical component of systemic treatment for patients with hepatobiliary tumors. Compared to other methods, surgery is the most effective way to remove tumors and improve survival rates, serving as the cornerstone of various treatment strategies. However, the large patient population sometimes burdens traditional surgical oncology. In recent years, rapidly advancing artificial intelligence (AI) technologies, characterized by efficiency, precision, and personalization, align well with the treatment philosophy of oncologic surgery. Increasing studies have shown that AI-assisted surgical oncology outperforms traditional approaches in many aspects. This review, based on machine learning, neural networks, and other AI techniques, discusses the various applications of AI throughout the entire process of hepatobiliary tumor surgical treatment, including diagnostic assistance, surgical decision-making, intraoperative support, postoperative monitoring, risk assessment, and medical education. It offers new insights and directions for the integration and application of AI in oncologic surgery.

Keywords: neural networks, surgical navigation, radiomics, postoperative monitoring, medical education

1. Introduction

Despite the rapid advancement of medical technology, malignant tumors remain a major threat to life and health (*1*). Among all cancers, primary liver cancer is one of the top five most common cancers globally and the second leading cause of cancer-related deaths, imposing a heavy burden on Chinese society (*2*). Compared to liver cancer, although gallbladder cancer is less common, its five-year survival rate is lower, and it has a higher degree of malignancy. Furthermore, the liver is a common metastatic site for other cancers, and liver metastasis often indicates that the disease has reached an advanced stage, with a lower survival rate. Over time, we have witnessed changing standards of treatment for cancer, ranging from nihilism (misconceptions, poor referrals, and debulking surgeries) to realism (formal R0 resections, complex/composite resections, laparascopic resections, and robotic resections) to modern-day activism (conservative surgery, brachytherapy, and targeted therapy). Examples of the conservative trend include treatment of liver cancer, which has moved from resection to ablation (RFA, TACE, MWA, and SIRT) (*66*). Currently, multiple treatment strategies exist for liver tumors (*3*), among which surgery offers the most complete removal of tumors, significantly improving survival rates and lifespan (*4*). For biliary tumors, treatment plans must be tailored based on the patient's liver function, number of tumors, and extent of metastasis, though surgery remains the most effective approach (*5*).

However, despite surgery being an irreplaceable component in the treatment of hepatobiliary tumors, many existing issues still interfere with the efficiency and speed of the surgical process. For example, when faced with complex anatomical structures, less experienced surgeons may require more time and effort to complete tumor resections. Additionally, when cirrhosis occurs, the fragile vascular physiology imposes stricter demands on the surgeon's expertise.

With the continuous development of computer science, artificial intelligence algorithms, including neural networks and deep learning, have shown remarkable potential. In the field of oncological

surgery, artificial intelligence (AI) models improve a range of processes, from preoperative assessment and intraoperative assistance to postoperative monitoring, continuously enhancing patient survival rates and quality of life, and sparking a revolution in traditional surgical models. The effectiveness of AI models is a topic of discussion, but existing studies have shown that AI-assisted surgeries, such as robotic liver resections, are comparable to traditional open liver resections in terms of treatment outcomes, while also reducing postoperative complications and improving survival rates (*6*).

2. Definition of artificial intelligence

2.1. General definitions for AI

In recent years, AI models have become increasingly prevalent in research, not only accelerating the collection, generation, transformation, and processing of data, but also assisting in experimental design and the formulation and validation of hypotheses based on experimental findings. These models have provided researchers with powerful tools, facilitating greater cross-disciplinary collaboration and integration (*7*) (Figure 1).

The field of artificial intelligence encompasses a vast range of learning algorithms, with machine learning models, particularly those based on neural networks, being among the most prominent. Commonly employed AI techniques in the healthcare domain include traditional machine learning models and deep learning models. Artificial intelligence serves as a technological nexus, bridging robotics and virtual reality with conventional surgical paradigms to facilitate their synergistic integration.

Broadly speaking, machine learning refers to the process of fitting predictive models to data or identifying patterns within data (*8*). Depending on whether the model is based on neural networks, machine learning can be classified into traditional machine learning and neural network-based machine learning. Furthermore, it can be categorized into supervised and unsupervised learning, depending on whether the training data requires classification and labeling. Traditional machine learning typically offers faster development and testing for a given problem, but often requires the dataset examples to have a consistent number of features (*8*). In practical applications, algorithms usually need to be adjusted according to the specific characteristics of the dataset, enabling faster and more accurate processing. This, in turn, increases the confidence in the derived conclusions and enhances the generalizability of the trained models (Figure 2).

2.2. Supervised learning and unsupervised learning

Supervised learning is the most commonly used form of machine learning. In supervised learning, the system is provided with features related to the learning objectives (such as patient demographics and risk factors) and the expected outcome measures (such as diagnosis or clinical events). The goal is to identify the relationship between these two elements within the dataset. When combined

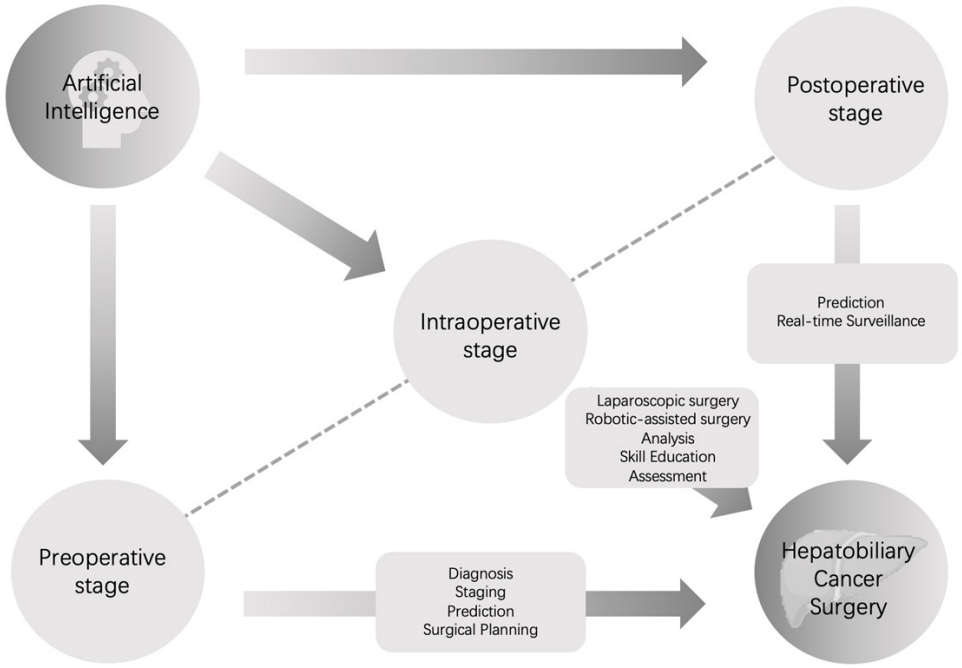

Figure 1. Integrating Artificial Intelligence Across Stages of Hepatobiliary Cancer Surgery. This figure illustrates the integration of artificial intelligence (AI) into various stages of hepatobiliary cancer surgery. AI supports the preoperative stage by enhancing diagnosis, staging, prediction, and surgical planning. During the intraoperative stage, AI facilitates laparoscopic and robotic-assisted surgeries, real-time analysis, skill education, and surgical assessment. In the postoperative stage, AI aids in prediction and real-time surveillance, ensuring better patient monitoring and outcomes.

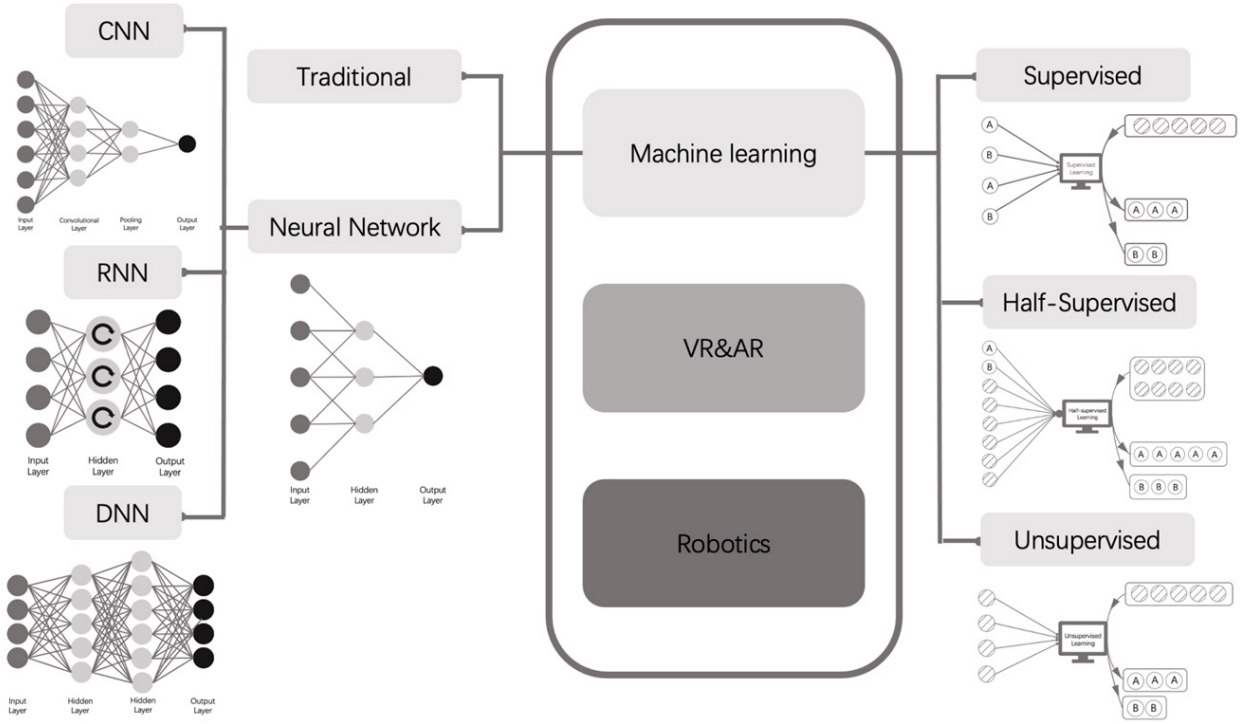

Figure 2. Framework of Machine Learning and Neural Network Applications in Medicine. This figure illustrates machine learning frameworks and neural networks in medical applications. Neural network models, including CNNs, RNNs, and DNNs, are shown on the left. The center highlights traditional and neural network-based machine learning, extending into VR, AR, and robotics. The right categorizes machine learning into supervised, semi-supervised, and unsupervised learning methods.

with other algorithms, supervised learning models can significantly enhance the speed of data processing.

In December 2023, Dong H developed a self-supervised learning model based on a sliding window (SW) approach (SWSSL) for anomaly detection in medical imaging. Validated with datasets of mammography and pneumonia X-ray images, SWSSL demonstrated its capability for specialized detection on high-resolution medical imaging datasets, helping to mitigate the problem of over-sampling in anomaly detection when relying solely on the SW method (*9*).

Beyond identifying abnormal attributes in instances, in January 2023, Tu Z and colleagues incorporated 2D image keypoints and texture from monocular video into a self-supervised learning model to achieve 3D organ reconstruction. Whether for joint movement or hand texture, self-supervised learning exhibited remarkable performance (*10*).

Unlike supervised learning, in unsupervised learning, the computer is provided with unlabeled data records (*13*), and through a self-reinforcing mechanism, it identifies and determines whether there are any underlying relationships between the input data. In other words, it learns from its own predictions and strengthens the associations between existing experiences and appropriate responses. This characteristic of unsupervised learning enables it to explore hidden relationships across multiple domains such as genomics, metabolomics, and biochemistry, providing researchers with new insights and fostering the development of interdisciplinary research directions. However, because unsupervised learning lacks associated constraints, the experiences derived from repeated self-reinforcement may not always be accurate or beneficial. The effectiveness of unsupervised learning is closely related to the consistency between the provided data characteristics and the task at hand. The higher the consistency, the stronger the effectiveness of unsupervised learning (*11*).

Similar to supervised learning, unsupervised learning can also identify abnormal structures in images by learning from normal images, enabling preoperative diagnosis and assessment of tumors. For instance, in April 2021, Baur C incorporated an unsupervised auto-learning model into the interpretation of brain MRI images, utilizing three different unsupervised auto-learning models to analyze a brain MRI dataset. Although none of the models perfectly reproduced the healthy model corresponding to the given images, the use of the unsupervised auto-learning model alleviated the need for manual segmentation of experimental data and highlighted the differences between the images in the dataset and the normal healthy model (*12*).

Beyond supervised and unsupervised learning, there exists a hybrid model that harnesses the strengths of both, known as semi-supervised learning. This approach is capable of analyzing substantial volumes of unlabeled data, concurrently leveraging a modest amount of labeled data to bolster the model's capacity for data pattern

recognition. As a result, it enhances the velocity and precision of extracting insights from extensive datasets, thereby alleviating the research burden and streamlining the analytical process for scientists (*13*).

2.3. Neural network

Neural network models represent the foundational cornerstone of deep learning, encompassing a spectrum of architectures such as traditional artificial neural networks, convolutional neural networks (CNNs), deep neural networks (DNNs), and recurrent neural networks (RNNs). Notably, CNNs have demonstrated exceptional efficacy in the recent empirical literature (*14*).

The canonical structure of a convolutional neural network is comprised of alternating convolutional and pooling layers. The convolutional layers are instrumental in identifying local feature connections from preceding layers, while pooling layers aggregate semantically analogous features into singular representations. This arrangement, when stacked with fully connected layers, forms the backbone of a conventional CNN (*15*). Advanced deep convolutional neural networks have notably ameliorated the generalization weakness of their traditional counterparts, securing their status as the algorithm of choice within the domain of medical image analysis. A case in point is the research by Huang J *et al*. in 2022, wherein a CNN-based model was crafted to discern features indicative of epilepsy and schizophrenia from static and dynamic brain MRI imagery, thereby enhancing the discriminative power of the CNN-learned features (*16*). Nonetheless, deep learning models are susceptible to overfitting on training datasets, necessitating rigorous external validation to ensure their generalizability and robustness (*17*).

2.4. Artificial intelligence-enhanced robotic surgery

The field of medical robotics has become increasingly prominent within the domain of surgical procedures, with the da Vinci Surgical System exemplifying a paradigmatic application of artificial intelligence in this context. Endorsed by the U.S. Food and Drug Administration in 2005 for its utility in soft tissue surgery, this system stands unparalleled. The system operates on a master-slave remote control paradigm, where the surgeon, positioned adjacent to the patient at the master console, directs the robot (*18*). Equipped with cameras and tremor-free instruments, the robot provides the surgeon with an enhanced, magnified 3D perspective of the surgical field (*65*). The slave arm executes the surgical maneuvers on the patient, while the surgeon views the internal organs through the endoscope and adjusts the position of the slave robot by manipulating the master manipulator (*18*). The robotic surgery system boasts several key advantages, including a broader range of motion compared to laparoscopic instruments, an expanded visual field for surgery, and heightened precision in operational maneuvers.

Within the specialty of urology, robotic radical cystectomy (RARC) has reached a level of maturity. RARC is associated with reduced blood loss and transfusion rates when juxtaposed with the traditional open radical cystectomy (ORC), while maintaining superior oncological outcomes and comparable postoperative complication rates (*20*). A systematic comparison of the safety and efficacy of da Vinci robotic surgery versus conventional surgery was conducted by Liu Z *et al*. in 2017. Their findings indicated that, in the context of cervical cancer, robotic surgery outperformed both traditional open and conventional laparoscopic approaches in terms of blood loss, surgical extent, and intraoperative complications (*21*). Despite the current limitations in cost-effectiveness associated with robotic surgery, the technology is evolving, with anticipated advancements on the horizon that promise to further refine its utility and efficiency.

AI-assisted surgical interventions represent an emerging trend in the future of oncological surgery. By developing intelligent models trained on real-world surgical datasets, robotic systems can acquire capabilities to perform routine procedural tasks. For instance, a preclinical study demonstrated the feasibility of autonomous small bowel end-to-end anastomosis in porcine models under laparoscopic settings, achieving operative independence from surgeon intervention (*67*). Similar applications hold transformative potential in hepatobiliary tumor resection, such as AI-guided suction devices for intraoperative hemorrhage clearance or automated systems for superficial wound closure. By analyzing multimodal historical imaging datasets including CT and MRI scans alongside intraoperative computer vision systems for real-time image interpretation, artificial intelligence achieves automated tumor-to-healthy tissue discrimination in robotic surgery, enabling submillimeter precision during oncological resection (*70*).

2.5. Virtual reality

Virtual reality (VR) technology engenders a comprehensively immersive experience by leveraging a triad of sensory modalities: visual, auditory, and tactile. This multifaceted approach integrates real-time interactive images and sounds, simulating a spectrum of sensations akin to those encountered in the physical world, thereby harnessing the capabilities of multi-sensory technology.

Virtual reality has been extensively integrated into surgical skill acquisition, demonstrating dual transformative capacities. Primarily, machine learning frameworks incorporating clustering algorithms enable quantitative profiling of trainees' learning curves through VR-derived kinematic data analytics. By predicting proficiency attainment thresholds—quantified as

required trial repetitions—these AI-powered systems assess individual competency trajectories, thereby facilitating personalized training protocols that optimize group training efficiency (*69*). Secondarily, within interactive VR surgical simulations, artificial intelligence dynamically adapts procedural pathways based on operator decisions while cross-referencing institutional databases to issue preemptive alerts regarding high-risk anatomical zones, such as error-prone dissection planes and vasculature proximity. AI-powered VR systems deliver personalized cognitive behavioral therapy (CBT) and mindfulness interventions for postoperative cancer patients, creating secure virtual environments to enhance therapeutic efficacy and improve quality of life (*68*).

In a pivotal 2019 study, Tao XM unveiled a revolutionary set of skin haptic interfaces, remarkable for their wireless control and power capabilities, eschewing the need for batteries. These innovative interfaces pave the way for augmenting VR and augmented reality (AR) experiences, transcending the traditional confines of vision and hearing (*22*). Their applications extend to material development, device design, integration strategies, and system layout. The utility of VR is already evident in various medical disciplines, including cardiac intervention (*23*), intensive care (*24*), laparoscopic surgery (*25*), and mental health (*26*). Anticipating future trends, the medical field is poised to witness an increasing integration of virtual and augmented reality technologies, heralding a new era in healthcare innovation.

3. Preoperative stage

Accurate preoperative diagnosis and assessment are critical components in the surgical management of hepatobiliary tumors. In line with clinical practice guidelines for hepatocellular carcinoma published by various countries, including China (*4*), Japan (*28*), South Korea (*29*), and the United Kingdom (*30*), definitive diagnosis of primary hepatocellular carcinoma can be established through pathology, immunohistochemistry, and radiomics. Regarding preoperative evaluation, the commonly utilized staging systems include the Barcelona Clinic Liver Cancer (BCLC) staging system (*29,30*), the modified International Union Against Cancer (mUICC) staging system (*28*), and the Chinese Liver Cancer (CNLC) staging system (*4*). These systems incorporate clinical characteristics such as tumor size and number, vascular and bile duct invasion, lymph node involvement, distant metastasis, and liver function status. Staging systems serve to aid in decision-making and prognostic assessment; thus, high-precision preoperative staging is a key determinant in the surgical treatment of hepatobiliary tumors.

Traditional preoperative risk prediction and surgical planning are subject to variations influenced by individual surgeons, potentially introducing bias. The incorporation of artificial intelligence-assisted diagnostics and staging evaluations can circumvent such variability, thereby optimizing surgical outcomes and contributing to a more standardized and refined approach to patient management.

3.1. AI-Enabled histopathology

The stratification of tumors and the assessment of microvascular invasion (MVI) are acknowledged as the two paramount prognostic indicators in the surgical management of hepatic malignancies (*31*). At present, the detection of MVI primarily relies on histopathological examination of postoperative specimens, underscoring the critical role of AI-driven models in preoperative evaluation of MVI for informed clinical decision-making. In a seminal study from 2009, Varghese *et al*. harnessed preoperative variables, including tumor volume, to train an Artificial Neural Network (ANN), revealing that the ANN outperformed conventional linear predictive models in accurately discerning Hepatocellular Carcinoma (HCC) grade and MVI status (*32*). Advancing this field, in 2020, Saillard *et al*. employed a pre-trained Convolutional Neural Network (CNN) to analyze HCC histopathological images, extracting features that were subsequently utilized to develop two distinct deep learning algorithms for the prediction of patient survival rates. These models demonstrated superior predictive accuracy over composite scoring systems in estimating survival rates for liver cancer, thereby validating the integrative application of AI algorithms in the preoperative prognostic assessment of HCC patients (*27*). Furthermore, the identification of specific immunogenic genes within histopathological images has been instrumental in shaping preoperative strategies. Illustratively, in 2022, Zeng *et al*. from France developed a suite of deep learning models, including Patch, Multiple Instance Learning (MIL), and Clustering Constrained Attention Multiple Instance Learning (CLAM), for the analysis of histological images. Notably, the CLAM model excelled in screening efficacy, showing promise in predicting patient responsiveness to immunotherapeutic interventions (*17*).

3.2. AI-radiomics

Integrating AI with hepatobiliary oncologic radiomics for enhanced preoperative diagnostics, surgical planning, and prognostic assessment: Mazzaferro V *et al*. in 2008 established that microvascular invasion, irrespective of its size or quantity, is a significant predictor of poorer overall survival and increased post-transplant recurrence in hepatocellular carcinoma patients undergoing liver transplantation, marking it as the most influential covariate impacting patient prognosis (*34*). Current preoperative assessments are limited to providing pre-emptive probabilities of MVI or associated

biomarkers (*34*). The deployment of AI models allows for a more nuanced prediction of MVI extent and a more accurate prognostic determination. A case in point is the work by Xia TY in 2023, who pioneered a radiomics methodology predicated on preoperative multiphase CT scans to prognosticate MVI, utilizing hybrid models to forecast MVI status and, consequently, patient recurrence survival rates (*33*).

Expanding beyond MVI, the evaluation of donor liver volume and vascular architecture is pivotal to the safety and postoperative survival rates associated with liver transplantation. Conventionally, the preoperative phase of living donor liver transplantation necessitates manual segmentation of the resection plane by surgeons based on CTA imaging of hepatic vasculature (*37*). This process is not only labor-intensive but also susceptible to inaccuracies due to the partial volume effect, which can obscure tumor margins. The incorporation of artificial intelligence significantly bolsters the reproducibility of tumor segmentation (*36*). Illustratively, between 2022 and 2023, Oh N developed a residual model based on pre-transplant CTA data, facilitating the construction of a 3D liver model. This model enabled automated segmentation of liver parenchyma and vascular structures, as well as volumetric assessment derived from these segmentations. When compared to manual surgical segmentation, artificial intelligence yielded more consistent and stable outcomes, demonstrating a higher correlation with actual values (*37*).

Although PET-CT possesses significant diagnostic and evaluative utility, its broader implementation is hindered by inherent limitations, such as fusion artifacts and motion-related image degradation. The deployment of artificial intelligence technologies offers a means to mitigate these issues by reducing image noise and augmenting image quality. Consequently, AI enhances the accuracy of preoperative diagnostic procedures, tumor staging, therapeutic decision-making, and the assessment of treatment responses (*38*).

In the context of metastatic liver cancer, artificial intelligence holds substantial promise. For instance, in the case of colorectal cancer, preoperative identification of high-risk patients with a poor prognosis is crucial to avoid unnecessary aggressive treatment. A pertinent example is the work by Keyl J *et al*. in 2022, who utilized a pre-trained convolutional neural network-based nnU-Net model to extract prognostic parameters from abdominal CT images of patients with colorectal liver metastases. This included the automatic segmentation of metastatic liver lesions, leading to the development of a personalized survival risk prediction model for advanced-stage colorectal cancer patients (*39*).

Furthermore, additional clinical indicators significantly influence the preoperative risk assessment of hepatobiliary tumors. In 2024, Jin Y *et al*. introduced a suite of five machine learning-based models, encompassing Logistic Regression (LR), Random Forest, Extreme Gradient Boosting (XGB), Light Gradient Boosting Machine (LGBM), and Artificial Neural Networks. These models were employed to assess various patient examination indicators, with the ANN model demonstrating superior performance. It was capable of early identification of patients at an elevated risk of Posthepatectomy Liver Failure (PHLF) (*35*).

4. Intraoperative stage

Within the realm of surgical interventions, the caliber of the surgeon's technical skills often surpasses perioperative care in its impact on surgical outcomes. Proficiency in surgical techniques is paramount for the prevention of intraoperative complications such as hemorrhage or vascular occlusion and may correlate with reduced procedural durations, consequently mitigating the risk of postoperative morbidity (*40*).

4.1. Artificial intelligence-enhanced laparoscopic surgery

Laparoscopic surgery has become widely recognized for its merits. When juxtaposed with open surgical approaches, laparoscopy is associated with more favorable rates of perioperative and postoperative complications, as well as abbreviated hospitalization periods (*41*). However, as the indications for laparoscopy broaden, several challenges have come to light. Notably, the intricate anatomical structures and vascular networks encircling the liver necessitate meticulous identification and circumvention during laparoscopic procedures. Furthermore, the insufflation of gas for pneumoperitoneum can induce liver displacement, distortion, and torsion of the hepatic hilum vessels (*19*), creating disparities between preoperative radiographic images and intraoperative realities, which augments the complexity of the surgery (*42*).

Incorporating artificial intelligence technologies such as Virtual Reality and Deep Learning (DL) in laparoscopic hepatectomy is considered to mitigate the aforementioned challenges to a significant extent. DL can be utilized to identify anatomical structures within the surgical field, thereby reducing the risk of adverse events. In 2020, Madani A *et al*. trained a pyramid scene parsing network model, composed of a convolutional neural network and a multi-scale pyramid pooling module, using several frames from laparoscopic cholecystectomy videos. The results demonstrated that this model could efficiently recognize key structures in the surgical area during laparoscopic cholecystectomy (LC) (*43*).

The integration of VR with surgical procedures has emerged as a hot topic in recent research. In 2022, Ramalhinho J interactively superimposed a 3D model of the liver, including the liver surface, vasculature, and virtual target tumors, onto laparoscopic liver views. Three methods were compared for participant tumor localization accuracy: unguided, single-screen display,

and augmented reality overlay. The conclusion was that any form of guided display improved performance and usability compared to unguided surgery, with the single-screen display showing the most significant results. However, participants expressed a preference for AR overlay that enhanced precision, which in turn augmented the performance and decision-making capabilities during laparoscopic surgery (*44*).

4.2. Robotic-assisted surgery

The field of robotic surgery has witnessed remarkable progress in recent years, with substantial evidence supporting the safety and efficacy of robotic hepatectomy as a viable alternative to laparoscopic hepatectomy. A study conducted by Jeong IG in 2017 indicated that robotic-assisted nephrectomy does not confer an increased risk of major complications when compared with laparoscopic approaches (*45*). Furthermore, a multicenter randomized controlled trial by Feng Q *et al*. in 2022 demonstrated that, for patients with mid to low rectal cancer, robotic surgery offers superior tumor resection, reduced surgical trauma, and enhanced postoperative recovery over conventional laparoscopic surgery (*46*). In 2024, Birgin E conducted a single-center randomized controlled single-blind study on patients with resectable liver malignancies, revealing no significant disparities in quality of life, perioperative morbidity, or oncological outcomes between those who underwent robotic hepatectomy and those who underwent laparoscopic hepatectomy (*47*).

In liver transplantation, the utilization of robotic systems is in its nascent stages. In April 2022, South Korea executed a pioneering procedure involving laparoscopic donor and recipient hepatectomy followed by robotic-assisted living donor liver transplantation. The robotic surgery system's advantages include stable visualization, facilitation of microsurgery, and incorporation of tremor correction and articular motion functionalities (*48*). In August 2023, Saudi Arabia marked a milestone by performing the world's first fully robotic living donor hepatectomy and liver transplantation implantation using the da Vinci Surgical System. This approach, in comparison to traditional hepatectomy, offers a three-dimensional perspective of the surgical field, enhanced visualization, and refined manipulation capabilities (*49*).

Despite the demonstrated precision, efficacy, and safety of robotic surgery systems in hepatobiliary tumor surgery, several challenges persist, including the constraints of limited operating space, restricted visual fields, difficulties in hepatic venous anastomosis due to excessive tension, and the high skill requirements for surgeons.

4.3. Artificial intelligence in the analysis of laparoscopic videos

The observation of surgical procedures is a rich educational resource for resident surgeons. A cardinal principle in medical education, particularly when acquiring new operative techniques, is encapsulated by the adage 'see one, do one, teach one'(*50*). By observing hepatobiliary surgical procedures, novice learners can closely scrutinize the intricacies of the operative process, thereby gaining a more profound comprehension of the anatomy and vascular architecture of abdominal organs such as the liver, as well as becoming intimately acquainted with the diseases under study and the procedural steps involved.

Laparoscopic surgery is particularly amenable to the development of audio-visual educational materials, with surgical videos providing an accurate depiction of the surgeon's viewpoint, thereby offering students essential insights into anatomical structures and the sequential steps of surgery (*51*). The task of manually indexing and analyzing these surgical videos is arduous and resource-intensive; thus, the employment of artificial intelligence for automated video indexing and as an adjunct in surgical pedagogy is not only warranted but also offers significant pedagogical benefits.

The task of automatically discerning surgical phases from video footage alone is inherently challenging. Initially, there is a paucity of inter-class distinctions between various phases, while substantial intra-class differences exist within the same phase. Additionally, the scene's clarity is often compromised due to factors such as camera movement and surgical smoke, which exacerbate the complexity of phase identification. Thirdly, the camera may not persistently capture the surgical field during intricate procedures, introducing extraneous imagery into the video record (*52*). Therefore, to attain a high degree of accuracy in the automated segmentation of surgical phases, it is essential to develop a model capable of concurrently harnessing video imagery characteristics, kinetic features, and spatiotemporal attributes.

Among the myriad of artificial intelligence algorithms, convolutional neural networks (CNNs) hold a distinct advantage in image and object recognition, frequently being employed to identify intraoperative characteristics in surgical videos, such as insufflation pressure and operating table position, tool usage and application—including the timestamps for the deployment and cessation of each instrument, as well as their usage patterns—video feature extraction and learning, such as operation recognition, and the prediction of remaining surgery time, thereby enhancing the efficiency of video review (*53*). In July 2016, a study from France introduced a novel CNN framework named EndoNet, designed for detection tasks like tool presence and phase identification, while also analyzing the impact of the volume of training data on the framework's performance. This addressed phase identification issues in laparoscopic surgery and pioneered a new method for

directly learning visual features from raw images (*54*). In May 2018, researchers from Hong Kong presented an innovative approach to surgical video analysis by integrating deep residual networks (ResNet) and long short-term memory networks (LSTM) to construct a novel recurrent convolutional neural network framework, SV-RCNet. This framework extracts visual features and temporal models from videos and is trained to recognize discriminative features in surgical videos, thereby accurately identifying surgical procedural steps (*52*). In March 2020, a study from Japan utilized a CNN model capable of identifying specific segments of laparoscopic surgery, assigning video clips to predefined surgical phases based on their characteristics, and constructed a large annotated surgical video dataset. Training CNNs requires a substantial amount of labeled data and significant parallel computing power, making this research conducive to the refinement of CNN models with potential applications in automated video indexing and surgical skill assessment (*55*).

Artificial intelligence is increasingly being employed for the identification of fundamental motion characteristics within surgical video contexts, particularly for simple procedural actions such as suturing, needle passing, and knot tying that are common in robotic minimally invasive surgery. The categorization of surgical gestures from video data is facilitated through the application of Linear Dynamical Systems (LDS), Bag of Features (BoF) models, and a synergistic approach combining both methods within a Multiple Kernel Learning (MKL) framework. These methodologies have been instrumental in the development of an integrated framework that amalgamates video and kinematic data, thereby enhancing the accuracy of surgical gesture recognition. This advanced capability not only aids in the execution of rudimentary surgical maneuvers and provides real-time feedback on procedural deficiencies, which can lead to reduced operative times and diminished surgical risks, but also serves to activate context-sensitive information displays. Specifically, when an AI model identifies a particular gesture, it can anticipate the forthcoming actions required by the surgeon and the tools that may be necessary, thus enabling the surgical team to proactively prepare for imminent procedural steps (*56*).

4.4. Artificial intelligence in surgical skill education

Within the paradigm of Robotic-Assisted Surgery (RAS), the conventional pedagogical approach of 'see one, do one, teach one' (*50*) has reached its limitations. The adoption of Virtual Reality models for the simulation of RAS procedures represents a more efficacious avenue for novice surgeons to acquire and refine their technical skills. While research has yet to fully substantiate the effectiveness of VR in mastering the intricacies of robotic surgery, the anticipated enhancements in VR model precision are poised to markedly transform the landscape of surgical training (*57*). In 2018, a forward-looking randomized controlled trial in the United Kingdom assessed the comparative efficacy of 2D video and 360-degree VR video in teaching single-handed surgical knotting. The study revealed that the immersive 360-degree VR video significantly outperformed the 2D modality in knotting skill acquisition, underscoring its potential as an educational tool (*58*).

4.5. Application of artificial intelligence in the video-assessment of surgical skills

The American Board of Surgery (ABS) recognized in 2023 the utility of Video-Based Assessment (VBA) as a complementary tool for evaluating the technical proficiency of surgeons, affirming its role in identifying and providing corrective feedback to underperforming surgical candidates (*59*). Machine learning techniques offer the promise of streamlining VBA processes, thereby augmenting the efficacy of skill evaluation. Nonetheless, the deployment of unsupervised deep learning models can engender what is often referred to as the 'black box' phenomenon, which obscures the rationale behind the scoring, thus impeding the ability of the assessed to discern the factors contributing to their performance outcomes (*60*).

5. Postoperative stage

5.1. Artificial intelligence for postoperative morbidity and survival prediction

Deficiencies in postoperative surveillance can result in the misclassification of patients at elevated risk for complications, potentially leading to their placement in general wards rather than intensive care units. In 2021, Loftus TJ utilized established random forest and nearest neighbor algorithms to demonstrate that inadequate triage is associated with increased mortality and morbidity rates (*61*). The principal aim of AI in the postoperative period is to prognosticate the likelihood of postoperative complications, promptly detect suboptimal triage scenarios, and facilitate real-time patient monitoring. The MySurgeryRisk AI system, which integrates electronic health record (EHR) data with machine learning algorithms—including generalized additive models and random forests—predicts postoperative complications with increasing accuracy as more features are incorporated into the model (*62*). In June 2021, Bonde A conducted a retrospective analysis, training a deep neural network (DNN)-based postoperative risk prediction model within a structured electronic medical data system. This analysis revealed that the model's performance escalated with an increased number of input variables, and even in the presence of incomplete data, the DNN model retained a high degree of precision.

This suggests that the integration of AI has transformed postoperative complications from an enigmatic risk into a foreseeable and manageable one (*63*).

For the majority of neoplasms, postoperative pathological imagery is intricately linked to patient prognosis. The deployment of convolutional neural network models on whole-slide imaging (WSI) of digital histological sections from patients who have undergone hepatectomy for hepatocellular carcinoma enables the generation of risk scores. These models can autonomously pinpoint the most pertinent risk areas within WSI, thereby facilitating the prediction of post-hepatectomy survival. Their predictive accuracy surpasses that of traditional prognostic models that combine clinical, biological and pathological characteristics. Nonetheless, there is a dearth of research attesting to the robust generalizability of these models (*27*).

5.2. AI-based real-time postoperative surveillance

AI-based real-time postoperative surveillance holds a distinct advantage in its capacity to merge instantaneous predictive analytics with clinical and digital workflows. The transformative potential of AI in enhancing patient survival rates following surgery is most notably realized through its capability to identify shifts in patient clinical trajectories in a timely manner. This facilitates a smooth transition between in-hospital and remote monitoring, such as through smartwatch-integrated remote electrocardiogram monitoring. Such technology encourages prompt medical engagement among postoperative patients, thereby reducing postoperative morbidity rates (*64*). This strategy not only bolsters patient outcomes but also optimizes the allocation of healthcare resources, contributing to a more efficient and sustainable healthcare delivery model.

6. Conclusion

In recent years, hepatobiliary tumors have persistently posed a significant threat to human health. The convergence of AI models, including neural networks, deep learning, robotic technology, and virtual reality, with surgical treatments for hepatobiliary tumors has the potential to yield a synergistic effect that surpasses the sum of its individual components. This integration aims to achieve the dual goals of reducing incidence and mortality rates, while simultaneously improving survival rates and prolonging survival times. Although AI faces a myriad of challenges in practical application, such as issues of medical ethics and morality, the need for clinical standardization, and concerns regarding model generalizability, the ongoing refinement and training of AI technologies are poised to exert a profound influence on the paradigms of hepatobiliary tumor surgery.

Funding: This work was supported by National Natural Science Foundation of China (81874056,81874182), the National Key Research and Development Plan of the Ministry of Science and Technology (2022YFE0125300), the Shanghai Natural Science Foundation Project (22ZR1413300), and the Public Health Bureau Foundation of Shanghai (202240240, 201940043).

Conflict of Interest: The authors have no conflicts of interest to disclose.

References

1. Siegel RL, Miller KD, Wagle NS, Jemal A. Cancer statistics, 2023. CA Cancer J Clin. 2023; 73:17-48.
2. European Association for the Study of the Liver. EASL Clinical Practice Guidelines: Management of hepatocellular carcinoma. J Hepatol. 2018; 69:182-236.
3. Vogel A, Martinelli E, ESMO Guidelines Committee. Updated treatment recommendations for hepatocellular carcinoma (HCC) from the ESMO Clinical Practice Guidelines. Ann Oncol. 2021; 32:801-805.
4. Xie D, Shi J, Zhou J, Fan J, Gao Q. Clinical practice guidelines and real-life practice in hepatocellular carcinoma: A Chinese perspective. Clin Mol Hepatol. 2023; 29:206-216.
5. Kubo S, Shinkawa H, Asaoka Y, *et al.* Liver Cancer Study Group of Japan Clinical Practice Guidelines for Intrahepatic Cholangiocarcinoma. Liver Cancer. 2022; 11:290-314.
6. Di Benedetto F, Magistri P, Di Sandro S, *et al.* Safety and Efficacy of Robotic vs Open Liver Resection for Hepatocellular Carcinoma. JAMA Surg. 2023; 158:46-54.
7. Wang H, Fu T, Du Y, *et al.* Scientific discovery in the age of artificial intelligence. Nature. 2023; 620:47-60.
8. Greener JG, Kandathil SM, Moffat L, Jones DT. A guide to machine learning for biologists. Nat Rev Mol Cell Biol. 2022; 23:40-55.
9. Dong H, Zhang Y, Gu H, Konz N, Zhang Y, Mazurowski MA. SWSSL: Sliding window-based self-supervised learning for anomaly detection in high-resolution images. IEEE Trans Med Imaging. 2023; 42:3860-3870.
10. Tu Z, Huang Z, Chen Y, Kang D, Bao L, Yang B, Yuan J. Consistent 3D hand reconstruction in video *via* self-supervised learning. IEEE Trans Pattern Anal Mach Intell. 2023; 45:9469-9485.
11. Bröker F, Holt LL, Roads BD, Dayan P, Love BC. Demystifying unsupervised learning: how it helps and hurts. Trends Cogn Sci. 2024; 28:974-986.
12. Baur C, Denner S, Wiestler B, Navab N, Albarqouni S. Autoencoders for unsupervised anomaly segmentation in brain MR images: A comparative study. Med Image Anal. 2021; 69:101952.
13. Handelman GS, Kok HK, Chandra RV, Razavi AH, Lee MJ, Asadi H. eDoctor: machine learning and the future of medicine. J Intern Med. 2018; 284:603-619.
14. Litjens G, Kooi T, Bejnordi BE, Setio AAA, Ciompi F, Ghafoorian M, van der Laak JAWM, van Ginneken B, Sánchez CI. A survey on deep learning in medical image analysis. Med Image Anal. 2017; 42:60-88.
15. LeCun Y, Bengio Y, Hinton G. Deep learning. Nature. 2015; 521:436-444.
16. Huang J, Wang M, Ju H, Shi Z, Ding W, Zhang D. SD-CNN: A static-dynamic convolutional neural network

for functional brain networks. Med Image Anal. 2023; 83:102679.
17. Zeng Q, Klein C, Caruso S, *et al.* Artificial intelligence predicts immune and inflammatory gene signatures directly from hepatocellular carcinoma histology. J Hepatol. 2022; 77:116-127.
18. Moustris GP, Hiridis SC, Deliparaschos KM, Konstantinidis KM. Evolution of autonomous and semi-autonomous robotic surgical systems: a review of the literature. Int J Med Robot. 2011; 7:375-392.
19. Di Saverio S, Catena F. Images in clinical medicine: Rotation of the liver in pneumoperitoneum. N Engl J Med. 2014; 371:e29.
20. Aron M, Gill IS. Robotic radical cystectomy: so far, so good--what next? Eur Urol. 2015; 67:361-362.
21. Liu Z, Li X, Tian S, Zhu T, Yao Y, Tao Y. Superiority of robotic surgery for cervical cancer in comparison with traditional approaches: A systematic review and meta-analysis. Int J Surg. 2017; 40:145-154.
22. Tao XM. Virtual and augmented reality enhanced by touch. Nature. 2019; 575:453-454.
23. Mahtab EAF, Egorova AD. Current and future applications of virtual reality technology for cardiac interventions. Nat Rev Cardiol. 2022; 19:779-780.
24. Bruno RR, Wolff G, Wernly B, Masyuk M, Piayda K, Leaver S, Erkens R, Oehler D, Afzal S, Heidari H, Kelm M, Jung C. Virtual and augmented reality in critical care medicine: the patient's, clinician's, and researcher's perspective. Crit Care. 2022; 26:326.
25. Jin C, Dai L, Wang T. The application of virtual reality in the training of laparoscopic surgery: A systematic review and meta-analysis. Int J Surg. 2021; 87:105859.
26. May M. How virtual reality therapy is shaping mental health. Nat Med. 2024; 30:1797-1799.
27. Saillard C, Schmauch B, Laifa O, *et al.* Predicting survival after hepatocellular carcinoma resection using deep learning on histological slides. Hepatology. 2020; 72:2000-2013.
28. Koga H, Iwamoto H, Suzuki H, Shimose S, Nakano M, Kawaguchi T. Clinical practice guidelines and real-life practice in hepatocellular carcinoma: A Japanese perspective. Clin Mol Hepatol. 2023; 29:242-251.
29. Korean Liver Cancer Association (KLCA), National Cancer Center (NCC) Korea. 2022 KLCA-NCC Korea practice guidelines for the management of hepatocellular carcinoma. Clin Mol Hepatol. 2022; 28:583-705.
30. Suddle A, Reeves H, Hubner R, Marshall A, Rowe I, Tiniakos D, Hubscher S, Callaway M, Sharma D, See TC, Hawkins M, Ford-Dunn S, Selemani S, Meyer T. British Society of Gastroenterology guidelines for the management of hepatocellular carcinoma in adults. Gut. 2024; 73:1235-1268.
31. Jonas S, Bechstein WO, Steinmüller T, Herrmann M, Radke C, Berg T, Settmacher U, Neuhaus P. Vascular invasion and histopathologic grading determine outcome after liver transplantation for hepatocellular carcinoma in cirrhosis. Hepatology. 2001; 33:1080-1086.
32. Cucchetti A, Piscaglia F, Grigioni AD, Ravaioli M, Cescon M, Zanello M, Grazi GL, Golfieri R, Grigioni WF, Pinna AD. Preoperative prediction of hepatocellular carcinoma tumour grade and micro-vascular invasion by means of artificial neural network: a pilot study. J Hepatol. 2010; 52:880-888.
33. Xia TY, Zhou ZH, Meng XP, Zha JH, Yu Q, Wang WL, Song Y, Wang YC, Tang TY, Xu J, Zhang T, Long XY, Liang Y, Xiao WB, Ju SH. Predicting microvascular invasion in hepatocellular carcinoma using CT-based radiomics model. Radiology. 2023; 307:e222729.
34. Mazzaferro V, Llovet JM, Miceli R, *et al.* Predicting survival after liver transplantation in patients with hepatocellular carcinoma beyond the Milan criteria: a retrospective, exploratory analysis. Lancet Oncol. 2009; 10:35-43.
35. Jin Y, Li W, Wu Y, Wang Q, Xiang Z, Long Z, Liang H, Zou J, Zhu Z, Dai X. Online interpretable dynamic prediction models for clinically significant posthepatectomy liver failure based on machine learning algorithms: a retrospective cohort study. Int J Surg. 2024; 110:7047-7057.
36. Liu Z, Wang S, Dong D, Wei J, Fang C, Zhou X, Sun K, Li L, Li B, Wang M, Tian J. The applications of radiomics in precision diagnosis and treatment of oncology: Opportunities and challenges. Theranostics. 2019; 9:1303-1322.
37. Oh N, Kim JH, Rhu J, Jeong WK, Choi GS, Kim J, Joh JW. Comprehensive deep learning-based assessment of living liver donor CT angiography: From vascular segmentation to volumetric analysis. Int J Surg. 2024; 110:6551-6557.
38. Dai J, Wang H, Xu Y, Chen X, Tian R. Clinical application of AI-based PET images in oncological patients. Semin Cancer Biol. 2023; 91:124-142.
39. Keyl J, Hosch R, Berger A, *et al.* Deep learning-based assessment of body composition and liver tumour burden for survival modelling in advanced colorectal cancer. J Cachexia Sarcopenia Muscle. 2023; 14:545-552.
40. Birkmeyer JD, Finks JF, O'Reilly A, Oerline M, Carlin AM, Nunn AR, Dimick J, Banerjee M, Birkmeyer NJ; Michigan Bariatric Surgery Collaborative. Surgical skill and complication rates after bariatric surgery. N Engl J Med. 2013; 369:1434-1442.
41. Koffron A, Geller D, Gamblin TC, Abecassis M. Laparoscopic liver surgery: shifting the management of liver tumors. Hepatology. 2006; 44:1694-1700.
42. Zhang Y, Zou Y, Liu PX. Point cloud registration in laparoscopic liver surgery using keypoint correspondence registration network. IEEE Trans Med Imaging. 2025; 44:749-760.
43. Madani A, Namazi B, Altieri MS, Hashimoto DA, Rivera AM, Pucher PH, Navarrete-Welton A, Sankaranarayanan G, Brunt LM, Okrainec A, Alseidi A. Artificial intelligence for intraoperative guidance: using semantic segmentation to identify surgical anatomy during laparoscopic cholecystectomy. Ann Surg. 2022; 276:363-369.
44. Ramalhinho J, Yoo S, Dowrick T, Koo B, Somasundaram M, Gurusamy K, Hawkes DJ, Davidson B, Blandford A, Clarkson MJ. The value of augmented reality in surgery - a usability study on laparoscopic liver surgery. Med Image Anal. 2023; 90:102943.
45. Jeong IG, Khandwala YS, Kim JH, Han DH, Li S, Wang Y, Chang SL, Chung BI. Association of robotic-assisted vs laparoscopic radical nephrectomy with perioperative outcomes and health care costs, 2003 to 2015. JAMA. 2017; 318:1561-1568.
46. Feng Q, Yuan W, Li T, Tang B, Jia B, Zhou Y, Zhang W, Zhao R, Zhang C, Cheng L, Zhang X, Liang F, He G, Wei Y, Xu J; REAL Study Group. Robotic versus laparoscopic surgery for middle and low rectal cancer (REAL): short-term outcomes of a multicentre randomised controlled trial. Lancet Gastroenterol Hepatol. 2022; 7:991-1004.

47. Birgin E, Heibel M, Hetjens S, Rasbach E, Reissfelder C, Téoule P, Rahbari NN. Robotic versus laparoscopic hepatectomy for liver malignancies (ROC'N'ROLL): a single-centre, randomised, controlled, single-blinded clinical trial. Lancet Reg Health Eur. 2024; 43:100972.
48. Lee KW, Choi Y, Hong SK, Lee S, Hong SY, Suh S, Han ES, Yi NJ, Suh KS. Laparoscopic donor and recipient hepatectomy followed by robot-assisted liver graft implantation in living donor liver transplantation. Am J Transplant. 2022; 22:1230-1235.
49. Broering DC, Raptis DA, Elsheikh Y. Pioneering fully robotic donor hepatectomy and robotic recipient liver graft implantation - a new horizon in liver transplantation. Int J Surg. 2024; 110:1333-1336.
50. Weiner SG. Invoking a medical axiom for buprenorphine initiation-see one, do one, teach one. JAMA Netw Open. 2023; 6:e2342980.
51. Celentano V, Smart N, McGrath J, *et al.* LAP-VEGaS practice guidelines for reporting of educational videos in laparoscopic surgery: a joint trainers and trainees consensus statement. Ann Surg. 2018; 268:920-926.
52. Jin Y, Dou Q, Chen H, Yu L, Qin J, Fu CW, Heng PA. SV-RCNet: workflow recognition from surgical videos using recurrent convolutional network. IEEE Trans Med Imaging. 2018; 37:1114-1126.
53. Garrow CR, Kowalewski KF, Li L, Wagner M, Schmidt MW, Engelhardt S, Hashimoto DA, Kenngott HG, Bodenstedt S, Speidel S, Müller-Stich BP, Nickel F. Machine learning for surgical phase recognition: a systematic review. Ann Surg. 2021; 273:684-693.
54. Twinanda AP, Shehata S, Mutter D, Marescaux J, de Mathelin M, Padoy N. EndoNet: a deep architecture for recognition tasks on laparoscopic videos. IEEE Trans Med Imaging. 2017; 36:86-97.
55. Kitaguchi D, Takeshita N, Matsuzaki H, Oda T, Watanabe M, Mori K, Kobayashi E, Ito M. Automated laparoscopic colorectal surgery workflow recognition using artificial intelligence: experimental research. Int J Surg. 2020; 79:88-94.
56. Zappella L, Béjar B, Hager G, Vidal R. Surgical gesture classification from video and kinematic data. Med Image Anal. 2013; 17:732-745.
57. Breda A, Territo A. Virtual reality simulators for robot-assisted surgery. Eur Urol. 2016; 69:1081-1082.
58. Yoganathan S, Finch DA, Parkin E, Pollard J. 360° virtual reality video for the acquisition of knot tying skills: a randomised controlled trial. Int J Surg. 2018; 54:24-27.
59. Pryor AD, Lendvay T, Jones A, Ibáñez B, Pugh C. An American Board of Surgery pilot of video assessment of surgeon technical performance in surgery. Ann Surg. 2023; 277:591-595.
60. Wu J, Hines OJ. Using artificial intelligence to assess surgeon skill. JAMA Surg. 2023; 158:e231140.
61. Loftus TJ, Ruppert MM, Ozrazgat-Baslanti T, Balch JA, Efron PA, Tighe PJ, Hogan WR, Rashidi P, Upchurch GR Jr, Bihorac A. Association of postoperative undertriage to hospital wards with mortality and morbidity. JAMA Netw Open. 2021; 4:e2131669.
62. Ren Y, Loftus TJ, Datta S, Ruppert MM, Guan Z, Miao S, Shickel B, Feng Z, Giordano C, Upchurch GR Jr, Rashidi P, Ozrazgat-Baslanti T, Bihorac A. Performance of a machine learning algorithm using electronic health record data to predict postoperative complications and report on a mobile platform. JAMA Netw Open. 2022; 5:e2211973.
63. Bonde A, Varadarajan KM, Bonde N, Troelsen A, Muratoglu OK, Malchau H, Yang AD, Alam H, Sillesen M. Assessing the utility of deep neural networks in predicting postoperative surgical complications: a retrospective study. Lancet Digit Health. 2021; 3:e471-e485.
64. Oikonomou EK, Khera R. Artificial intelligence-enhanced patient evaluation: bridging art and science. Eur Heart J. 2024; 45:3204-3218.
65. Lee N. Robotic surgery: where are we now? Lancet. 2014; 384:1417.
66. Joshi RM, Telang B, Soni G, Khalife A.. Overview of perspectives on cancer, newer therapies, and future directions. Oncol Transl Med. 2024; 10:105-109.
67. Saeidi H, Opfermann JD, Kam M, Wei S, Leonard S, Hsieh MH, Kang JU, Krieger A. Autonomous robotic laparoscopic surgery for intestinal anastomosis. Sci Robot. 2022; 7:eabj2908.
68. Horesh D, Kohavi S, Shilony-Nalaboff L, Rudich N, Greenman D, Feuerstein JS, Abbasi MR. Virtual reality combined with artificial intelligence (VR-AI) reduces hot flashes and improves psychological well-being in women with breast and ovarian cancer: a pilot study. Healthcare (Basel). 2022; 10:2261.
69. Gao Y, Kruger U, Intes X, Schwaitzberg S, De S. A machine learning approach to predict surgical learning curves. Surgery. 2020; 167:321-327.
70. Moglia A, Georgiou K, Georgiou E, Satava RM, Cuschieri A. A systematic review on artificial intelligence in robot-assisted surgery. Int J Surg. 2021; 95:106151.

Received July 3, 2025; Revised July 29, 2025; Accepted August 2, 2025.

[§]These authors contributed equally to this work.

*Address correspondence to:
Kenji Karako, Hepato-Biliary-Pancreatic Surgery Division, Department of Surgery, Graduate School of Medicine, The University of Tokyo, Tokyo 113-8655, Japan.
E-mail: tri.leafs@gmail.com

Weiping Zhu, Department of Hepatic Surgery, Fudan University Shanghai Cancer Center, Shanghai Medical College, Fudan University, Shanghai, 200032, China.
E-mail: wpzhush@hotmail.com

Released online in J-STAGE as advance publication August 4, 2025.

Original Article

DOI: 10.5582/bst.2025.01178

Survival benefit of adjuvant chemotherapy and individualized prognosis in resected cHCC-CCA

Bo Sun[1,2,§], Yimeng Wang[1,3,§], Ruyu Han[1,3], Yuren Xia[1,4], Meng Zhao[1,5], Liyu Sun[1,3], Xiaochen Ma[1,3], Tianqiang Song[1,3], Xiangdong Tian[1,6,*], Wenchen Gong[1,7,*], Lu Chen[1,3,*]

[1] Tianjin Medical University Cancer Institute and Hospital, National Clinical Research Center for Cancer, National Key Laboratory of Druggability Evaluation and Systematic Translational Medicine, Tianjin Key Laboratory of Digestive Cancer, Tianjin's Clinical Research Center for Cancer, Tianjin, China;
[2] The Second Department of Breast Cancer, Tianjin Medical University Cancer Institute and Hospital, Tianjin, China;
[3] Department of Hepatobiliary Cancer, Liver cancer research center, Tianjin Medical University Cancer Institute and Hospital, Tianjin, China;
[4] Department of Pediatric Oncology, Tianjin Medical University Cancer Institute and Hospital, Tianjin, China;
[5] Department of Clinical laboratory, Tianjin Medical University Cancer Institute and Hospital, Tianjin, China;
[6] Department of Endoscopy, Tianjin Medical University Cancer Institute and Hospital, Tianjin, China;
[7] Department of Pathology, Tianjin Medical University Cancer Institute and Hospital, Tianjin, China.

SUMMARY: Combined hepatocellular-cholangiocarcinoma (cHCC-CCA) is a rare malignancy with poor prognosis and unclear benefit from adjuvant chemotherapy. To identify the appropriate candidates for postoperative adjuvant chemotherapy in cHCC-CCA, we developed a prognostic model to predict patient outcomes and stratify populations accordingly. This retrospective study included 75 cHCC-CCA patients treated at Tianjin Medical University Cancer Institute and Hospital from 2009 to 2019. Prognostic factors were identified via univariate and multivariate Cox regression. Model performance was assessed using ROC curves, calibration plots, and decision curve analysis. Propensity score matching (PSM) was applied to reduce bias. Adjuvant chemotherapy significantly improved overall survival (OS) in Kaplan–Meier (p = 0.029) and PSM analyses (p = 0.0011). Five independent prognostic factors were identified: macrovascular invasion, lymph node metastasis, the largest tumor size >5 cm, the high expression of CD8, and the high expression of FOXP3. The nomogram showed good predictive performance. Among high-risk patients stratified by the nomogram, those receiving adjuvant chemotherapy had longer OS (p = 0.013), while no significant benefit was observed in the low-risk group (p = 0.084). Adjuvant chemotherapy improves postoperative survival in cHCC-CCA. The nomogram provides individualized risk stratification and may inform treatment decisions.

Keywords: cHCC-CCA, adjuvant chemotherapy, prognostic nomogram, overall survival, propensity score matching

1. Introduction

cHCC-CCA is a rare primary liver malignancy characterized by the dual histopathological features of hepatocellular carcinoma (HCC) and cholangiocarcinoma (CCA) (*1-4*). Despite its relatively low incidence, cHCC-CCA demonstrates highly aggressive biological behavior due to its pronounced molecular and histological heterogeneity (*5-10*). As a result, CHC patients have a higher postoperative recurrence rate and significantly worse long-term survival compared to individuals with either HCC or CCA alone. Surgical resection currently stands as the sole potentially curative treatment for cHCC-CCA (*11,12*). However, the postoperative recurrence rate surpasses 50%, and the absence of standardized adjuvant treatment strategies poses a significant challenge to enhancing long-term survival outcomes for these patients (*1,13-15*).

In recent years, adjuvant chemotherapy has been extensively demonstrated to markedly enhance the prognosis of different solid tumors post-surgery (*16-18*). However, the clinical use of adjuvant chemotherapy in cHCC-CCA is contentious due to the insufficient high-quality supporting evidence. This issue is partly due to the rarity of cHCC-CCA and limited disease-specific understanding (*19*). In addition, reliable prognostic models based on large-scale real-world data are lacking, making it difficult to accurately identify appropriate candidates for adjuvant therapy and predict therapeutic efficacy (*12*).

With the progress in precision medicine, creating personalized postoperative management plans for patients with cHCC-CCA is now a pressing clinical

concern (*20-22*). Nomograms, which are practical predictive tools based on multivariate analysis, can combine clinicopathological features and molecular biomarkers to offer personalized quantitative survival predictions (*23*). While nomograms have been widely used to assess prognosis in different cancers, there is currently no validated nomogram model for predicting postoperative survival in patients with cHCC-CCA. Consequently, the potential clinical utility of nomograms in guiding adjuvant treatment decisions for cHCC-CCA remains unexplored (*24*).

In this study, we systematically reviewed the clinical and follow-up data of 75 patients with cHCC-CCA who underwent curative resection at Tianjin Medical University Cancer Institute and Hospital between 2009 and 2019. We successfully developed a prognostic nomogram model with strong predictive performance by combining conventional clinicopathological characteristics with tumor immune microenvironment indicators based on rigorous univariate and multivariate Cox regression analyses. This model accurately predicted 2-year and 3-year survival probabilities and demonstrated practical clinical utility through decision curve analysis (DCA). Additionally, using propensity score matching (PSM), we confirmed the survival benefit of adjuvant chemotherapy across different risk strata.

The study findings offer strong evidence to support individualized postoperative management and adjuvant treatment decision-making for patients with cHCC-CCA. This support may advance the clinical application of precise therapeutic strategies, leading to enhanced long-term survival outcomes in this complex patient group.

2. Materials and Methods

2.1. Patient selection

This retrospective study included 75 patients diagnosed with combined hepatocellular-cholangiocarcinoma (cHCC-CCA) who underwent curative resection at Tianjin Medical University Cancer Institute and Hospital between January 2009 and December 2019. The study was approved by the institutional ethics committee (Approval ID: bc20240058), and all participants provided written informed consent. The study was conducted in accordance with the Declaration of Helsinki. All patients had pathologically confirmed cHCC-CCA without evidence of distant metastasis or macrovascular invasion, and complete follow-up data were available.

Inclusion criteria were as follows (A-E):
A. Age ≥ 18 years.
B. Pathological confirmation of cHCC-CCA.
C. Underwent curative (R0) resection.
D. Availability of complete clinical and follow-up data.
E. No macrovascular invasion or distant metastasis at diagnosis.

Exclusion criteria were as follows (A-D):
A. Follow-up duration less than 1 month.
B. History of other malignancies.
C. Non-R0 resection.
D. Incomplete clinical data.

2.2. Data collection

Clinical data were collected retrospectively, including (A-F):
A. Demographic information: sex, age, HBV infection, and Liver cirrhosis.
B. The liver function parameters included albumin (ALB), total bilirubin (TBIL), and prothrombin time (PT).
C. Tumor characteristics included the largest tumor size, microvascular invasion, presence of satellite nodules and CD8, CD20, FOXP3, PD-L1 expression level.
D. Serum tumor markers included alpha-fetoprotein (AFP).
E. Treatment information: whether adjuvant chemotherapy was administered.
F. Follow-up data: overall survival (OS) and survival status.

2.3. Survival analysis

Survival curves were produced utilizing the Kaplan–Meier method, and group differences were evaluated through the log-rank test. OS was defined as the time from the surgery date to the death date or last follow-up. Survival differences between the adjuvant chemotherapy and non-chemotherapy groups were examined in the total cohort (n = 75), within risk-level-stratified subgroups, and in the PSM-matched cohort. Statistical significance was determined as a two-sided P-value of < 0.05.

2.4. Quantification of immune cell infiltration in tumor tissues of patients with cHCC-CCA

Immune cell infiltration in tumor tissues was quantified using formalin-fixed paraffin-embedded (FFPE) samples from patients with cHCC-CCA. Ten high-power fields (HPF, ×200 magnification) were randomly chosen for each patient to guarantee unbiased sampling. Immunohistochemical (IHC) staining with validated markers specific to immune cell populations was used to identify immune cells. Positively stained cells with distinct membrane and cytoplasmic patterns were manually counted in each field. The average count of immune cells per HPF was calculated for each patient, and an overall mean immune cell density was calculated to establish a stratification threshold. Patients were then grouped into categories (*e.g.*, high *vs*. low immune cell infiltration) based on comparisons with this threshold. This standardized approach ensures reproducibility and facilitates the evaluation of immune microenvironment

heterogeneity in cHCC-CCA.

2.5. Identification of prognostic factors and nomogram construction

Univariate Cox proportional hazards regression analysis was employed to identify potential prognostic factors for OS, with a screening threshold set at $p < 0.157$ to prevent the exclusion of crucial variables (*25*). Variables with $p < 0.157$ were subsequently included in multivariate Cox regression analysis to determine independent prognostic factors. Following these findings, five variables (macrovascular invasion, lymph node metastasis, largest tumor size > 5 cm, CD8 expression, and FOXP3 expression) were integrated into the final nomogram for predicting the probabilities of 2- and 3-year survival.

The postoperative risk score for cHCC-CCA is determined by the following formula: 44.88 × (the largest tumor size) + 59.65 × (the high expression of FOXP3 status) + 100 × (the low expression of CD8 status) + 65.2 × (major vascular invasion status) + 80.53 × (lymph node metastasis status). In this scoring system, variables are assigned numerical values according to specific criteria (A-F).

A: The largest tumor size: 1 if > 5 cm, 0 if ≤ 5 cm;
B: FOXP3 status: 1 if high expression, 0 if low expression;
C: CD8 status: 1 if low expression, 0 if high expression;
D: Major vascular invasion: 1 if present, 0 if absent;
E: Lymph node metastasis: 1 if present, 0 if absent.
F: Patients were categorized into high-risk (total score > 130) or low-risk (total score ≤ 130) groups according to their cumulative scores.

2.6. IHC staining

Consecutive sections of FFPE tissues were prepared and processed using a Ventana BenchMark XT apparatus (Ventana Medical Systems). The sections underwent dewaxing, followed by antigen retrieval at 95°C for 30 min in EDTA repair solution. Subsequently, the sections were exposed to primary antibodies against CD8 (SP57, Ventana Medical Systems, Tucson, AZ, USA), CD20 (L26, Ventana, Tucson, AZ, USA), FOXP3 (236A/E7, ab20034, Abcam, Cambridge, UK), and programmed death ligand 1 (PD-L1) (SP263, Ventana, Tucson, AZ, USA) at 37°C for 32 min. Following this, the sections were treated with an HRP-conjugated secondary antibody (multimer HRP, Ventana) for 10 min at room temperature. Positive signals were detected using diaminobenzidine and then counterstained with hematoxylin.

2.7. Evaluation of model performance

The nomogram's calibration performance was evaluated by generating calibration curves from 100 bootstrap resamples, showing strong agreement between the predicted and observed survival outcomes.

To assess the clinical utility of the model, DCA was conducted to evaluate the net clinical benefit over a range of threshold probabilities. The nomogram consistently showed superior clinical decision-making advantages in comparison to the traditional staging system for both 2-year and 3-year survival predictions.

2.8. PSM

To reduce potential confounding variables affecting the assessment of adjuvant chemotherapy, PSM was utilized to equalize the baseline characteristics between the chemotherapy and non-chemotherapy cohorts. The propensity scores were calculated using clinical and pathological variables, including sex, age, HBV infection status, presence of cirrhosis, the largest tumor size, satellite nodules, microvascular and macrovascular invasion, lymph node metastasis, and immune markers.

A 1:2 nearest-neighbor matching algorithm was utilized, yielding a matched cohort of 19 patients in the chemotherapy group and 38 patients in the non-chemotherapy group. The baseline characteristics post-matching were adequately balanced ($p > 0.05$).

Subsequent survival analysis was conducted on the matched cohort to further confirm the survival advantage of adjuvant chemotherapy after accounting for confounding variables.

2.9. Software

All statistical analyses were conducted using R software (version 4.4.3) and SPSS software (version 29.0). Nomogram construction and validation utilized the R packages "rms", "survival", and "timeROC". Calibration curves were generated through bootstrap resampling. The DCA was conducted using the "ggDCA" package. All statistical tests were two-sided, with significance set at $p < 0.05$.

3. Results

3.1. Patient enrollment and study flow

This retrospective cohort study was conducted at Tianjin Medical University Cancer Institute and Hospital, involving patients diagnosed with cHCC-CCA who underwent curative resection from January 2009 to December 2019. Following rigorous inclusion and exclusion criteria, the final analysis comprised 75 patients.

Among these patients, 19 (25.3%) received adjuvant chemotherapy, while 56 (74.7%) did not. Comprehensive clinicopathological characteristics and follow-up data were gathered, and long-term follow-up was conducted

to assess the impact of adjuvant chemotherapy on OS. Histopathologic and immunophenotypic analyses confirmed the biphenotypic differentiation of the tumor, with both hepatocellular and cholangiocellular components identified (Figures 1A-G). The overall workflow of patient screening, inclusion, and cohort analysis is summarized in a schematic diagram (Figure 1H).

3.2. Efficacy of adjuvant chemotherapy

Kaplan–Meier survival analysis revealed that patients who received adjuvant chemotherapy had a significantly better OS compared to those who did not receive adjuvant chemotherapy (p = 0.029; Figure 2A). PSM was used to mitigate potential confounding factors influencing the evaluation of adjuvant chemotherapy. Following matching, 57 patients were enrolled, with 19 and 38 patients in the chemotherapy and non-chemotherapy groups, respectively. The baseline characteristics after matching were well balanced (Table 1).

The proportion of male patients was 73.7% in the chemotherapy group and 84.2% in the non-chemotherapy group (p = 0.553). The median age was 54 years (IQR: 49–65) and 55.5 years (IQR: 52–63) in the two groups, respectively (p = 0.617). HBV infection rates (68.4% *vs*. 68.4%, p = 0.838) and cirrhosis rates (31.6% *vs*. 36.8%, p = 0.695) were similar between the two groups.

No significant differences were noted in laboratory parameters, such as ALB, TBIL, and PT. The percentage of patients with AFP levels > 40 ng/mL was 31.6% in the chemotherapy group and 57.9% in the non-chemotherapy group (p = 0.061).

There were no significant differences between the two groups regarding satellite nodules (15.8% *vs*. 21.1%, p = 0.906), microvascular invasion (5.3% *vs*.

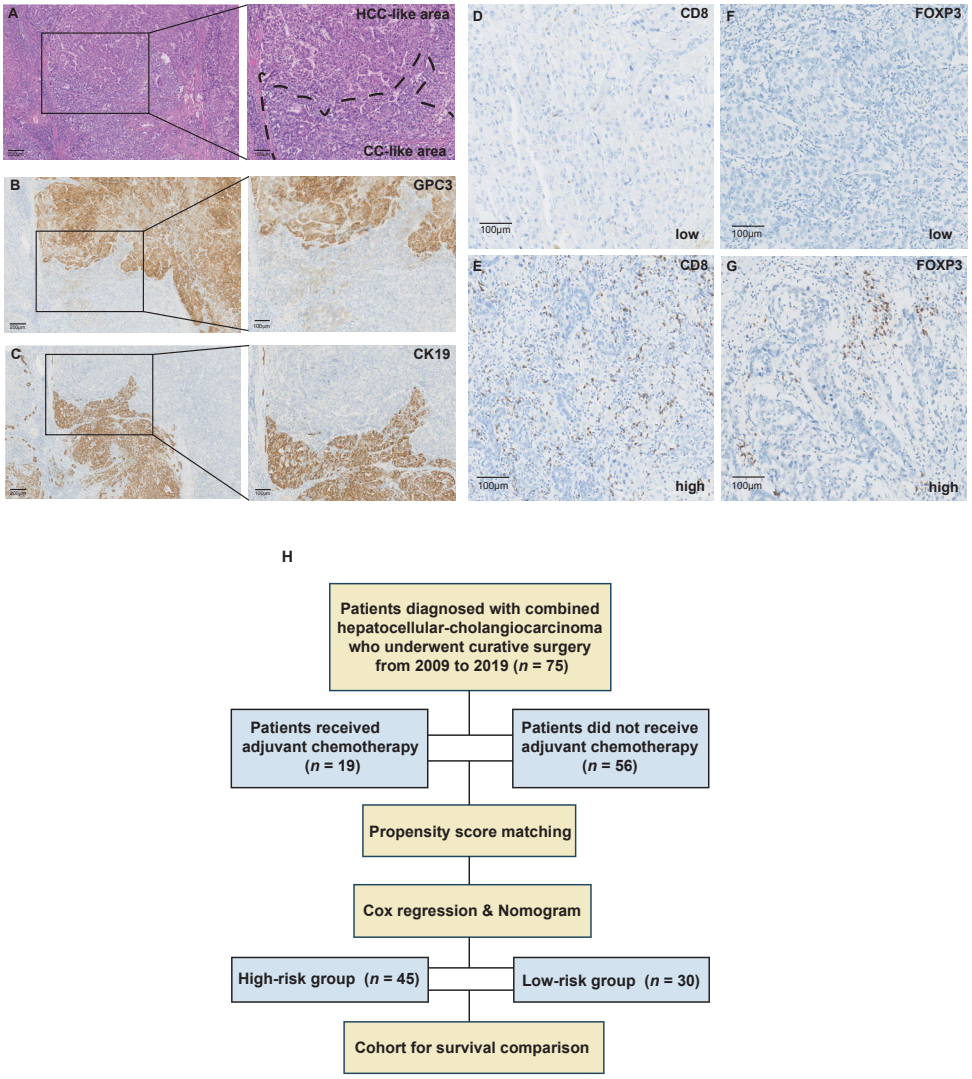

Figure 1. Histopathological features and study design of patients with cHCC-CCA. (A) H&E staining showing distinct HCC-like and CC-like regions. **(B–C)** GPC3 and CK19 immunostaining confirming dual hepatocellular and cholangiocellular phenotypes. **(D–G)** CD8 and FOXP3 staining indicating low and high immune cell infiltration. **(H)** Study flowchart: patient selection, treatment grouping, risk stratification, and PSM.

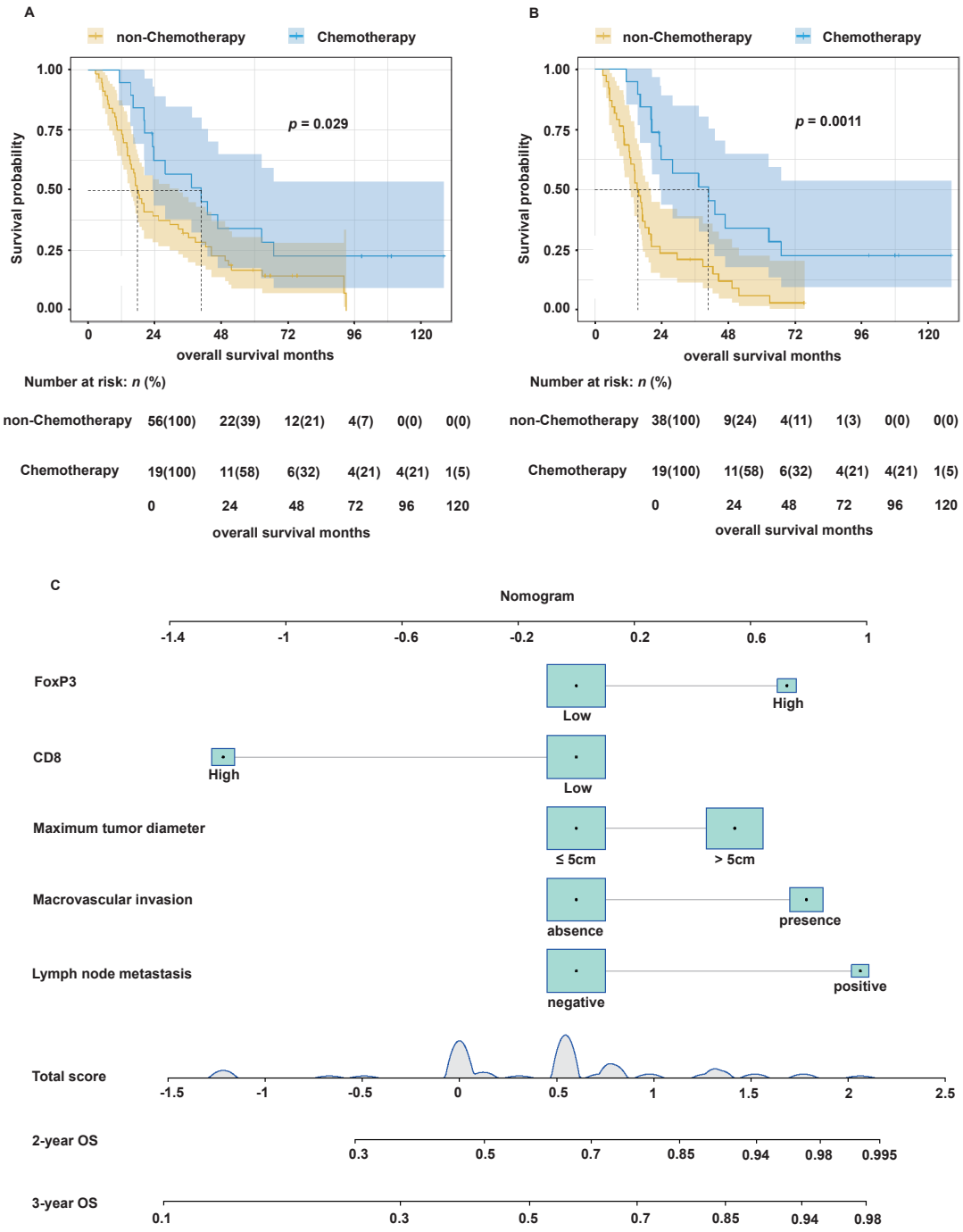

Figure 2. Survival outcomes and prognostic nomogram. (A) Kaplan–Meier curve comparing chemotherapy vs. non-chemotherapy in the unmatched cohort. **(B)** Kaplan–Meier curve after PSM showing improved survival with chemotherapy. **(C)** Nomogram incorporating five variables to predict 2- and 3-year overall survival.

10.5%, $p = 0.869$), or macrovascular invasion (26.3% *vs*. 23.7%, $p = 1.000$).

Regarding immune microenvironment markers, the high expression of CD8 was observed in 5.3% of patients in the chemotherapy group and 0% in the non-chemotherapy group ($p = 0.3330$). The high expression of FOXP3 was observed in 5.3% and 2.6% of patients, respectively ($p = 1.000$). The results of PSM-matched survival analysis indicated that patients who received adjuvant chemotherapy had significantly better overall survival than those who did not ($p = 0.0011$) (Figure 2B), further confirming the survival benefit of adjuvant chemotherapy.

3.3. Construction of the nomogram model

Univariate and multivariate Cox regression analyses were conducted to determine independent prognostic factors for OS. The univariate analysis (Table 2) revealed that macrovascular invasion (HR = 1.767, 95% CI: 1.015–3.076, $p = 0.044$), lymph node metastasis (HR = 2.596, 95% CI: 1.099–6.132, $p = 0.030$), the largest

Table 1. Clinicopathologic characteristics of patients in two groups

Characteristic	Median (IQR) or number (%)		*p*-value
	Chemotherapy group (*n* =19)	Non-Chemotherapy group (*n* =38)	
Sex			0.553
Male	14 (73.7)	32 (84.2)	
Female	5 (26.3)	6 (15.8)	
Age	54 (49-65)	55.5 (52-63)	0.617
HBV			0.887
Present	13 (68.4)	27 (71.1)	
Absent	6 (31.6)	11 (28.9)	
Liver cirrhosis			0.695
Present	6 (31.6)	14 (36.8)	
Absent	13 (68.4)	24 (63.2)	
ALB (g/L)	43.1 (38.1-48.0)	41.85 (39.125-44.275)	0.326
TBIL (μmol/L)	19.0 (13.3-22.9)	16.8 (12.775-21.25)	0.660
PT (sec)	11.1 (10.6-11.8)	11.2 (10.9-11.7)	0.209
AFP (ng/mL)			0.061
> 40	6 (31.6)	22 (57.9)	
≤ 40	13 (68.4)	16 (42.1)	
Satellite lesions			0.906
Present	3 (15.8)	8 (21.1)	
Absent	16 (84.2)	30 (78.9)	
Microvascular invasion			0.869
Present	1 (5.3)	4 (10.5)	
Absent	18 (94.7)	34 (89.5)	
Macrovascular invasion			1.000
Present	5 (26.3)	9 (23.7)	
Absent	14 (73.7)	29 (76.3)	
Lymphatic node metastasis			0.170
Present	4 (21.1)	2 (5.3)	
Absent	15 (78.9)	36 (94.7)	
Largest tumor size (cm)			0.707
>5	11 (57.9)	20 (52.6)	
≤5	8 (42.1)	18 (47.4)	
CD8			0.333
High	1 (5.3)	0	
Low	18 (94.7)	38 (100)	
CD20			0.523
High	6 (31.6)	9 (23.7)	
Low	13 (68.4)	29 (76.3)	
FOXP3			1.000
High	1 (5.3)	1 (2.6)	
Low	18 (94.7)	37 (97.4)	
PD-L1			1.000
High	2 (10.5)	4 (10.5)	
Low	17 (89.5)	34 (89.5)	

Abbreviation: IQR, interquartile ranges; HBV, Hepatitis B Virus; ALB, albumin; TBIL, total bilirubin; PT, prothrombin time; AFP, alpha-fetoprotein.

tumor size > 5 cm (HR = 1.640, 95% CI: 0.993–2.709, p = 0.053), the high expression of CD8 (HR = 0.407, 95% CI: 0.174–0.951, p = 0.038), and the high expression of FOXP3 (HR = 1.935, 95% CI: 0.825–4.537, p = 0.129) were linked to OS..

Multivariate Cox analysis further confirmed that macrovascular invasion (HR = 1.964, 95% CI: 1.074–3.591, p = 0.028), lymph node metastasis (HR = 3.712, 95% CI: 1.424–9.674, p = 0.007), the largest tumor size > 5 cm (HR = 1.661, 95% CI: 1.001–2.768, p = 0.050), the high expression of CD8 (HR = 0.285, 95% CI: 0.113–0.718, p = 0.008), and the high expression of FOXP3 (HR = 3.350, 95% CI: 1.192–9.415, p = 0.022) were independent prognostic factors (Table 2).

Based on these five independent prognostic factors, a nomogram was developed to predict the 2- and 3-year survival rates (Figure 2C). Lymph node metastasis, macrovascular invasion, the largest tumor size diameter > 5 cm, and the high expression of FOXP3 had adverse effects on prognosis, while the high expression of CD8 was a beneficial prognostic factor.

3.4. Validation of the nomogram model

The calibration curves for predicting the 2-year and 3-year OS closely matched the ideal 45-degree reference line, demonstrating excellent agreement between the predicted and observed survival probabilities (Figures

Table 2. Univariate and multivariate analyses of prognostic factors based on OS

Variable	Univariate		Multivariate	
	HR (95%CI)	*p*-value	HR (95%CI)	*p*-value
Sex				
Male	Reference		Reference	
Female	1.594 (0.877-2.896)	0.126	1.513 (0.804-2.846)	0.199
Age	1.014 (0.981-1.048)	0.399		
HBV				
Present	Reference			
Absent	0.830 (0.493-1.399)	0.484		
Liver cirrhosis				
Present	Reference			
Absent	1.006 (0.604-1.677)	0.981		
ALB (g/L)	0.972 (0.914-1.034)	0.372		
TBIL (μmol/L)	1.002 (0.982-1.023)	0.819		
PT (sec)	1.013 (0.770-1.334)	0.925		
AFP (ng/ml)				
≤40	Reference			
> 40	1.101 (0.670-1.808)	0.705		
Satellite lesions				
Present	Reference			
Absent	1.027 (0.546-1.929)	0.935		
Microvascular invasion				
Present	Reference			
Absent	1.768 (0.756-4.133)	0.189		
Macrovascular invasion				
Present	Reference		Reference	
Absent	1.767 (1.015-3.076)	0.044	1.964 (1.074-3.591)	0.028
Lymphatic node metastasis				
Present	Reference		Reference	
Absent	2.596 (1.099-6.132)	0.030	3.712 (1.424-9.674)	0.007
Largest tumor size (cm)				
≤ 5	Reference		Reference	
> 5	1.640 (0.993-2.709)	0.053	1.661 (1.001-2.768)	0.050
CD8				
High	Reference		Reference	
Low	0.407 (0.174-0.951)	0.038	0.285 (0.113-0.718)	0.008
CD20				
High	Reference			
Low	0.729 (0.413-1.287)	0.276		
FOXP3				
High	Reference		Reference	
Low	1.935 (0.825-4.537)	0.129	3.350 (1.192-9.415)	0.022
PD-L1				
High	Reference			
Low	1.557 (0.762-3.181)	0.225		

Abbreviation: HR, hazard ratios; HBV, Hepatitis B Virus; ALB, albumin; TBIL, total bilirubin; PT, prothrombin time; AFP, alpha-fetoprotein.

3A and 3B). The DCA further demonstrated that the nomogram model offered greater net clinical benefit in predicting 2- and 3-year OS compared to the "treat-all" or "treat-none" strategies (Figures 3C and 3D). Time-dependent ROC curve analysis indicated an area under the ROC curve (AUC) of 0.694 for 2-year OS and 0.689 for 3-year OS (Figure 3E), indicating moderate predictive accuracy.

3.5. Risk stratification based on the nomogram

Based on the calculated risk scores, the patients were categorized into high- (n = 45) and low-risk (n = 30) groups. Kaplan–Meier survival curves revealed a significantly poorer prognosis for patients in the high-risk group compared to those in the low-risk group (p = 0.00031; Figure 3F), validating the effectiveness of the nomogram stratification.

In the low-risk group, the group that received adjuvant chemotherapy did not demonstrate a superior survival prognosis (p = 0.084) (Figure 4A); conversely, in the high-risk group, patients who underwent adjuvant chemotherapy exhibited significantly improved survival compared to those who did not undergo adjuvant chemotherapy (p = 0.013) (Figure 4B).

4. Discussion

cHCC-CCA is a rare primary liver malignancy characterized by the coexistence of HCC and CCA

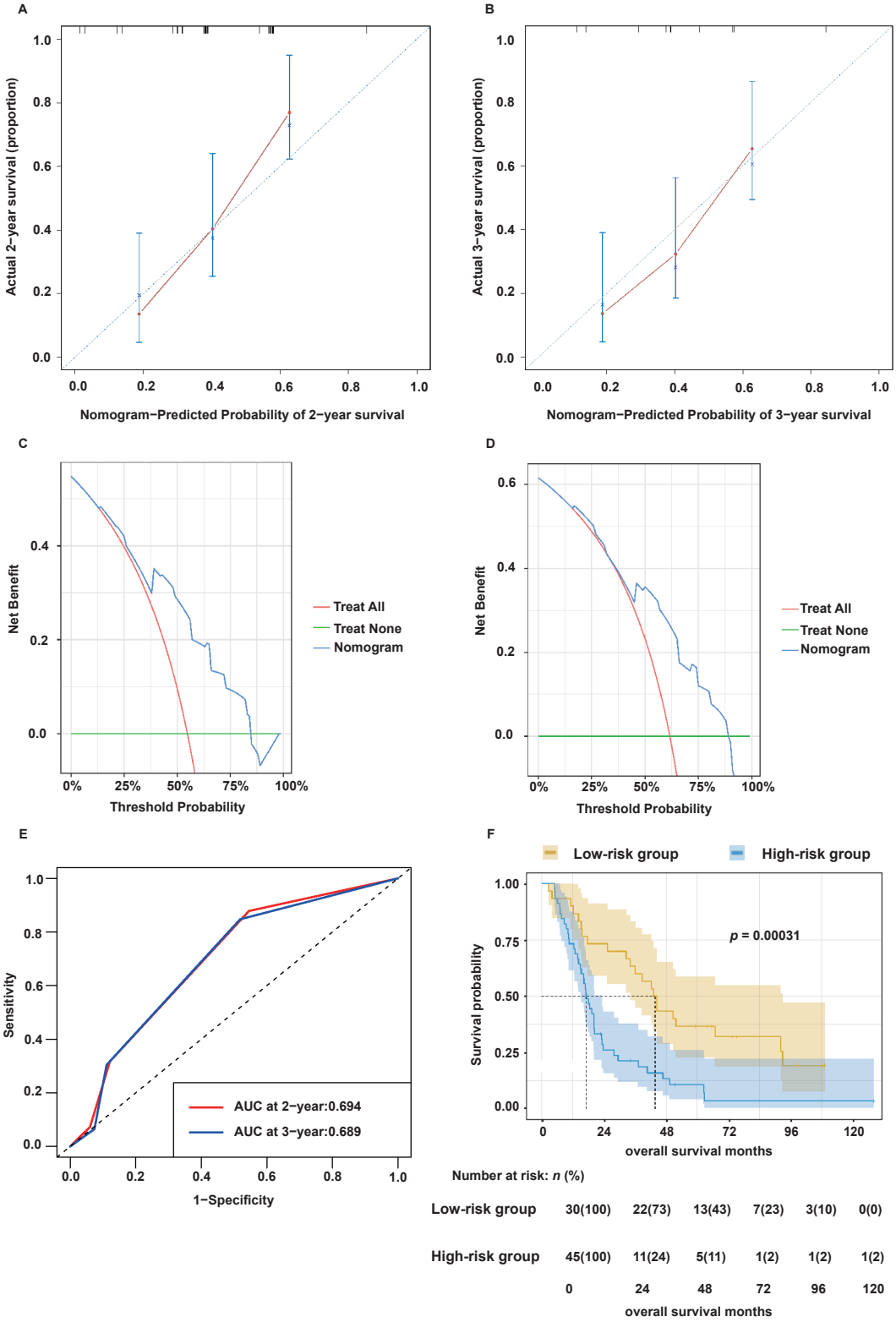

Figure 3. Nomogram validation and risk stratification. (A–B) Calibration plots for 2- and 3-year survival. **(C–D)** Decision curve analysis (DCA) showing clinical utility of the nomogram. **(E)** ROC curves with AUCs of 0.694 (2-year) and 0.689 (3-year). **(F)** Kaplan–Meier curve showing worse survival in the high-risk group.

components. Owing to its complex molecular features and dual histological differentiation, cHCC-CCA displays more aggressive biological behavior, a higher postoperative recurrence rate, and significantly poorer long-term survival compared to either HCC or CCA alone. Curative resection is the sole potentially effective treatment for cHCC-CCA; however, the postoperative recurrence rate exceeds 50%, and there is no established standard adjuvant therapy (*1,21,26*). Enhancing postoperative survival through adjuvant interventions

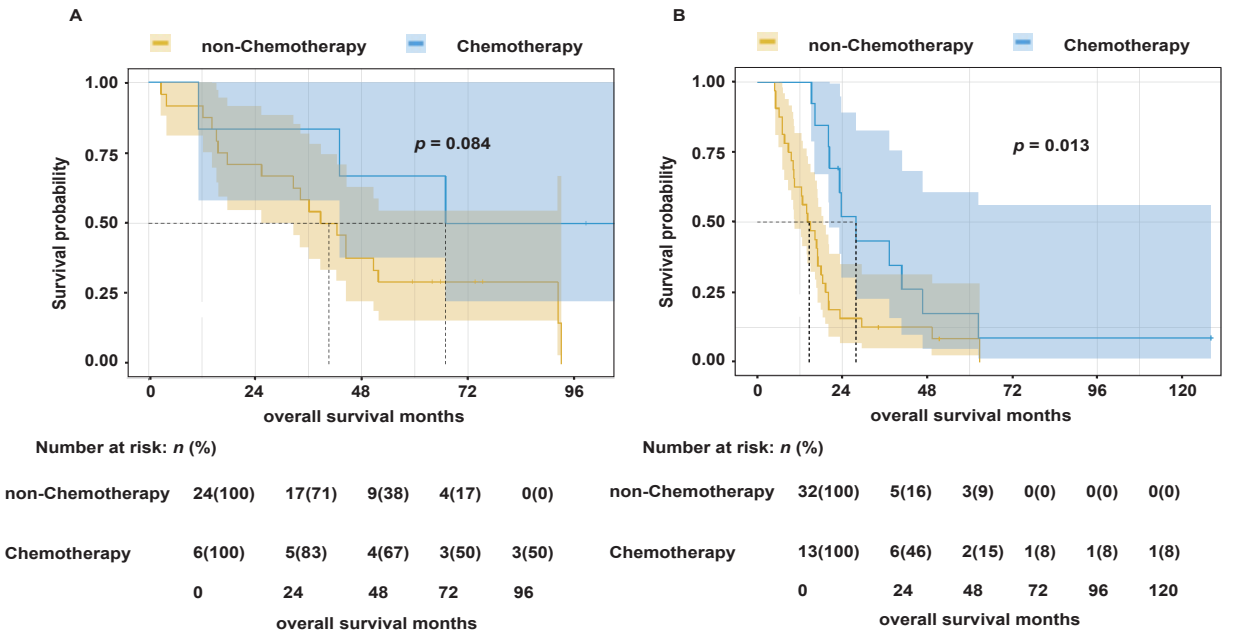

Figure 4. Subgroup survival analysis by risk classification. (A) No significant survival difference in the low-risk group (p = 0.084). **(B)** Chemotherapy significantly improved survival in the high-risk group (p = 0.013).

poses a critical clinical challenge.

In this study, we systematically evaluated the survival benefits of adjuvant chemotherapy after resection in cHCC-CCA patients and established a robust nomogram-based prognostic model using real-world clinical data. This model provides a practical and scientifically grounded tool for individualized postoperative management of patients with cHCC-CCA.

Our main findings showed that adjuvant chemotherapy significantly enhanced the OS of patients with cHCC-CCA. Notably, survival benefits were evident in both high- and low-risk subgroups identified using the nomogram model. This survival benefit remained statistically significant even after PSM, which effectively reduced confounding factors (p = 0.029). In contrast to prior studies with small sample sizes and limited stratified analysis, our study employed robust statistical methods and thorough subgroup analyses, offering more compelling evidence to support the clinical use of adjuvant chemotherapy in cHCC-CCA (*3,27*).

For the development of the prognostic model, we integrated traditional clinicopathological factors like macrovascular invasion, lymph node metastasis, and the largest tumor size, alongside novel immune microenvironment-related markers such as CD8 and FOXP3. Subsequent multivariate Cox regression analysis validated the high expression of CD8 as a favorable prognostic factor (HR = 0.285, p = 0.008), while identifying the high expression of FOXP3 as an independent adverse prognostic factor (HR = 3.350, p = 0.022). These results emphasize the pivotal role of the tumor immune microenvironment in the prognosis of cHCC-CCA and propose potential targets for forthcoming immunotherapy strategies (*23*).

The developed nomogram model exhibited strong predictive performance. Time-dependent ROC curve analyses indicated moderate predictive accuracy, with AUC values of 0.694 for 2-year OS and 0.689 for 3-year OS. Calibration curves demonstrated excellent concordance between predicted survival probabilities and actual outcomes. Decision curve analysis (DCA) illustrated that the nomogram model yielded superior clinical net benefit compared with conventional staging systems for both 2-year and 3-year survival predictions. The population can be stratified into high- and low-risk categories based on the nomogram scores. Postoperative adjuvant chemotherapy did not confer a significant survival benefit for patients in the low-risk category. These results highlight the model's potential as a reliable and intuitive clinical tool to guide personalized treatment decisions and accurately evaluate the benefits of adjuvant chemotherapy.

Despite the significant findings of this study, there are several limitations. Firstly, it was retrospective and carried out at a single center with a relatively small sample size, potentially introducing a selection bias. Secondly, the small sample size utilized for identifying immune microenvironment markers may have impacted the model's generalizability. Lastly, external validation with independent multicenter prospective cohorts is necessary to validate the model's robustness and broader applicability.

In summary, this study not only systematically verified, for the first time, the important role of adjuvant chemotherapy in postoperative survival benefits in cHCC-CCA but also successfully constructed a

prognostic prediction model based on clinicopathological features and immune microenvironmental indices, which possesses good predictive ability and clinical practicability and can screen out the patient population that can benefit from adjuvant chemotherapy(*28*). Future studies should focus on integrating multi-omics data, such as genomic, transcriptomic, and proteomic profiles, and conduct large-scale prospective validations to further optimize and refine the prognostic models. These efforts will ultimately contribute to the advancement of precision medicine and standardized management strategies for patients with postoperative cHCC-CCA, thereby improving long-term survival outcomes (*29*).

Our study showed that adjuvant chemotherapy markedly enhanced postoperative OS in patients with cHCC-CCA. Furthermore, the nomogram model, developed using multivariate analysis, exhibited excellent predictive performance and strong clinical applicability, offering an efficient tool for personalized survival prediction and adjuvant treatment decision-making in cHCC-CCA patients. This model is of significant value for clinical implementation and the progression of precision medicine in cHCC-CCA management.

Acknowledgements

Lu Chen would like to thank the 2023/2024 IHPBA Kenneth Warren Fellowship for the financial support.

Funding: This work was supported by the National Natural Science Foundation of China (grants 82373365, 82173317, 82203423, 82472991 and 82372894), Tianjin Natural Science Foundation (23JCYBJC00600), Joint Funds of the Natural Science Foundation of Tianjin (No.25JCLZJC00350), Tianjin Key Medical Discipline Construction Project (TJYXZDXK-009A).

Conflict of Interest: The authors have no conflicts of interest to disclose.

References

1. Beaufrère A, Calderaro J, Paradis V. Combined hepatocellular-cholangiocarcinoma: An update. J Hepatol. 2021; 74:1212-1224.
2. Calderaro J, Ghaffari Laleh N, Zeng Q, *et al*. Deep learning-based phenotyping reclassifies combined hepatocellular-cholangiocarcinoma. Nat Commun. 2023; 14:8290.
3. Li X, Ramadori P, Pfister D, Seehawer M, Zender L, Heikenwalder M. The immunological and metabolic landscape in primary and metastatic liver cancer. Nat Rev Cancer. 2021; 21:541-557.
4. Xue R, Chen L, Zhang C, *et al*. Genomic and Transcriptomic Profiling of Combined Hepatocellular and Intrahepatic Cholangiocarcinoma Reveals Distinct Molecular Subtypes. Cancer Cell. 2019; 35:932-947.e938.
5. Nguyen CT, Caruso S, Maille P, *et al*. Immune Profiling of Combined Hepatocellular- Cholangiocarcinoma Reveals Distinct Subtypes and Activation of Gene Signatures Predictive of Response to Immunotherapy. Clin Cancer Res. 2022; 28:540-551.
6. Harding JJ, Khalil DN, Fabris L, Abou-Alfa GK. Rational development of combination therapies for biliary tract cancers. J Hepatol. 2023; 78:217-228.
7. Gong W, Zhang S, Tian X, Chen W, He Y, Chen L, Ding T, Ren P, Shi L, Wu Q, Sun Y, Chen L, Guo H. Tertiary lymphoid structures as a potential prognostic biomarker for combined hepatocellular-cholangiocarcinoma. Hepatol Int. 2024; 18:1310-1325.
8. Chen X, Dong L, Chen L, *et al*. Epigenome-wide development and validation of a prognostic methylation score in intrahepatic cholangiocarcinoma based on machine learning strategies. Hepatobiliary Surg Nutr. 2023; 12:478-494.
9. Chen L, Yin G, Wang Z, Liu Z, Sui C, Chen K, Song T, Xu W, Qi L, Li X. A predictive radiotranscriptomics model based on DCE-MRI for tumor immune landscape and immunotherapy in cholangiocarcinoma. Biosci Trends. 2024; 18:263-276.
10. Yang S, Qian L, Li Z, *et al*. Integrated Multi-Omics Landscape of Liver Metastases. Gastroenterology. 2023; 164:407-423.e417.
11. Dar FS, Abbas Z, Ahmed I, *et al*. National guidelines for the diagnosis and treatment of hilar cholangiocarcinoma. World J Gastroenterol. 2024; 30:1018-1042.
12. Ye L, Schneider JS, Ben Khaled N, Schirmacher P, Seifert C, Frey L, He Y, Geier A, De Toni EN, Zhang C, Reiter FP. Combined Hepatocellular-Cholangiocarcinoma: Biology, Diagnosis, and Management. Liver Cancer. 2024; 13:6-28.
13. Jeong H, Kim KP, Jeong JH, Hwang DW, Lee JH, Kim KH, Moon DB, Lee MA, Park SJ, Chon HJ, Park JH, Lee JS, Ryoo BY, Yoo C. Adjuvant gemcitabine plus cisplatin versus capecitabine in node-positive extrahepatic cholangiocarcinoma: the STAMP randomized trial. Hepatology. 2023; 77:1540-1549.
14. Leone V, Ali A, Weber A, Tschaharganeh DF, Heikenwalder M. Liver Inflammation and Hepatobiliary Cancers. Trends Cancer. 2021; 7:606-623.
15. Trikalinos NA, Zhou A, Doyle MBM, Fowler KJ, Morton A, Vachharajani N, Amin M, Keller JW, Chapman WC, Brunt EM, Tan BR. Systemic Therapy for Combined Hepatocellular-Cholangiocarcinoma: A Single-Institution Experience. J Natl Compr Canc Netw. 2018; 16:1193-1199.
16. Kataoka K, Mori K, Nakamura Y, *et al*. Survival benefit of adjuvant chemotherapy based on molecular residual disease detection in resected colorectal liver metastases: subgroup analysis from CIRCULATE-Japan GALAXY. Ann Oncol. 2024; 35:1015-1025.
17. Moris D, Palta M, Kim C, Allen PJ, Morse MA, Lidsky ME. Advances in the treatment of intrahepatic cholangiocarcinoma: An overview of the current and future therapeutic landscape for clinicians. CA Cancer J Clin. 2023; 73:198-222.
18. Stoop TF, Sugawara T, Oba A, *et al*. Adjuvant Chemotherapy After Resection of Localized Pancreatic Adenocarcinoma Following Preoperative FOLFIRINOX. JAMA Oncol. 2025; 11:276-287.
19. He GQ, Li Q, Jing XY, Li J, Gao J, Guo X. Persistent response to combination therapy of pemigatinib and chemotherapy in a child of combined hepatocellular-cholangiocarcinoma with FGFR2 fusion. Mol Cancer. 2024; 23:269.

20. Rosenberg N, Van Haele M, Lanton T, *et al*. Combined hepatocellular-cholangiocarcinoma derives from liver progenitor cells and depends on senescence and IL-6 trans-signaling. J Hepatol. 2022; 77:1631-1641.
21. Pinter M, Scheiner B, Pinato DJ. Immune checkpoint inhibitors in hepatocellular carcinoma: emerging challenges in clinical practice. Lancet Gastroenterol Hepatol. 2023; 8:760-770.
22. Gan X, Dong W, You W, Ding D, Yang Y, Sun D, Li W, Ding W, Liang Y, Yang F, Zhou W, Dong H, Yuan S. Spatial multimodal analysis revealed tertiary lymphoid structures as a risk stratification indicator in combined hepatocellular-cholangiocarcinoma. Cancer Lett. 2024; 581:216513.
23. Calderaro J, Di Tommaso L, Maillé P, *et al*. Nestin as a diagnostic and prognostic marker for combined hepatocellular-cholangiocarcinoma. J Hepatol. 2022; 77:1586-1597.
24. Heng Q, Hou M, Leng Y, Yu H. Establishment of a prognostic nomogram and risk stratification system for patients with combined hepatocellular-cholangiocarcinoma. Sci Rep. 2025; 15:16726.
25. Heinze G, Wallisch C, Dunkler D. Variable selection – A review and recommendations for the practicing statistician. Biom J. 2018; 60:431-449.
26. Claasen M, Ivanics T, Beumer BR, de Wilde RF, Polak WG, Sapisochin G, JNM IJ. An international multicentre evaluation of treatment strategies for combined hepatocellular-cholangiocarcinoma(☆). JHEP Rep. 2023; 5:100745.
27. Kelley RK, Rimassa L, Cheng AL, *et al*. Cabozantinib plus atezolizumab versus sorafenib for advanced hepatocellular carcinoma (COSMIC-312): a multicentre, open-label, randomised, phase 3 trial. Lancet Oncol. 2022; 23:995-1008.
28. Yang H, Cheng J, Zhuang H, *et al*. Pharmacogenomic profiling of intra-tumor heterogeneity using a large organoid biobank of liver cancer. Cancer Cell. 2024; 42:535-551.e538.
29. Liu Q, Zhang X, Qi J, *et al*. Comprehensive profiling of lipid metabolic reprogramming expands precision medicine for HCC. Hepatology. 2025; 81:1164-1180.

Received June 23, 2025; Revised July 10, 2025; Accepted July 14, 2025.

[§]These authors contributed equally to this work.

**Address correspondence to:*
Xiangdong Tian, Wenchen Gong, and Lu Chen, Tianjin Medical University Cancer Institute and Hospital, West Huan-Hu Road, Ti Yuan Bei, Hexi District, Tianjin 300060, China.
E-mail: xiangdongtian@tmu.edu.cn (XT); gongwenchen@tmu.edu.cn (WG); chenlu@tmu.edu.cn (LC)

Released online in J-STAGE as advance publication July 16, 2025.

Original Article

DOI: 10.5582/bst.2025.01162

Conversion therapy followed by surgery and adjuvant therapy improves survival in Barcelona C stage hepatocellular carcinoma — A propensity score-matched analysis

Yinbiao Cao[1,§], Liru Pan[1,§], Zikun Ran[1,2,§], Wenwen Zhang[1], Junfeng Li[1], Xuerui Li[1], Tianyu Jiao[1], Zhe Liu[1], Tao Wan[1], Haowen Tang[1], Shichun Lu[1,*]

[1] First Medical Center of Chinese People's Liberation Army General Hospital, Beijing, China;
[2] School of Medicine, Nankai University, Tianjin, China.

SUMMARY: Conversion therapy with a combination of tyrosine kinase inhibitor and anti-programmed death-1 antibody sequential surgery and postoperative adjuvant therapy has shown improved survival benefits in patients with Barcelona C stage (BCLC-C) hepatocellular carcinoma (HCC). We aimed to compare the survival benefits in a retrospective cohort of patients with BCLC-C HCC who underwent surgery after conversion therapy with adjuvant therapy and surgery alone. The conversion therapy group was derived from a prospective clinical study, and from January 2015 to September 2023, we selected patients diagnosed with BCLC-C HCC who underwent liver resection at Chinese PLA General Hospital as the surgical group. The primary endpoint in the comparison of survival benefits between conversion therapy and surgery-alone groups was recurrence-free survival. Propensity score matching was applied to reduce any potential bias in the study. By the end of follow-up, the conversion therapy group mRFS was 37.8 months, with postoperative 1-, 2- and 3-year RFS rates of 66.8%, 54.6%, and 48.3%. In the surgery group, the mRFS was 3.0 months, and postoperative 1- , 2- and 3-year RFS rates of 22.4%, 17.5%, and 15.0%, respectively. On multivariable Cox regression analyses, conversion therapy significantly reduced HCC-related mortality and HCC recurrence rates compared with surgery alone. For BCLC-C HCC patients, conversion therapy with adjuvant therapy is in relationship with increased survival in comparison with surgery alone.

Keywords: hepatocellular carcinoma, salvage surgery, tyrosine kinase inhibitor, anti-programmed death-1 antibody, portal vein tumor thrombosis, propensity score matching

1. Introduction

Liver cancer is the fourth leading cause of cancer-related death, and it is the second leading cause of cancer-related death in males (*1*). Approximately 70-80% of individuals with HCC are diagnosed during their progressive stage and have a poor prognosis (*2*). Barcelona Clinic Liver Cancer (BCLC) staging is the most commonly used international staging method for HCC. Individuals with BCLC–C-stage HCC have a short survival period (approximately 3-6 months) (*3,4*). Currently, there is no effective therapy to achieve a favorable prognosis for individuals with BCLC-C stage HCC. BCLC–C-stage HCC mainly presents with vascular invasion and extrahepatic metastasis. Individuals with HCC combined with portal vein tumor thrombus (PVTT) have a natural survival of 2.7-4 months, while patients with HCC combined with lymph node metastasis have a median disease-free survival (mRFS) and overall survival (mOS) of only 5.9 months and 11 months, with 1-year, 3-year, and 5-year OS rates were 36.4%, 13.6%, and 13.6% (*5,6*). An international consensus on treating individuals with BCLC–C-stage HCC combined with vascular invasion alone is unavailable. According to the EASL and NCCN guidelines, combined vascular invasion is a contraindication to surgical treatment for individuals with HCC (*7,8*). In addition, patient prognosis is not considerably improved after preoperative adjuvant therapy, and surgery is not the best treatment option for such individuals. However, Chinese guidelines indicate that patients with PVTT grade 2 or less can be treated surgically (*9*). Surgery is not recommended worldwide for patients with PVTT grade 3 or higher or with lymph node metastases alone, and systemic drug-based supportive therapy is preferred.

The advent of immunotherapy combined with targeted regimens has provided novel insights into treating advanced HCC. Numerous clinical trials suggest

that a combination regimen based on immunotherapy combined with targeted therapy effectively prolongs the survival duration of individuals with advanced HCC (*10*). Based on previous research, implementing immunotherapy combined with targeted regimens (conversion therapy) in patients with advanced HCC preoperatively and sequential surgical treatment after the patient has achieved oncologic benefit has become an effective practice, and postoperative adjuvant therapy based on pathologic findings may further prolong patient survival (*11*). Despite the initial effectiveness, further studies using large sample sizes are required to demonstrate its efficacy and safety. The current historical-prospective study explored the safety and efficacy of conversion therapy sequential surgical therapy to treat BCLC–C-stage HCC. Meanwhile, the previous research of our team pointed out that serum alpha-fetoprotein (AFP) level has a significant impact on the efficacy assessment and prognosis of HCC patients receiving conversion therapy, which was also given further exploration in this study (*12*).

2. Material and Methods

2.1. Sample sources

Individuals with BCLC–C-stage HCC received surgical treatment at the Department of Hepatobiliary and Pancreatic Surgery, General Hospital of the Chinese People's Liberation Army. Patients in the conversion therapy group of this study were derived from a prospective clinical study, registration number ChiCTR1900023914 (A Research of programmed death-1 (PD-1) Inhibitors Combined with Lenvatinib for Advanced Unresectable Liver Cancer as the Conversion Therapy: A Prospective Open-label Exploratory Clinical Study). Patients in the surgery group were selected from January 2015 to September 2023, which had a high degree of homogeneity in the study site and surgeon team in addition to the intervention. Patients were followed up till December 2024. Informed consent was obtained from all patients to be included in the study. We obtained written informed consent for treatment and the use of patient data for clinical research before treatment. Patients who received preoperative conversion therapy and sequential surgery with postoperative treatment served as the conversion therapy and postoperative treatment group, whereas patients who received no conversion therapy and were treated directly with surgery served as the surgery alone group. The major observational endpoint of this research was recurrence-free survival (RFS), and the secondary endpoint was overall survival (OS) because of the diverse treatments available to patients after postoperative recurrence. In addition, the association between the patient's serum AFP levels at the time of initial diagnosis and preoperatively and the treatment outcome was also studied as a secondary observational endpoint.

2.2. Selection criteria

The inclusion criteria for this research were as stated: (1) Age 18-80 years; (2) Eastern Cooperative Oncology Group Performance Status (ECOG-PS) score of 0 ; (3) Diagnosis of HCC according to the guidelines of the American Association for the Study of Liver Diseases (AASLD) or postoperative pathology; (4) R_0 resection confirmed by postoperative pathology; (5) Administration of PD-1 antibody in combination with tyrosine kinase inhibitor (TKI) for sequential surgical resection; (6) Tumor stage of BCLC-C during initial diagnosis; the exclusion criteria were as stated: (1) Previous treatment with PD-1 antibody, TKI, or any other combination regimen; (2) Cancer history other than HCC in the last 5 years; (3) Concurrent major systemic diseases.

2.3. Data collection

Relevant information was collected from patients at the initial visit, including gender, age, viral hepatitis, initial liver function Child-Pugh score, ECOG-PS score, maximum tumor diameter, number of tumor lesions, serum AFP level (patients were differentiated into AFP high (AFPH) and AFP low (AFPL) groups based on whether or not the AFP was positive (> 20 μg/mL)), other local treatment received preoperatively, pre-combined therapy portal vein tumor thrombosis (PVTT), hepatic vein tumor thrombosis/inferior vena cava tumor thrombosis (HVTT/IVCTT), and lymph node metastasis.

The conversion therapy group received a combination of TKI and PD-1 antibody as the downstaging protocol. Conversion therapy is subjected to unresectable tumors, aiming to make surgery feasible and improve overall survival by local or systemic therapy (*13*). Conversion protocols are mainly made concerning achieving a high objective response rate (ORR) (Appendix Table S1). The postoperative therapy protocols were guided based on pathological examination findings: 1) Patients who reached a pathological complete response (PCR) would only receive initial PD-1 antibodies consistently for another 6 months, otherwise, 2) Patients would receive initial combination therapy protocol for 6–12 months depending on imaging examination findings by follow-up.

Intraoperative data were collected from patients, including the surgical approach (simple hepatectomy, superimposed thrombectomy or portal vein reconstruction, *etc*.), the extent of hepatectomy (≥ 3 Couinaud's segments were considered extensive hepatectomy), intraoperative bleeding, and perioperative blood transfusion. Information on postoperative complications included postoperative Clavein-Dindo score, postoperative biliary fistula (diagnosed by

bilirubin > 3 times serum bilirubin level in the operative area drainage fluid on postoperative day 3), postoperative bleeding, duration of postoperative hospitalization, and postoperative Child-Pugh score at 5 days (*14,15*).

Information on immunotherapy combined with a targeted regimen was collected from patients. Additionally, one infusion of PD-1 was used as 1 treatment cycle. Efficacy assessment by abdominal enhancement magnetic resonance imaging (MRI, urine routine, blood routine, thyroid function, coagulation function, liver and kidney function, cardiac enzyme profile, and tumor markers were carried out approximately every 3 months. The maximum diameter of the tumor after combined treatment was collected from patients. The tumor treatment effect was assessed by the modified Response Evaluation Criteria in Solid Tumors (m-Recist) (*16*). The proportion of residual tumor cells in the postoperative pathology was used to evaluate the response to tumor treatment. The absence of microscopically visible residual tumor cells in the pathology specimens indicated a pathological complete response (pCR). For pathological findings, the major pathological response (MPR) was defined as surviving tumor activity < 10% (*17,18*). Treatment-related adverse events were assessed by the common terminology criteria for adverse events (CTCAE 5.0) evaluation criteria (*19*). In this study, the JSH typing criteria were adopted to define the grade of post-conversion cancer emboli according to the location of emboli still present in the vasculature after combined treatment (regardless of their oncological activity) due to the absence of a uniform and clear definition (*20*).

2.4. Surgical evaluation and postoperative adjuvant medication and follow-up in the conversion therapy group

Surgical treatment was performed when the following indications were met: (1) Preoperative liver function Child-Pugh score grade A/B; (2) Postoperative residual liver volume ≥ 35% of standard liver volume during the lack of cirrhosis and ≥ 45% of standard liver volume in cirrhosis; (3) 15-min retention rate < 20% for indocyanine green; (4) Structural integrity of the planned preserved hepatic parenchymal inflow and outflow tracts; (5) Patent biliary drainage or an intra- and extra-hepatic biliary structure that can be completely reconstructed; (6) Eastern U.S. Oncology Collaborative Group score of 0 to 1; (7) ASA rating ≤ grade 3. (*21*)

2.5. Selection of surgical modality and procedures

(1) Hepatectomy: A reverse L-shaped incision was made in the right upper abdomen to open the tissue layer by layer or to establish a laparoscopic operating system. Subsequently, the abdominal cavity was explored for ascites, distant metastases in lymph nodes or other organ tissues, and local tumor infiltration. The liver segment where the tumor was located was targeted and the resection line was marked along > 2 cm beyond the tumor. Afterward, the liver parenchyma was fragmented by the Cavitation Ultrasonic Surgical Aspirator (CUSA)/ ultrasonic knife/clamp, and the exposed Glisson system and the veins of the hepatic venous system were ligated or sutured. The primary branches of the Glisson system or the main trunk of the hepatic venous system were dissected with a linear Endo-GIA stapler. The sections were covered with hemostatic material after energy instrumentation and suturing for hemostasis.

(2) Vascular thrombectomy and reconstruction: Vascular clamping was performed on both ends of the branches where the portal vein cancer embolus was located. Subsequently, the vessel wall was incised longitudinally along the direction of the vessel. The clamp was used to remove all the visually visible cancerous tissues to investigate whether the tumor invaded the contralateral vessel. After the examination, the distal vascular clamp was released to ensure proper blood flow. After confirming no residual tumor tissue in the vascular system, the vessel wall incision was closed with transverse plastic sutures using 4-0/5-0 prolene sutures. If the angle between the residual portal vein and the main trunk was still acute after suturing, the angle was straightened and adjusted to an obtuse angle by ligating again on the resected side to ensure a smooth flow signal within it.

(3) Abdominal lymph node dissection: according to the patient's preoperative imaging data and intraoperative exploration results, the metastatic lymph nodes with definite and suspicious metastases in the abdominal cavity were removed by dissection after ligation of lymphatic vessels and sent for pathological examination.

2.6. Statistical analysis

Comparison of continuous variables conforming to normal distribution between two groups was carried out using the *t*-test, whereas the Mann-Whitney *U*-test was utilized for comparing the continuous variables not conforming to normal distribution. The chi-square and Fisher's exact tests were used to compare categorical data. Survival status between the two groups was compared using the Kaplan-Meier method for the log-rank test. Univariate survival analysis was introduced in a multivariate Cox proportional risk model to explore important risk factors for recurrence. Continuous variables were dichotomized and then included in the analysis to determine adjusted risk ratios and 95% confidence intervals (CIs). Propensity score matching was applied in the two patient groups to reduce the potential bias in this study. Variables associated with long-term survival were chosen for propensity score generation, including age, gender, and hepatitis etiology; Child-Pugh score, ECOG-PS, and serum AFP level; other

local treatments; tumor diameters; multiple or single tumors; BCLC stage; and surgery procedures, major or minor hepatectomy, perioperative blood loss, and perioperative blood transfusion. All statistical analyses were performed using SPSS 26.0 and R 4.1.2. Statistical significance was obtained at $P < 0.05$.

3. Results

3.1. Patients' related basic information

In total, 88 patients from the prospective study were included in the study, 123 patients diagnosed with BCLC–C-stage HCC and subjected to surgery at the Department of Hepatobiliary and Pancreatic Surgery, General Hospital of the Chinese People's Liberation Army, from January 2015 to September 2023, were recruited into this study. Eventually, 211 individuals with BCLC–C-stage HCC were included in this research after screening by the inclusion and exclusion criteria, and 176 patients comprised the PSM cohort (patients in the conversion therapy group were completely matched) (Figure 1).

3.2. Baseline characteristics of patients

The baseline features of the two groups in this study are demonstrated in Table 1. In the total cohort, the group of patients receiving combination therapy had a higher rate of HBV infection ($P = 0.027$), previous local treatments ($P = 0.035$), multiple tumor number ($P = 0.003$) and minor hepatectomy ($P = 0.024$) at the initial diagnosis. No considerable variations were noted between the two groups in terms of all variables after PSM. All patients were diagnosed as BCLC–C-stage HCC by preoperative imaging or postoperative pathology.

3.3. Evaluation of the effect of immunotherapy combined with targeted therapy and toxic side effects in the conversion therapy group

The dosing regimens of the 88 patients receiving immunotherapy combined with the targeted therapy regimen are demonstrated in Table 2. These patients were given a dosing regimen of 3-20 cycles with a median of 5 cycles. According to the m-Recist criteria, 12 patients achieved complete response (CR), 58 achieved partial response (PR), 16 had stable disease (SD), and 2 had progressive disease (PD). Before the combined treatment, 75 individuals in the conversion therapy group developed vascular invasion, including 68 with PVTT, and 20 with HVTT. After conversion therapy, 68 patients had vascular invasion, including 61 with PVTT and 11 with HVTT. In addition, 27 patients had a decrease in PVTT of at least one grade, and 7 had complete disappearance of PVTT. In addition, the HVTT decreased by at least one grade in 15 patients, and the HVTT disappeared completely in 9 patients. Moreover, 34 patients in the conversion therapy group had lymph node metastases before the combined treatment, but this number decreased to 17 after the combined treatment. And postoperative pathological findings confirmed that the primary tumor foci eventually reached pCR in 21 patients, and MPR in 48 patients. During immunotherapy combined with targeted therapy, 64 individuals in the conversion therapy group experienced adverse events during treatment, 44 of whom had a CTCAE event grade ≥ 2 (Table 2). No patient abandoned the treatment regimen or failed to undergo surgery due to the side effects accompanying the treatment process.

3.4. Surgical procedures and postoperative complications

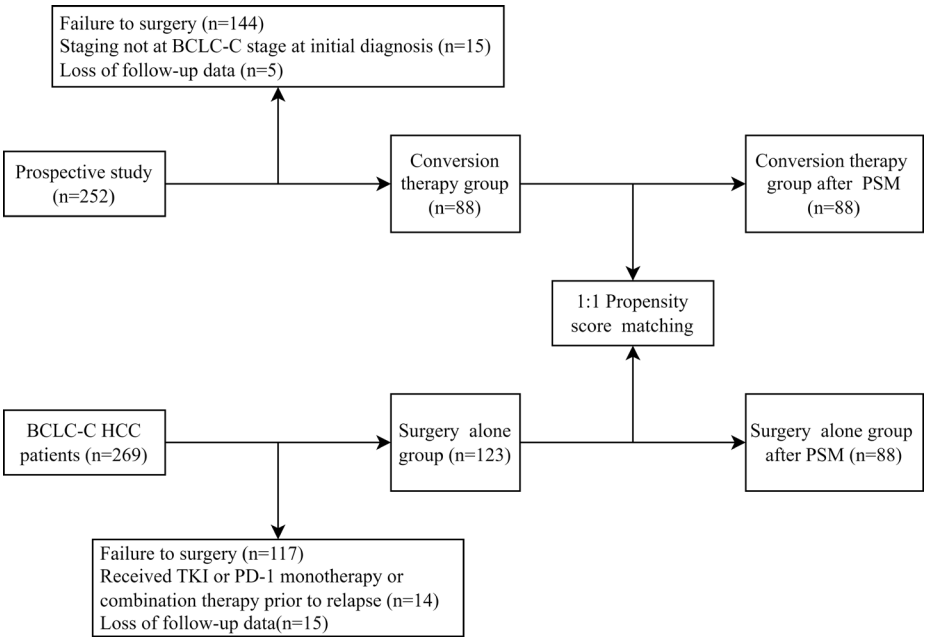

Figure 1. Flowchart of this research.

Table 1. Comparison of characteristics between BCLC-C HCC patients undergoing conversion therapy and postoperative treatment or surgery alone

Variables *n* (%)	Before PSM			After PSM		
	Conversion therapy (*n* = 88)	Surgery (*n* = 123)	*P*	Conversion therapy (*n* = 88)	Surgery (*n* = 88)	*P*
Age (years)	54 (24-73)	55 (29-80)	0.917	54 (24-73)	55 (30-80)	0.642
Gender			0.528			1.000
Male	77 (87.5)	111 (90.2)		77 (87.5)	77 (87.5)	
Female	11 (12.5)	12 (9.6)		11 (12.5)	11 (12.5)	
Etiology of hepatitis			0.027			0.551
HBV	76 (86.4)	94 (76.4)		76 (86.4)	80 (90.9)	
HCV	6 (6.8)	5 (4.1)		6 (6.8)	3 (3.4)	
No hepatitis	6 (6.8)	24 (19.5)		6 (6.8)	5 (5.7)	
Child-pugh grade			0.329			0.406
A	86 (97.7)	117 (95.1)		86 (97.7)	84 (95.5)	
B	2 (2.3)	6 (4.9)		2 (2.3)	4 (4.5)	
ECOG PS			1.000			1.000
0	88	123		88	88	
1	0	0		0	0	
2	0	0		0	0	
3	0	0		0	0	
4	0	0		0	0	
5	0	0		0	0	
AFP (ng/mL)			0.706			0.861
> 20	66 (75)	95 (77.2)		66 (75)	67 (76.1)	
≤ 20	22 (25)	28 (22.8)		22 (25)	21 (23.9)	
Previous local treatment			0.035			0.150
Yes	24 (27.3)	19 (15.4)		24 (27.2)	16 (18.2)	
No	64 (72.7)	104 (84.6)		64 (72.8)	72 (81.8)	
Tumor diameter (cm)	9.11±4.25	8.43±4.04	0.549	8.6 (2.7-19.9)	8.5 (2-25)	0.589
Tumor number			0.003			0.082
Single	61 (77.3)	106 (86.2)		61 (69.3)	71 (80.7)	
Multiple	27 (22.7)	17 (13.8)		27 (30.7)	17 (15.3)	
BCLC stage			1.000			1.000
A	0	0		0	0	
B	0	0		0	0	
C	88 (100)	123 (100)		88 (100)	88 (100)	
D	0	0		0	0	
Surgical procedure			0.152			0.364
Thrombectomy	37 (52.7)	64 (52.0)		37 (42.0)	43 (48.9)	
En-bloc	51 (47.3)	59 (48.0)		51 (58.0)	45 (51.1)	
Extent of resection			0.024			0.165
Major	49 (55.7)	87 (70.7)		49 (55.7)	58 (65.9)	
Minor	39 (44.3)	36 (29.3)		39 (44.3)	30 (34.1)	
Intraoperative blood loss (mL)	300 (50-2400)	300 (50-3000)	0.077	300 (50-2400)	300 (50-2500)	0.680
Perioperative blood transfusion			0.496			
Yes	37 (42.0)	46 (37.4)		37 (42.0)	30 (34.1)	0.277
No	51 (58.0)	77 (62.6)		51 (58.0)	58 (65.9)	

Abbreviations: HBV, hepatitis B virus; HCV, hepatitis C virus; AFP, alpha-fetoprotein; ECOG PS, Eastern Cooperative Oncology Group performance status.

In the conversion therapy group, 51 patients underwent hepatectomy alone, and 37 had hepatectomy combined with thrombectomy. In contrast, 59 patients underwent hepatectomy alone, and 64 had hepatectomy combined with thrombectomy in the surgery group. Considerable variations were not observed between the two groups ($P = 0.152$). The mean intraoperative bleeding volumes were 300 mL (50-2,400 mL) and 300 mL (50-3,000 mL) in the two groups, respectively. In addition, major variations were not observed between the two groups in terms of perioperative blood transfusion, postoperative hospital days, postoperative biliary fistula, bleeding, and other complications, Child-Pugh score, and Clavein-Dindo score (Table 3). In the cohort after PSM, there were no significant statistical differences in surgery-related complication indicators between the two groups of patients.

3.5. Follow-up results

By the end of follow-up, 38 patients in the conversion therapy group experienced recurrence and mRFS was 37.8 months, with postoperative 1-, 2- and 3-year RFS rates of 66.8%, 54.6%, and 48.3%, respectively. In the surgery group, 93 patients experienced recurrence, with an mRFS of 3.1 months and postoperative 1-, 2-

and 3-year RFS rates of 27.2%, 21.1%, and 18.5%, respectively. Sixteen patients in the conversion therapy group died and did not reach mOS yet, with 1-, 2-, 3-, and 5-year OS rates of 96.6%, 82.8%, 77.2%, and 58.1%, respectively. In the surgery group, 85 patients died, with a mOS of 26.8 months and 1-, 2-, 3-, and 5-year OS rates of 66.7%, 53.7%, 38.2%, and 28.9%, respectively. The survival curves for RFS and OS of patients in both groups are shown in Figure 2.

For patients with combined macrovascular invasion, the 1-, 2-, and 3-year RFS rates in the conversion therapy group compared with the surgery group were 66.6% *vs*. 27.0%, 52.1% *vs*. 20.9%, and 45.0% *vs*. 17.3%, respectively; the 1-, 2-, 3-, and 5-year OS rates in the two groups were 96.0% *vs*. 66.7%, 79.8% *vs*. 53.3%, 74.7% *vs*. 38.3% and 57.3% *vs*. 29.6%. As for patients with lymph node metastasis, the 1-, 2-, and 3-year RFS rates were 63.7 % *vs*. 20%, 57.0% *vs*. 20%, 50.6% *vs*. 20%, respectively; the 1-, 2-, 3-, and 5-year OS rates in both groups were 94.4% *vs*. 60%, 82.9% *vs*. 40%, 79.4% *vs*. 20% and 67% *vs*. 20% (Figure 2).

In the propensity model, 33 patients in the conversion therapy group developed recurrence and mRFS was 37.8 months, with postoperative 1-, 2- and 3-year RFS rates of 66.8%, 54.6%, and 48.3%, respectively. In the surgery group, 60 patients developed recurrence, with an mRFS of 3.0 months and 1-, 2- and 3-year RFS rates of 22.4%, 17.5% and 15.0%, respectively. Thirteen patients in the conversion therapy group died and did not attain mOS, with 1-, 2-, 3-, and 5-year OS rates of 96.6%, 82.8%, 77.2%, and 58.1%, respectively. In the surgery group, 55 patients died, with a mOS of 22.7 months and 1-, 2-, 3-, and 5-year postoperative OS rates of 63.6%, 48.9%, 33.5%, and 21.8%, respectively. Survival curves for RFS and OS of the PSM cohort and subgroup for combined macrovascular invasion and lymph node metastasis are illustrated in Figure 3.

Table 2. Tumor response and adverse events to conversion therapy

No. of patients	Conversion therapy cohort, No. (%)
Response to conversion therapy	
CR	12 (13.6)
PR	58 (65.9)
SD	16 (18.2)
PD	2 (2.3)
Tumor pathology	
PCR	21 (23.9)
MPR	48 (54.5)
Adverse events (CTCAE)	
Grade 0	24 (27.2)
Grade 1	20 (22.7)
Grade 2	29 (33.0)
Grade 3	15 (17.1)
Grade 4	0 (0)
Grade 5	0 (0)

Abbreviations: CR, complete response; PR, partial response; SD, stable disease; PD, progressive disease; PCR, pathological complete response; MPR, major pathological response; CTCAE, common terminology criteria for adverse events.

3.6. Analysis of serum AFP levels with patient outcome and prognosis

Analysis of the relationship between AFP levels before and after treatment and patient prognosis in patients receiving conversion therapy revealed that OS (Figure 4A) and RFS (Figure 4B) were significantly higher in patients with negative AFP levels before conversion therapy than in patients with positive AFP levels before conversion therapy (P = 0.016/0.026). AFP-positive patients reached median relapse-free survival at 21.6 months. The efficacy of AFP level after conversion therapy was more significant (P = 0.0025/< 0.001) in suggesting OS (Figure 4C) and RFS (Figure 4D) of patients. No significant correlation was observed between the AFP level at the time of the initial diagnosis and the proportion of residual tumor (Figure 4E), and there was a significant correlation between the proportion of residual tumor in surgically resected specimens and AFP level after conversion therapy (Figure 4F, P = 0.0047, R^2= 0.089). However, among the other indicators of efficacy assessment, AFP levels at initial consultation and after

Table 3. Comparison of surgery-related complications in the conversion therapy or surgery group

Variables *n* (%)	Before PSM			After PSM		
	Conversion therapy (*n* = 88)	Surgery (*n* = 123)	*P*	Conversion therapy (*n* = 88)	Surgery (*n* = 88)	*P*
Postoperative Child-pugh grade on day 5			< 0.001			< 0.001
A	74 (84.1)	71 (56.3)		74 (84.1)	50 (56.9)	
B	14 (15.9)	50 (42.2)		14 (15.9)	37 (42.0)	
C	0 (0)	2 (27.8)		0 (0)	1 (1.1%)	
Postoperative hospital stays	9 (4-33)	9 (4-40)	0.756	9 (4-33)	9 (4-40)	0.691
Perioperative mortality	0 (0)	2 (1.6)	0.511	0 (0)	1 (1.1%)	0.316
Complications						
Clavien-Dindo classification			0.25			0.53
3	4	10		4	5	
4	14	20		14	12	
5	0	3		0	1	

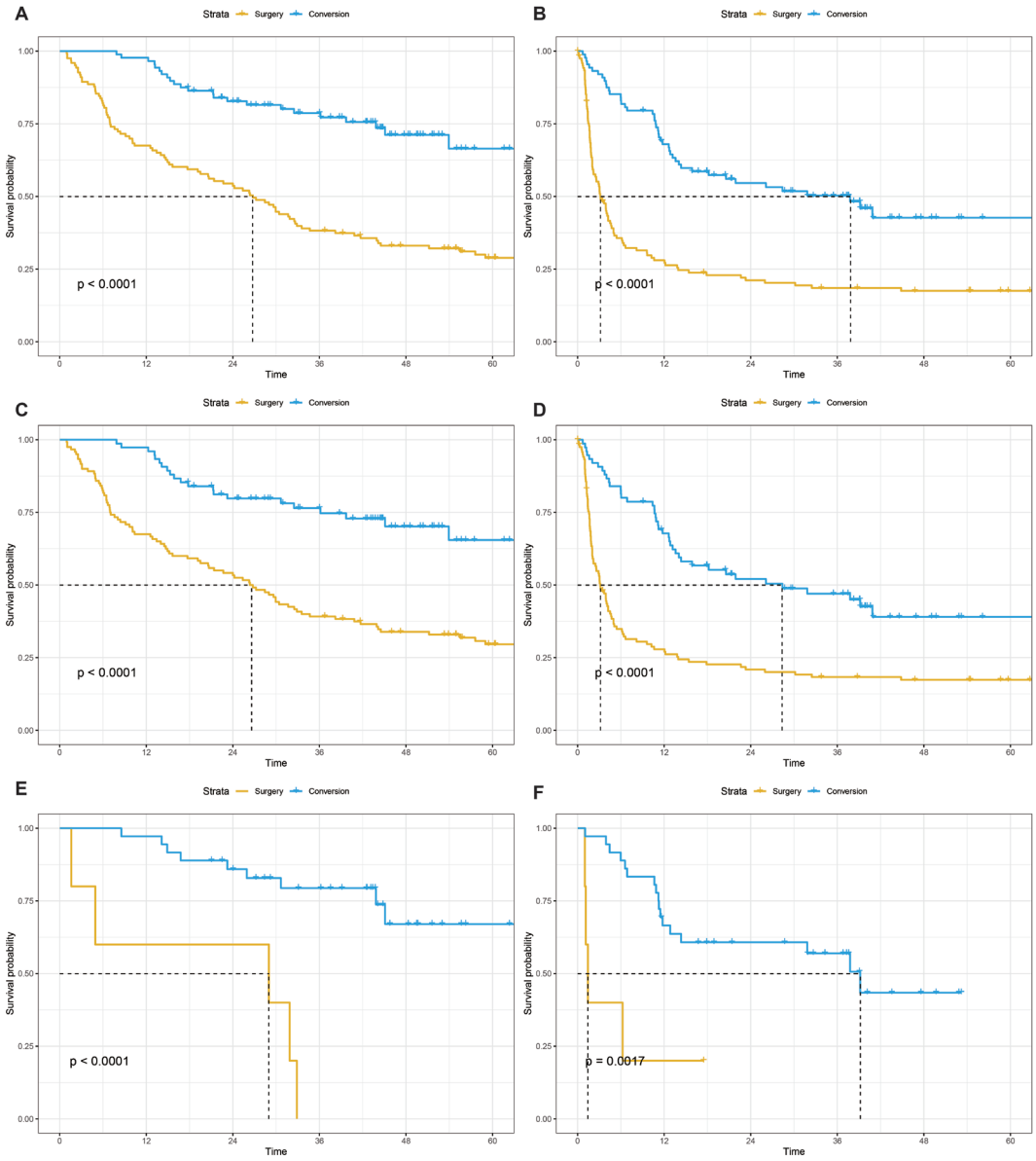

Figure 2. (A) Overall survival (OS) curves for the conversion therapy groups and surgery groups, (B) Recurrence-free survival (RFS) curves for the conversion groups and surgery-alone groups, (C) Overall survival (OS) curves for patients with macrovascular invasion in two groups, (D) Recurrence-free survival (RFS) curves for patients with macrovascular invasion in two groups. (E) Overall survival (OS) curves for patients with lymph node metastasis in two groups. (F)Recurrence-free survival (RFS) curves for patients with lymph node metastasis in two groups.

treatment were significantly correlated with the results of mRecist assessment and the results of pathologic assessment (Figures 4G-J).

3.7. COX analysis results

According to univariate COX regression analysis, preoperative CHILD grading, intraoperative blood loss, perioperative blood transfusion, and conversion therapy were correlated with postoperative recurrence of individuals with BCLC–C-stage HCC ($P < 0.1$) and were included in the COX multivariate analysis. The final results suggested a significant correlation between conversion therapy and postoperative OS in individuals with BCLC–C-stage HCC. Moreover, the above factors still exhibited a statistical correlation with OS in the cohort after PSM. Multivariate Cox analysis in the PSM cohort revealed that conversion therapy remains the only independent risk factor associated with postoperative survival in patients with BCLC-C stage HCC. The final results suggested that conversion therapy was remarkably linked to postoperative OS in individuals with BCLC–C-stage HCC (Table 4). In terms of postoperative recurrence in patients at the BCLC-C stage, univariate Cox analysis results from the overall cohort suggest that conversion therapy, tumor diameter, surgical procedure, intraoperative blood loss, and perioperative blood transfusion are associated with postoperative RFS. After incorporating these into a multivariate Cox analysis, it was found that only conversion therapy is an independent

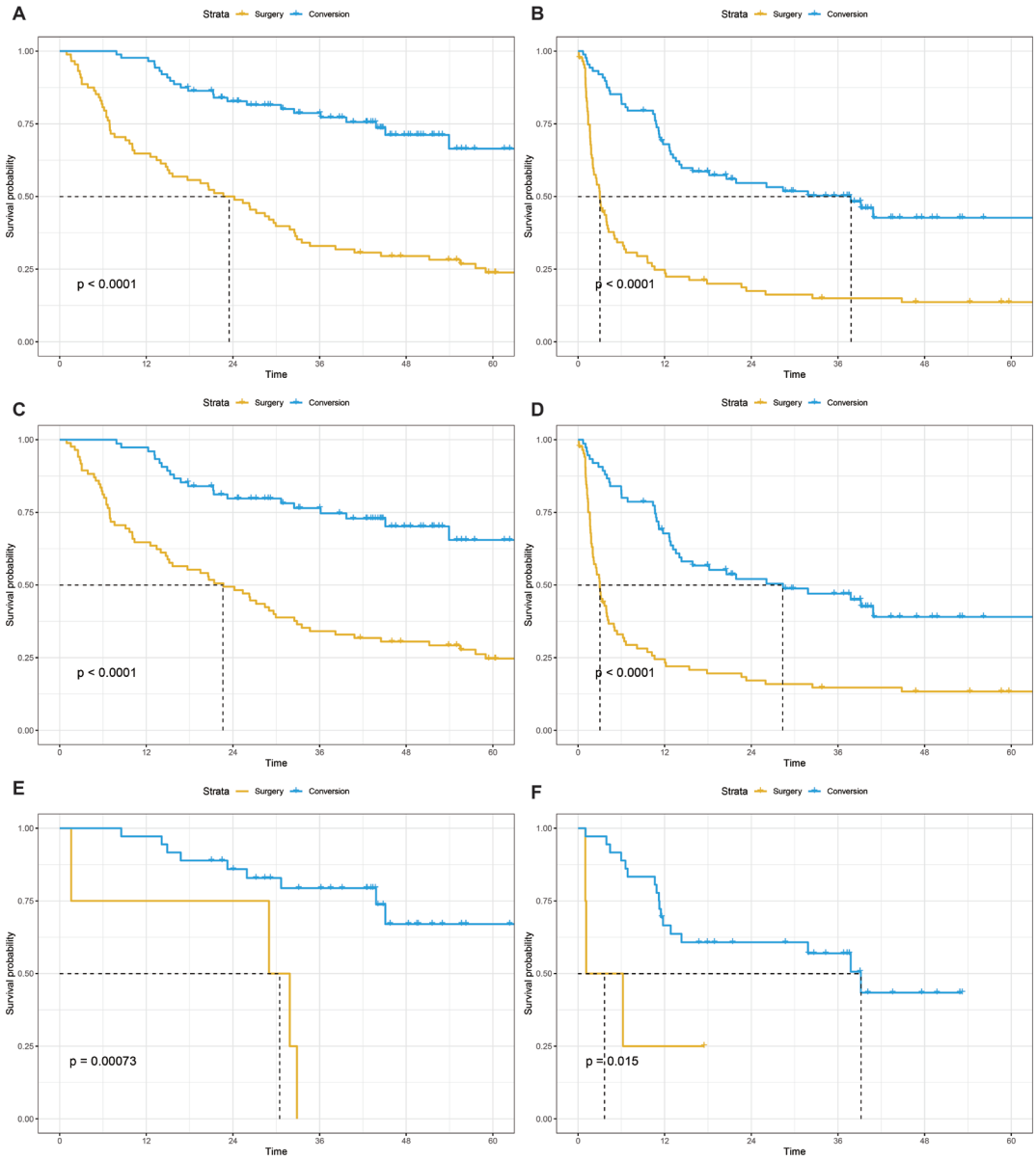

Figure 3. (A) Overall survival (OS) curves for the conversion therapy groups and surgery groups in propensity model, (B) Recurrence-free survival (RFS) curves for the conversion groups and surgery-alone groups in propensity model, (C) Overall survival (OS) curves for patients with macrovascular invasion in two groups in propensity model, (D) Recurrence-free survival (RFS) curves for patients with macrovascular invasion in two groups in propensity model. (E) Overall survival (OS) curves for patients with lymph node metastasis in two groups in the propensity model. (F)Recurrence-free survival (RFS) curves for patients with lymph node metastasis in the two groups in propensity model.

risk factor for postoperative recurrence. Similar results were observed in the cohort after PSM (Table 5).

4. Discussion

Individuals with BCLC–C-stage HCC have poor treatment outcomes and short survival duration. Surgery is the radical means to treat HCC (*22*). In previous clinical practice, patients with BCLC-C stage were recommended by most guidelines and consensus to undergo systemic combined treatment to delay tumor progression because of the poor outcome of surgical treatment (*8*). However, immunotherapy combined with targeted sequential surgical regimens significantly improved the prognosis of individuals with BCLC–C-stage HCC (*12,23*). In addition, the stage-reducing effect of conversion therapy furthered the opportunity for surgery in patients with stage BCLC-C. A total of 211 individuals with BCLC–C-stage HCC were included in this research. Among them, 88 patients received conversion therapy sequential surgical treatment before surgery, and 123 received surgery directly. The comparison of recurrence-free survival and survival rates between the two groups suggested that patients with BCLC–C-stage HCC treated with conversion therapy sequential surgery had a significantly better prognosis than their counterparts who underwent direct surgery. Therefore, conversion therapy may provide a significant

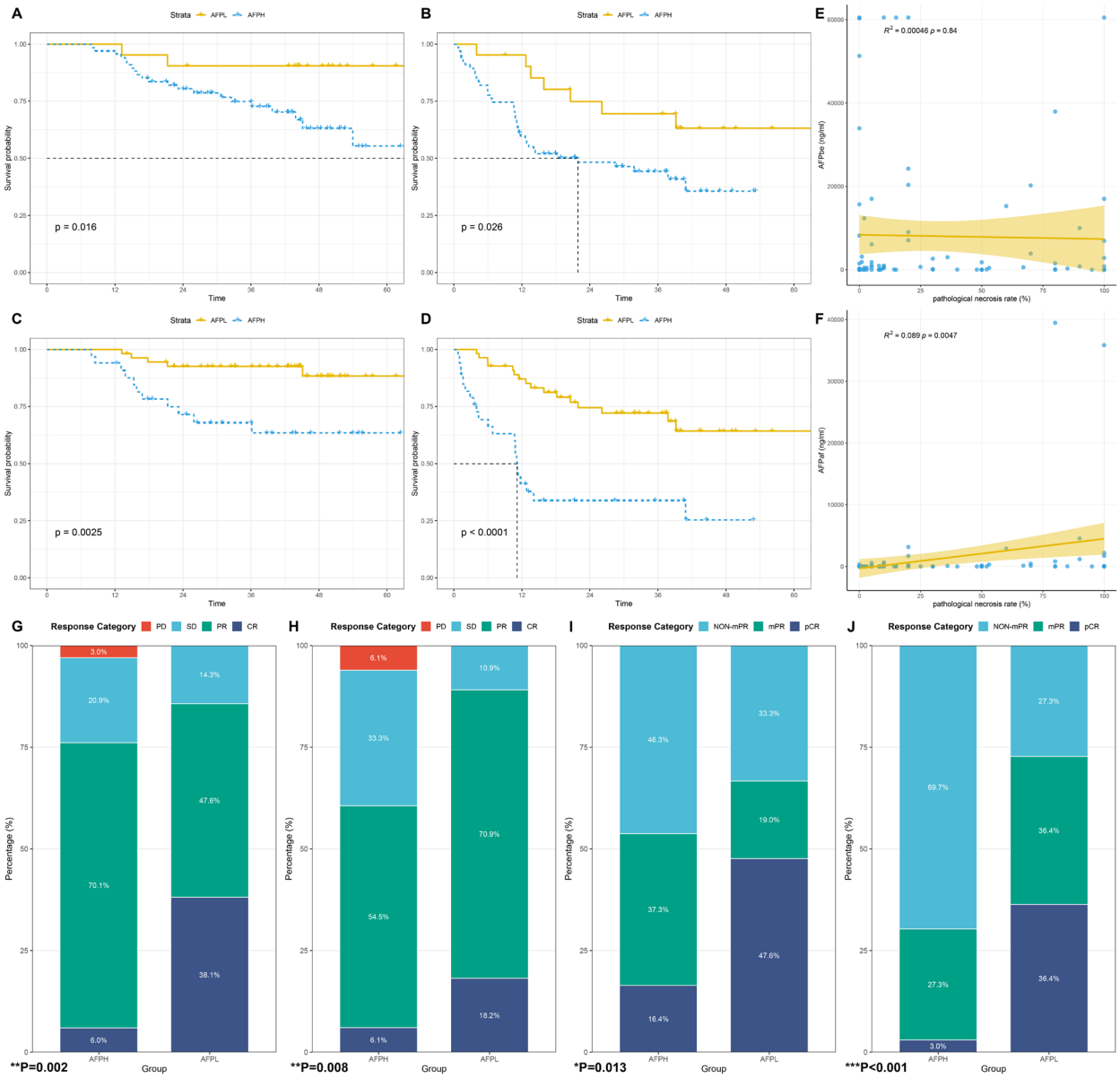

Figure.4 (A) Overall survival (OS) curves for the initial AFPH groups and AFPL groups, (B) Recurrence-free survival (RFS) curves for the initial AFPH groups and AFPL groups, (C) Overall survival (OS) curves for the AFPH groups and AFPL groups after conversion therapy, (D) Recurrence-free survival (RFS) curves for the AFPH groups and AFPL groups after conversion therapy. (E) Correlation between initial AFP levels and percentage of pathological necrosis. (F) Correlation between AFP levels after conversion therapy and percentage of pathological necrosis. (G) Relationship between initial AFP and mRecist assessment results. (H) Relationship between AFP after conversion therapy and mRecist assessment results. (I). Relationship between initial AFP and results of pathologic evaluation. (J). Relationship between AFP after conversion therapy and results of pathologic evaluation.

survival benefit for individuals with BCLC–C-stage HCC. According to the results of the COX multifactorial regression model, preoperative immunotherapy combined with targeted sequential surgical therapy was a significant protective factor for overall survival(HR = 0.212, $P < 0.001$) and recurrence-free survival (HR = 0.387, $P < 0.001$) in patients with BCLC–C-stage HCC. In contrast, individuals with BCLC–C-stage HCC underwent transhepatic artery chemoembolization with sorafinib to achieve mOS of 12 months, and 1- and 2-year OS rates were 47% and 24%, respectively (*24*). Whereas advanced hepatocellular carcinoma is treated by applying SBRT, the 6 and 12-month PFS was 58% and 40% (*25*). Therefore, conversion therapy with sequential surgical treatment protocols has better efficacy than previous combination therapies.

Macrovascular invasion is a common clinical condition in individuals with BCLC-C stage HCC. After conversion therapy, 27 patients had downgraded PVTT, 7 patients had complete disappearance of PVTT, and 15 patients had downgraded HVTT, 9 patients had complete disappearance of HVTT. PVTT is more likely to result in intrahepatic and hematogenous metastases, increasing portal vein pressure, and the risk of ruptured esophagogastric varices (*26*). Patients with hepatic vein thrombosis are not only at higher risk of pulmonary

Table 4. Univariate and multivariate Cox-regression analyses of overall survival in HCC patients with PVTT undergoing conversion therapy or surgery alone

Variables	UV HR (95% CI)	*P*	MV HR (95% CI)	*P*
Before PSM				
Age (> 60 *vs*. ≤ 60 years)	0.958 (0.620-1.483)	0.849		
Gender (Male *vs*. Female)	1.055 (0.549-2.028)	0.871		
HBsAg (Positive *vs*. Negative)				
No hepatitis	-	-		
HBV	1.065 (0.613-1850)	0.823		
HCV	0.744 (0.247-2.245)	0.600		
Child-pugh grade (B *vs*. A)	2.115 (0.925-4.835)	0.076	1.357 (0.573-3.209)	0.488
AFP (> 20 *vs*. ≤ 20 ng/mL)	1.317 (0.814-2.130)	0.262		
Previous local treatment (Yes *vs*. No)	0.828 (0.502-1.365)	0.459		
Tumor diameter (cm)	1.032 (0.986-1.080)	0.178		
Tumor number (Multiple *vs*. Single)	1.070 (0.656-1.747)	0.785		
Surgical procedure (Thrombectomy *vs*. En-bloc)	1.169 (0.791-1.729)	0.433		
Extent of resection (Major *vs*. Minor)	1.103 (0.722-1.685)	0.649		
Intraoperative blood loss (> 400 *vs*. ≤ 400 mL)	1.911 (1.290-2.830)	0.001	1.510 (0.965-2.362)	0.071
Perioperative blood transfusion (Yes *vs*. No)	1.670 (1.116-2.500)	0.013	1.352 (0.846-2.160)	0.207
Conversion therapy (Yes *vs*. No)	0.235 (0.138-0.403)	< 0.001	0.242 (0.141-0.415)	< 0.001
After PSM				
Age (> 60 *vs*. ≤ 60 years)	1.003 (0.590-1.705)	0.991		
Gender (Male *vs*. Female)	0.783 (0.400-1.533)	0.475		
HBsAg (Positive *vs*. Negative)				
No hepatitis	-	-		
HBV	2.216 (0.695-7.068)	0.179		
HCV	1.834 (0.370-9.096)	0.458		
Child-pugh grade (B *vs*. A)	4.355 (1.728-10.972)	0.002	4.212 (1.604-11.057)	0.004
AFP (> 20 *vs*. ≤ 20 ng/mL)	1.146 (0.668-1.966)	0.620		
Previous local treatment (Yes *vs*. No)	0.936 (0.526-1.664)	0.822		
Tumor diameter (cm)	1.024 (0.968-1.084)	0.403		
Tumor number (Multiple *vs*. Single)	1.126 (0.634-1.998)	0.686		
Surgical procedure (Thrombectomy *vs*. En-bloc)	0.913 (0.565-1.476)	0.710		
Extent of resection (Major *vs*. Minor)	1.132 (0.684-1.872)	0.630		
Intraoperative blood loss (> 400 *vs*. ≤ 400 mL)	1.750 (1.086-2.817)	0.021	1.267 (0.754-2.129)	0.372
Perioperative blood transfusion (Yes *vs*. No)	1.893 (1.158-3.094)	0.011	1.705 (0.988-2.941)	0.055
Conversion therapy (Yes *vs*. No)	0.225 (0.122-0.414)	< 0.001	0.212 (0.114-0.391)	< 0.001

Abbreviations: HBV, hepatitis B virus; HCV, hepatitis C virus; AFP, alpha-fetoprotein.

metastasis but also at risk of sudden death due to the dislodgment of the hepatic vein thrombus (*27*). A meta-analysis has noted that patients with microvascular invasion treated surgically have a median overall survival of 14.39 months, 1-year OS was 54.47% and 3-year OS was 23.20%, the 1- and 3-year RFS were 27.70% and 10.06%, respectively (*28*). Compared with the results reported in our study, it can be found that the application of the combined treatment regimen significantly prolonged the OS and RFS of the patients, providing a clear survival benefit for the patients. Conversion therapy effectively reduced tumor load and prolonged patient survival. Thus, a combination regimen to downgrade the tumor followed by sequential surgical procedures was effective. The reduction in tumor volume allows patients to complete radical resection of the tumor within a smaller resection area, and the larger residual liver volume provides sufficient opportunity to undergo other local treatment options or even secondary surgical treatment after tumor-resistant recurrence (*14*). And the retreating cancer embolus prepares an adequate length of blood vessels. Therefore, patients who would otherwise require cancer embolization or even portal vein resection and reconstruction can complete en-bloc resection through hepatectomy alone. This protocol simplifies the surgical procedure, ensures a higher percentage of en-bloc resection, and improves the procedure's safety (*29*).

A subset of individuals with BCLC–C-stage HCC will develop extrahepatic metastases. The vast majority of patients with extrahepatic lesions in this study had abdominal lymph node metastases, and only one patient in the surgery group had localized diaphragmatic invasion. Currently, non-surgical treatments, such as PD-1 antibodies, targeted agents, or other localized treatment options, are still recommended for patients with hepatocellular carcinoma combined with lymph node metastases. In this study, 34 patients in the conversion therapy group were diagnosed by imaging data with lymph node metastasis at the initial diagnosis. However, lymph node metastases were detected in only 17 individuals in the postoperative pathological specimen examination. During the conversion process, it was observed that several patients in the conversion therapy group showed shrinkage or even the disappearance

Table 5. Univariate and multivariate Cox-regression analyses of recurrence-free survival in HCC patients with PVTT undergoing conversion therapy or surgery alone

Variables	UV HR (95% CI)	*P*	MV HR (95% CI)	*P*
Before PSM				
Age (> 60 *vs*. ≤ 60 years)	1.048 (0.716-1.534)	0.809		
Gender (Male *vs*. Female)	0.884 (0.516-1.515)	0.653		
HBsAg (Positive *vs*. Negative)				
No hepatitis	-	-		
HBV	0.942 (0.583-1.520)	0.805		
HCV	0.711 (0.285-1.770)	0.463		
Child-pugh grade (B *vs*. A)	1.490 (0.656-3.384)	0.340		
AFP (> 20 *vs*. ≤ 20 ng/mL)	1.258 (0.828-1.911)	0.282		
Previous local treatment (Yes *vs*. No)	0.975 (0.638-1.490)	0.907		
Tumor diameter (cm)	1.040 (0.997-1.084)	0.066	1.037 (0.992-1.084)	0.106
Tumor number (Multiple *vs*. Single)	1.128 (0.734-1.734)	0.582		
Surgical procedure (Thrombectomy *vs*. En-bloc)	1.467 (1.040-2.070)	0.029	1.175 (0.822-1.679)	0.376
Extent of resection (Major *vs*. Minor)	1.332 (0.916-1.938)	0.133		
Intraoperative blood loss (> 400 *vs*. ≤ 400 mL)	1.604 (1.137-2.261)	0.007	1.310 (0.877-1.957)	0.187
Perioperative blood transfusion (Yes *vs*. No)	1.477 (1.028-2.122)	0.035	1.202 (0.789-1.831)	0.392
Conversion therapy (Yes *vs*. No)	0.391 (0.267-0.572)	< 0.001	0.394 (0.268-0.580)	< 0.001
After PSM				
Age (> 60 *vs*. ≤ 60 years)	1.043 (0.663-1.643)	0.855		
Gender (Male *vs*. Female)	0.748 (0.423-1.324)	0.319		
HBsAg (Positive *vs*. Negative)				
No hepatitis	-	-		
HBV	1.500 (0.654-3.436)	0.338		
HCV	1.063 (0.300-3.771)	0.924		
Child-pugh grade (B *vs*. A)	1.606 (0.589-4.384)	0.355		
AFP (> 20 *vs*. ≤ 20 ng/mL)	1.164 (0.731-1.853)	0.522		
Previous local treatment (Yes *vs*. No)	1.056 (0.649-1.717)	0.827		
Tumor diameter (cm)	1.031 (0.980-1.084)	0.238		
Tumor number (Multiple *vs*. Single)	1.212 (0.739-1.987)	0.447		
Surgical procedure (Thrombectomy *vs*. En-bloc)	1.287 (0.856-1.936)	0.225		
Extent of resection (Major *vs*. Minor)	1.298 (0.846-1.991)	0.223		
Intraoperative blood loss (> 400 *vs*. ≤ 400 mL)	1.417 (0.941-2.133)	**0.096**	1.108 (0.696-1.763)	**0.666**
Perioperative blood transfusion (Yes *vs*. No)	1.544 (1.001-2.382)	**0.050**	1.527 (0.935-2.495)	0.091
Conversion therapy (Yes *vs*. No)	0.390 (0.253-0.600)	**< 0.001**	0.387 (0.251-0.597)	**< 0.001**

Abbreviations: HBV, hepatitis B virus; HCV, hepatitis C virus; AFP, alpha-fetoprotein; ECOG PS, Eastern Cooperative Oncology Group performance status; PVTT, portal vein tumor thrombus.

of lymph nodes. The location of the lymph nodes present at the initial diagnosis was carefully explored intraoperatively, and some tissues were excised for pathological examination, suggesting that there were no definite tumor cells. Therefore, the immunotherapy combined with targeted therapy effectively attenuated the tumors metastasizing in local lymph nodes. However, the need for radical debulking of sites where lymph node lesions have disappeared after conversion therapy remains to be investigated.

Serum AFP levels have previously been used as a tumor marker for the diagnosis of hepatocellular carcinoma. More and more studies have pointed out that AFP levels may also indicate the effectiveness of treatment during tumor therapy in hepatocellular carcinoma (*30*). In this study, serum AFP levels were significantly associated with OS, RFS, mRecist, pathologic evaluation, and the percentage of pathologic tumor cell remnants in patients who underwent conversion therapy. This suggests that AFP levels after conversion therapy can be used to predict patient outcomes and evaluate the timing of surgery. At the same time, AFP levels at the time of initial diagnosis also correlated with these indicators, suggesting that serum AFP levels at the time of initial diagnosis can be used to predict the efficacy of immunotherapy and the prognosis of patients. However, no matter before or after treatment, patients in the high AFP group always showed shorter survival and poorer therapeutic effects, which we believe is related to the inhibitory tumor immune microenvironment caused by high AFP levels and further research is urgently needed to explore the related mechanisms (*31,32*).

Also of interest in this study was the postoperative adjuvant therapy that the patients received. In this study, patients will undergo postoperative targeted combination immunotherapy after surgery based on pathology findings. To date, 43 individuals in this cohort have completed postoperative adjuvant therapy. We believe that postoperative adjuvant therapy plays a positive role in preventing postoperative recurrence in patients, while its mechanism and efficacy still need to be revealed

by further research. A postoperative adjuvant program based on a combination of surgical and pathologic findings to guide the process provides a clear plan for discontinuation of the drug. This has helped to minimize adverse drug reactions and economic burden for patients.

Sixty-four patients in the conversion therapy group experienced adverse events during conversion therapy, 44 of whom had a CTCAE event grade ≥ 2. No patients discontinued the conversion regimen due to treatment-related adverse events and considerable variations were not observed between the two groups regarding bleeding volume, intraoperative blood transfusion, and postoperative hospitalization days. In the conversion therapy group, five patients developed postoperative biliary fistula, one developed postoperative bleeding, one suffered from pancreatitis, and one had postoperative secondary portal thrombosis (right anterior branch). The non-significant differences in Clavein-Dindo scores between the two groups suggest the safety of immunotherapy combined with targeted sequential surgical regimens. Compared with traditional surgical treatment of liver cancer, the difference in perioperative complication rates was not statistically significant, confirming the safety and feasibility of this protocol.

There are certain limitations to this study. The nature of this historical-prospective study leads to some bias and the sample size included in the subgroup was small. Moreover, statistically positive outcomes were difficult to obtain in some patients. Nevertheless, this study contains the largest cohort and assesses the efficacy and safety of immunotherapy combined with targeted sequential surgical therapy in individuals with advanced HCC. It provides a detailed analysis of the efficacy and safety of treatment in multiple subgroups of patients.

Funding: None.

Conflict of Interest: The authors have no conflicts of interest to disclose.

References

1. Devarbhavi H, Asrani SK, Arab JP, Nartey YA, Pose E, Kamath PS. Global burden of liver disease: 2023 update. J Hepatol. 2023; 79:516-537.
2. Thomas MB, Jaffe D, Choti MM, *et al*. Hepatocellular carcinoma: consensus recommendations of the National Cancer Institute Clinical Trials Planning Meeting. J Clin Oncol. 2010; 28:3994-4005.
3. Cabibbo G, Enea M, Attanasio M, Bruix J, Craxì A, Cammà C. A meta-analysis of survival rates of untreated patients in randomized clinical trials of hepatocellular carcinoma. Hepatology. 2010; 51:1274-1283.
4. Bruix J, Reig M, Sherman M. Evidence-Based Diagnosis, Staging, and Treatment of Patients With Hepatocellular Carcinoma. Gastroenterology. 2016; 150:835-853.
5. Llovet JM, Bustamante J, Castells A, Vilana R, Ayuso Mdel C, Sala M, Brú C, Rodés J, Bruix J. Natural history of untreated nonsurgical hepatocellular carcinoma: rationale for the design and evaluation of therapeutic trials. Hepatology. 1999; 29:62-67
6. Lee CW, Chan KM, Lee CF, Yu MC, Lee WC, Wu TJ, Chen MF. Hepatic resection for hepatocellular carcinoma with lymph node metastasis: clinicopathological analysis and survival outcome. Asian J Surg. 2011; 34:53-62.
7. European Association for the Study of the Liver. EASL Clinical Practice Guidelines on the management of hepatocellular carcinoma. J Hepatol. 2025; 82:315-374.
8. Benson AB, D'Angelica MI, Abbott DE, *et al*. Hepatobiliary Cancers, Version 2.2021, NCCN Clinical Practice Guidelines in Oncology. J Natl Compr Canc Netw. 2021; 19:541-565.
9. Korean Liver Cancer Association (KLCA) and National Cancer Center (NCC) Korea. 2022 KLCA-NCC Korea practice guidelines for the management of hepatocellular carcinoma. Clin Mol Hepatol. 2022; 28:583-705.
10. Llovet JM, Kudo M, Merle P, *et al*. Lenvatinib plus pembrolizumab versus lenvatinib plus placebo for advanced hepatocellular carcinoma (LEAP-002): A randomised, double-blind, phase 3 trial. Lancet Oncol. 2023; 24:1399-1410.
11. Cao Y, Tang H, Hu B, *et al*. Comparison of survival benefit between salvage surgery after conversion therapy versus surgery alone for hepatocellular carcinoma with portal vein tumor thrombosis: a propensity score analysis. HPB (Oxford). 2023; 25:775-787.
12. Pan Y, Yang L, Cao Y, Jun H, Tang H, Zhang W, Wan T, Jiao T, Hu B, Lu S. Factors influencing the prognosis patients with Barcelona Clinic Liver Cancer stage C hepatocellular carcinoma undergoing salvage surgery after conversion therapy. Transl Cancer Res. 2023; 12:1852-1862.
13. Tang H, Cao Y, Jian Y, Li X, Li J, Zhang W, Wan T, Liu Z, Tang W, Lu S. Conversion therapy with an immune checkpoint inhibitor and an antiangiogenic drug for advanced hepatocellular carcinoma: A review. Biosci Trends. 2022; 16:130-141.
14. Clavien PA, Barkun J, de Oliveira ML, Vauthey JN, Dindo D, Schulick RD, de Santibañes E, Pekolj J, Slankamenac K, Bassi C, Graf R, Vonlanthen R, Padbury R, Cameron JL, Makuuchi M. The Clavien-Dindo classification of surgical complications: five-year experience. Ann Surg. 2009; 250:187-196.
15. Koch M, Garden OJ, Padbury R, *et al*. Bile leakage after hepatobiliary and pancreatic surgery: a definition and grading of severity by the International Study Group of Liver Surgery. Surgery. 2011; 149:680-688.
16. Llovet JM, Lencioni R. mRECIST for HCC: Performance and novel refinements. J Hepatol. 2020; 72:288-306.
17. Cottrell TR, Thompson ED, Forde PM, *et al*. Pathologic features of response to neoadjuvant anti-PD-1 in resected non-small-cell lung carcinoma: A proposal for quantitative immune-related pathologic response criteria (irPRC). Ann Oncol. 2018; 29:1853-1860.
18. Cloyd JM, Wang H, Egger ME, *et al*. Association of Clinical Factors With a Major Pathologic Response Following Preoperative Therapy for Pancreatic Ductal Adenocarcinoma. JAMA Surg. 2017; 152:1048-1056.
19. Common Terminology Criteria for Adverse Events (CTCAE) v5.0. *https://ctep.cancer.gov/protocoldevelopment/electronic_applications/ctc.htm#ctc_50* (accessed January 11, 2023).
20. Kudo M, Kawamura Y, Hasegawa K, *et al*. Management of Hepatocellular Carcinoma in Japan: JSH Consensus Statements and Recommendations 2021 Update. Liver

Cancer. 2021; 10:181-223.
21. Tang H, Zhang W, Cao J, *et al*. Chinese expert consensus on sequential surgery following conversion therapy based on combination of immune checkpoint inhibitors and antiangiogenic targeted drugs for advanced hepatocellular carcinoma (2024 edition). Biosci Trends. 2025; 18:505-524.
22. Iijima H, Kudo M, Kubo S, Kurosaki M, Sakamoto M, Shiina S, Tateishi R, Osamu N, Fukumoto T, Matsuyama Y, Murakami T, Takahashi A, Miyata H, Kokudo N. Report of the 23rd nationwide follow-up survey of primary liver cancer in Japan (2014-2015). Hepatol Res. 2023; 53:895-959.
23. Zhu XD, Huang C, Shen YH, Xu B, Ge NL, Ji Y, Qu XD, Chen L, Chen Y, Li ML, Zhu JJ, Tang ZY, Zhou J, Fan J, Sun HC. Hepatectomy After Conversion Therapy Using Tyrosine Kinase Inhibitors Plus Anti-PD-1 Antibody Therapy for Patients with Unresectable Hepatocellular Carcinoma. Ann Surg Oncol. 2023; 30:2782-2790.
24. Zhao Y, Wang WJ, Guan S, Li HL, Xu RC, Wu JB, Liu JS, Li HP, Bai W, Yin ZX, Fan DM, Zhang ZL, Han GH. Sorafenib combined with transarterial chemoembolization for the treatment of advanced hepatocellular carcinoma: a large-scale multicenter study of 222 patients. Ann Oncol. 2013; 24:1786-1792.
25. Sharma D, Thaper D, Kamal R, Yadav HP. Role of palliative SBRT in barcelona clinic liver cancer-stage C hepatocellular carcinoma patients. Strahlenther Onkol. 2023; 199:838-846.
26. Kawai T, Yashima Y, Sugimoto T, Sato T, Kanda M, Enomoto N, Sato S, Obi S. Emergency endoscopic variceal ligation following variceal rupture in patients with advanced hepatocellular carcinoma and portal vein tumor thrombosis: a retrospective study. World J Surg Oncol. 2016; 14:52.
27. Papp E, Keszthelyi Z, Kalmar NK, Papp L, Weninger C, Tornoczky T, Kalman E, Toth K, Habon T. Pulmonary embolization as primary manifestation of hepatocellular carcinoma with intracardiac penetration: a case report. World J Gastroenterol. 2005; 11:2357-2359.
28. Huang DQ, Tran A, Tan EX, Nerurkar SN, Teh R, Teng MLP, Yeo EJ, Zou B, Wong C, Esquivel CO, Bonham CA, Nguyen MH. Characteristics and outcomes of hepatocellular carcinoma patients with macrovascular invasion following surgical resection: a meta-analysis of 40 studies and 8,218 patients. Hepatobiliary Surg Nutr. 2022; 11:848-860.
29. Jiao T, Tang H, Zhang W, Hu B, Wan T, Cao Y, Zhang Z, Wang Y, Cao J, Cui M, Lu S. Long-term survival and portal vein patency with novel PVTT surgery approach in advanced HCC patients with Vp3/4 PVTT following combination therapy of TKIs and PD-1 inhibitors. BMC Surg. 2023; 23:384.
30. Lim TS, Rhee H, Kim GM, Kim SU, Kim BK, Park JY, Ahn SH, Han KH, Choi JY, Kim DY. Alpha-Fetoprotein, Des-Gamma-Carboxy Prothrombin, and Modified RECIST Response as Predictors of Survival after Transarterial Radioembolization for Hepatocellular Carcinoma. J Vasc Interv Radiol. 2019; 30:1194-1200.e1.
31. Munson PV, Adamik J, Butterfield LH. Immunomodulatory impact of α-fetoprotein. Trends Immunol. 2022; 43:438-448
32. He H, Chen S, Fan Z, Dong Y, Wang Y, Li S, Sun X, Song Y, Yang J, Cao Q, Jiang J, Wang X, Wen W, Wang H. Multi-dimensional single-cell characterization revealed suppressive immune microenvironment in AFP-positive hepatocellular carcinoma. Cell Discov. 2023; 9:60.

Received June 2, 2025; Revised July 20, 2025; Accepted July 23, 2025.

[§]These authors contributed equally to this work.
**Address correspondence to:*
Shichun Lu, Faculty of Hepato-Pancreato-Biliary Surgery, First Medical Center of Chinese People's Liberation Army General Hospital, No.28 Fuxing Road, Haidian District, Beijing, China.
E-mail: lusc_plagh@163.com

Released online in J-STAGE as advance publication July 26, 2025.

Appendix Data

Table S1. Conversion therapy protocols

Conversion therapy protocols	No. of patients, No. (%)
Sintilimab+lenvatinib	66 (75.0)
pembrolizumab+lenvatinib	8 (9.1)
Tislelizumab+lenvatinib	5 (5.7)
Toripalimab+lenvatinib	5 (5.7)
Camrelizumab+apatinib	1 (1.1)
Toripalimab+apatinib	1 (1.1)
Camrelizumab + lenvatinib	1 (1.1)
Navulizumab+lenvatinib	1 (1.1)

Original Article

DOI: 10.5582/bst.2025.01208

Textbook outcome and survival following laparoscopic versus open right hemihepatectomy for hepatocellular carcinoma: A propensity score-matched study

Jun Ji, Ding Hu, Jiaao Wang, Ziqi Hou, Zhihong Zhang, Haichuan Wang*, Jiwei Huang*

Division of Liver Surgery, Department of General Surgery, West China Hospital, Sichuan University, Chengdu, China.

SUMMARY: The role of laparoscopy for complex resections like right hemihepatectomy for hepatocellular carcinoma (HCC) remains contentious, and its assessment is often hampered by traditional metrics that fail to reflect the comprehensive quality of perioperative management. Therefore, this study used the textbook outcome (TO), a composite endpoint, to compare the laparoscopic (LRH) and open (ORH) approaches for HCC within a propensity score-matched (PSM) analysis. We retrospectively analyzed 435 patients who underwent curative-intent right hemihepatectomy. After 1:3 PSM, a final cohort of 121 patients who underwent LRH and 242 who underwent ORH was included for analysis. Results indicated that the rate of TO achievement was comparable between the LRH and ORH groups (62.0% *vs*. 65.3%, $p = 0.563$), with intraoperative complications (17.4%), post-hepatectomy liver failure (14.9%), and major postoperative complications (13.5%) as the primary barriers to achieving a TO. No significant differences in overall survival (OS) or disease-free survival (DFS) were observed, although the LRH group had a significantly shorter duration of hospitalization ($p = 0.006$). In multivariable Cox regression models, achieving a TO was confirmed as an independent protective factor for both OS (HR: 0.46, 95% CI: 0.34-0.63, $p < 0.001$) and DFS (HR: 0.44, 95% CI: 0.33-0.58, $p < 0.001$). For right hemihepatectomy, clinical practice should focus on maximizing the rate of TO achievement through systematic perioperative management, as a key strategy to improve long-term prognosis.

Keywords: liver cancer, minimally invasive surgery, textbook outcome, prognosis, postoperative complications

1. Introduction

Primary liver cancer (PLC) represents a significant global health burden, ranking as the sixth most common malignancy and the third leading cause of cancer-related mortality, with over 906,000 new cases diagnosed worldwide in 2020 (*1*). Hepatocellular carcinoma (HCC), the predominant histological subtype, comprises approximately 80% of the total PLC burden (*2*). For patients with HCC, surgical resection is the cornerstone of curative therapy for those with resectable lesions and well-preserved liver function, offering five-year survival rates of over 50% in selected cases (*3*).

With advances in minimally invasive principles and techniques, laparoscopic liver resection has emerged as a key alternative to open surgery, owing to its advantages in reducing perioperative trauma and shortening the duration of hospitalization, all while maintaining comparable oncological safety (*4,5*). However, the widespread use of laparoscopy in complex liver resections is limited by a steep learning curve and increased technical demands. Among hepatectomy procedures, right hemihepatectomy is particularly challenging due to its extensive resection volume and the intricate anatomy involved, posing significant demands on both the patient's physiological reserve and the surgeon's technical skill, which translates to heightened perioperative risks (*6*). Although studies have confirmed the safety and feasibility of laparoscopic hemihepatectomy (*7,8*), existing large-scale comparative analyses have largely focused on isolated perioperative endpoints. This fails to provide a comprehensive assessment of the overall quality of surgery and limits our understanding of how the perioperative course impacts the long-term prognosis.

Conventional quality assessment, which relies on single-outcome parameters, fails to capture the comprehensive characteristics of perioperative management (*9*). As a composite measure of multiple perioperative outcomes, the textbook outcome (TO) offers a more robust and comprehensive evaluation of overall surgical performance. In liver surgery, a standardized definition for the TO, established through an international Delphi consensus, includes five core

domains: intraoperative incidents, general postoperative complications, liver surgery-related postoperative complications, mortality, and oncological resection margin (*10*). Crucially, the achievement of a TO is associated with improved long-term survival in patients undergoing hepatectomy (*11,12*). This association elevates the TO from a simple quality benchmark to a clinically significant prognostic factor.

Whether the laparoscopic approach confers an advantage in achieving the TO for liver surgery remains unclear. While some studies have suggested a benefit for the laparoscopic approach (*13*), other comparative analyses have reported no significant difference in the rate of TO achievement between the two approaches (*14,15*). Interestingly, evidence from a multicenter study suggests that although laparoscopic surgery results in a higher rate of TO achievement in minor liver resection, this advantage disappears with major liver resection (*16*). In addition, as the complexity of surgery increases, the rate of TO achievement tends to decrease (*17*). Collectively, these results suggest that the relationship between surgical procedures and the TO may be a complex dependency, indicating that a "one-size-fits-all" assessment is inadequate and that distinct procedures may have specific TO profiles.

To the extent known, no study has specifically evaluated the role of laparoscopy in achieving a TO within the challenging setting of right hemihepatectomy. Therefore, this study aimed to compare the rates of TO achievement and associated risk factors between laparoscopic (LRH) and open (ORH) right hemihepatectomy for HCC in a propensity score-matched cohort and to further explore the impact of the TO as a comprehensive outcome indicator on long-term survival.

2. Methods

2.1. Study population

This retrospective cohort study was conducted in accordance with the Declaration of Helsinki and adhered to the Strengthening the Reporting of Cohort, Cross-sectional, and Case-control Studies in Surgery (STROCSS) guidelines (*18*). The study protocol was approved by the Ethics Committee of West China Hospital, Sichuan University (Approval No. 2025-93), and the requirement for individual patient consent was waived due to the retrospective design. The study was registered with ClinicalTrials.gov as NCT06950827.

We retrospectively analyzed the clinical data on consecutive patients who underwent curative-intent LRH or ORH for HCC at our center between January 2018 and January 2023. The inclusion criteria were as follows: (i) age ≥ 18 years; (ii) pathologically confirmed HCC confined to the right hemiliver; (iii) elective surgery; and (iv) Child-Pugh class A or B liver function and an American Society of Anesthesiologists (ASA) classification of I, II, or III. The exclusion criteria were: (*i*) pathologically confirmed cholangiocarcinoma, combined hepatocellular-cholangiocarcinoma, or metastatic liver malignancies; (*ii*) history of previous upper abdominal surgery; (*iii*) concomitant resection of adjacent organs (other than the gallbladder) or major vascular/biliary reconstruction; (*iv*) presence of adjacent organ invasion (other than the gallbladder), major vascular or biliary tumor thrombus, or distant metastases; and (*v*) incomplete or missing critical data.

2.2. Perioperative strategy and surgical procedure

A standardized perioperative management strategy was adopted. Preoperatively, the surgical plans for all complex cases were discussed by a multidisciplinary team (MDT). The perioperative assessment of liver function reserve included Child-Pugh and albumin-bilirubin (ALBI) grading, the indocyanine green retention rate at 15 minutes (ICG-R15) test, and computed tomography (CT) volumetry measurement.

Right hemihepatectomy was performed using a standardized anterior approach (*19*). For the LRH group, following routine surgical exploration and cholecystectomy, intraoperative laparoscopic ultrasonography was utilized to define the anatomical relationship between the lesions and key structures, particularly the middle hepatic vein (MHV). The hepatic hilum was then dissected to isolate the right Glissonean pedicle, which was temporarily clamped to delineate a clear ischemic line. Alternatively, indocyanine green fluorescence staining technique could be applied to visualize the intersegmental boundaries. Using the demarcated border and the MHV as primary anatomical landmarks, parenchymal transection proceeded in a caudal-to-cranial direction. The parenchymal transection continued deep to the level of the hilar plate, where the right hilar structures were dissected. The transection then progressed superiorly, culminating in the dissection of the main trunk of the right hepatic vein (RHV) at the second hepatic hilum. The right hemiliver was mobilized by dissecting the perihepatic ligaments, the short hepatic veins, and any surrounding adhesions. The specimen was placed in a retrieval bag and extracted through an accessory incision in the lower abdomen. After ensuring hemostasis and absence of bile leakage from the cut surface, an abdominal drain was placed in the surgical field. The procedure for the ORH group, performed through a reverse "L" or right subcostal incision, was similar to that for the LRH group. For both groups, blood inflow was controlled by intermittent use of the Pringle maneuver as required.

Postoperatively, patients were managed following an established Enhanced Recovery after Surgery (ERAS) pathway, which included intensive care for high-risk individuals, dynamic fluid resuscitation, hepatoprotective

therapy, thrombosis prophylaxis, and meticulous drainage management.

2.3. Definitions and outcomes

We used electronic medical records to retrospectively analyze the clinical data on patients, including their baseline characteristics, oncological information, intraoperative details, and pathological results. A comprehensive list of variables and a comparison of them between groups is detailed in Table 1. Preoperative liver function reserve was assessed using the ALBI score, calculated with the formula: (log10 bilirubin [μmol/L] × 0.66) - (albumin [g/L] × 0.085), and patients were stratified into three grades (*20*). The Barcelona Clinic Liver Cancer (BCLC) staging system was used for tumor staging (*21*). Major vascular or biliary invasion was defined as tumor involvement of the main hilar structures or invasion into the inferior vena cava or the confluence of the three main hepatic veins. Resection margin status was classified based on the shortest distance from the tumor to the transection plane, with an R0 resection (negative margin) defined as a tumor-free margin of ≥ 1 mm. The primary outcome was the achievement of a TO. A TO was considered to have been achieved if all of the following criteria were simultaneously met: absence

Table 1. Characteristics of HCC patients who underwent open or laparoscopic right hemihepatectomy before and after PSM

Variables	Before PSM			After PSM		
	ORH (*n* = 309)	LRH (*n* = 126)	*p* value	ORH (*n* = 242)	LRH (*n* = 121)	*p* value
Baseline Characteristics						
Age (years)	53 (46-64)	55.0 (48-64)	0.335	54 (47-64)	55 (48-64)	0.706
Sex (male)	270 (87.4)	106 (84.1)	0.359	210 (86.8)	102 (84.3)	0.525
BMI (kg/m²)	22.7 (20.9-24.7)	22.4 (20.2-24.5)	0.370	22.7 (20.7-24.8)	22.5 (20.2-24.5)	0.624
Diabetes mellitus	28 (9.1)	16 (12.7)	0.293	22 (9.1)	16 (13.2)	0.275
HBV infection	261 (84.5)	104 (82.5)	0.666	203 (83.9)	101 (83.5)	1.000
HCV infection	9 (2.9)	8 (6.3)	0.105	8 (3.3)	8 (6.6)	0.177
ALT (U/L)	39 (25-58)	36 (22-59)	0.356	36 (25-56)	36 (22-59)	0.455
Cirrhosis	186 (60.2)	68 (54.0)	0.240	142 (58.7)	67 (55.4)	0.574
ALBI grade			0.430			0.779
I	244 (79.0)	104 (82.5)		194 (80.2)	99 (81.8)	
II&III	65 (21.0)	22 (17.5)		48 (19.8)	22 (18.2)	
Tumor characteristics						
Tumor size > 5 cm	219 (65.8)	67 (53.1)	**< 0.001**	155 (64.1)	67 (55.4)	0.110
Multiple tumors	85 (27.5)	22 (17.5)	**0.028**	53 (21.9)	22 (18.2)	0.492
AFP > 400 ng/mL	122 (39.5)	39 (31.0)	0.101	83 (34.3)	38 (31.4)	0.637
BCLC stage			**< 0.001**			0.080
0&A	163 (52.8)	92 (73.0)		152 (62.8)	87 (71.9)	
B	46 (14.9)	17 (13.5)		32 (13.2)	17 (14.0)	
C	100 (32.4)	17 (13.5)		58 (24.0)	17 (14.0)	
Tumor differentiation			0.209			0.606
Well-differentiated	6 (1.9)	5 (4.0)		5 (2.1)	4 (3.3)	
Moderately differentiated	159 (51.5)	72 (57.1)		134 (55.4)	70 (57.9)	
Poorly differentiated	144 (46.6)	49 (38.9)		103 (42.6)	47 (38.8)	
Microvascular invasion	90 (29.1)	28 (22.2)	0.155	63 (26.0)	27 (22.3)	0.519
Preoperative therapy	71 (23.0)	18 (14.3)	**0.049**	48 (19.8)	18 (14.9)	0.312
Subsequent therapy	207 (67.0)	86 (68.3)	0.823	155 (64.0)	84 (69.4)	0.348
Operative details						
Operating time (min)	215 (180-260)	260 (226-292)	**< 0.001**	214.5 (180-260)	260 (227-293)	**< 0.001**
Blood loss (mL)	300 (200-500)	300 (200-400)	**0.019**	300 (200-500)	300 (200-450)	0.159
Blood transfusion	53 (17.2)	14 (11.1)	0.143	34 (14.0)	14 (11.6)	0.622
Resection margin < 1 cm	178 (57.6)	61 (48.4)	0.090	135 (55.8)	58 (47.9)	0.181
Conversion to open	/	13 (10.3)		/	13 (10.7)	
Outcomes						
Intraoperative complication	62 (20.1)	24 (19.0)	0.895	39 (16.1)	24 (19.8)	0.381
Bile leak	17 (5.5)	3 (2.4)	0.210	12 (5.0)	3 (2.5)	0.402
Post-hepatectomy liver failure	56 (18.1)	23 (18.3)	1.000	32 (13.2)	22 (18.2)	0.215
Major complication	53 (17.2)	14 (11.1)	0.143	36 (14.9)	13 (10.7)	0.330
Readmission	22 (7.1)	5 (4.0)	0.276	19 (7.9)	5 (4.1)	0.262
In-hospital mortality	13 (4.2)	4 (3.2)	0.788	8 (3.3)	3 (2.5)	0.758
Margin-positive resection	31 (10.0)	9 (7.1)	0.464	18 (7.4)	9 (7.4)	1.000
Textbook outcome achieved	180 (58.3)	79 (62.7)	0.451	158 (65.3)	75 (62.0)	0.563
Duration of hospitalization (days)	9.0 (7.0-10.0)	8.0 (6.0-10.0)	**0.002**	8.0 (7.0-10.0)	8.0 (6.0-10.0)	**0.006**

AFP, alpha-fetoprotein; ALBI, albumin-bilirubin; ALT, alanine aminotransferase; BCLC, Barcelona Clinic Liver Cancer; BMI, body mass index; HBV, hepatitis B virus; HCV, hepatitis C virus; IQR, interquartile range; LRH, laparoscopic right hemihepatectomy; ORH, open right hemihepatectomy; PSM, propensity score matching. Data are presented as n (%) or median (IQR). Values in bold were statistically significant.

of intraoperative grade ≥ 2 incidents (*22*); absence of a postoperative grade B or C bile leak or post-hepatectomy liver failure (PHLF) (*23,24*); absence of major postoperative complications (defined as Clavien-Dindo grade ≥ III) (*25*); absence of 90-day readmission, in-hospital, or 90-day mortality and an R0 resection margin (*10*). Secondary outcomes included overall survival (OS) and disease-free survival (DFS). OS was defined as the interval from the date of surgery to death from any cause or the date of the last follow-up. DFS was defined as the interval from the date of surgery to the first documented tumor recurrence or death from any cause. In addition, the duration of hospitalization was defined as the total number of days from the date of admission to the date of discharge.

Patients underwent follow-up assessments at 1 and 3 months after surgery, and every 3 to 6 months thereafter, or more frequently if clinically indicated. Standard evaluations included serum tumor marker levels, liver function tests, and imaging (typically contrast-enhanced CT, MRI, or contrast-enhanced ultrasound). Tumor recurrence was defined as the appearance of new intrahepatic lesions, local recurrence at the resection margin, or distant metastases on routine follow-up imaging. The data cutoff date for this study was January 1, 2025. Patients who were alive and who had not experienced an endpoint event by this date were censored at the time of their last follow-up.

2.4. Statistical analysis

Continuous variables are expressed as the mean ± standard deviation (SD) or median with interquartile range (IQR) based on their distribution, and they were compared using the Student's *t*-test or Mann-Whitney *U* test, respectively. Categorical variables are expressed as numbers (n) and percentages (%), and they were compared using the Pearson's χ^2 test or Fisher's exact test, as appropriate. To minimize selection bias inherent in this non-randomized study, a 1:3 propensity score matching (PSM) was performed. A binary logistic regression model was constructed to calculate a propensity score for each patient, including baseline covariates that could influence the choice of surgical approach. These covariates were: age, sex, BMI, presence of cirrhosis, ALBI grade, maximum tumor size, presence of multiple lesions, AFP > 400 ng/mL, and history of preoperative therapy. We used a nearest-neighbor matching algorithm without replacement, with a caliper width set at 0.1. The balance of covariates before and after matching was assessed using the standardized mean difference (SMD), with an SMD < 0.1 considered indicative of a satisfactory balance. To explore the independent predictors for achieving a TO and for survival outcomes, multivariable logistic regression and Cox proportional hazards regression models were constructed, respectively (*15,16*). The variable selection process for these models followed a two-step method: variables with statistical significance ($p < 0.1$) in univariate analysis were subsequently entered into the multivariable models (*12*). The proportional hazards assumption for all Cox models was verified. All statistical analyses were performed using the software R (version 4.3.0, R Foundation for Statistical Computing, Vienna, Austria). For all analyses, a two-tailed *p*-value < 0.05 was considered statistically significant, unless otherwise specified. For pairwise subgroup comparisons in the survival analysis, the Bonferroni correction was applied to account for multiple comparisons, and a *p*-value < 0.0125 was considered statistically significant for these specific analyses.

3. Results

3.1. Patient characteristics

A total of 435 patients who underwent curative-intent right hemihepatectomy for HCC were included in the initial cohort for this study (Figure 1). The cohort was predominantly male ($n = 376$, 86.4%), with a median age of 54 years (IQR, 47-64). Most patients had a background of chronic hepatitis B (83.9%), and liver function reserve was generally well-preserved, with 80.0% of patients classified as ALBI grade I ($n = 348$). In terms of oncological features, 58.6% of patients had BCLC stage 0 or A, the median maximum tumor diameter was 6.5 cm (IQR, 4.5-9.5 cm), and 24.6% presented with multiple tumors. Detailed clinical characteristics are shown in Table 1.

Prior to PSM, the cohort consisted of 126 patients who underwent LRH and 309 who underwent ORH. Significant imbalances were observed between the two groups across several variables (Table 1). Specifically, compared to the ORH group, the LRH group presented with smaller tumors (tumor size > 5 cm: 53.1% *vs*. 65.8%, $p < 0.001$), fewer multiple tumors (17.5% *vs*. 27.5%, $p = 0.028$), an earlier BCLC stage ($p < 0.001$), and a lower frequency of preoperative therapy (14.3% *vs*. 23.0%, $p = 0.049$). After PSM, a final cohort of 121 patients in the LRH group and 242 patients in the ORH group was generated for analysis. Following matching, all baseline variables were well-balanced, with all *p*-values > 0.05 and SMDs < 0.1 for all matching covariates (Table 1; Supplemental Figure S1, *https://www.biosciencetrends.com/action/getSupplementalData.php?ID=267*).

3.2. Perioperative outcomes and TO achievement

The perioperative outcomes for the matched cohort are detailed in Table 1. The LRH group was associated with a longer operating time compared to the ORH group (median: 260 *vs*. 214.5 min, $p < 0.001$). However, the two groups were comparable in terms of intraoperative blood loss, blood transfusion rates, and the incidence of

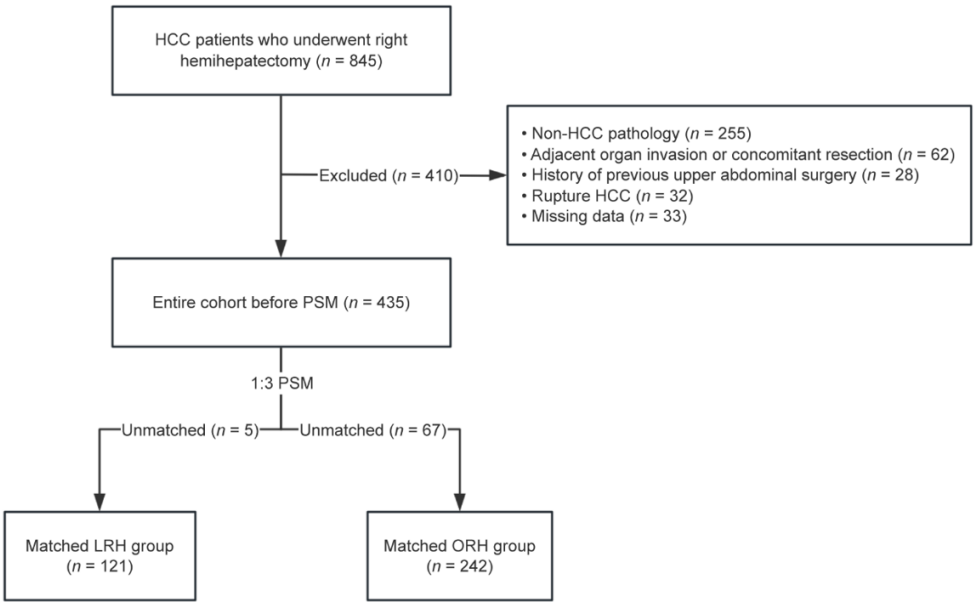

Figure 1. Flow diagram for patient selection.

narrow margins. Of the 121 patients in the LRH group, 13 (10.7%) required conversion to open surgery due to intraoperative difficulties.

In the entire matched cohort (n = 363), the overall rate of TO achievement was 64.2% (n = 233). An analysis of the individual components precluding a TO revealed that intraoperative complications were the primary barrier, affecting 17.4% of patients, followed by post-hepatectomy liver failure (PHLF) (14.9%) and major postoperative complications (13.5%) (Table 1 and Figure 2). When the two surgical approaches were compared, there were no significant differences in the rates of any individual TO components, which culminated in a comparable overall rate of TO achievement between the LRH and ORH groups (62.0% *vs*. 65.3%, p = 0.563). Notably, although the median duration of hospitalization was identical at 8 days for both groups, the Mann-Whitney U test revealed a significant difference in the overall distribution of the duration of hospitalization (p = 0.006), favoring the LRH group.

To investigate the risk factors for TO achievement, a logistic regression analysis was performed (Table 2). After adjusting for competing variables, the multivariable model demonstrated that factors such as intraoperative blood loss > 400 mL (OR: 0.22, 95% CI: 0.13-0.39, p < 0.001), BCLC stage C (*vs*. 0/A; OR: 0.26, 95% CI: 0.13-0.49, p < 0.001), the presence of cirrhosis (OR: 0.51, 95% CI: 0.30-0.86, p = 0.012), poorer liver function (ALBI grade 2/3 *vs*. 1; OR: 0.54; 95% CI:, 0.29-0.99; p = 0.046), and a tumor size > 5 cm (OR: 0.55, 95% CI: 0.30-0.98, p = 0.043) were each independently associated with lower odds of achieving a TO. Notably, the surgical approach was not an independent predictor of TO achievement (p = 0.536).

3.3. Survival analysis

The median follow-up for the matched cohort was 66.2 months (95% CI: 64.5–67.9 months). An initial Kaplan-Meier analysis was performed to directly compare the impact of the two surgical approaches on long-term survival (Figure 3). This analysis showed that although the LRH group tended to have better outcomes in both median OS and DFS, these differences were not statistically significant (median OS: 44.7 *vs*. 35.0 months, p = 0.179; median DFS: 20.7 *vs*. 16.6 months, p = 0.181). The comparable 5-year OS rates (39.1% *vs*. 37.4%) and 5-year DFS rates (24.2% *vs*. 21.4%) further corroborated this finding. To further explore the interactive effects of the surgical approach and TO on prognosis, a stratified four-subgroup survival analysis was performed (Figure 4). After applying a strict Bonferroni correction for multiple subgroup comparisons (significance level: p < 0.0125), we found that regardless of the surgical approach used, patients in whom a TO was achieved had significantly better DFS and OS than in those whom it was not achieved. The 5-year OS rate for patients in whom a TO was achieved was 49.9%, in stark contrast to only 17.5% for those in the non-TO group (Log-rank p < 0.001). A similarly large difference in DFS was observed (5-year DFS rate: 31.5% *vs*. 6.6%; p < 0.001). In contrast, there were no statistically significant differences in OS and DFS between the two surgical approaches, either within the group in whom a TO was achieved or in the group in whom it was not achieved.

In order to identify independent prognostic factors for long-term survival, Cox proportional hazards regression analysis was performed (Tables 3 and 4). For OS, the multivariable analysis identified the achievement of a

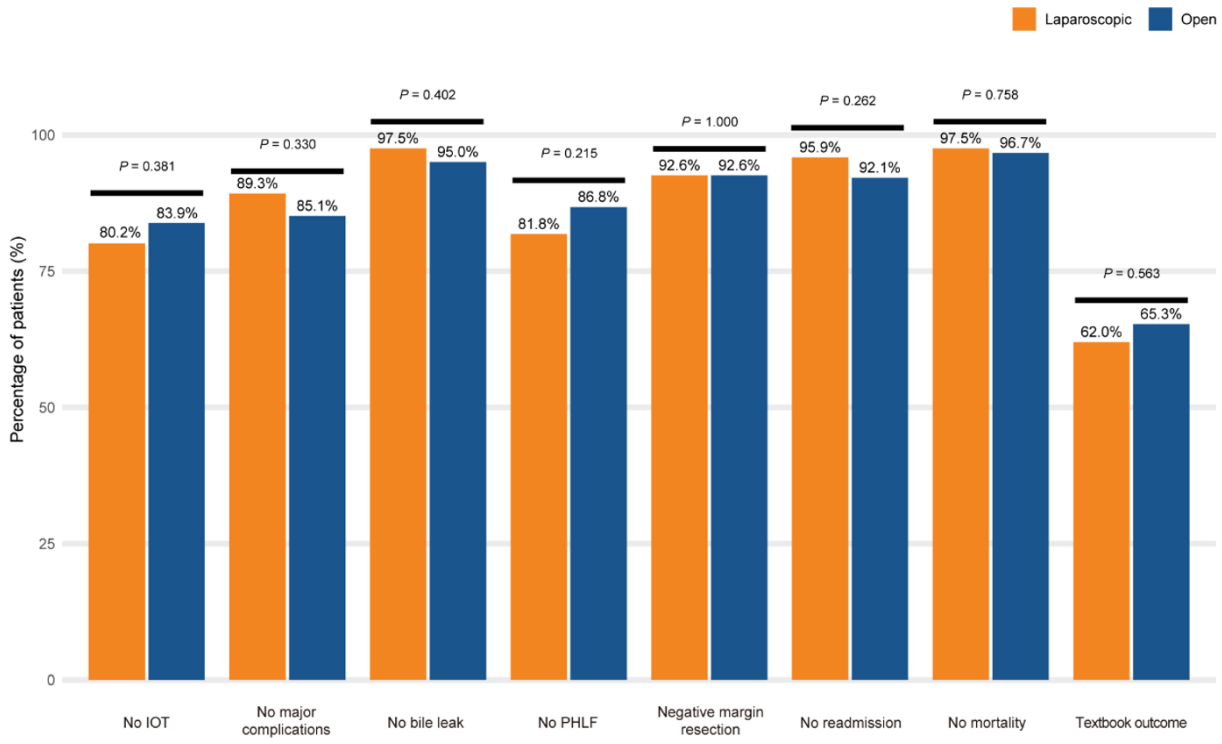

Figure 2. Textbook outcome individual components after PSM: Comparison between laparoscopic and open right hemihepatectomy for HCC. PSM, propensity score matching; HCC, hepatocellular carcinoma; IOT, intervention other than tumor resection; PHLF, post-hepatectomy liver failure.

Table 2. Univariate and multivariate logistic regression analyses to predict textbook outcome in right hemihepatectomy for HCC

Variables	Univariate analysis		Multivariate analysis	
	OR (95% CI)	*p* value	OR (95% CI)	*p* value
Age (> 65 years)	0.99 (0.59-1.70)	0.970		
Sex (male)	1.18 (0.64-2.16)	0.585		
BMI (≥ 25 kg/m²)	0.84 (0.50-1.42)	0.517		
Diabetes mellitus	0.66 (0.33-1.31)	0.228		
HBV infection	0.75 (0.40-1.35)	0.354		
HCV infection	0.71 (0.26-2.02)	0.500		
Cirrhosis	0.52 (0.33-0.80)	0.004	0.51 (0.30-0.86)	**0.012**
ALBI grade II&III *vs*. I	0.45 (0.26-0.76)	0.003	0.54 (0.29-0.99)	**0.046**
Tumor size (> 5 cm)	0.49 (0.31-0.78)	0.003	0.55 (0.30-0.98)	**0.043**
Multiple tumors	0.65 (0.39-1.09)	0.098	0.37 (0.13-1.04)	0.060
AFP (> 400 ng/mL)	0.96 (0.61-1.53)	0.877		
BCLC stage				
B *vs*. 0&A	0.54 (0.29-1.04)	0.062	1.10 (0.33-3.68)	0.873
C *vs*. 0&A	0.17 (0.10-0.30)	< 0.001	0.26 (0.13-0.49)	**< 0.001**
Tumor differentiation				
moderately differentiated *vs*. well-differentiated	1.26 (0.26-4.94)	0.751		
poorly differentiated *vs*. well-differentiated	0.59 (0.12-2.31)	0.463		
Microvascular invasion	0.65 (0.40-1.07)	0.087	1.13 (0.62-2.10)	0.690
Preoperative therapy	0.90 (0.52-1.57)	0.699		
Operating time (> 300 min)	0.31 (0.16-0.57)	< 0.001	0.52 (0.24-1.10)	0.087
Blood loss (> 400 mL)	0.19 (0.11-0.31)	< 0.001	0.22 (0.13-0.39)	**< 0.001**
Resection margin (< 1 cm)	0.51 (0.32-0.78)	0.002	0.70 (0.42-1.18)	0.183
Surgical approach (LRH *vs*. ORH)	0.87 (0.55-1.37)	0.536		

AFP, alpha-fetoprotein; ALBI, albumin-bilirubin; BCLC, Barcelona Clinic Liver Cancer; BMI, body mass index; CI, confidence interval; HBV, hepatitis B virus; HCV, hepatitis C virus; LRH, laparoscopic right hemihepatectomy; OR, odds ratio; ORH, open right hemihepatectomy. Variables with $p < 0.1$ in univariate analysis were included in the multivariate model. Values in bold were statistically significant ($p < 0.05$) in multivariate analysis.

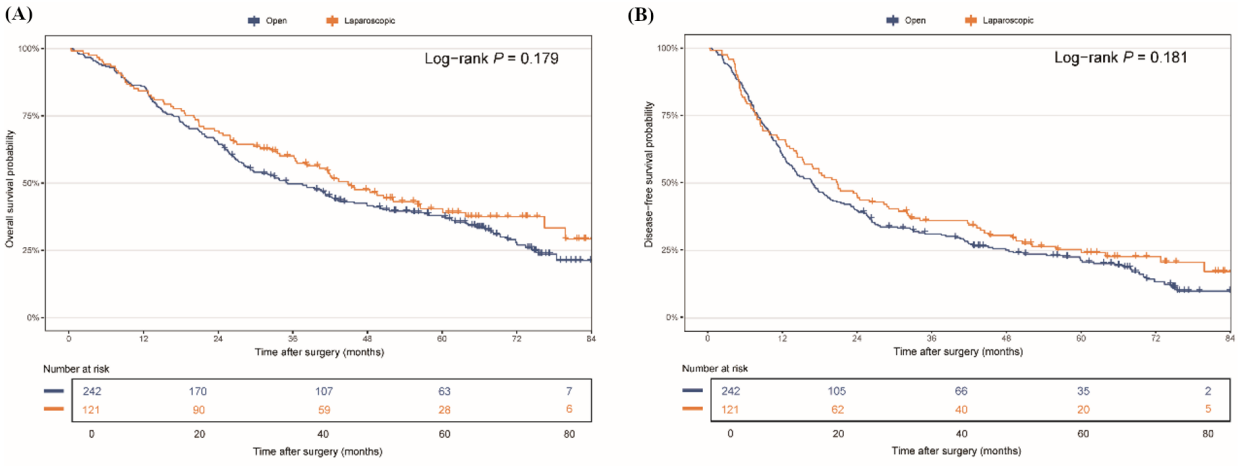

Figure 3. Kaplan-Meier survival curves after PSM: (A) overall survival and (B) disease-free survival comparing laparoscopic versus open right hemihepatectomy for HCC. LRH, laparoscopic right hemihepatectomy; ORH, open right hemihepatectomy; PSM, propensity score matching; HCC, hepatocellular carcinoma.

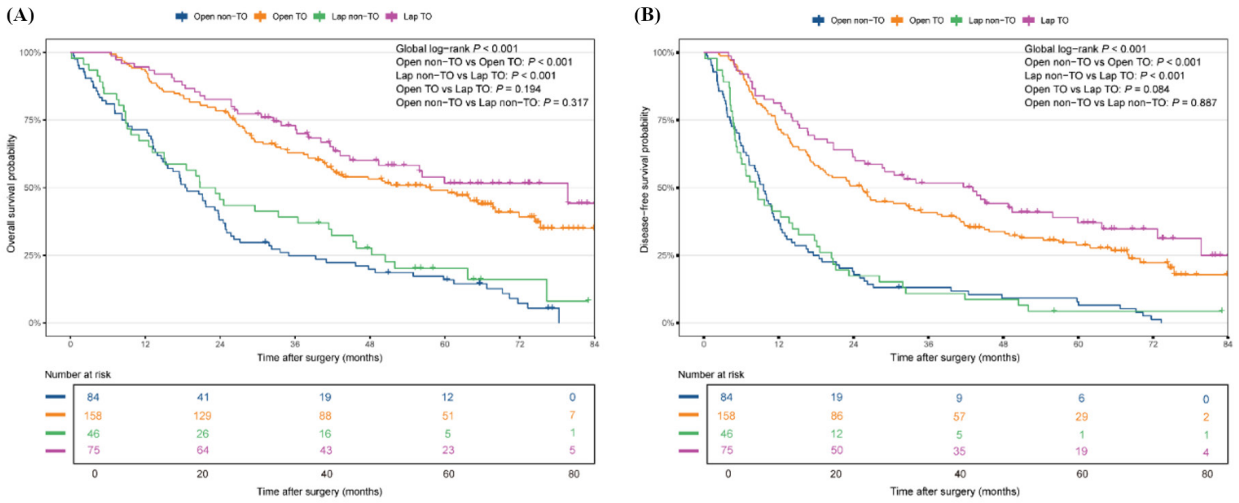

Figure 4. Kaplan-Meier curves for (A) overall survival and (B) disease-free survival, stratified by surgical approach and textbook outcome achievement. TO, textbook outcome; Lap, laparoscopic right hemihepatectomy; Open, open right hemihepatectomy; PSM, propensity score matching; HCC, hepatocellular carcinoma.

TO as an independent protective factor (HR: 0.46, 95% CI: 0.34-0.63, $p < 0.001$). Concurrently, BCLC stage C (HR: 1.86, 95% CI: 1.31-2.65, $p < 0.001$), microvascular invasion (HR: 1.66, 95% CI: 1.23-2.23, $p < 0.001$), and a resection margin < 1 cm (HR: 1.36, 95% CI: 1.03-1.80, $p = 0.030$) were identified as independent risk factors for OS. Regarding DFS, the multivariable analysis similarly confirmed that achievement of a TO was an independent protective factor (HR: 0.44, 95% CI: 0.33-0.58, $p < 0.001$). Independent risk factors associated with worse DFS were: the presence of cirrhosis (HR: 1.42, 95% CI: 1.10-1.83, $p = 0.007$), multiple tumors (HR: 1.84, 95% CI: 1.15-2.95, $p = 0.011$), BCLC stage C (HR: 1.79, 95% CI: 1.27-2.51, $p < 0.001$), poor tumor differentiation (HR: 2.70, 95% CI: 1.08-6.73, $p = 0.033$), microvascular invasion (HR: 2.46, 95% CI: 1.85-3.27, $p < 0.001$), and a resection margin < 1 cm (HR: 1.42, 95% CI: 1.11-1.83, $p = 0.006$).

4. Discussion

TO, a standardized multidimensional metric in liver surgery (*10,17*), provides a robust tool for comprehensively measuring the optimal clinical course for patients postoperatively. In recent years, laparoscopic techniques have been widely adopted in liver surgery, owing to advantages such as smaller incisions and superior high-definition, variable-angle visualization (*8,19*). However, their use in right hemihepatectomy, a procedure hampered by a steep learning curve and the risk of major postoperative complications, remains limited to high-volume centers, and the perioperative evaluation metrics in related cohort studies have often been one-dimensional. The current study focused specifically on the homogeneous, standardized, and complex procedure of right hemihepatectomy for HCC.

Table 3. Univariate and multivariate Cox regression analyses to predict overall survival in right hemihepatectomy for HCC

Variables	Univariate analysis		Multivariate analysis	
	HR (95% CI)	*p* value	HR (95% CI)	*p* value
Age (> 65 years)	1.16 (0.85-1.59)	0.337		
Sex (male)	0.92 (0.65-1.32)	0.657		
BMI (≥ 25 kg/m²)	1.21 (0.89-1.64)	0.231		
Diabetes mellitus	0.95 (0.62-1.47)	0.826		
HBV infection	1.15 (0.80-1.65)	0.445		
HCV infection	1.10 (0.58-2.07)	0.773		
Cirrhosis	1.49 (1.14-1.94)	0.003	1.14 (0.86-1.51)	0.377
ALBI grade II&III *vs*. I	1.28 (0.94-1.75)	0.122		
Tumor size (> 5 cm)	1.73 (1.31-2.28)	< 0.001	1.20 (0.89-1.62)	0.232
Multiple tumors	1.22 (0.89-1.67)	0.209		
AFP (> 400 ng/mL)	1.25 (0.96-1.63)	0.102		
BCLC stage				
B *vs*. 0&A	1.66 (1.13-2.43)	0.010	1.30 (0.88-1.94)	0.191
C *vs*. 0&A	3.41 (2.53-4.59)	< 0.001	1.86 (1.31-2.65)	**< 0.001**
Tumor differentiation				
moderately differentiated *vs*. well-differentiated	1.67 (0.62-4.54)	0.311		
poorly differentiated *vs*. well-differentiated	3.00 (1.10-8.15)	0.031	2.39 (0.86-6.60)	0.094
Microvascular invasion	2.15 (1.62-2.84)	< 0.001	1.66 (1.23-2.23)	**< 0.001**
Preoperative therapy	1.29 (0.94-1.79)	0.118		
Operating time (> 300 min)	1.37 (0.96-1.95)	0.084	0.80 (0.54-1.18)	0.255
Blood loss (> 400 mL)	1.67 (1.27-2.18)	< 0.001	1.20 (0.88-1.64)	0.241
Resection margin (< 1 cm)	1.70 (1.31-2.21)	< 0.001	1.36 (1.03-1.80)	**0.030**
Surgical approach (LRH *vs*. ORH)	0.83 (0.63-1.09)	0.179		
Textbook outcome	0.34 (0.26-0.44)	< 0.001	0.46 (0.34-0.63)	**< 0.001**

AFP, alpha-fetoprotein; ALBI, albumin-bilirubin; BCLC, Barcelona Clinic Liver Cancer; BMI, body mass index; CI, confidence interval; HBV, hepatitis B virus; HCV, hepatitis C virus; HR, hazard ratio; LRH, laparoscopic right hemihepatectomy; ORH, open right hemihepatectomy. Variables with $p < 0.1$ in univariate analysis were included in the multivariate model. Values in bold were statistically significant ($p < 0.05$) in multivariate analysis.

Our primary finding was that mature laparoscopic and open approaches had comparable performance in achieving a TO. A distinct advantage for the laparoscopic group, however, was observed in quicker postoperative recovery, which aligns with ERAS principles, as evinced by a significantly shorter duration of hospitalization. Consistent with previous findings, we confirmed that neither the difference in surgical approach nor the speediness of recovery translated directly into a significant long-term survival benefit. More importantly, we found that, irrespective of the approach, patients in whom a TO was achieved had far superior long-term survival, then establishing TO achievement as an independent prognostic factor *via* multivariable survival regression analyses. Therefore, these findings suggest that when evaluating and selecting options for complex liver surgery, the clinical focus should systematically shift from the choice of surgical approach alone to fostering a perioperative environment conducive to achieving a TO, thereby improving long-term prognosis.

Previous studies have reported a considerable variation in the rate of TO achievement following liver surgery, ranging from 22.1% to 80.5% (*12-14,26-29*). Whether laparoscopy results in a higher rate of TO achievement remains open to discussion, with some studies considering it advantageous (*13,28*) and others not (*14,26*). This heterogeneity in findings appears to be closely linked to the amalgamation of different types of procedures and complexities in study cohorts (*16,30*), as a laparoscopic benefit is more readily observed in studies with a higher proportion of patients with early-stage disease and undergoing minor hepatectomy. This underscores the need to evaluate outcomes within specific procedural contexts. Our study, conducted at a high-volume liver surgery center, focused exclusively on right hemihepatectomy. In this specific setting, the overall rate of TO achievement in the matched cohort was 64.2%, and performance between the laparoscopic and open groups was comparable (62.0% *vs*. 65.3%, $p = 0.563$). The reasons for this finding of equivalence are multifaceted. First, the inherent technical difficulty, high physiological impact (*6,29*), and potentially heavy tumor burden of right hemihepatectomy likely act as the primary determinants of the outcome (*12*). This may create a "ceiling effect," largely diluting the theoretical advantages of a minimally invasive approach that are more evident with simpler procedures (*16*). Our data also confirmed that intraoperative events, PHLF, and major complications are the main challenges hindering the achievement of a TO in patients in this cohort. Secondly, the dimensions of TO and the differences in TO standards among different studies also warrant consideration (*14,31*). The standard used in our study derives from a Delphi consensus (*10*). However, the

Table 4. Univariate and multivariate Cox regression analyses to predict disease-free survival in right hemihepatectomy for HCC

Variables	Univariate analysis		Multivariate analysis	
	HR (95% CI)	*p* value	HR (95% CI)	*p* value
Age (> 65 years)	1.00 (0.75-1.33)	0.984		
Sex (male)	1.06 (0.76-1.49)	0.712		
BMI (≥ 25 kg/m²)	1.11 (0.84-1.46)	0.482		
Diabetes mellitus	1.04 (0.72-1.51)	0.820		
HBV infection	1.18 (0.85-1.62)	0.322		
HCV infection	1.35 (0.79-2.32)	0.270		
Cirrhosis	1.61 (1.26-2.04)	< 0.001	1.42 (1.10-1.83)	**0.007**
ALBI grade II&III *vs*. I	1.15 (0.87-1.53)	0.336		
Tumor size (> 5 cm)	1.55 (1.22-1.98)	< 0.001	1.24 (0.94-1.64)	0.128
Multiple tumors	1.56 (1.19-2.06)	0.001	1.84 (1.15-2.95)	**0.011**
AFP (> 400 ng/mL)	1.23 (0.97-1.57)	0.090	1.05 (0.81-1.36)	0.727
BCLC stage				
B *vs*. 0&A	1.82 (1.30-2.54)	< 0.001	0.81 (0.47-1.41)	0.460
C *vs*. 0&A	3.41 (2.57-4.53)	< 0.001	1.79 (1.27-2.51)	**< 0.001**
Tumor differentiation				
moderately differentiated *vs*. well-differentiated	2.08 (0.85-5.09)	0.108		
poorly differentiated *vs*. well-differentiated	3.61 (1.47-8.86)	0.005	2.70 (1.08-6.73)	**0.033**
Microvascular invasion	3.21 (2.47-4.16)	< 0.001	2.46 (1.85-3.27)	**< 0.001**
Preoperative therapy	1.29 (0.96-1.74)	0.095	1.20 (0.88-1.64)	0.257
Operating time (> 300 min)	1.26 (0.90-1.75)	0.173		
Blood loss (> 400 mL)	1.33 (1.03-1.71)	0.027	0.90 (0.67-1.20)	0.477
Resection margin (< 1 cm)	1.57 (1.24-1.98)	< 0.001	1.42 (1.11-1.83)	**0.006**
Surgical approach (LRH *vs*. ORH)	0.84 (0.66-1.08)	0.182		
Textbook outcome	0.35 (0.28-0.45)	< 0.001	0.44 (0.33-0.58)	**< 0.001**

AFP, alpha-fetoprotein; ALBI, albumin-bilirubin; BCLC, Barcelona Clinic Liver Cancer; BMI, body mass index; CI, confidence interval; HBV, hepatitis B virus; HCV, hepatitis C virus; HR, hazard ratio; LRH, laparoscopic right hemihepatectomy; ORH, open right hemihepatectomy. Variables with $p < 0.1$ in univariate analysis were included in the multivariate model. Values in bold were statistically significant ($p < 0.05$) in multivariate analysis.

variable "no extended duration of hospitalization" did not reach the 80% expert consensus threshold when this consensus was reached and was therefore not included in the final criteria. This precisely explains an important phenomenon in our study, that is, there was no TO advantage in the LRH group, but it had a significantly shorter duration of hospitalization, confirming its value in ERAS that exists outside the current TO definition (*26*). While some studies incorporate duration of hospitalization in the TO, its judgment criteria (such as the median or 75th percentile) are readily affected by variations in different diseases, regional levels of medicine, and cultural beliefs. Finally, our use of PSM effectively controlled for the common selection bias of assigning patients with smaller tumor burdens to the LRH group, thus reducing the risk of false-positive results and providing a more realistic analysis. The results for intraoperative blood loss reflect this matching effect. While the LRH group had a more favorable distribution of blood loss before matching ($p = 0.019$), this advantage was offset after PSM, which may be related to the balance of patients at risk of intraoperative bleeding between the two groups. The concept of a TO is valuable for identifying weak links in specific medical processes. At our center, intraoperative incidents, PHLF, and major postoperative complications were the three primary challenges hindering achievement of a TO (Figure 2). Multivariable logistic regression analysis (Table 2) further confirmed that the achievement of a TO was independently associated with several clinical factors, including patient condition (cirrhosis, ALBI grade 2/3), tumor burden and aggressiveness (BCLC stage C, tumor size > 5 cm), and intraoperative blood loss > 400 mL, which is consistent with previous studies (*27,32,33*). Crucially, these factors for a TO are also, to a large extent, well-established risk factors for long-term survival. This provides a clear mechanistic explanation for why TO so effectively predicts prognosis (*12,34*) (Figure 4). Cox regression analyses (Tables 3 and 4) revealed that achieving a TO was an independent protective factor for both OS and DFS. The independent risk factors for DFS constituted a comprehensive profile of tumor biology, including cirrhosis, BCLC stage C, multiple tumors, poor differentiation, MVI, and a resection margin < 1 cm. This is logical, as these factors point to a higher potential for residual disease or early recurrence. In contrast, the list of risk factors in the multivariable model for OS was more refined, consisting of BCLC stage C, MVI, and a resection margin < 1 cm. In summary, the evidence chain linking the "barriers to a TO", "predictors of a TO", and the "prognostic value of a TO" indicates that a procedure that successfully navigates these short-term risks to achieve a TO is inherently more likely to yield long-term survival benefits. To improve

the quality of complex liver surgery, a systematic perioperative strategy centered on achieving a TO should be adopted (*34*).

To the extent known, this is the first cohort study to systematically compare the impact of laparoscopic versus open techniques on both TO achievement and survival in the context of right hemihepatectomy for HCC. We also acknowledge that our study had several limitations. First, this was a retrospective study; even though we controlled for measurable confounders with PSM, we cannot entirely rule out the potential for unmeasured bias. Second, the statistical power for some subgroup analyses was limited by sample size, which may explain why some notable clinical trends did not reach statistical significance. Finally, our study's evaluation lacks data on cost-effectiveness and patient-reported outcomes.

In conclusion, this cohort study of right hemihepatectomy for HCC demonstrated that the laparoscopic and open approaches have comparable performance in achieving a TO and in survival, although laparoscopy offers an advantage in shortening the duration of hospitalization. Our findings confirm that, irrespective of the chosen approach, the achievement of a TO is an independent protective factor that determines prognosis. Therefore, fostering a perioperative environment conducive to achieving a TO is an effective management strategy to improve long-term prognosis. Future studies should be conducted to further refine and standardize the criteria for a TO in liver surgery and to explore its characteristics across different liver diseases and procedures.

Acknowledgements

We would like to thank all the staff in our team for their support.

Funding: This work was supported by a grant from the National Key Research and Development Program of China (No. 2023YFB3810004 for Huang J).

Conflict of Interest: The authors have no conflicts of interest to disclose.

References

1. Rumgay H, Arnold M, Ferlay J, Lesi O, Cabasag CJ, Vignat J, Laversanne M, McGlynn KA, Soerjomataram I. Global burden of primary liver cancer in 2020 and predictions to 2040. J Hepatol. 2022; 77:1598-1606.
2. Rumgay H, Ferlay J, de Martel C, Georges D, Ibrahim AS, Zheng R, Wei W, Lemmens *VS*oerjomataram I. Global, regional and national burden of primary liver cancer by subtype. Eur J Cancer. 2022; 161:108-118.
3. Reveron-Thornton RF, Teng MLP, Lee EY, *et al*. Global and regional long-term survival following resection for HCC in the recent decade: A meta-analysis of 110 studies. Hepatol Comm. 2022; 6:1813-1826.
4. Goh EL, Chidambaram S, Ma S. Laparoscopic *vs* open hepatectomy for hepatocellular carcinoma in patients with cirrhosis: A meta-analysis of the long-term survival outcomes. Int J Surg. 2018; 50:35-42.
5. Yoh T, Cauchy F, Soubrane O. Oncological resection for liver malignancies: Can the laparoscopic approach provide benefits? Ann Surg. 2022; 275:182-188.
6. Kawaguchi Y, Fuks D, Kokudo N, Gayet B. Difficulty of laparoscopic liver resection: Proposal for a new classification. Ann Surg. 2018; 267:13-17.
7. Fichtinger RS, Aldrighetti LA, Abu Hilal M, *et al*. Laparoscopic Versus Open Hemihepatectomy: The ORANGE II PLUS multicenter randomized controlled trial. J Clin Oncol. 2024; 42:1799-1809.
8. Li G, Mugaanyi J, Li Z, Bao Y, Lu C, Huang J. A comparative study of laparoscopic and open approaches for right hemihepatectomy in hepatocellular carcinoma patients: Safety and short-term outcomes. Med Sci Monit. 2024; 30:e942096.
9. Kolfschoten NE, Kievit J, Gooiker GA, van Leersum NJ, Snijders HS, Eddes EH, Tollenaar RA, Wouters MW, Marang-van de Mheen PJ. Focusing on desired outcomes of care after colon cancer resections; Hospital variations in 'textbook outcome'. Eur J Surg Oncol. 2013; 39:156-163.
10. Gorgec B, Benedetti Cacciaguerra A, Pawlik TM, *et al*. An International Expert Delphi Consensus on Defining Textbook Outcome in Liver Surgery (TOLS). Ann Surg. 2023; 277:821-828.
11. Li Q, Liu H, Gao Q, Xue F, Fu J, Li M, Yuan J, Chen C, Zhang D, Geng Z. Textbook outcome in gallbladder carcinoma after curative-intent resection: A 10-year retrospective single-center study. Chinese Medical Journal. 2023; 136:1680-1689.
12. Sindayigaya R, Tzedakis S, Tribillon E, Gavignet C, Mazzotta A, Nassar A, Marchese U, Soubrane O, Fuks D. Assessing textbook outcome after single large hepatocellular carcinoma resection. HPB (Oxford). 2023; 25:1093-1101.
13. Hobeika C, Nault JC, Barbier L, Schwarz L, Lim C, Laurent A, Gay S, Salame E, Scatton O, Soubrane O, Cauchy F. Influence of surgical approach and quality of resection on the probability of cure for early-stage HCC occurring in cirrhosis. JHEP Rep. 2020; 2:100153.
14. Hobeika C, Cauchy F, Fuks D, *et al*. Laparoscopic versus open resection of intrahepatic cholangiocarcinoma: Nationwide analysis. Br J Surg. 2021; 108:419-426.
15. Endo Y, Tsilimigras DI, Munir MM, *et al*. Textbook outcome in liver surgery: Open *vs* minimally invasive hepatectomy among patients with hepatocellular carcinoma. J Gastrointestinal Surgery. 2024; 28:417-424.
16. Luo SY, Qin L, Qiu ZC, Xie F, Zhang Y, Yu Y, Leng SS, Wang ZX, Dai JL, Wen TF, Li C. Comparison of textbook outcomes between laparoscopic and open liver resection for patients with hepatocellular carcinoma: A multicenter study. Surg Endosc. 2025; 39:2052-2061.
17. Mohamed A, Nicolais L, Fitzgerald TL. Textbook outcome as a composite measure of quality in hepaticopancreatic surgery. J Hepatobiliary Pancreat Sci. 2023; 30:1172-1179.
18. Agha R, Mathew G, Rashid R, Kerwan A, Al-Jabir A, Sohrabi C, Franchi T, Nicola M, Agha M. Revised Strengthening the reporting of cohort, cross-sectional and case-control studies in surgery (STROCSS) guideline: An update for the age of artificial intelligence. Premier J Sci. 2025.
19. Peng Y, Li B, Xu H, Guo S, Wei Y, Liu F. Is the anterior

approach suitable for laparoscopic right hemihepatectomy in patients with large HCC (5-10 cm)? A propensity score analysis. Surg Endosc. 2022; 36:6024-6034.
20. Johnson PJ, Berhane S, Kagebayashi C, *et al*. Assessment of liver function in patients with hepatocellular carcinoma: A new evidence-based approach—The ALBI Grade. J Clinical Oncol. 2015; 33:550-558.
21. Reig M, Forner A, Rimola J, *et al*. BCLC strategy for prognosis prediction and treatment recommendation: The 2022 update. J Hepatol. 2022; 76:681-693.
22. Kazaryan AM, Rosok BI, Edwin B. Morbidity assessment in surgery: Refinement proposal based on a concept of perioperative adverse events. ISRN Surg. 2013; 2013:625093.
23. Koch M, Garden OJ, Padbury R, *et al*. Bile leakage after hepatobiliary and pancreatic surgery: A definition and grading of severity by the International Study Group of Liver Surgery. Surgery. 2011; 149:680-688.
24. Sultana A, Brooke-Smith M, Ullah S, *et al*. Prospective evaluation of the International Study Group for Liver Surgery definition of post hepatectomy liver failure after liver resection: An international multicentre study. HPB (Oxford). 2018; 20:462-469.
25. Clavien PA, Barkun J, de Oliveira ML, *et al*. The Clavien-Dindo classification of surgical complications: Five-year experience. Ann Surg. 2009; 250:187-196.
26. Endo Y, Tsilimigras DI, Munir MM, *et al*. Textbook outcome in liver surgery: Open *vs* minimally invasive hepatectomy among patients with hepatocellular carcinoma. J Gastrointest Surg. 2024; 28:417-424.
27. Ruzzenente A, Poletto E, Conci S, Campagnaro T, Valle BD, De Bellis M, Guglielmi A. Factors related to textbook outcome in laparoscopic liver resections: A single Western centre analysis. J Gastrointest Surg. 2022; 26:2301-2310.
28. Azoulay D, Ramos E, Casellas-Robert M, Salloum C, Llado L, Nadler R, Busquets J, Caula-Freixa C, Mils K, Lopez-Ben S, Figueras J, Lim C. Liver resection for hepatocellular carcinoma in patients with clinically significant portal hypertension. JHEP Rep. 2021; 3:100190.
29. Xu Z, Lv Y, Zou H, Jia Y, Du W, Lu J, Liu Y, Shao Z, Zhang H, Sun C, Zhu C. Textbook outcome of laparoscopic hepatectomy in the context of precision surgery: A single center experience. Dig Liver Dis. 2024; 56:1368-1374.
30. Sweigert PJ, Ramia JM, Villodre C, Carbonell-Morote S, De-la-Plaza R, Serradilla M, Pawlik TM. Textbook outcomes in liver surgery: A systematic review. J Gastrointest Surg. 2023; 27:1277-1289.
31. de Graaff MR, Elfrink AKE, Buis CI, *et al*. Defining Textbook Outcome in liver surgery and assessment of hospital variation: A nationwide population-based study. Eur J Surg Oncol. 2022; 48:2414-2423.
32. Dawood ZS, Khalil M, Waqar U, Banani I, Alidina Z, Pawlik TM. Use of textbook outcome as a quality metric in hepatopancreaticobiliary surgery: A systematic review and meta-analysis. J Gastrointest Surg. 2025; 29:102005.
33. Tsilimigras DI, Mehta R, Merath K, *et al*. Hospital variation in Textbook Outcomes following curative-intent resection of hepatocellular carcinoma: An international multi-institutional analysis. HPB (Oxford). 2020; 22:1305-1313.
34. Merath K, Chen Q, Bagante F, *et al*. A multi-institutional international analysis of textbook outcomes among patients undergoing curative-intent resection of intrahepatic cholangiocarcinoma. JAMA Surg. 2019; 154:e190571.

Received July 4, 2025; Revised July 28, 2025; Accepted August 1, 2025.

**Address correspondence to:*
Jiwei Huang and Haichuan Wang, Division of Liver Surgery, Department of General Surgery, West China Hospital, Sichuan University, #37 Guoxue Alley, Wuhou District, Chengdu, Sichuan Province, China 610041.
E-mail: huangjiwei@wchscu.cn (JH); haichuan.wang@wchscu.edu.cn (HW)

Released online in J-STAGE as advance publication August 4, 2025.

Original Article

DOI: 10.5582/bst.2025.01040

A new strategy of laparoscopic anatomical right hemihepatectomy *via* a hepatic parenchymal transection-first approach guided by the middle hepatic vein

Nan You[1,§], Yongkun Li[1,§], Qifan Zhang[2,§], Chaoqun Wang[1], Ke Wu[1], Zheng Wang[1], Qian Ren[1], Jing Li[1], Lu Zheng[1,*]

[1] Department of Hepatobiliary Surgery, The Second Affiliated Hospital, Third Military Medical University (Army Medical University), Chongqing, China;
[2] Division of Hepatobiliopancreatic Surgery, Department of General Surgery, Nanfang Hospital, Southern Medical University, Guangzhou, Guangdong, China.

SUMMARY: Laparoscopic anatomical right hemihepatectomy (LARH) is a highly challenging procedure due to the lack of an appropriate surgical approach. This study aimed to investigate the safety and efficacy of LARH *via* a hepatic parenchymal transection-first approach (HPF) guided by the middle hepatic vein (MHV) (HPFM) to treat hepatocellular carcinoma (HCC) by comparison with the extrahepatic Glissonian approach (EG). Between January 2017 and December 2019, a total of 105 HCC patients who underwent LARH, of whom 48 underwent HPFM, were included in this study. After a 1:1 propensity score matching, 41 LARH-HPFM were compared to 41 LARH-EG. We have analyzed perioperative and oncologic outcomes of the two different operative approaches for HCC treatments. Quality of two operative approaches was defined by textbook outcome (TO). The LARH-HPF group was associated with shorter mean operative time (P = 0.029) and less blood loss (P = 0.023). The LARH-HPFM did not increase the postoperative overall complication rates (P = 0.248) when compared with the LARH-EG. The results of univariable and multivariable analyses indicated that LARH-HPFM provided a clinical benefit for operative time and blood loss. In addition, patients who received LARH-HPFM cumulated more TO criteria (P = 0.017), and achieved higher rate of TO (46.3% *vs*. 24.4%; 2.68, 95% CI 1.05 - 6.86, P = 0.040) compared with those who received LARH-EG. These findings indicate LARH-HPFM is safe and feasible for HCC with certain advantages over LARH-EG, but there are still many problems worth further exploration.

Keywords: laparoscopic liver resection, anatomical, right hemihepatectomy, parenchymal transection-first, middle hepatic vein

1. Introduction

Laparoscopic liver surgery, a widely considered safe and feasible surgical practice without compromising oncological outcome, has expanded from initial local hepatectomy to anatomical hepatectomy (*1*). Nowadays, with increasing experience and developments in surgical techniques and instruments, an increasing number of reports have confirmed the feasibility and safety of laparoscopic anatomical right hemihepatectomy (LARH) in selected patients (*2-4*). However, due to the unique anatomical structure, complexity in identifying the boundary of right hemihepatectomy, surgical complication, LARH can be very challenging and technically demanding procedure (*5*). There are many technical tips for LARH, and the core technical tip is how to choose an appropriate laparoscopic approach, which is a main determinant of surgical success (*6*). To date, the approaches for LARH roughly include Glissonian approach (which can be divided into three types: the extrahepatic, intrahepatic, and transfissural approaches) (*7*), hilar dissection approach (HD) (*8*). However, all these approaches have certain drawbacks. Through continuous learning and exploration, we have carried out laparoscopic anatomical liver resection *via* a hepatic parenchymal transection-first approach (HPF) guided by the middle hepatic vein (MHV) (LARH-HPFM) (*9,10*) and applied it to LARH. LARH-HPFM is a feasible and effective technique. The specific strategy described here may help laparoscopic surgeons safely perform this challenging procedure. Therefore, the study aims to provide our initial experience using the HPF and

compare the surgical outcomes with the extrahepatic Glissonian approach (EG).

2. Materials and Methods

2.1. Patients and data

The data of patients who underwent laparoscopic liver resection in the Second Affiliated Hospital, Third Military Medical University (Army Medical University) between January 2017 and December 2019 were retrospectively collected. The selection criteria for patients in this study included (1) male or female patients aged 18–75 years, (2) liver function classified as Child–Pugh class A or B; (3) histologically confirmed hepatocellular carcinoma (HCC) and (4) patients underwent LARH with lesions localized in the right liver. The following patients were excluded: (1) the presence of severe dysfunction of organs, (2) LARH combined with the resection of other parts of the liver and/or other organs except for cholecystectomy. To standardize HCC management, our institution formed a multidisciplinary tumor board where all new cases were presented for joint decision-making. Patients with hepatitis B virus (HBV) received the whole course of antiviral treatment. The prophylactic antibiotic therapy was intravenously administered 30 min before the surgery and maintained until the second postoperative day. Post-operative management included hemostasis, hepatic function protection, analgesia, rehydration and other symptomatic and supportive care. This study was conducted in accordance with the Declaration of Helsinki and relevant ethical guidelines. It was approved by the Ethics Committee of the Second Affiliated Hospital of the Third Military Medical University (Army Medical University) and registered in the Chinese Clinical Trial Registry prior to the enrollment of the first subject (Registration ID: ChiCTR2400086625).

2.2. Methods

The patient was placed in a reversed Trendelenburg and left semilateral position with head up 30° and leg splitting (Figure 1A). The surgeon stood on the right side of the patient, the camera assistant stood between the spread legs, and the assistant and monitor were on the left side of the patient, facing the surgeon (Figure 1B). The trocars were inserted according to the 5-port-method (Figure 1C). To prepare for extracorporeal Pringle's maneuver, a 3-mm length incision was made between left two ports through which a self-designed tube (Figure 2) would be inserted for holding a cotton tape around the hepatoduodenal ligament. Central venous pressure (CVP) was kept lower than 5 cmH_2O.

In the LARH-HPFM group, operation began with division of liver ligaments and right liver mobilization. Intraoperative laparoscopic ultrasonography (IOUS) was performed on the liver surface to determine the courses of main trunk of the MHV. Parenchymal dissection proceeded from the caudal to cranial side along the markings of the MHV (right of the vein), exposing the MHV on the cutting plane of the liver remnant. The caudate process was cut from the back side. Short

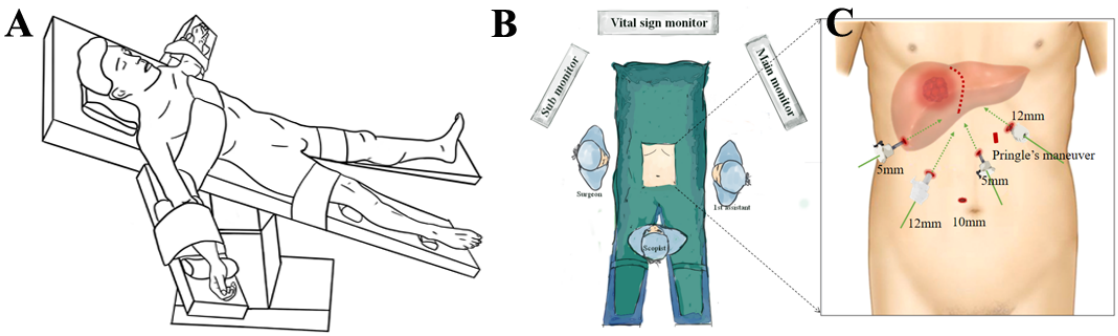

Figure 1. (A) Patient position. (B) The position of operators and instruments. (C) Diagrams of trocar placement for LARH-HPFM. Two 12-mm trocars, two 5-mm trocars and one 10-mm trocar are used. The incision was made 3 mm in length for insertion of extracorporeal Pringle's maneuver. *Abbreviation*: LARH-HPFM, laparoscopic anatomical right hemihepatectomy *via* a hepatic parenchymal transection-first approach guided by the middle hepatic vein.

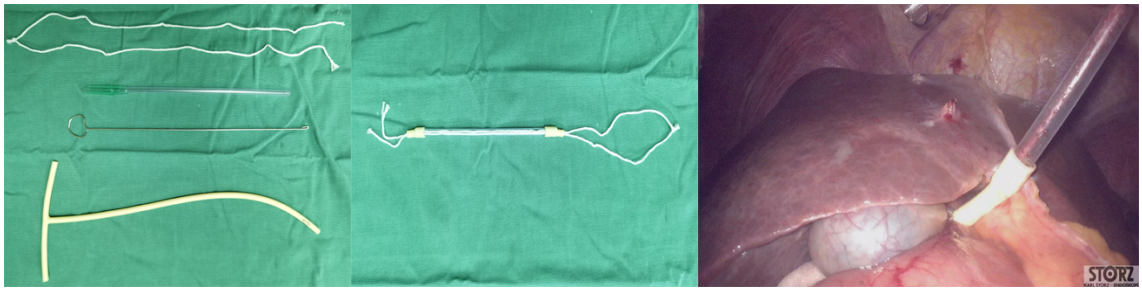

Figure 2. An illustration and image of the laparoscopic first hepatic hilum blood flow occlusion device.

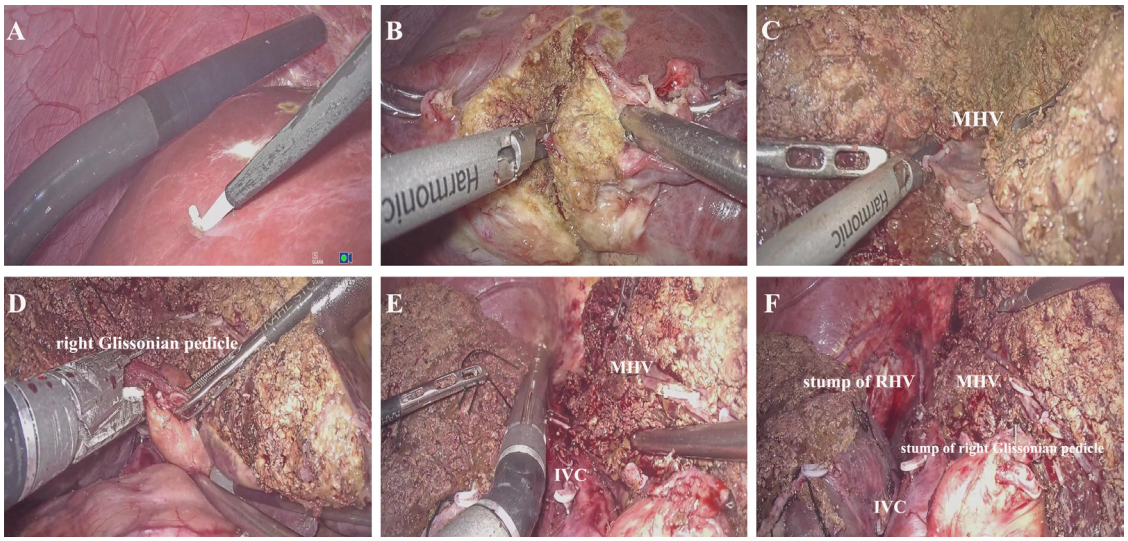

Figure 3. Laparoscopic technique and procedure for LARH-HPFM. (A) IOUS was used to mark the the tumor range and central position and to determine the courses of main trunk of MHV; **(B)** Parenchymal resection was carried out firstly using harmonic scalpel; **(C)** Parenchymal transection along the MHV; **(D)** exposing and dividing right Glissonian pedicle; **(E)** exposing and dividing RHV; **(F)** Findings after anatomic hemihepatectomy. *Abbreviation*: LARH-HPFM, laparoscopic anatomical right hemihepatectomy *via* a hepatic parenchymal transection-first approach guided by the middle hepatic vein; MHV,Middle hepatic vein.

hepatic veins were clipped. After sufficient opening of the hepatic parenchyma around the ventral and dorsal side of the right Glissonian pedicle, the right Glissonian pedicle was isolated by cotton tape and then transected. It is noteworthy that transecting was done while the tape was retracted toward the contralateral side. Then, parenchymal dissection was advanced from the caudal to cranial side along the plane consisting of ventral side of the inferior vena cava (IVC), MHV and ischemic line. After accomplishing parenchymal dissection, the right hepatic vein (RHV) was divided (Figure 3).

In the LARH-EG group, the peritoneum of the hepatoduodenal ligament was meticulously dissected at the hepatic hilum and the dorsal side of the hepatoduodenal ligament. The dissection was performed between the hepatic parenchyma and the bifurcation of the right Glissonian pedicle. The right Glissonian pedicle was encircled laparoscopically. When the corresponding Glissonian pedicle was occluded, we marked the ischemic line by electrocautery on the liver capsule. The superficial parenchyma was dissected along the demarcation line, while the deeper tissue was dissected along the MHV. The caudate process was cut from the back side. Short hepatic veins were clipped. After sufficient parenchymal dissection, so that the whole bifurcating Glissonian pedicle was exposed, the right Glissonian pedicle was transected by a laparoscopic linear stapler. After accomplishing parenchymal dissection, the RHV was divided (Figure 4).

2.3. Propensity score matching (PSM)

The PSM analysis is a useful method and widely used in retrospective studies to reduce confounding and selection bias (*11*). In our research, the LARH-HPFM group and the LARH-EG group were compared with a 1:1 PSM analysis in an attempt to minimize intergroup disparities. A propensity score for each patient was calculated using logistic regression based on the imbalanced variables, and a 1:1 the nearest-neighbor matching method was performed between the two groups. Patients who fail to meet the matching criteria were excluded.

2.4. Surgical outcomes

The following analyzed variables were included: operative time, estimated blood loss (EBL), intraoperative transfusion, conversion, bowel function recovery, postoperative hospital stay, postoperative liver function, postoperative complications according to Clavien–Dindo grade (*12*) and mortality. Prolonged operative time was defined as ≥ 240 min (*13*). Massive hemorrhage during operation was defined as EBL > 400 mL (*14*). All patients were regularly followed at the outpatient department every 1-3 months for the first year and every 3-6 months thereafter. All patients underwent routine blood tests, liver function tests, tumor markers tests, and abdominal ultrasound and computed tomography (CT) or magnetic resonance imaging (MRI) were performed when necessary. The follow-up ended in February 2023.

The quality of surgical care was assessed using textbook outcome (TO), which was considered in patients fulfilling and cumulating all of the following 6 previously described endpoints (*15*): R0 (≥ 1 cm) surgical margin, absence of perioperative transfusion, absence of postoperative complications (considering all Dindo-Clavien grades), absence of prolonged length

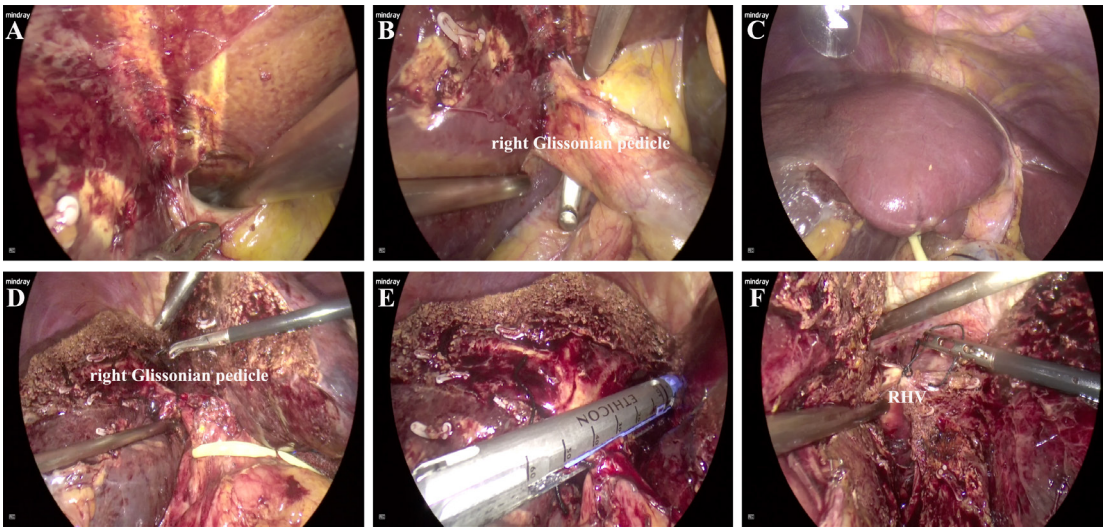

Figure 4. Laparoscopic technique and procedure for LARH-GA. (A) The peritoneum of the hepatoduodenal ligament was meticulously dissected at the hepatic hilum and the dorsal side of the hepatoduodenal ligament; **(B)** The golden finger was inserted into the latent anatomic space between the hepatic parenchyma and the bifurcation of the right Glissonian pedicles; **(C)** When the right Glissonian pedicle was isolated and occluded, the ischemic line was marked by electrocautery on the liver capsule; **(D)** After sufficient parenchymal dissection, the right Glissonian pedicle was exposed; **(E)** Right Glissonian pedicle was transected by a laparoscopic linear stapler with 60-mm blue cartridge; **(F)** RHV was isolated and ligated. *Abbreviation*: LARH-HPFM, laparoscopic anatomical right hemihepatectomy *via* a hepatic parenchymal transection-first approach guided by the middle hepatic vein; RHV, Right hepatic vein.

of stay (LOS) as defined as a postoperative stay < 50th percentile of the total cohort (LOS ≤ 10 days), absence of unplanned readmission, and absence of postoperative mortality.

2.5. Statistical analysis

The characteristics of patients were expressed as mean ± standard deviation or median with interquartile range for continuous variables and frequency with proportion for categorical variables. Differences between the groups were compared using *t* test for continuous data and Chi-square test for categorical variables. Survival curves were estimated by the Kaplan–Meier method with log-rank comparison. Prior to multivariate logistic regression modeling, multicollinearity among candidate predictors was assessed using Pearson correlation; variables with $|r| > 0.7$ were excluded. Variables significant in univariate analysis ($p < 0.05$) or deemed clinically relevant based on prior knowledge were included as candidates for the multivariate logistic regression model. The final model was constructed using backward stepwise selection (removal criterion $p \geq 0.05$), retaining variables significant at $p < 0.05$ or considered clinically essential. The $p < 0.05$ were considered statistically significant. Statistical analyses and PSM were performed using R version 4.3.1 and SPSS version 26.0 (IBM SPSS, Inc, Chicago, IL).

3. Results

3.1. Baseline characteristics

Between January 2017 and December 2019, a total of 105 HCC patients who underwent LARH were included in this study, of whom 48 patients underwent LARH-HPFM and 57 the LARH-EG.

All patients underwent blood biochemistry and tumor markers analyses, imaging examination (Figure 5), indocyanine green clearance test, and 3-dimensional reconstruction (Figure 6) before the operation. The patients' baseline characteristics in the two groups are shown in Table 1. The two groups differed before PSM in terms of ALB ($p = 0.017$). After PSM, 41 patients in each group were well-matched and the baseline demographics were comparable (Table 1).

3.2. Surgical data and postoperative outcomes

The Table 2 summarized the surgical data and postoperative outcomes between LARH-HPFM and LARH-EG group. The operative time was shorter in the LARH-HPFM group than in the LARH-EG group ($p = 0.029$). The blood loss in LARH-HPFM group was less than that of LARH-EG group ($p = 0.023$). The Pringle's time of LARH-HPFM group was shorter than that of LARH-EG group ($p = 0.035$). One patients in the LARH-HPFM group and two patients in the LARH-EG group converted to formal open surgery due to difficult control of intraoperative bleeding and intra-abdominal adhesions.

For postoperative recovery, there were no significant differences between the RH-HPFM and LARH-EG groups in terms of length of stay, diet recovery, and conversion rates. In terms of postoperative liver function, there were no significant differences in serum ALT, total bilirubin and albumin levels between LARH-HPFM group and LARH-EG group at 1, 3 and 5 days

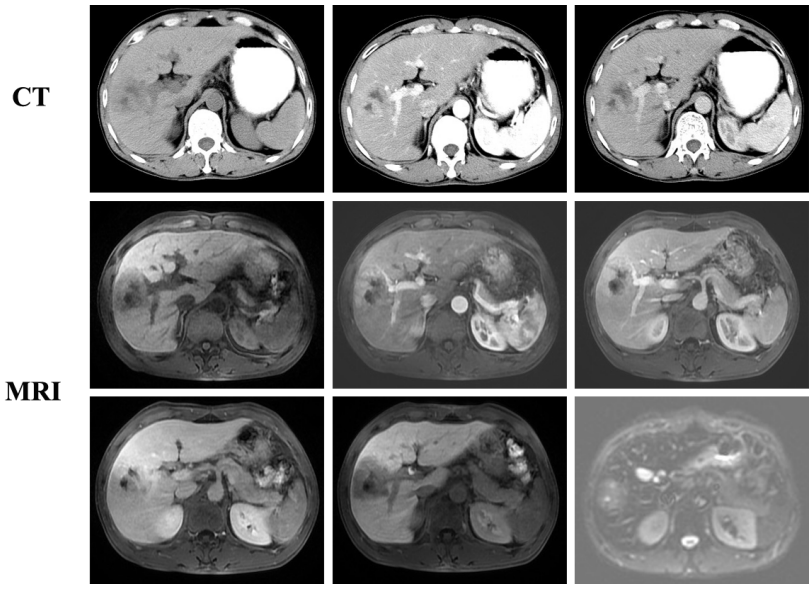

Figure 5. Preoperative CT (A) and MRI (B) of the liver.

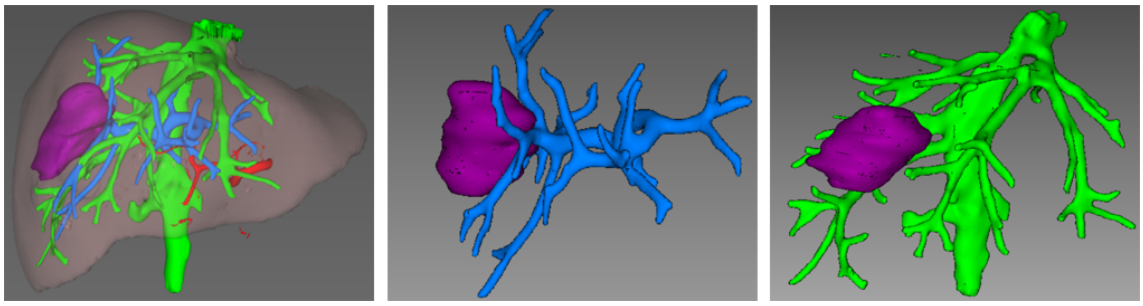

Figure 6. Preoperative 3D-CT reconstruction.

after surgery. In terms of complications, there was no significant difference in the total complication rate between LARH-HPFM group and LARH-EG group (29.3% *vs.* 41.5%, $p = 0.248$). Similarly, there were no significant differences in the type of complications and the incidence of grade I and grade II complications between the two groups. No patients suffered Grade III and above complications in LARH-HPFM group. In the LARH-EG group, one patient suffered from pleural effusion was submitted to thoracentesis with continuous chest drainage, and one intra-abdominal collection secondary to bile leak, treated with ultrasound-guided abdominal puncture and drainage, who were noted as grade III complications. There was no mortality case within 30 days in both groups.

3.3. Univariable and multivariable analyses of risk factors associated with EBL ≥ 400 mL in HCC patients undergoing LARH-HPFM or LARH-EG after PSM

All univariable and multivariable analyses of risk factors associated with EBL ≥ 400 mL in two groups after PSM are shown in Figure 7. Univariable analysis identified surgical approaches, cirrhosis, maximum tumor diameter > 5 cm, macrovascular invasion as risk factors of EBL ($p < 0.05$). Multivariate analysis revealed that maximum tumor diameter > 5 cm (8.59, 95% CI 1.91 - 38.77, $p = 0.005$), cirrhosis (7.17, 95% CI 1.71 - 30.12, $p = 0.007$) and macrovascular invasion (12.51, 95% CI 1.67 - 93.64, $p = 0.014$) were independent risk factors for EBL ≥ 400 mL. However, LARH-HPFM (compared to LARH-EG) (0.14, 95% CI 0.04 - 0.53, $p = 0.004$) was protective factors for EBL ≥ 400 mL.

3.4. Univariable and multivariable analyses of risk factors associated with prolonged operative time in HCC patients undergoing LARH-HPFM or LARH-EG after PSM

All univariable and multivariable analyses of risk factors associated with operative time ≥ 240 min in two groups after PSM are shown in Figure 8. Univariable analysis identified surgical approaches, maximum tumor diameter > 5 cm, tumor encapsulation incomplete, and macrovascular invasion as risk factors of prolonged operative time ($p < 0.05$). Multivariate analysis revealed that maximum tumor diameter > 5 cm (5.89, 95% CI 1.54 - 22.52, $p = 0.010$) and macrovascular invasion (11.69,

Table 1. Patient characteristics before and after PSM

Variables	Before PSM		*p*	After PSM		*p*
	LARH-HPFM *n* = 48	LARH-EG *n* = 57		LARH-HPFM *n* = 41	LARH-EG *n* = 41	
Age (years), mean (SD)	52.29 ± 10.45	54.6 ± 11.45	0.288	52.34 ± 10.50	52.56 ± 11.6	0.929
Gender, *n* (%)						
Male	38 (79.2)	39 (68.4)	0.215	32 (78.0)	31 (75.6)	0.794
Female	10 (20.8)	18 (31.6)		9 (22.0)	10 (24.4)	
BMI (kg/m^2), mean (SD)	23.30 ± 2.96	23.39 ± 2.94	0.873	23.24 ± 3.16	23.37 ± 3.19	0.852
ASA II, *n* (%)	24 (48.9)	26 (43.7)		20 (48.8)	14 (34.1)	0.179
Child-Pugh B, *n* (%)	9 (18.8)	7 (12.3)	0.358	7 (17.1)	8 (19.5)	0.775
BCLC stage B, *n* (%)	10 (20.8)	18 (31.6)	0.483	8 (19.5)	14 (34.1)	0.135
Previous abdominal surgery, *n* (%)	5 (10.4)	10 (17.5)	0.298	5 (12.2)	5 (12.2)	1.000
Hepatitis B viral infection, *n* (%)	34 (75.6)	37 (77.1)	0.862	35 (85.4)	36 (87.8)	0.746
Cirrhosis, *n* (%)	9 (18.8)	11 (19.3)	0.943	9 (22.0)	6 (14.6)	0.391
Clinically significant portal hypertension, *n* (%)	4 (8.3)	4 (7.0)	0.800	2 (4.9)	3 (7.3)	0.644
ICG-R15 (%), mean (SD)	7.17 ± 2.94	7.72 ± 2.25	0.278	7.49 ± 2.95	7.56 ± 2.25	0.867
Hypertension, *n* (%)	9 (18.8)	7 (12.3)	0.358	7 (17.1)	3 (7.3)	0.177
Diabetes mellitus, *n* (%)	6 (12.5)	6 (10.5)	0.751	5 (12.2)	4 (9.8)	0.724
Heart disease, *n* (%)	3 (6.7)	2 (4.2)	0.593	2 (4.9)	1 (2.4)	0.556
Largest tumor size(cm), mean (SD)	5.38 ± 1.61	5.35 ± 2.31	0.952	5.37 ± 1.59	5.17 ± 2.04	0.630
Surgical margin (cm), mean (SD)	3.08 ± 0.74	2.91 ± 0.58	0.186	3.15 ± 0.73	2.98 ± 0.61	0.253
Microvascular invasion, *n* (%)						
M1, *n* (%)	8 (16.7)	11 (19.3)	0.921	4 (9.8)	8 (19.5)	0.207
M2, *n* (%)	4 (8.3)	4 (7.0)		4 (9.8)	1 (2.4)	
Macrovascular invasion, *n* (%)	7 (14.6)	9 (15.8)	0.062	5 (12.2)	6 (14.6)	0.746
Tumor encapsulation incomplete, *n* (%)	37 (77.1)	42 (73.7)	0.688	30 (73.2)	30 (73.2)	1.000
Edmondson–Steiner grade, *n* (%)						
I/II	31 (64.6)	40 (70.2)	0.542	26 (63.4)	28 (68.3)	0.641
III/IV	17 (35.4)	17 (29.8)		15 (36.6)	13 (31.7)	
HGB (g/L), mean (SD)	139.10 ± 16.96	133.00 ± 16.90	0.069	139.85 ± 15.9	137.63 ± 14.79	0.515
AST (IU/L), mean (SD)	29.70 (17.00-139.30)	37.10 (12.20-306.30)	0.069	29.00 (17.00-139.30)	33.50 (10.90-113.50)	0.970
ALT (IU/L), mean (SD)	35.00 (11.00-152.00)	36.10 (16.10-287.40)	0.412	32.30 (10.70-144.80)	33.50 (10.10-156.10)	0.742
TB (μmol/L), mean (SD)	16.25 ± 7.70	15.42 ± 6.50	0.551	15.93 ± 8.16	15.51 ± 6.19	0.796
ALB (g/L), mean (SD)	44.67 ± 4.62	42.49 ± 4.53	0.017	44.29 ± 4.67	43.63 ± 4.24	0.505
PT (s), mean (SD)	11.44 ± 1.05	11.70 ± 1.18	0.232	11.39 ± 1.05	11.71 ± 1.10	0.185
INR, mean (SD)	1.02 ± 0.11	1.04 ± 0.12	0.190	1.01 ± 0.107	1.04 ± 0.10	0.266
PLT (109 /L), mean (SD)	185.0 ± 72.15	175.0 ± 62.89	0.453	190.29 ± 74.68	174.07 ± 59.29	0.279

Abbreviation: PSM, propensity score matching; LARH, laparoscopic anatomical right hemihepatectomy; HPFM, hepatic parenchymal transection-first approach (HPF) guided by the middle hepatic vein (MHV); EG, Glissonian approach; BMI, body mass index; ASA, American society of aneshesiologists physical status classification system; SD, standard deviation.

95% CI 1.96 - 69.83, 0.007) were independent risk factors for prolonged operative time. However, LARH-HPFM (compared to LARH-EG) (0.23, 95% CI 0.06 - 0.81, p = 0.023) was protective factor for prolonged operative time.

3.5. Distribution of TO criteria and number of cumulated TO criteria

LARH-HPFM cumulated more TO criteria (p = 0.025) and had higher rate of TO (46.3% *vs*. 24.4%; 2.68, 95% CI 1.05 - 6.86, p = 0.038) than LARH-EG. The distribution of TO criteria and the cumulated number of TO criteria according to LARH-HPFM and LARH-EG is displayed in Figure 9A and B.

3.6. Survival

The median follow-up time in the LARH-HPFM group was 40.2 months and in the LARH-EG group was 37.1 months (p = 0.871). The oncological outcomes between LARH-HPFM group and LARH-EG group did not differ with regard to overall survival (OS) (p = 0.539) and disease-free survival (DFS) (p = 0.846). The 1- and 3-year OS rates were 97.6% and 67.7%, respectively, in the LARH-HPFM group and 95.1% and 76.7%, respectively,

Table 2. Intraoperative data and postoperative outcomes

	LARH-HPFM *n* = 41	LARH-EG *n* = 41	*p*
Surgical data			
Operative time (min), mean (SD)	207.59 ± 37.70	226.44 ± 39.30	0.029
Blood loss (mL), mean (SD)	333.90 ± 94.52	382.32 ± 94.01	0.023
Conversion to open, *n* (%)	1 (2.4)	2 (4.9)	1.000
Pringle time (min), mean (SD)	41.7 ± 13.35	47.68 ± 11.89	0.035
Postoperative outcomes			
TO	19 (46.34)	10 (24.39)	0.038
No. of cumulated TO creteria, mean (SD)	5.15 ± 1.04	4.59 ± 1.18	0.025
Mortality within 30d, *n* (%)	0	0	NA
Perioperative transfusion, *n* (%)	7 (17.1)	16 (39.0)	0.027
Prolonged hospitalization time, *n* (%)	7 (17.1)	13 (31.7)	0.123
Negative margins, *n* (%)	35 (85.4)	33 (80.5)	0.557
Readmission, *n* (%)	3 (7.3)	3 (7.3)	1.000
Complications, *n* (%)	12 (29.3)	17 (41.5)	0.248
Clavien–Dindo classification, *n* (%)			0.364
I, *n* (%)	10 (24.4)	11 (26.8)	
II, *n* (%)	2 (4.9)	4 (9.8)	
III, *n* (%)	0	2 (4.9)	
Liver decompensation, *n* (%)	0	2 (4.9)	0.494
Ascites, *n* (%)	10 (24.4)	7 (17.1)	0.414
Hemorrhage, *n* (%)	1 (2.4)	3 (7.3)	0.305
Bile leakage, *n* (%)	1 (2.4)	1 (2.4)	1.000
Pulmonary infection, *n* (%)	4 (9.8)	5 (12.2)	0.724
Pleural effusion, *n* (%)	1 (2.4)	3 (7.3)	0.305
Hospitalization time(days), mean (SD)	10.07 ± 3.67	11.56 ± 4.38	0.099
Bowel function recovery (days), mean (SD)	2.95 ±0.77	3.46 ± 1.53	0.060
Postoperative liver function			
POD1			
TB, μmol/L, mean (SD)	29.07 ± 15.06	30.71 ± 21.44	0.691
AST, IU/L, mean (SD)	240.44 ±212.60	292.95 ± 261.66	0.322
ALT, IU/L, mean (SD)	239.80 ± 179.83	274.29 ± 211.02	0.428
POD3			
TB, μmol/L, mean (SD)	27.00 ± 16.65	31.07 ± 17.21	0.279
AST, IU/L, mean (SD)	61.59 ± 42.27	65.12 ± 60.66	0.760
ALT, IU/L, mean (SD)	120.15 ± 87.95	116.02 ± 76.17	0.821
POD5			
TB, μmol/L, mean (SD)	22.51 ± 10.95	26.02 ± 12.77	0.185
AST, IU/L, mean (SD)	39.78 ± 16.30	38.02 ± 23.35	0.694
ALT, IU/L, mean (SD)	65.22 ± 33.77	53.37 ± 25.87	0.078

Abbreviation: LARH, laparoscopic anatomical right hemihepatectomy; HPFM, hepatic parenchymal transection-first approach guided by the middle hepatic vein; EG, Glissonian approach; TO, textbook outcome; POD, post-operative day; SD, standard deviation.

in the LARH-EG group (Figure 10A). The 1-and 3-year DFS rates were 87.8% and 63.6%, respectively, in the LARH-HPFM group and 90.2% and 72.0%, respectively, in the LARH-EG group (Figure 10B).

4. Discussion

In recent years, laparoscopic major hepatectomies are increasingly used in different centers worldwide, while LARH is the most commonly performed laparoscopic major liver resection (*16*). Although recent studies demonstrated the safety and reproducibility of LARH with favorable surgical outcomes in comparison with open surgery, this procedure remains technically challenging with a steep learning curve (*17,18*). In LARH, the main difficulty lies in the choice of surgical approach. The choice of laparoscopic surgical approach for a LARH is not simply a "road of entry" but a series of strategic decisions on how to accomplish the surgical goals while ensuring the safety and effectiveness of the surgery (*19,20*).

The Glissonian approach and HD can be used in LARH. HD is difficult and time-consuming to operate under the laparoscope and is suitable for the treatment of bileduct stones and portal vein tumor thrombus (PVTT) (*21,22*). The Glisson approach is based on hepatectomy with Glissonian pedicle transection proposed by Takasaki. It can be divided into the extrahepatic, intrahepatic, and transfissural approaches (*23,24*). It has a better safety profile, shortens the separation time of Glissonian pedicle, and advances the laparoscopic surgical process. If there is liver cirrhosis, severe fatty liver disease, Glissonian pedicle anatomical variation, short portal vessels, narrow hepatic hilar region, or difficulty in exposure of the hilar plate, and due to limitations of endoscopic instruments, the Glissonian approach is harder (*25-28*). The Laennec capsule can be used as a marker and

Characteristics	Univariate analysis			Multivariate analysis		
	OR	95%CI	P-value	OR	95%CI	P-value
LARH-HPFM vs. LARH-EG	0.26	0.11 , 0.66	0.005	0.14	0.04 , 0.53	0.004
Male	0.68	0.24 , 1.89	0.454			
Age>60	1.16	0.44 , 3.06	0.759			
ASA II	0.4	0.16 , 1.01	0.053			
BMI≥24kg/m2	1.27	0.40 , 4.01	0.688			
Hypertension	0.48	0.11 , 2.00	0.313			
Diabetes mellitus	0.97	0.24 , 3.91	0.965			
Previous abdominal surgery	0.79	0.20 , 3.03	0.729	0.38	0.05 , 2.73	0.334
Clinically significant portal hypertension	1.98	0.52 , 7.64	0.319	0.37	0.06 , 2.49	0.31
Cirrhosis	3.52	1.29 , 9.61	0.014	7.17	1.71 , 30.12	0.007
BCLC stage B	1.31	0.49 , 3.48	0.591			
Child-Pugh B	0.71	0.16 , 3.17	0.65			
Edmondson–Steiner III/IV	1.35	0.54 , 3.37	0.523			
Tumor diameter>5 cm	3.52	1.29 , 9.61	0.014	8.59	1.91 , 38.77	0.005
Tumor encapsulation incomplete	1.87	0.74 , 4.76	0.186	1.75	0.52 , 5.90	0.37
Microvascular invasion	1.49	0.51 , 4.34	0.468			
Macrovascular invasion	6.91	1.39 , 34.38	0.018	12.51	1.67 , 93.64	0.014
PLT≥100×109 /L	0.63	0.19 , 2.06	0.44			
ALT>44 U/L	1.08	0.43 , 2.71	0.864			
AST>44 U/L	2.61	0.90, 7.52	0.077			
ALB≥35 g/L	1.7	0.35 , 8.11	0.508			
TBIL>17 mol/L	1.49	0.58 , 3.83	0.408			
PT>12 s	2.96	0.91 , 9.64	0.071	1.68	0.35 , 8.05	0.514
HBV infection	0.44	0.15 , 1.27	0.128			

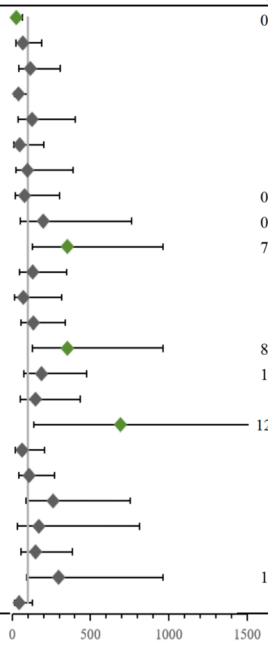

Figure 7. Univariable and multivariable analyses of risk factors associated with EBL > 400 mL in HCC patients undergoing LARH-HPFM or LARH-EG after PSM. *Abbreviation*: EBL, estimated blood loss; LARH, laparoscopic anatomical right hemihepatectomy; HPFM, hepatic parenchymal transection-first approach guided by the middle hepatic vein; EG, Glissonian approach; PSM, propensity score matching; ASA, American society of Aneshesiologists physical status classification system.

Characteristics	Univariate analysis			Multivariate analysis		
	OR	95%CI	P-value	OR	95%CI	P-value
LARH, HPFM vs. LARH, EG	0.32	0.12 , 0.90	0.030	0.23	0.06 , 0.81	0.023
Male	0.8	0.26 , 2.44	0.696			
Age>60	0.87	0.29 , 2.59	0.805			
ASA II	0.68	0.25 , 1.84	0.445			
BMI≥24kg/m2	2.09	0.72 , 6.07	0.176			
Hypertension	1.86	0.47 , 7.31	0.375			
Diabetes mellitus	2.27	0.55 , 9.36	0.255			
Previous abdominal surgery	1.11	0.26 , 4.74	0.884	0.940	0.15 , 6.03	0.945
Clinically significant portal	1.78	0.28 , 11.40	0.544			
Cirrhosis	0.8	0.27 , 2.37	0.693	0.660	0.18 , 2.43	0.531
BCLC stage B	2.27	0.80 , 6.43	0.121			
Child-Pugh B	1.96	0.61 , 6.32	0.259			
Edmondson–Steiner III/IV	0.43	0.14 , 1.33	0.145			
Tumor diameter>5 cm	3.24	1.17 , 9.03	0.024	5.890	1.54 , 22.52	0.010
Tumor encapsulation incomplete	3.2	1.17 , 8.75	0.023	3.650	0.99 , 13.44	0.052
Macrovascular invasion	9.96	2.35 , 42.19	0.002	11.690	1.96 , 69.83	0.007
Microvascular invasion	1.09	0.34 , 3.53	0.888			
PLT≥100×109 /L	2.25	0.68 , 7.41	0.183			
ALT>44 U/L	1.04	0.38 , 2.86	0.94			
AST>44 U/L	0.62	0.18 , 2.11	0.441			
ALB≥35 g/L	0.4	0.05 , 3.53	0.411			
TBIL>17 mol/L	1.73	0.63 , 4.77	0.291			
PT>12 s	2.79	0.87 , 8.89	0.083			
HBV infection	0.41	0.11 , 1.50	0.177			

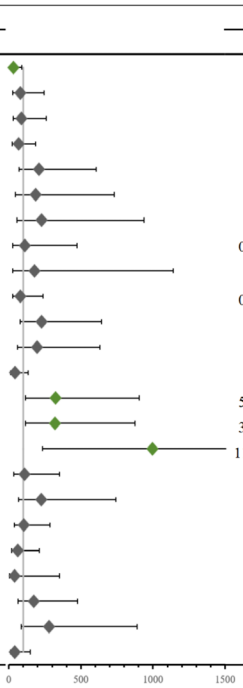

Figure 8. Univariable and multivariable analyses of risk factors associated with prolonged operative time in HCC patients undergoing LARH-HPFM or LARH-EG after PSM. *Abbreviation*: EBL, estimated blood loss; LARH, laparoscopic anatomical right hemihepatectomy; HPFM, hepatic parenchymal transection-first approach guided by the middle hepatic vein; EG, Glissonian approach; PSM, propensity score matching; ASA,A merican society of aneshesiologists physical status classification system.

approach for anatomical hepatectomy. The surgeon can achieve anatomical separation and management of the right Glissonian pedicle without anatomical damage to the liver parenchyma. The Laennec capsule approach for hepatectomy with Glissonian's pedicle transection is essentially an extrahepatic, extrathecal approach that can overcome some of the shortcomings of the conventional extrahepatic, extrathecal approach and is safe and effective (*29-31*).

The "easy first" strategy can be used for the LARH

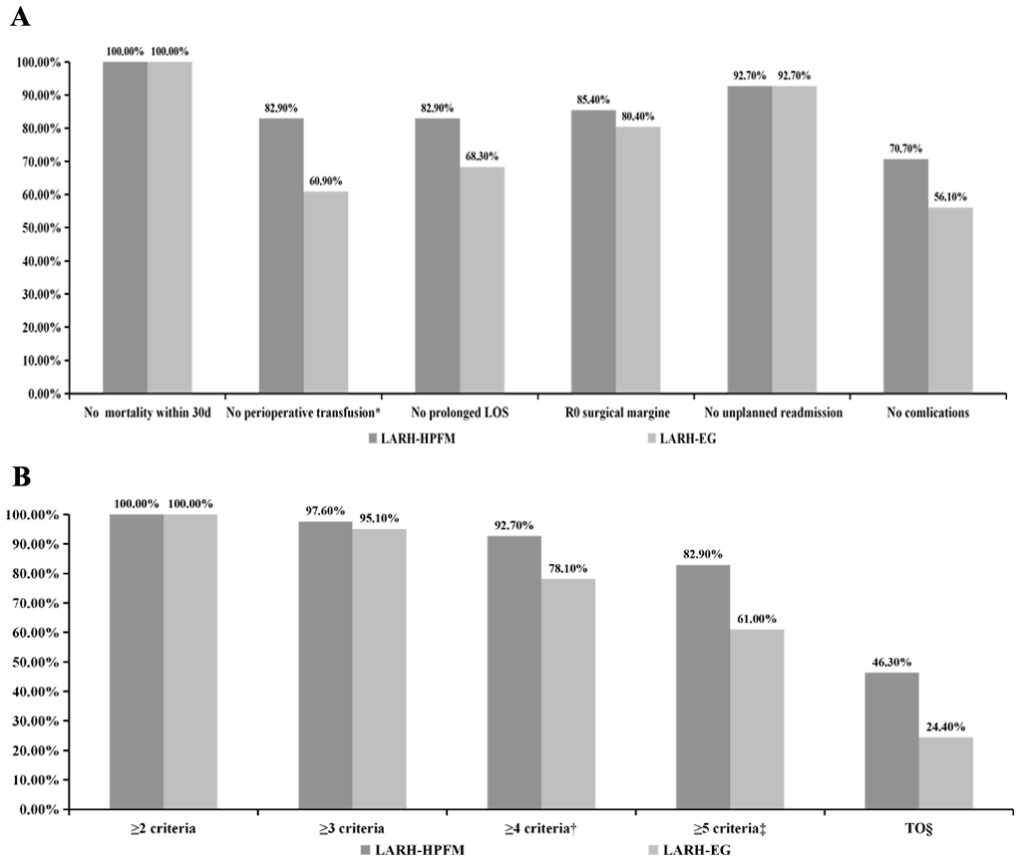

Figure 9. Distribution of TO criteria and number of cumulated TO criteria according to the type of surgical approach in the matched population. (A) TO criteria distribution. Levels of significance: **p* = 0.027. **(B)** Distribution of number of cumulated TO criteria. Levels of significance: †*p* = 0.061; ‡*p* = 0.027; §*p* = 0.038. *Abbreviation*: TO, textbook outcome. LOS, length of stay.

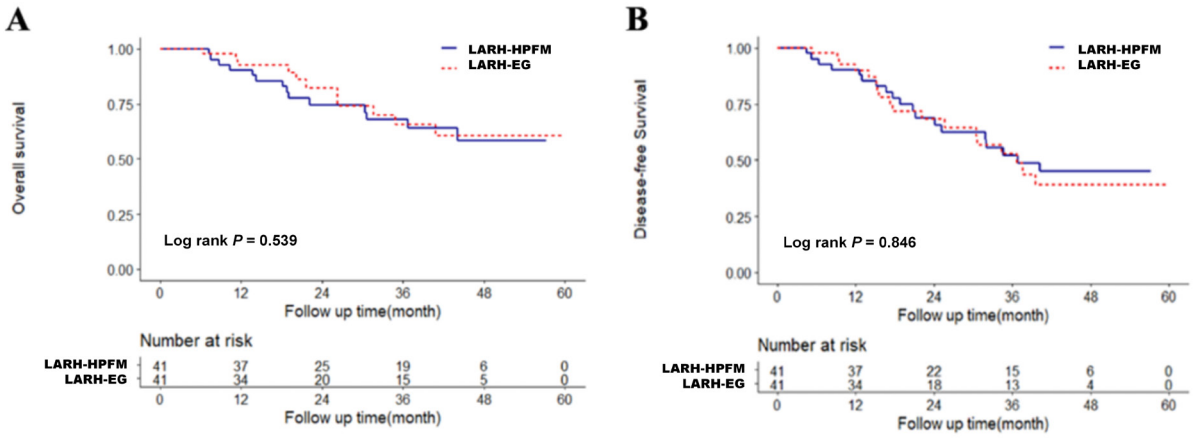

Figure 10. The survival curve between LARH-HPFM and LARH-GA groups, (A) OS rates and (B) DFS rates. *Abbreviation*: LARH, laparoscopic anatomical right hemihepatectomy; HPFM, hepatic parenchymal transection-first approach guided by the middle hepatic vein; EG, Glissonian approach; OS, overall survival; DFS, disease-free survival.

approach. According to the anatomical characteristics of the right hemiliver, the site that is relatively easy to dissect is dissected first to simplify the complex operation. We have explored this by using the HPFM for laparoscopic left hemihepatectomy in the early stage. By prioritizing the transection of the liver parenchyma, the left Glissonian pedicle is fully exposed, and the Glissonian pedicle is handled under adequate space conditions, making laparoscopic anatomical hepatectomy progression less difficult (*9*). Is this technique suitable for right hemihepatectomy? Based on the experience of other centers, combined with our own clinical experience, we continuously explored and practiced different sequences of the LARH approach and carried out LARH *via* HPFM. The resection was completed through the MHV as marker and fully exposing right Glissonian pedicle. To a certain extent, this technique overcomes the difficulties of complicated LARH operations, high

technical risks, and long learning curves and can more simply and intuitively guide the transected liver plane, simplify the surgical procedure, shorten the surgical time, and reduce the risks of bleeding and postoperative complications, which is consistent with the concept of precision hepatectomy and amounts to a certain technical model. Of note, LARH-HPFM proved significantly superior to the LARH-EG in TO. The HPFM is both safe and effective for various liver resections, including right anterior hepatectomy, central hepatectomy, segment 4 segmentectomy, segment 8 segmentectomy, and others.

The precautions for LARH-HPFM are listed as follows: (*i*) Preoperative high resolution thin-sliced enhanced CT scanning, helical CT arterial portography, 3D reconstruction visualization system and magnetic resonance cholangiopancreatography (MRCP) are used to accurately assess and judge the location and courses of vessels and bile duct, and individualized treatment is performed according to the variation (*32*). (*ii*) IOUS is an important step. In the absence of IOUS, preoperative image analysis and liver anatomical surface marking can be used to locate the position of the MHV and its relationship with the tumor, as well as the location of the larger vein branches (*33*). The hepatectomy section can be delineated to improve the accuracy of the surgery. According to the intraoperative conditions, IOUS can be used to repeatedly adjust the liver transection plane. To reduce gas interference, water can be injected into the transection. (*iii*) In the first longitudinal liver transection plane, the left or right Glissonian pedicle can be temporarily clipped to form the ischemic line, and the pre-resection line can be determined. Generally, the Cantlie line can also be selected. It is better to expose the MHV to determine the liver transection plane to achieve anatomical hepatectomy. Active exposure of the MHV avoids the massive hemorrhage caused by accidental injury of the hepatic vein during the operation; the anatomical level of the Laennec capsule can be fully utilized for blunt separation while separating and protecting the vein (*34*). (*iv*) The procedure should be performed under CVP (3-5 cmH_2O) and intermittent blockage of the first hepatic portal to reduce the blood oozing from the wound during separation (*35*). (*v*) Full dissection was performed to expose the Glissonian pedicle so that the endoscopic linear stapler could be placed. The whole Glissonian pedicle was accurately exposed and identified, and then the transection could be done using endoscopic linear stapler. Hepatic parenchymal was sufficiently transected first to help protect the preserved lateral ducts and hepatic vein trunk, and long-arm detachment forceps were used to test-clamp target hepatic pedicle to accurately identify the right Glissonian pedicle. Attention needs to be paid to the protection of the IVC, and the endoscopic linear stapler must be inserted under direct vision and without violence to prevent damage to the IVC. (*vi*) According to the situation and experience of the surgeon, direct cauterization using bipolar or unipolar electrocoagulation, titanium clips, or vascular clips (first using the separation forceps to lift part of the venous wall) can be used to stop bleeding. Suturing can be used to stop bleeding if necessary, and an appropriate amount of absorbable hemostatic gauze can significantly reduce bleeding (*36*). (*vii*) The use of a special device, the "Goldfinger" (a specialized curved dissector) is conducive to the anatomical separation of the Glisson pedicle and can reduce iatrogenic injury.

The application value of the LARH-HPFM in laparoscopic anatomical hepatectomy is mainly reflected in the following aspects: (*i*) It follows the "easy first" strategy and avoids the fine anatomical separation of Glissonian pedicle and bypasses the surgical obstacles caused by the complex anatomical variation of the Glissonian pedicle. (*ii*) Adequately thinning the hepatic parenchymal and maintaining enough tension to expand the relative gap to expose the transection plane can help determine the position of the Glissonian pedicle in the parenchyma and the direction and angle of the endoscopic linear stapler placement, improving the efficiency of the endoscopic linear stapler, avoiding the risk of injury and bleeding caused by dissecting and separating the Glissonian pedicle without adequate exposure, simplifying the surgical procedure somewhat, shortening the operation time, and improving the safety of the operation. (*iii*) The use of mature anatomical landmarks to set the transection plane of the liver parenchyma avoided accidental injury caused by the wrong dissection level and direction, and the scope of resection can be easily and precisely located. (*iv*) The ineffective liver tissue without inflow and outflow tract can be completely removed, the possibility of postoperative tumor recurrence and postoperative complications can be reduced, so as to improve the survival rate of patients.

For HCC treatment, any surgical approach aims to improve the survival rate of patients. Previous studies demonstrated that the Glissonian approach could improve the postoperative survival in patients with HCC. The principal reason for this is that Glissonian approach could prevent intraoperative spread of cancer cells dislodged by surgical manipulation by isolating the blood supply of the tumor-bearing area from that of the other parts of the liver (*37,38*). Meanwhile, we found that the oncological outcomes were similar between the two groups. Previous reports (*39,40*) have demonstrated increased blood loss and blood transfusion are negative effects on the recurrence and prognosis of patients with HCC after hepatectomy. Moreover, favouring TO significantly improved the probability of cure. Based on these results, the LARH-HPFM seems to be a better choice to improve survival rates of the HCC patients. However, our results are limited to small sample size and further studies need to evaluate the oncological results.

In this study, several limitations need to be addressed. The potential effects of a learning curve in

the laparoscopic approach may exist objectively. To limit the influence of learning curve as less as possible, we included patients who underwent LARH-HPFM only after the time period that we had passed the learning curve. The study is a retrospective analysis with small sample size, which may introduce potential selection bias. Although we introduced the PSM method to minimize selection bias, confounding variables could not be completely avoided. The follow-up period was not long enough, and a longer follow-up time is required in future studies to verify the effect of LARH-HPFM. This was a single-centre study, which may have limited the generalizability of the results. Therefore, further multicenter prospective or retrospective studies with large sample sizes and long-term follow-up are required to confirm these results.

The goal of laparoscopic anatomical hepatectomy is to simplify the complex surgery, with reasonable design, accurate efficacy, and high safety. We will combine the "easy first" strategy with LARH, and HPFM will be used. By preferentially dissecting the hepatic parenchyma, the Glissonian pedicle of the corresponding hepatic segment is fully exposed, and the Glissonian pedicle is treated with enough space to reduce the difficulty of progression of the laparoscopic anatomical hepatectomy and make its application easier. However, the selection of various approaches is not fixed and independent. It is necessary to conduct a comprehensive preoperative evaluation through careful image reading and three-dimensional reconstruction before surgery and to make a rational selection with a combination of various accesses according to their technical characteristics, the equipment, the surgical style, the lesion localization, and the individual characteristics of each case.

In conclusion, LARH-HPFM is safe and feasible for HCC with certain advantages over LARH-EG, but there are still many problems worth further exploration.

Funding: This work was supported by a grant from the general program of Chongqing medical scientific research project (Joint project of Chongqing Health Commission and Science and Technology Bureau) (2023MSXM004) and Chongqing health appropriate technology promotion project (2024jstg025). Medical research project of Chongqing Municipal Health Commission (2023WSJK054). Young Doctor Incubation Program of the Second Affiliated Hospital of Army Medical University (2022YQB031).

Conflict of Interest: The authors have no conflicts of interest to disclose.

References

1. Aghayan DL, Kazaryan AM, Fretland ÅA, Røsok B, Barkhatov L, Lassen K, Edwin B. Evolution of laparoscopic liver surgery: 20-year experience of a Norwegian high-volume referral center. Surg Endosc. 2022; 36:2818-2826.
2. Kim JH, Kim H. Laparoscopic Right Hemihepatectomy Using the Glissonean Approach: Detachment of the Hilar Plate (with Video). Ann Surg Oncol. 2021; 28:459-464.
3. Willems E, D'Hondt M, Kingham TP, *et al*. Comparison Between Minimally Invasive Right Anterior and Right Posterior Sectionectomy *vs* Right Hepatectomy: An International Multicenter Propensity Score-Matched and Coarsened-Exact-Matched Analysis of 1,100 Patients. J Am Coll Surg. 2022; 235:859-868.
4. Peng Y, Li B, Xu H, Guo S, Wei Y, Liu F. Is the anterior approach suitable for laparoscopic right hemihepatectomy in patients with large HCC (5-10 cm)? A propensity score analysis. Surg Endosc. 2022; 36:6024-6034.
5. Nitta H, Sasaki A, Katagiri H, Kanno S, Umemura A. Is Laparoscopic Hepatectomy Safe for Giant Liver Tumors? Proposal from a Single Institution for Totally Laparoscopic Hemihepatectomy Using an Anterior Approach for Giant Liver Tumors Larger Than 10 cm in Diameter. Curr Oncol. 2022; 29:8261-8268.
6. Wang S, Yue Y, Zhang W, Liu Q, Sun B, Sun X, Yu D. Dorsal approach with Glissonian approach for laparoscopic right anatomic liver resections. BMC Gastroenterol. 2021; 21:138.
7. Lee MJ, Kim JH, Jang JH. Tailored Strategy for Dissecting the Glissonean Pedicle in Laparoscopic Right Posterior Sectionectomy: Extrahepatic, Intrahepatic, and Transfissural Glissonean Approaches (with Video). World J Surg. 2022; 46:1962-1968.
8. Liao KX, Yu F, Cao L, Wang BL, Li XS, Wang XJ, Li JW, Fan YD, Chen J, Zheng SG. Laparoscopic Glissonian pedicle versus hilar dissection approach hemihepatectomy: A prospective, randomized controlled trial. J Hepatobiliary Pancreat Sci. 2022; 29:629-640.
9. Liu Q, Li J, Zhou L, Gu H, Wu K, You N, Wang Z, Wang L, Zhu Y, Gan H, Zheng L. Liver Parenchyma Transection-First Approach for Laparoscopic Left Hemihepatectomy: A Propensity Score Matching Analysis. World J Surg. 2021; 45:615-623.
10. You N, Wu K, Li J, Zheng L. Laparoscopic liver resection of segment 8 *via* a hepatic parenchymal transection-first approach guided by the middle hepatic vein. BMC Gastroenterol. 2022; 22:224.
11. Zhu P, Liao W, Zhang WG, Chen L, Shu C, Zhang ZW, Huang ZY, Chen YF, Lau WY, Zhang BX, Chen XP. A prospective study using propensity score matching to compare long-term survival outcomes after robotic-assisted, laparoscopic, or open liver resection for patients with BCLC stage 0-A hepatocellular carcinoma. Ann Surg. 2023; 277:e103-e111.
12. Kaibori M, Ichihara N, Miyata H, Kakeji Y, Nanashima A, Kitagawa Y, Yamaue H, Yamamoto M, Endo I. Surgical outcomes of laparoscopic versus open repeat liver resection for liver cancers: A report from a nationwide surgical database in Japan. J Hepatobiliary Pancreat Sci. 2022; 29:833-842.
13. Fagenson AM, Pitt HA, Lau KN. Perioperative Blood Transfusions or Operative Time: Which Drives Post-Hepatectomy Outcomes? Am Surg. 2022; 88:1644-1652.
14. Lin ZY, Zhang XP, Zhao GD, Li CG, Wang ZH, Liu R, Hu MG. Short-term outcomes of robotic versus open hepatectomy among overweight patients with hepatocellular carcinoma: a propensity score-matched study. BMC Surg. 2023; 23: 153.
15. D'Silva M, Cho JY, Han HS, Yoon YS, Lee HW, Lee

JS, Lee B, Jo Y, Lee E, Kang M, Park Y. The value of analyzing textbook outcomes after laparoscopic hepatectomy-a narrative review. Transl Cancer Res. 2023; 12:631-637.
16. Liang X, Zheng J, Xu J, Tao L, Cai J, Liang Y, Feng X, Cai X. Laparoscopic anatomical portal territory hepatectomy using Glissonean pedicle approach (Takasaki approach) with indocyanine green fluorescence negative staining: how I do it. HPB (Oxford). 2021; 23:1392-1399.
17. Hoogteijling TJ, Sijberden JP, Primrose JN, Morrison-Jones V, Modi S, Zimmitti G, Garatti M, Sallemi C, Morone M, Abu Hilal M. Laparoscopic right hemihepatectomy after future liver remnant modulation: A single surgeon's experience. Cancers (Basel).2023; 15:2851.
18. Görgec B, Suhool A, Al-Jarrah R, Fontana M, Tehami NA, Modi S, Abu Hilal M. Surgical technique and clinical results of one- or two-stage laparoscopic right hemihepatectomy after portal vein embolization in patients with initially unresectable colorectal liver metastases: A case series. Int J Surg. 2020; 77:69-75.
19. Kim JH. Pure laparoscopic right hepatectomy using modified liver hanging maneuver: Technical evolution from caudal approach toward ventral approach. J Gastrointest Surg. 2018; 22:1343-1349.
20. Gao J, Zheng J, Zhu Z, Xu J, Qi W, Chen J, Liang X. Laparoscopic orthotopic right hemihepatectomy by anterior approach combined with inferior vena cava thrombectomy. Ann Surg Oncol. 2022; 29:5548-5549.
21. Liu F, Wei Y, Chen K, Li H, Wang W, Wu H, Wen T, Li B. The extrahepatic Glissonian versus hilar dissection approach for laparoscopic formal right and left hepatectomies in patients with hepatocellular carcinoma. J Gastrointest Surg. 2019; 23:2401-2410.
22. Rotellar F, Luján J, Almeida A, Benito A, Hidalgo F, López-Olaondo L, Martí-Cruchaga P, Zozaya G. Full laparoscopic vascular reconstruction for portal tumoral invasion during a right hepatectomy using the caudal approach. Ann Surg Oncol. 2022; 29:5543-5544.
23. Cho SC, Kim JH. Laparoscopic left hemihepatectomy using the extrahepatic Glissonean approach: Technical tips for entering gaps. J Surg Oncol. 2022; 126:1430-1433.
24. Wan H, Xie K, Wu H. Parenchymal sparing laparoscopic segmentectomy III and IV with indocyanine green fluorescence negative stain method using Glisson pedicle approach. J Gastrointest Surg. 2023; 27:203-204.
25. Zheng K, He D, Liao A, Wu H, Yang J, Jiang L. Laparoscopic segmentectomy IV using hepatic round ligament approach combined with fluorescent negative staining method. Ann Surg Oncol. 2022; 29:2980-2981.
26. Zheng Z, Xie H, Liu Z, Wu X, Peng J, Chen X, He J, Zhou J. Laparoscopic central hepatectomy using a parenchymal-first approach: How we do it. Surg Endosc. 2022; 36:8630-8638.
27. Kim JH. Laparoscopic anatomical segmentectomy using the transfissural Glissonean approach. Langenbecks Arch Surg. 2020; 405:365-372.
28. Morimoto M, Tomassini F, Berardi G, *et al*. Glissonean approach for hepatic inflow control in minimally invasive anatomic liver resection: A systematic review. J Hepatobiliary Pancreat Sci. 2022; 29:51-65.
29. Hanzawa S, Monden K, Hioki M, Sadamori H, Ohno S, Takakura N. How-I-do-it: laparoscopic left medial sectionectomy utilizing a cranial approach to the middle hepatic vein and Laennec's capsule. Langenbecks Arch Surg. 2021; 406:2091-2097.
30. Morimoto M, Matsuo Y, Nonoyama K, Denda Y, Murase H, Kato T, Imafuji H, Saito K, Takiguchi S. Glissonean pedicle isolation focusing on the Laennec's capsule for minimally invasive anatomical liver resection. J Pers Med. 2023; 13:1154.
31. Hu W, Zhang G, Chen M, Zhong C, Li M, Sun X, Li K, Wang Z. Laennec's approach for laparoscopic anatomical hemihepatectomy. World J Surg Oncol. 2021; 19:295.
32. Sheng W, Yuan C, Wu L, Yan J, Ge J, Lei J. Clinical application of a three-dimensional reconstruction technique for complex liver cancer resection. Surg Endosc. 2022; 36:3246-3253.
33. Kamiyama T, Kakisaka T, Orimo T. Current role of intraoperative ultrasonography in hepatectomy. Surg Today. 2021; 51:1887-1896.
34. Joechle K, Vega EA, Okuno M, Simoneau E, Ogiso S, Newhook TE, Ramirez DL, Holmes AA, Soliz JM, Chun YS, Tzeng CD, Lee JE, Vauthey JN, Conrad C. Middle hepatic vein roadmap for a safe laparoscopic right hepatectomy. Ann Surg Oncol. 2019; 26:296.
35. Liu TS, Shen QH, Zhou XY, Shen X, Lai L, Hou XM, Liu K. Application of controlled low central venous pressure during hepatectomy: A systematic review and meta-analysis. J Clin Anesth. 2021; 75:110467.
36. Yang SY, Feng JK, Yan ML, Guo L, Duan YF, Ye JZ, Liu ZH, Xiang YJ, Xu L, Xue J, Shi J, Lau WY, Cheng SQ, Guo WX. Laparoscopic and open liver resection for hepatocellular carcinoma with type 2 diabetes mellitus: multicenter propensity score-matched study. Hepatol Int. 2023; 17:1251-1264.
37. Tsuruta K, Okamoto A, Toi M, Saji H, Takahashi T. Impact of selective Glisson transection on survival of hepatocellular carcinoma. Hepatogastroenterology. 2002; 49:1607-1610.
38. Tian F, Leng S, Chen J, Cao Y, Cao L, Wang X, Li X, Wang J, Zheng S, Li J. Long-term outcomes of laparoscopic liver resection versus open liver resection for hepatocellular carcinoma: A single-center 10-year experience. Front Oncol. 2023; 13:1112380.
39. Harada N, Shirabe K, Maeda T, Kayashima H, Ishida T, Maehara Y. Blood transfusion is associated with recurrence of hepatocellular carcinoma after hepatectomy in Child-Pugh class A patients. World J Surg 2015;39:1044-1051.
40. Suh SW, Lee SE, Choi YS. Influence of intraoperative blood loss on tumor recurrence after surgical resection in hepatocellular carcinoma. J Pers Med. 2023; 13:1115.

Received February 10, 2025; Revised July 30, 2025; Accepted August 5, 2025.

[§]These authors contributed equally to this work.
**Address correspondence to:*
Lu Zheng, Department of Hepatobiliary Surgery, The Second Affiliated Hospital, Third Military Medical University (Army Medical University), Chongqing 400037, China.
E-mail: zhenglu@tmmu.edu.cn

Released online in J-STAGE as advance publication August 8, 2025.

Original Article

DOI: 10.5582/bst.2025.01170

Radiotherapy enhances triple therapy for conversion and survival in patients with unresectable hepatocellular carcinoma with portal vein tumor thrombus

Ying Zhou[1], Minghong Yao[2], Tianfu Wen[1], Chuan Li[1,*]

[1] Division of Liver Surgery, Department of General Surgery, West China Hospital, Sichuan University, Chengdu, China;
[2] Chinese Evidence-based Medicine Center and CREAT Group, West China Hospital, Sichuan University, Chengdu, China.

SUMMARY: Triple therapy (TT), consisting of transarterial chemoembolization, immune checkpoint inhibitors, and tyrosine kinase inhibitors, is recommended as a conversion therapy for patients with unresectable hepatocellular carcinoma (uHCC). However, patients with uHCC with portal vein tumor thrombosis (PVTT) have a limited response to TT alone. This study evaluated whether combining TT with radiotherapy (TTR) could increase conversion resection rates and improve the prognosis of uHCC with PVTT. A total of 123 patients treated at our institution from 2020-2024 were retrospectively analyzed, comprising 103 patients receiving TT and 20 receiving TTR. The overlap weighting (OW) method was used to minimize bias. Compared with the TT group, patients in the TTR group had a significantly greater early tumor shrinkage rate (85.0% *vs.* 59.2%, $p = 0.029$). Moreover, conversion resection rates were significantly higher in the TTR group (65.0% *vs.* 35.0%, $p = 0.012$), and the median overall survival (OS) was notably prolonged (median OS not reached *vs.* 31.9 months, $p = 0.031$). Following OW adjustment of the data, we obtained similar results. Multivariate analysis confirmed TTR as an independent protective factor for both OS (HR = 0.354, 95% CI = 0.127-0.984, $p = 0.046$) and the conversion resection rate (OR = 0.261, 95% CI = 0.081-0.838, $p = 0.024$). Treatment-related adverse events were manageable. Thus, TTR offers an improved conversion resection rate and survival outcomes compared with TT alone in patients with uHCC with PVTT and represents a promising therapeutic strategy.

Keywords: unresectable hepatocellular carcinoma, portal vein tumor thrombosis, radiotherapy, conversion resection

1. Introduction

Hepatocellular carcinoma (HCC) is a highly aggressive malignancy and the third leading cause of cancer-related mortality in patients worldwide; it is responsible for more than 800,000 deaths annually (*1*). Liver resection remains the primary curative treatment for HCC, with reported 5-year overall survival (OS) rates ranging from 50% to 70% (*2*). However, owing to its asymptomatic onset and rapid progression, over 60% of patients present with intermediate or advanced disease, precluding curative surgery (*2*). Although recent advances in both systemic and locoregional therapies have improved long-term outcomes in these patients (*3*), the OS rates remain unsatisfactory, particularly in patients with portal vein tumor thrombosis (PVTT).

Conversion therapy has emerged as a promising strategy for initially unresectable HCC (uHCC), enabling curative-intent resection and improved survival (*2*). Various conversion therapy regimens have been investigated (*4*), among which triple therapy (TT), which combines immune checkpoint inhibitors (ICIs), tyrosine kinase inhibitors (TKIs), and transarterial chemoembolization (TACE), has shown superior efficacy and is endorsed by the Chinese expert consensus (*4-7*). Compared with TACE or systemic therapy alone, TT significantly improves resection rates, OS, and progression-free survival (PFS) in patients with uHCC (*5*). However, PVTT is an independent risk factor in these patients, affecting the conversion resection rate, OS and PFS (*8,9*). PVTT progression accelerates disease progression, portal hypertension, hepatic decompensation, and related complications, with reported median growth rates of up to 0.9 mm/day (*10*). These observations highlight the urgent need for targeted PVTT management during conversion therapy. Emerging evidence suggests that stereotactic body radiotherapy (SBRT) combined with systemic therapy may improve outcomes compared with systemic therapy alone in patients with uHCC with PVTT (*11,12*).

On the basis of these observations, we hypothesized that in these patients, TT augmented with RT (TTR) may represent a more effective conversion therapy than TT. To investigate this premise, we conducted this study.

2. Materials and Methods

2.1. Study population

This study enrolled patients with uHCC with PVTT who received conversion therapy with either TT or TTR at our center between January 2020 and January 2024. The inclusion criteria for this study were as follows: 1) age ≥ 18 years; 2) liver function classified as Child–Pugh class A or B; 3) a diagnosis of HCC according to the American Association for the Study of Liver Diseases guidelines or by postoperative pathological examination; 4) Barcelona Clinic Liver Cancer (BCLC) stage C disease, with confirmed portal vein involvement as verified by imaging; 5) Eastern Cooperative Oncology Group (ECOG) performance status score of 0–1; and 6) no history of other malignancies. The exclusion criteria were as follows: patients aged <18 years, patients with recurrent HCC, individuals with extrahepatic metastases, and those presenting spontaneous tumor rupture. PVTTs was radiologically confirmed *via* pretreatment imaging and classified according to the Japan Liver Cancer Study Group criteria as follows: VP1 (third-order branch involvement), VP2 (second-order branch involvement), VP3 (first-order branch involvement), and VP4 (main trunk or contralateral branch involvement) (*13*). This study was approved by the Ethics Committee of West China Hospital of Sichuan University (No. 2025-795) and conformed to the Strengthening the Reporting of Observational Studies in Epidemiology (STROBE) guidelines for reporting observational studies (*14*).

2.2. Treatment

Treatment regimens were individually tailored by a multidisciplinary team (MDT). Eligible patients received one of the following targeted therapy regimens: lenvatinib (12 mg/day for patients weighing ≥ 60 kg; 8 mg/day for patients weighing < 60 kg), apatinib (250 mg/day), sorafenib (400 mg twice daily), donafenib (200 mg twice daily), bevacizumab (15 mg/kg every 3 weeks), or regorafenib (160 mg/day). The ICIs administered included atezolizumab (1200 mg every 3 weeks), sintilimab (200 mg every 3 weeks), toripalimab (240 mg every 3 weeks), camrelizumab (200 mg every 2 weeks), and tislelizumab (200 mg every 3 weeks).

TACE procedures were performed under local anesthesia *via* right femoral artery access. Following arteriography of the celiac trunk and superior mesenteric artery to assess the liver's arterial vascularization, chemotherapy agents, including 5-fluorouracil (800–1000 mg) and epirubicin-adriamycin (30–40 mg), were administered according to the body surface area. Subsequently, lipiodol and polyvinyl alcohol foam embolization particles were selectively injected into the hepatic segmental artery corresponding to the target tumor site. The volume of embolization agents ranged from 5 to 30 mL, with the dose adjusted on the basis of the tumor's location, size, and number.

For patients who underwent radiotherapy, the target area was delineated by experienced radiation oncologists under CT guidance. The gross tumor volume (GTV) encompassed the portal vein filling defect and adjacent primary hepatic lesions. To generate the clinical target volume (CTV), the GTV was expanded by 5 mm, and an additional margin of 5 mm was subsequently added to the CTV to form the planning target volume (PTV). Decisions regarding the prescribed radiation dose and fractionation schedule were determined by tumor location and volume, as well as proximity to critical anatomical structures. The linear-quadratic (LQ) formalism along with the biologically effective dose (BED) derived from the LQ model was used to evaluate the effect of fractionated irradiation. The BED was calculated using the following equation: $BED = nd \times [1 + d/(\alpha/\beta)]$, where n represents the number of radiation fractions, d denotes the fraction size, and an α/β ratio of 10 was used to determine the BED delivered to the tumor (*15*). Ultimately, the radiotherapy regimen and dosage were individualized for each patient according to tumor dimensions and proximity to intrahepatic lesions.

2.3. Efficacy assessment and follow-up

Tumor response and PVTT response was assessed according to the modified Response Evaluation Criteria in Solid Tumors (mRECIST) version 1.1 (*16*) at 3-month intervals, with subsequent therapeutic strategies (including surgical interventions) determined by MDT consensus. Early tumor shrinkage (ETS) was defined as a reduction of at least 10% from baseline in the sum of the longest diameters of target lesions at the first tumor assessment (*17*). A major pathological response (MPR) was defined as 10% or fewer residual viable tumor cells (indicating ≥90% necrosis), whereas a pathological complete response (pCR) was characterized by the absence of viable tumor cells in the resected tissue. For patients exhibiting either disease progression to treatment or grade ≥ 3 treatment-related adverse events (trAEs), the current regimen was discontinued and second-line alternatives were evaluated. OS was calculated from treatment initiation to death from any cause or last follow-up (1 March 2025). PFS was defined as the time from first treatment to progressive disease (PD) or death or recurrence from any reason

(*18*). Recurrence-free survival (RFS) was defined as the time interval from conversion resection to the occurrence of recurrence.

2.4. Definitions

The albumin-bilirubin (ALBI) grade was computed using the following established formula: ALBI score = (log10 bilirubin [μmol/L] × 0.66) + (albumin [g/L] × -0.085) (*19*). ALBI values were divided into 3 grades as follows: grade 1 (ALBI score < -2.60), grade 2 (-2.60 ≤ ALBI score ≤ -1.39), and grade 3 (ALBI score > -1.39) (*19*). Thrombocytopenia was defined as a platelet count <100×10⁹/L (*20*). Perioperative complications were assessed according to the Clavien-Dindo grading system (*21*), with grade ≥3 complications considered severe complications (*20*).

2.5. Statistical analysis

Categorical variables are presented as frequency counts and percentages, with between-group comparisons performed using Pearson's chi-square test or Fisher's exact test. Continuous variables are expressed as the means ± standard deviations, and group comparisons were conducted using independent Student's *t* tests or Mann-Whitney *U* tests. Survival outcomes were analyzed using the Kaplan-Meier method. Factors with a *p* value of less than 0.1 in the univariate analysis were subsequently entered into the multivariate analysis. A *p* value of less than 0.05 was considered statistically significant. To further address potential confounding, we applied overlap weighting (OW). All the statistical analyses were conducted using R software (version 4.4.2) or SPSS (version 23.0) for Windows.

3. Results

3.1. Patient characteristics

This study initially identified 159 uHCC patients with PVTT. After applying the predefined inclusion/exclusion criteria (Figure 1), 36 patients were excluded, yielding a final cohort of 123 patients: 103 who received TT and 20 who received TTR. The baseline characteristics were well balanced between the groups (Table 1). The predominant etiology among the HCC patients was hepatitis B virus (HBV) infection (91.9%). The mean tumor diameter was 8.42 cm. The extent of PVTT was as follows: VP2, 7 (5.7%) patients; VP3, 72 (58.5%) patients and VP4, 44 (35.8%) patients. A total of 94.3% of the patients suffered from VP3 or VP4 PVTT. After applying OW, the TT and TTR groups each had a weighted effective sample size (ESS) of 15.38, and their baseline clinical characteristics were well balanced (Table 1).

The median total prescribed dose in the TTR group was 40 Gy (range: 24-50 Gy), delivered in a median of 5 fractions (range: 3-25). The BED_{10} ranged from 59.5- 85.5Gy. As listed in Supplemental Table S1 (*https://www.biosciencetrends.com/action/getSupplementalData.php?ID=266*), lenvatinib was the predominant TKI in both cohorts (TT: 85.4%; TTR: 85.0%). Similarly, camrelizumab was the most frequently administered ICI in the two groups (TT: 81.6%; TTR: 75.0%)

3.2. Comparison of the tumor response between the two groups

As shown in Supplemental Figure S1 (*https://www.biosciencetrends.com/action/getSupplementalData.php?ID=266*), according to mRECIST, the TT group exhibited a complete response (CR) in 13 patients (12.6%), a partial response (PR) in 35 patients (34.0%), stable disease (SD) in 29 patients (28.2%), and progressive disease (PD) in 26 patients (25.2%). In contrast, the TTR group demonstrated CR in 4 patients (20.0%), PR in 10 patients (50.0%), SD in 4 patients (20.0%), and PD in 2 patients (10.0%). Compared

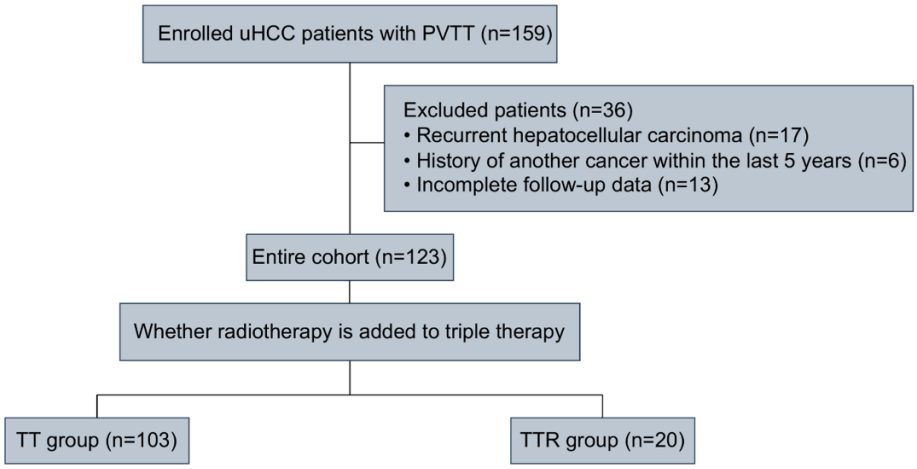

Figure 1. Flowchart of this study.

Table 1. Comparison of the baseline characteristics between the TT group and the TTR group

Variables	Primary cohort			OW cohort		
	TT group	TTR group	SMD	TT group	TTR group	SMD
n	103	20		15.38	15.38	
Age (years)	52.2 ± 10.8	49.7 ± 12.2	0.215	50.8 ± 11.1	50.8 ± 11.6	< 0.001
Gender			0.181			< 0.001
Female	10 (9.7%)	1 (5.0%)		0.9 (6.1%)	0.9 (6.1%)	
Male	93 (90.3%)	19 (95.0%)		14.4 (93.9%)	14.4 (93.9%)	
Platelet ($\times 10^9$/L)	172 ± 88.2	174 ± 84.8	0.033	176.7 ± 91.8	176.7 ± 86.3	< 0.001
ALBI, *n* (%)			0.019			< 0.001
Grade 1	66 (64.1%)	13 (65.0%)		10.1 (65.6%)	10.1 (65.6%)	
Grade 2	37 (35.9%)	7 (35.0%)		5.3 (34.4%)	5.3 (34.4%)	
History of hepatitis			0.007			< 0.001
HBV-related	94 (91.3%)	19 (95.0%)		14.7 (95.4%)	14.7 (95.4%)	
Non-HBV	1 (1.0%)	1 (5.0%)		0.7 (4.6%)	0.7 (4.6%)	
AFP (ng/mL)			0.099			< 0.001
≥ 400	62 (60.2%)	13 (65.0%)		9.9 (64.5%)	9.9 (64.5%)	
< 400	41 (39.8%)	7 (35.0%)		5.5 (35.5%)	5.5 (35.5%)	
Tumor number			0.206			< 0.001
Multiple	62 (60.2%)	10 (50.0%)		8.1 (52.7%)	8.1 (52.7%)	
Single	41 (39.8%)	10 (50.0%)		7.3 (47.3%)	7.3 (47.3%)	
Tumor diameter (cm)			0.596			< 0.001
< 5	15 (14.6%)	8 (40.0%)		4.9 (31.7%)	4.9 (31.7%)	
≥ 5	88 (85.4%)	12 (60.0%)		10.5 (68.3%)	10.5 (68.3%)	
PVTT			0.106			< 0.001
vp2	6 (5.8%)	1 (5.0%)		7.1 (5.8%)	7.2 (5.8%)	
vp3	61 (59.2%)	11 (55.0%)		71.5 (58.3%)	70.2 (56.8%)	
vp4	36 (35.0%)	8 (40.0%)		43.9 (35.8%)	46.3 (37.4%)	

OW, overlap weighting; ECOG PS, Eastern Cooperative Oncology Group Performance Status; TBil, total bilirubin; ALT, alanine aminotransferase; AST, aspartate aminotransferase; ALB, albumin; AFP, alpha fetoprotein; ALBI, albumin-bilirubin; HBV, hepatitis B virus; HCV, hepatitis C virus; up to seven, up to seven criteria.

Table 2. The best tumor responses in the TT group and TTR group

mRECIST 1.1	Primary cohort			OW cohort		
	TT group (*n* = 103)	TTR group (*n* = 20)	*p*	TT group (*n* = 15.38)	TTR group (*n* = 15.38)	*p*
Overall response						
CR, *n* (%)	13 (12.6%)	4 (20.0%)	0.382	1.90 (12.3%)	2.41 (15.7%)	0.693
PR, *n* (%)	35 (34.0%)	10 (50.0%)	0.173	5.00 (32.5%)	7.81 (50.8%)	0.154
SD, *n* (%)	29 (28.2%)	4 (20.0%)	0.451	4.64 (30.2%)	3.44 (22.4%)	0.489
PD, *n* (%)	26 (25.2%)	2 (10.0%)	0.137	3.84 (24.9%)	1.72 (11.2%)	0.127
ORR, n (%)	48 (46.6%)	14 (70.0%)	0.095	6.90 (44.8%)	10.22 (66.5%)	0.085
DCR, *n* (%)	77 (74.8%)	18 (90.0%)	0.241	11.54 (75.1%)	13.66 (88.8%)	0.126
PVTT						
CR, *n* (%)	34 (33.0%)	12 (60.0%)	**0.042**	5.05 (32.9%)	9.14 (59.4%)	**0.037**
Non-CR/Non-PD, *n* (%)	57 (55.3%)	7 (35.0%)	0.155	8.58 (55.8%)	5.40 (35.1%)	0.112
PD, *n* (%)	12 (11.7%)	1 (5.0%)	0.691	1.75 (11.4%)	0.84 (5.5%)	0.461
Early tumor shrinkage	61 (59.2%)	17 (85.0%)	**0.029**	9.74 (63.3%)	13.09 (85.1%)	**0.028**

OW, overlap weight; mRECIST, modified Response Evaluation Criteria in Solid Tumors; CR, Complete response; PR, Partial response; SD, Stable disease; PD, Progressive disease; ORR, objective response rate; DCR, disease control rate; PVTT, portal vein tumor thrombosis; TT, triple therapy; TTR, triple therapy with radiotherapy.

with the TT group, the TTR group demonstrated a numerically greater objective response rate (ORR; 70.0% *vs.* 46.6%; $p = 0.095$) and disease control rate (DCR; 90.0% *vs.* 74.8%; $p = 0.241$), although these differences did not reach statistical significance (Table 2). Notably, 85.0% of TTR patients achieved ETS, compared to 59.2% of TT patients ($p = 0.029$). In contrast, as shown in Table 2, the CR rate for PVTT was significantly improved in the TTR cohort (60.0% *vs.* 33.0%; $p = 0.042$). After applying OW, the CR rate of PVTT was 32.9% in TT group and 59.4% in TTR group ($p = 0.037$). Furthermore, 8 (22.2%) patients in the TT group and 3 (23.1%) patients in the TTR group achieved a pCR ($p = 1.000$). MPR was observed in 15 (41.7%) patients in the TT group and 7 (53.8%) patients in the TTR group ($p = 0.449$).

3.3. Factors independently associated with conversion resection

Thirteen (65.0%) patients in the TTR group and 36 (35.0%) patients in the TT group successfully underwent conversion resection. The conversion resection rate was significantly greater in the TTR cohort than in the TT cohort (p = 0.012). As presented in Table 3, multivariate analysis revealed that VP4 PVTT (OR = 3.278, 95% CI = 1.291-8.322, p = 0.012), ALBI grade 2 (OR = 2.831, 95% CI = 1.068-7.509, p = 0.037) and TTR (OR = 0.261, 95% CI = 0.081-0.838, p = 0.024) were independently associated with conversion resection rate. Among these factors, the TTR was a protective factor.

3.4. Safety of conversion resection

All of the patients underwent R0 resection. Among the 49 patients who successfully underwent liver resection following conversion therapy, severe postoperative complications were observed in 7 (19.4%) patients in the TT group and in 1 (7.7%) patient in the TTR group. Of these, 2 patients in the TT group experienced two or more postoperative complications simultaneously. The incidence of severe postoperative complications was comparable between the two groups (p = 0.663). Detailed information on these severe complications is provided in Supplemental Table S2 (*https://www.biosciencetrends.com/action/getSupplementalData.php?ID=266*).

3.5. Comparison of Survival Outcomes in the TTR and TT groups

The median follow-up duration was 35.3 months for the TT group and 32.9 months for the TTR group. During follow-up, 47 patients (45.6%) in the TT group and 4 patients (20.0%) in the TTR group died. The median OS (mOS) was 31.9 months (95% CI: 23.1-40.8) in the TT group, whereas it was not reached in the TTR group (p = 0.031). After applying OW, the mOS remained significantly longer in the TTR group (not reached) compared to the TT group (31.9 month; 95% CI: 25.9-not reached, p = 0.014). The 1-, 2-, 3-, and 4-year OS rates for patients in the TTR group were 94.7%, 89.5%, 82.0%, and 70.3%, respectively, whereas those for the TT group were 81.0%, 61.7%, 47.3%, and 41.1%, respectively (Figure 2A, p = 0.031). Disease progression occurred in 65 patients (63.1%) in the TT group and 9 patients (45.0%) in the TTR group. The median PFS (mPFS) was 35.5 months for the TTR group and 18.7 months for the TT group (p = 0.074). After applying OW, the mPFS was 35.5 months in the TTR group and 21.9 months in the TT group (p = 0.071). The 1-, 2-, 3-, and 4-year PFS rates for the TTR group were 85.0%, 63.8%, 45.3%, and 45.3%, respectively, whereas those for the TT group were 58.1%, 44.0%, 29.9%, and 29.9%, respectively (Figure 2B, p = 0.074).

We further compared the survival outcomes between patients who underwent successful conversion resection and those who did not across the two groups. Among patients who successfully underwent conversion resection, RFS and OS were similar between the TT and TTR groups (Supplemental Figure S2, p = 0.830; p = 0.670, *https://www.biosciencetrends.com/action/getSupplementalData.php?ID=266*). However, among patients who failed to undergo conversion resection, the OS was significantly better in the TTR group than in the TT group (Figure 3, p = 0.034).

We applied the Benjamini-Hochberg (BH) procedure for multiple comparison correction to these primary endpoints, minimizing the risk of false positives and ensuring the robustness of the data and validity of the results (Supplemental Table S3, *https://www.biosciencetrends.com/action/getSupplementalData.php?ID=266*).

Table 3. Univariate and multivariate analyses of factors associated with successful conversion resection

Variable	UV OR (95% CI)	*p*	MV OR (95% CI)	*p*
Age (≤ 60 *vs.* > 60 years)	0.779 (0.264-2.296)	0.651		
Gender (Male *vs.* Female)	0.507 (0.126-2.033)	0.338		
ALT (≤ 40 *vs.* > 40 U/L)	1.221 (0.452-3.302)	0.694		
AST (≤ 35 *vs.* > 35 U/L)	0.358 (0.071-1.818)	0.215		
HBeAg (Positive *vs.* Negative)	2.157 (0.750-6.204)	0.154		
AFP (≥ 400 *vs.* < 400 ng/mL)	0.910 (0.387-2.135)	0.828		
Tumor number (Single *vs.* Multiple)	0.925 (0.375-2.279)	0.865		
Tumor diameter (≥ 5 *vs.*< 5 cm)	1.900 (0.645-5.592)	0.244		
PVTT (Vp4 *vs.* Vp2/VP3)	2.780 (1.234-6.267)	**0.014**	3.278 (1.291-8.322)	**0.012**
ALBI grade (Grade 2 *vs.* Grade 1)	2.349 (1.059-5.213)	**0.036**	2.831 (1.068-7.509)	**0.037**
Thrombocytopenia (Yes *vs.* No)	1.136 (0.469-2.751)	**0.778**		
Treatment group (TTR group *vs.* TT group)	0.289 (0.106-0.790)	**0.015**	0.261 (0.081-0.838)	**0.024**

PVTT, portal vein tumor thrombosis; ALT, alanine aminotransferase; AST, aspartate aminotransferase; HBeAg, hepatitis B virus e antigen; AFP, alpha fetoprotein; ALBI, albumin-bilirubin; TT, triple therapy; TTR, triple therapy with radiotherapy; UV, univariate; MV, multivariate; OR, odds ratio.

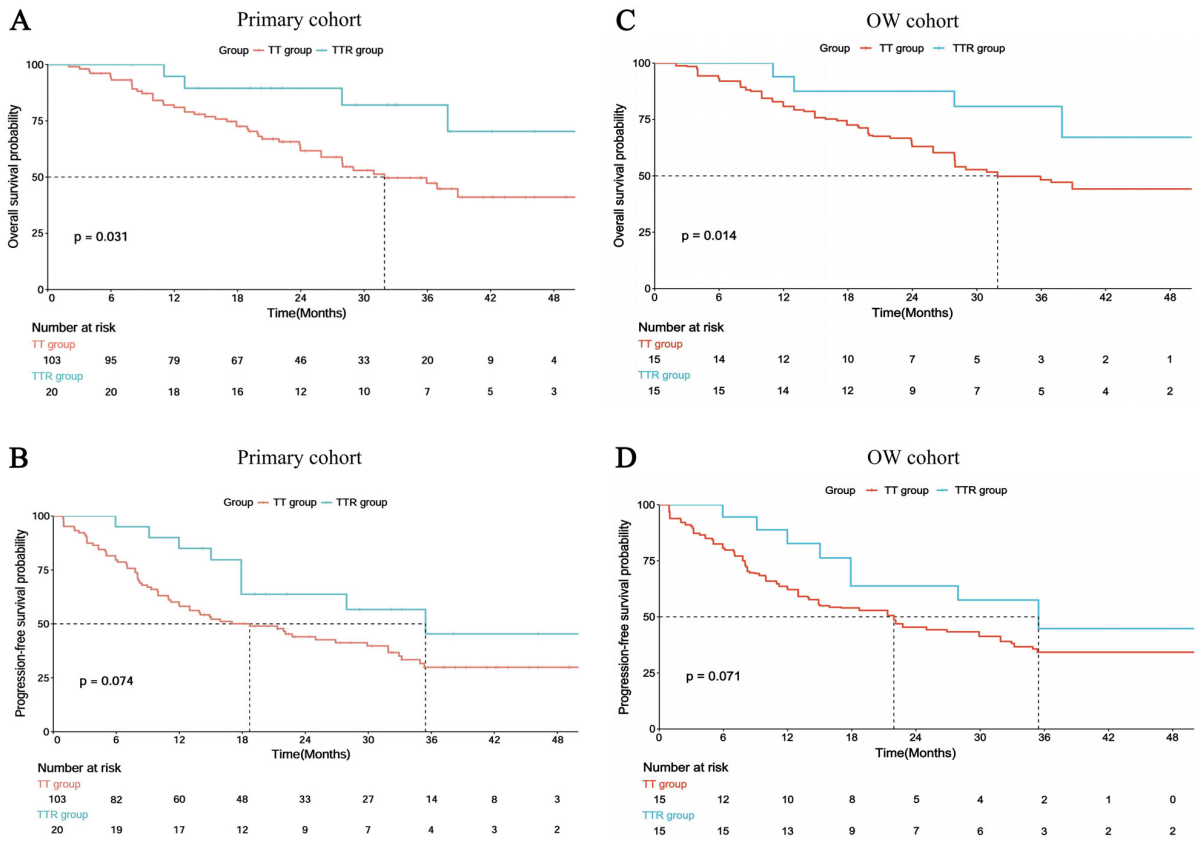

Figure 2. Overall survival and progression-free survival curves for the TT group and the TTR group.

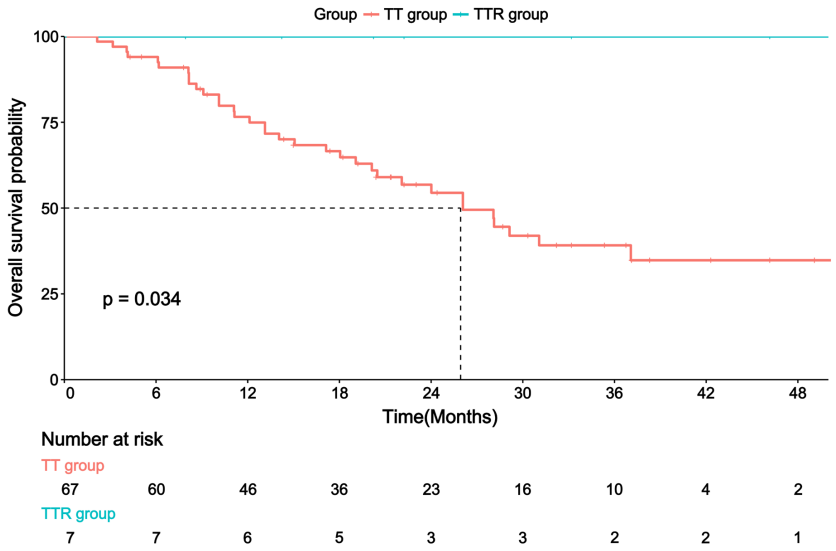

Figure 3. Overall survival curves for the TT group and the TTR group who failed to receive conversion resection.

3.6. Factors independently associated with OS and PFS

As shown in Table 4, univariate analysis suggested that male sex, thrombocytopenia, and treatment group had potential prognostic value in predicting OS. However, multivariate analysis confirmed that only thrombocytopenia (HR = 2.020, 95% CI = 1.035-3.940, $p = 0.039$) and TTR (HR = 0.354, 95% CI = 0.127-0.984, $p = 0.046$) were independently associated with OS. The TTR was identified as a protective factor for OS in this study.

Univariate analysis also revealed male sex, tumor diameter, and treatment group as potential prognostic factors for PFS (Supplemental Table S4, *https://www.biosciencetrends.com/action/getSupplementalData.php?ID=266*). However, multivariate analysis revealed

Table 4. Univariate and multivariate analyses of independent factors associated with overall survival

Variable	UV HR (95% CI)	*p*	MV HR (95% CI)	*p*
Age (≤ 60 *vs.* > 60 years)	0.972 (0.486-1.942)	0.935		
Gender (Male *vs.* Female)	0.481 (0.217-1.071)	0.073		
ALT (≤ 40 *vs.* > 40 U/L)	0.882 (0.496-1.568)	0.668		
AST (≤ 35 *vs.* > 35 U/L)	1.717 (0.721-4.087)	0.222		
HBeAg (Positive *vs.* Negative)	1.456 (0.684-3.098)	0.330		
AFP (≥ 400 *vs.* < 400 ng/mL)	1.010 (0.577-1.766)	0.972		
Tumor number (Single *vs.* Multiple)	1.190 (0.684-2.072)	0.538		
Tumor diameter (≥ 5 *vs.*< 5 cm)	1.555 (0.730-3.310)	0.252		
PVTT (Vp4 *vs.* Vp2/VP3)	0.669 (0.361-1.238)	0.200		
ALBI grade (Grade 2 *vs.* Grade 1)	1.288 (0.729-2.274)	0.383		
Thrombocytopenia (Yes *vs.* No)	2.027 (1.037-3.960)	**0.032**	2.020 (1.035-3.940)	**0.039**
Treatment group (TTR group *vs.* TT group)	0.342 (0.123-0.951)	**0.040**	0.354 (0.127-0.984)	**0.046**

PVTT, portal vein tumor thrombosis; ALT, alanine aminotransferase; AST, aspartate aminotransferase; HBeAg, hepatitis B virus e antigen; AFP, alpha fetoprotein; ALBI, albumin-bilirubin; TT, triple therapy; TTR, triple therapy with radiotherapy; UV, univariate; MV, multivariate; HR, hazard ratio.

that only male sex was independently associated with poorer PFS (HR = 2.038, 95% CI = 1.000-4.138, p = 0.049).

3.7. Adverse reactions

As listed in Supplemental Table S5 (*https://www.biosciencetrends.com/action/getSupplementalData.php?ID=266*), among all 123 treated patients, the most common trAE was hypothyroidism, which was observed in 25 patients (20.3%), followed by thrombocytopenia in 24 patients (19.5%) and hand-foot skin reactions in 19 patients (15.4%). Overall, all trAEs were generally manageable in both cohorts, with no treatment-related deaths occurring.

4. Discussion

The prognosis of uHCC with PVTT remains dismal. The BRIDGE study reported an mOS of approximately 15 months for patients with BCLC stage C, whereas patients with untreated PVTT had an mOS of only 2.4-4.0 months (*22*). Tumor invasion of the portal venous system promotes aggressive intrahepatic spread and, once beyond the hepatic portal veins, induces hemodynamic instability *via* reduced portal perfusion (*23,24*), leading to rapid hepatic decompensation, portal hypertension, and associated complications that severely constrain treatment options (*25*). Most patients with PVTT are ineligible for resection at diagnosis; a national cohort study in Korea revealed that only 15.1% of these patients underwent liver resection at diagnosis (*26*). Numerous studies have suggested that the combination of TACE with ICIs and TKIs could achieve a better ORR than existing first-line systemic therapies (*27,28*). For example, Yang *et al*. demonstrated that patients with initial uHCC who received triple conversion therapy had a significantly higher rate of liver resection than did those receiving TACE alone (34.6% *vs.* 23.5%) (*27*). Additionally, Wu *et al*. reported that 54.5% of patients with uHCC could progress to resectable HCC after TT (*28*). Accordingly, the Chinese expert consensus recommended the use of TT for conversion therapy for patients with initial uHCC (*29*). Conversion therapy may offer a potential opportunity for radical liver resection and improved OS in these patients. Our study confirmed that TTR may result in a higher rate of successful conversion resection and longer OS than in patients with initial uHCC.

Systemic therapy is recommended for patients with HCC with BCLC stage C disease by both the American Association for the Study of Liver Diseases and the European Association for the Study of the Liver (*3,30*). Recent advancements in systemic therapy have significantly improved outcomes for patients with advanced HCC (*3*). For example, the Imbrave-150 study demonstrated that the mOS for patients receiving atezolizumab plus bevacizumab was 19.2 months, which was significantly greater than that for patients treated with sorafenib (*31*). The ORR in the Imbrave-150 study, assessed by mRECIST, also increased to 35% (*31*). However, despite these advancements, both the OS and ORR for current first-line systemic therapies for patients with uHCC remain suboptimal. In the STAH trial, the median OS for patients receiving sorafenib plus TACE was 12.8 months, while the LAUNCH Phase III trial reported a median OS of 17.8 months with TACE plus Lenvatinib (*32,33*). Building on these findings, the OS in our TTR group has not yet been reached, suggesting that the combination of triple therapy with radiotherapy may offer more substantial survival benefits for patients with uHCC with PVTT.

PVTT is a well-established negative prognostic factor in conversion therapy for initial uHCC, independently limiting resection feasibility (*8,9*). Studies have consistently shown that therapies such as TACE, ICIs, and TKIs are less effective in patients

with PVTT than in those without (*34-36*). For example, Chuma *et al*. reported an ORR of 37.5% in patients with HCC with more than 50% liver occupation, compared with only 26.7% in those with VP4 PVTT (*36*). Additionally, Xiang *et al*. confirmed that TACE yielded a prognosis similar to that of best supportive care in HCC patients with VP4 PVTT (*34*). In clinical practice, PVTT growth velocity is notably rapid. Gon *et al*. indicated that the average growth rate of PVTT was as high as 0.9 mm/day (*10*). Therefore, conversion therapy for patients with uHCC with PVTT necessitates tailored treatment strategies specifically targeting the PVTT. However, previous studies on conversion therapy for these patients did not adequately address this issue. Studies have also demonstrated that, compared with systemic therapy alone, combining radiotherapy with systemic therapy improves both the ORR and OS in patients with PVTT (*12,37*). For example, Hu *et al.* (*12*) reported an ORR of 47.5% for patients with uHCC treated with camrelizumab-apatinib combined with radiotherapy, which was significantly greater than that for patients receiving camrelizumab-apatinib alone. In our study, we similarly reported that the conversion resection rate was significantly greater in the TTR group than in the TT group. These pronounced survival benefits likely result from the synergistic effects of radiotherapy, immune checkpoint inhibition, antiangiogenic therapy, and local interventions (*38-40*). As a local modality, radiotherapy not only induces lethal DNA damage in tumor cells but also triggers immunogenic cell death, which stimulates systemic antitumor immunity and enhances the infiltration of cytotoxic immune cells, thereby amplifying the effects of immunotherapy (*41-43*). Furthermore, antiangiogenic agents can enhance the efficacy of radiotherapy by normalizing the tumor vasculature and creating an immunologically favorable tumor microenvironment (*44,45*).

In this study, the ORR was greater in the TTR group (70.0%) than in the TT group (46.6%), although the difference was not statistically significant, likely due to the smaller TTR sample size. Interestingly, the conversion resection rate was significantly greater in the TTR group than in the TT group. Many patients in the TTR group exhibited meaningful tumor shrinkage, though these reductions did not meet the mRECIST criteria for PR or CR. Therefore, to better capture these effects, we refined the mRECIST standard by applying ETS and found that 59.2% of TT patients and 85.0% of TTR patients achieved ETS ($p = 0.029$). Furthermore, the evaluation of treatment efficacy indicated a higher CR rate for PVTT in the TTR group ($p = 0.042$), demonstrating the TTR regimen's capacity to elicit tumor responses. Furthermore, while OS was notably longer in the TTR group than in the TT group, the difference in PFS between the two groups was not statistically significant. Multivariate analysis indicated that conversion therapy did not independently contribute to PFS. A significant number of patients in both groups underwent conversion resection, and following liver resection, patients' PFS increased. Additionally, previous studies have highlighted that in advanced HCC, the correlation between PFS and OS may be weaker (*46*). While PFS primarily reflects tumor progression, OS captures a broader range of factors, including prolonged survival and delayed treatment effects. Notably, immunotherapy often induces delayed immune responses, which may not be immediately reflected in PFS but can significantly impact OS over time. This aligns with findings from other studies, such as the IMbrave-150 trial, where PFS improvements did not directly correlate with OS benefits; however, the combination of immune checkpoint inhibitors and targeted therapies led to substantial long-term survival gains. The delayed immune effects of TTR may account for the lack of significant short-term improvement in PFS. Radiotherapy induces immunogenic cell death, triggering systemic immune responses that enhance the effects of subsequent therapies. However, these effects may take months to fully manifest. While PFS reflects early tumor responses, it may not capture the long-term, cumulative benefits of treatment, which are more accurately represented by OS (*47*). Moreover, factors such as tumor biology, individual patient characteristics, and treatment regimens can influence PFS outcomes. These may explain the lack of a significant difference in PFS between the two groups.

Notably, the OS was significantly longer in the entire TTR group than in the TT group, particularly in patients who failed to undergo conversion resection. Previous studies have indicated that the OS of patients with uHCC with PVTT is extremely poor, especially those with VP3-4 PVTT (*48*). Some studies have even suggested that the mOS of these patients without any treatment is only 2.7 months. In the present study, however, the OS was notably greater than that reported in previous studies (*49*). These findings suggest that TTR may serve as a viable treatment option, even for patients who are not eligible for liver resection, as it may still lead to a favorable prognosis. However, given the small sample size of the TTR group, further studies are needed to confirm these results.

This study had several limitations. First, this was a single-center study with a small sample size in the TTR group. Second, as with many previous studies, we were unable to standardize the use of ICIs and TKIs in our clinical practice (*50*). This variation was due to differences in the drugs covered by medical insurance in different regions of China.

In conclusion, our results demonstrate that the addition of RT to TT significantly enhances both the conversion resection rate and OS in patients with uHCC patients with PVTT compared with TT alone. This combined modality approach offers a safe and effective therapeutic strategy for managing these patients.

Funding: This work was supported by grants from the National Key R&D Program of China (No.2022YFC2503701), the Science and Technological Supports Project of Sichuan Province (No.2024YFFK0313), the Natural Science Foundation of Sichuan Province (2024NSFSC0637), and the 1·3·5 project for disciplines of excellence–Clinical Research Incubation Project, West China Hospital, Sichuan University (No.2022HXFH012).

Conflict of Interest: The authors have no conflicts of interest to disclose.

References

1. Sung H, Ferlay J, Siegel RL, Laversanne M, Soerjomataram I, Jemal A, Bray F. Global Cancer Statistics 2020: GLOBOCAN Estimates of Incidence and Mortality Worldwide for 36 Cancers in 185 Countries. CA: a cancer journal for clinicians. 2021; 71:209-249.
2. Li B, Qiu J, Zheng Y, Shi Y, Zou R, He W, Yuan Y, Zhang Y, Wang C, Qiu Z, Li K, Zhong C, Yuan Y. Conversion to Resectability Using Transarterial Chemoembolization Combined With Hepatic Arterial Infusion Chemotherapy for Initially Unresectable Hepatocellular Carcinoma. Ann Surg Open. 2021; 2:e057.
3. Liver EAftSot. EASL Clinical Practice Guidelines on the management of hepatocellular carcinoma. J Hepatol. 2025; 82:315-374.
4. Bi X, Zhao H, Zhao H, *et al*. Consensus of Chinese Experts on Neoadjuvant and Conversion Therapies for Hepatocellular Carcinoma: 2023 Update. Liver Cancer. 2025; 14:223-238.
5. Tang Z, Bai T, Wei T, Wang X, Chen J, Ye J, Li S, Wei M, Li X, Lin Y, Tang J, Li L, Wu F. TACE combined Lenvatinib plus Camrelizumab versus TACE alone in efficacy and safety for unresectable hepatocellular carcinoma: a propensity score-matching study. BMC cancer. 2024; 24:717.
6. Wu J, Wu J, Li S, Luo M, Zeng Z, Li Y, Fu Y, Li H, Liu D, Ou X, Lin Z, Wei S, Yan M. Effect of transcatheter arterial chemoembolization combined with lenvatinib plus anti-PD-1 antibodies in patients with unresectable hepatocellular carcinoma: A treatment with Chinese characteristics. Bioscience trends. 2024; 18:42-48.
7. Li J, Kong M, Yu G, Wang S, Shi Z, Han H, Lin Y, Shi J, Song J. Safety and efficacy of transarterial chemoembolization combined with tyrosine kinase inhibitors and camrelizumab in the treatment of patients with advanced unresectable hepatocellular carcinoma. Front Immunol. 2023; 14:1188308.
8. Xuexian Z, Ruidong W, Yuhan D, Qingwei L, Feng X, Hong R, Jun Z, Wei L. Safety and efficacy of DEB-TACE in combination with lenvatinib and camrelizumab for the treatment of unresectable hepatocellular carcinoma (uHCC): a two-centre retrospective study. Front Immunol. 2024; 15:1422784.
9. Yang H, Yang T, Qiu G, Liu J. Efficacy and Safety of TACE Combined with Lenvatinib and PD-(L)1 Inhibitor in the Treatment of Unresectable Hepatocellular Carcinoma: A Retrospective Study. J Hepatocell Carcinoma. 2023; 10:1435-1443.
10. Gon H, Kido M, Tanaka M, Kinoshita H, Komatsu S, Tsugawa D, Awazu M, Toyama H, Matsumoto I, Itoh T, Fukumoto T. Growth velocity of the portal vein tumor thrombus accelerated by its progression, alpha-fetoprotein level, and liver fibrosis stage in patients with hepatocellular carcinoma. Surgery. 2018; 164:1014-1022.
11. Ji X, Zhang A, Duan X, Wang Q. Stereotactic body radiotherapy versus lenvatinib for hepatocellular carcinoma with portal vein tumor thrombosis: a propensity matching score analysis. Radiat Oncol. 2024; 19:143.
12. Hu Y, Zhou M, Tang J, *et al*. Efficacy and Safety of Stereotactic Body Radiotherapy Combined with Camrelizumab and Apatinib in Patients with Hepatocellular Carcinoma with Portal Vein Tumor Thrombus. Clinical cancer research : an official journal of the American Association for Cancer Research. 2023; 29:4088-4097.
13. Kokudo T, Hasegawa K, Matsuyama Y, Takayama T, Izumi N, Kadoya M, Kudo M, Ku Y, Sakamoto M, Nakashima O, Kaneko S, Kokudo N, Liver Cancer Study Group of J. Survival benefit of liver resection for hepatocellular carcinoma associated with portal vein invasion. J Hepatol. 2016; 65:938-943.
14. von Elm E, Altman DG, Egger M, Pocock SJ, Gøtzsche PC, Vandenbroucke JP. The Strengthening the Reporting of Observational Studies in Epidemiology (STROBE) statement: guidelines for reporting observational studies. Lancet (London, England). 2007; 370:1453-1457.
15. Son SH, Jang HS, Lee H, Choi BO, Kang YN, Jang JW, Yoon SK, Kay CS. Determination of the α/β ratio for the normal liver on the basis of radiation-induced hepatic toxicities in patients with hepatocellular carcinoma. Radiation oncology (London, England). 2013; 8:61.
16. Freites-Martinez A, Santana N, Arias-Santiago S, Viera A. Using the Common Terminology Criteria for Adverse Events (CTCAE - Version 5.0) to Evaluate the Severity of Adverse Events of Anticancer Therapies. Actas dermo-sifiliograficas. 2021; 112:90-92.
17. Kudo M, Yamashita T, Finn RS, Galle PR, Ducreux M, Cheng AL, Tsuchiya K, Sakamoto N, Hige S, Take R, Yamada K, Nakagawa Y, Takahashi H, Ikeda M. Depth and Duration of Response Are Associated with Survival in Patients with Unresectable Hepatocellular Carcinoma: Exploratory Analyses of IMbrave150. Liver cancer. 2025; 1-16.
18. Hatanaka T, Kakizaki S, Hiraoka A, *et al*. Predictive factors and survival outcome of conversion therapy for unresectable hepatocellular carcinoma patients receiving atezolizumab and bevacizumab: Comparative analysis of conversion, partial response and complete response patients. Aliment Pharmacol Ther. 2024; 60:1361-1373.
19. Johnson PJ, Berhane S, Kagebayashi C, *et al*. Assessment of liver function in patients with hepatocellular carcinoma: a new evidence-based approach-the ALBI grade. J Clin Oncol. 2015; 33:550-558.
20. Qiu ZC, Dai JL, Zhang Y, Xie F, Yu Y, Leng SS, Wen TF, Li C. Association of the Number of Concurrent Metabolic Syndrome Risk Factors with Textbook Outcomes Following Liver Resection for Patients with Hepatocellular Carcinoma: A Multicenter Study. Ann Surg Oncol. 2025; 32:399-407.
21. Clavien PA, Barkun J, de Oliveira ML, *et al*. The Clavien-Dindo classification of surgical complications: five-year experience. Annals of surgery. 2009; 250:187-196.
22. Llovet JM, Bustamante J, Castells A, Vilana R, Ayuso Mdel C, Sala M, Brú C, Rodés J, Bruix J. Natural history

of untreated nonsurgical hepatocellular carcinoma: rationale for the design and evaluation of therapeutic trials. Hepatology (Baltimore, Md). 1999; 29:62-67.
23. Kitao A, Zen Y, Matsui O, Gabata T, Nakanuma Y. Hepatocarcinogenesis: multistep changes of drainage vessels at CT during arterial portography and hepatic arteriography--radiologic-pathologic correlation. Radiology. 2009; 252:605-614.
24. Shi B, Bian C, Li Z, Chen J, Yang D, Li Y, Hao X, Ping Y. Imaging findings of hepatocellular carcinoma with portal vein tumor thrombosis secondary to hepatic portal vein collateral circulation: a cross-sectional study. Journal of gastrointestinal oncology. 2023; 14:334-351.
25. Fujiwara K, Kondo T, Fujimoto K, *et al*. Clinical risk factors for portal hypertension-related complications in systemic therapy for hepatocellular carcinoma. J Gastroenterol. 2024; 59:515-525.
26. Jo HS, Park PJ, Yu YD, Choi YJ, Yu SH, Kim DS, Korean Liver Cancer A. Clinical significance of surgical resection for hepatocellular carcinoma with portal vein invasion: a nationwide cohort study. Hepatobiliary Surg Nutr. 2024; 13:814-823.
27. Yang DL, Ye L, Zeng FJ, *et al*. Erratum: Multicenter, retrospective GUIDANCE001 study comparing transarterial chemoembolization with or without tyrosine kinase and immune checkpoint inhibitors as conversion therapy to treat unresectable hepatocellular carcinoma: Survival benefit in intermediate or advanced, but not early, stages. Hepatology. 2025; 82:E40.
28. Wu XK, Yang LF, Chen YF, Chen ZW, Lu H, Shen XY, Chi MH, Wang L, Zhang H, Chen JF, Huang JY, Zeng YY, Yan ML, Zhang ZB. Transcatheter arterial chemoembolisation combined with lenvatinib plus camrelizumab as conversion therapy for unresectable hepatocellular carcinoma: a single-arm, multicentre, prospective study. EClinicalMedicine. 2024; 67:102367.
29. Tang H, Zhang W, Cao J, *et al*. Chinese expert consensus on sequential surgery following conversion therapy based on combination of immune checkpoint inhibitors and antiangiogenic targeted drugs for advanced hepatocellular carcinoma (2024 edition). Biosci Trends. 2025; 18:505-524.
30. Singal AG, Llovet JM, Yarchoan M, *et al*. AASLD Practice Guidance on prevention, diagnosis, and treatment of hepatocellular carcinoma. Hepatology. 2023; 78:1922-1965.
31. Finn RS, Qin S, Ikeda M, *et al*. Atezolizumab plus Bevacizumab in Unresectable Hepatocellular Carcinoma. N Engl J Med. 2020; 382:1894-1905.
32. Park JW, Kim YJ, Kim DY, Bae SH, Paik SW, Lee YJ, Kim HY, Lee HC, Han SY, Cheong JY, Kwon OS, Yeon JE, Kim BH, Hwang J. Sorafenib with or without concurrent transarterial chemoembolization in patients with advanced hepatocellular carcinoma: The phase III STAH trial. Journal of hepatology. 2019; 70:684-691.
33. Peng Z, Fan W, Zhu B, *et al*. Lenvatinib Combined With Transarterial Chemoembolization as First-Line Treatment for Advanced Hepatocellular Carcinoma: A Phase III, Randomized Clinical Trial (LAUNCH). Journal of clinical oncology : official journal of the American Society of Clinical Oncology. 2023; 41:117-127.
34. Xiang X, Lau WY, Wu ZY, Zhao C, Ma YL, Xiang BD, Zhu JY, Zhong JH, Li LQ. Transarterial chemoembolization versus best supportive care for patients with hepatocellular carcinoma with portal vein tumor thrombus: A multicenter study. Eur J Surg Oncol. 2019; 45:1460-1467.
35. Wang DX, Yang X, Lin JZ, Bai Y, Long JY, Yang XB, Seery S, Zhao HT. Efficacy and safety of lenvatinib for patients with advanced hepatocellular carcinoma: A retrospective, real-world study conducted in China. World J Gastroenterol. 2020; 26:4465-4478.
36. Chuma M, Uojima H, Hiraoka A, *et al*. Analysis of efficacy of lenvatinib treatment in highly advanced hepatocellular carcinoma with tumor thrombus in the main trunk of the portal vein or tumor with more than 50% liver occupation: A multicenter analysis. Hepatol Res. 2021; 51:201-215.
37. Zhu M, Liu Z, Chen S, Luo Z, Tu J, Qiao L, Wu J, Fan W, Peng Z. Sintilimab plus bevacizumab combined with radiotherapy as first-line treatment for hepatocellular carcinoma with portal vein tumor thrombus: A multicenter, single-arm, phase 2 study. Hepatology. 2024; 80:807-815.
38. Dawson LA, Winter KA, Knox JJ, *et al*. Stereotactic Body Radiotherapy vs Sorafenib Alone in Hepatocellular Carcinoma: The NRG Oncology/RTOG 1112 Phase 3 Randomized Clinical Trial. JAMA oncology. 2025; 11:136-144.
39. Sample JW. Beyond monotherapy: Combining radiotherapy with sintilimab and bevacizumab for hepatocellular carcinoma with portal vein tumor thrombus. Hepatology (Baltimore, Md). 2024; 80:757-758.
40. Li S, Li K, Wang K, *et al*. Low-dose radiotherapy combined with dual PD-L1 and VEGFA blockade elicits antitumor response in hepatocellular carcinoma mediated by activated intratumoral CD8(+) exhausted-like T cells. Nature communications. 2023; 14:7709.
41. Wu TD, Madireddi S, de Almeida PE, *et al*. Peripheral T cell expansion predicts tumour infiltration and clinical response. Nature. 2020; 579:274-278.
42. Lin X, Liu Z, Dong X, *et al*. Radiotherapy enhances the anti-tumor effect of CAR-NK cells for hepatocellular carcinoma. J Transl Med. 2024; 22:929.
43. Zhang Y, Hong W, Zheng D, Li Z, Hu Y, Chen Y, Yang P, Zeng Z, Du S. Increased IFN-β indicates better survival in hepatocellular carcinoma treated with radiotherapy. Clinical and experimental immunology. 2024; 218:188-198.
44. Zhao CN, Chiang CL, Chiu WK, Chan SK, Li CJ, Chen WW, Zheng DY, Chen WQ, Ji R, Lo CM, Jabbour SK, Chan CA, Kong FS. Treatments of transarterial chemoembolization (TACE), stereotactic body radiotherapy (SBRT) and immunotherapy reshape the systemic tumor immune environment (STIE) in patients with unresectable hepatocellular carcinoma. Journal of the National Cancer Center. 2025; 5:38-49.
45. Goh MJ, Park HC, Yu JI, Kang W, Gwak GY, Paik YH, Lee JH, Koh KC, Paik SW, Sinn DH, Choi MS. Impact of Intrahepatic External Beam Radiotherapy in Advanced Hepatocellular Carcinoma Patients Treated with Tyrosine Kinase Inhibitors. Liver cancer. 2023; 12:467-478.
46. Llovet JM, Montal R, Villanueva A. Randomized trials and endpoints in advanced HCC: Role of PFS as a surrogate of survival. Journal of hepatology. 2019; 70:1262-1277.
47. Vaes RDW, Hendriks LEL, Vooijs M, De Ruysscher D. Biomarkers of Radiotherapy-Induced Immunogenic Cell Death. Cells. 2021; 10.
48. Jiao T, Tang H, Zhang W, Hu B, Wan T, Cao Y, Zhang

Z, Wang Y, Cao J, Cui M, Lu S. Long-term survival and portal vein patency with novel PVTT surgery approach in advanced HCC patients with Vp3/4 PVTT following combination therapy of TKIs and PD-1 inhibitors. BMC Surg. 2023; 23:384.
49. Xiao Y, Li K, Zhao Y, Yang S, Yan J, Xiang C, Zeng J, Lu Q, Zhang C, Li G, Li G, Dong J. Efficacy of radiotherapy in combined treatment of hepatocellular carcinoma patients with portal vein tumor thrombus: a real-world study. BMC Surg. 2024; 24:54.
50. Tan HY, Liu SQ, Zheng JL, Liu HY, Liu YH, Dai GH, Feng HG. Efficacy of radiotherapy combined with hepatic arterial infusion chemotherapy, TKI and ICI for hepatocellular carcinoma with portal vein tumor thrombus: a retrospective cohort study. Abdom Radiol (NY). 2025; 50:1320-1329.

Received June 18, 2025; Revised July 27, 2025; Accepted August 1, 2025.

*Address correspondence to:
Chuan Li, Division of Liver Surgery, Department of General Surgery, West China Hospital, Sichuan University, Chengdu 610041, China.
E-mail: lichuan@scu.edu.cn

Released online in J-STAGE as advance publication August 4, 2025.

BST
BioScience Trends

Guide for Authors

1. Scope of Articles

BioScience Trends (Print ISSN 1881-7815, Online ISSN 1881-7823) is an international peer-reviewed journal. *BioScience Trends* devotes to publishing the latest and most exciting advances in scientific research. Articles cover fields of life science such as biochemistry, molecular biology, clinical research, public health, medical care system, and social science in order to encourage cooperation and exchange among scientists and clinical researchers.

2. Submission Types

Original Articles should be well-documented, novel, and significant to the field as a whole. An Original Article should be arranged into the following sections: Title page, Abstract, Introduction, Materials and Methods, Results, Discussion, Acknowledgments, and References. Original articles should not exceed 5,000 words in length (excluding references) and should be limited to a maximum of 50 references. Articles may contain a maximum of 10 figures and/or tables. Supplementary Data are permitted but should be limited to information that is not essential to the general understanding of the research presented in the main text, such as unaltered blots and source data as well as other file types.

Brief Reports definitively documenting either experimental results or informative clinical observations will be considered for publication in this category. Brief Reports are not intended for publication of incomplete or preliminary findings. Brief Reports should not exceed 3,000 words in length (excluding references) and should be limited to a maximum of 4 figures and/or tables and 30 references. A Brief Report contains the same sections as an Original Article, but the Results and Discussion sections should be combined.

Reviews should present a full and up-to-date account of recent developments within an area of research. Normally, reviews should not exceed 8,000 words in length (excluding references) and should be limited to a maximum of 10 figures and/or tables and 100 references. Mini reviews are also accepted, which should not exceed 4,000 words in length (excluding references) and should be limited to a maximum of 5 figures and/or tables and 50 references.

Policy Forum articles discuss research and policy issues in areas related to life science such as public health, the medical care system, and social science and may address governmental issues at district, national, and international levels of discourse. Policy Forum articles should not exceed 3,000 words in length (excluding references) and should be limited to a maximum of 5 figures and/or tables and 30 references.

Communications are short, timely pieces that spotlight new research findings or policy issues of interest to the field of global health and medical practice that are of immediate importance. Depending on their content, Communications will be published as "Comments" or "Correspondence". Communications should not exceed 1,500 words in length (excluding references) and should be limited to a maximum of 2 figures and/or tables and 20 references.

Editorials are short, invited opinion pieces that discuss an issue of immediate importance to the fields of global health, medical practice, and basic science oriented for clinical application. Editorials should not exceed 1,000 words in length (excluding references) and should be limited to a maximum of 10 references. Editorials may contain one figure or table.

News articles should report the latest events in health sciences and medical research from around the world. News should not exceed 500 words in length.

Letters should present considered opinions in response to articles published in *BioScience Trends* in the last 6 months or issues of general interest. Letters should not exceed 800 words in length and may contain a maximum of 10 references. Letters may contain one figure or table.

3. Editorial Policies

For publishing and ethical standards, *BioScience Trends* follows the Recommendations for the Conduct, Reporting, Editing, and Publication of Scholarly Work in Medical Journals issued by the International Committee of Medical Journal Editors (ICMJE, *https://icmje.org/recommendations*), and the Principles of Transparency and Best Practice in Scholarly Publishing jointly issued by the Committee on Publication Ethics (COPE, *https://publicationethics.org/resources/guidelines-new/principles-transparency-and-best-practice-scholarly-publishing*), the Directory of Open Access Journals (DOAJ, *https://doaj.org/apply/transparency*), the Open Access Scholarly Publishers Association (OASPA, *https://oaspa.org/principles-of-transparency-and-best-practice-in-scholarly-publishing-4*), and the World Association of Medical Editors (WAME, *https://wame.org/principles-of-transparency-and-best-practice-in-scholarly-publishing*).

BioScience Trends will perform an especially prompt review to encourage innovative work. All original research will be subjected to a rigorous standard of peer review and will be edited by experienced copy editors to the highest standards.

Ethical Approval of Studies and Informed Consent: For all manuscripts reporting data from studies involving human participants or animals, formal review and approval, or formal review and waiver, by an appropriate institutional review board or ethics committee is required and should be described in the Methods section. When your manuscript contains any case details, personal information and/or images of patients or other individuals, authors must obtain appropriate written consent, permission and release in order to comply with all applicable laws and regulations concerning privacy and/or security of personal information. The consent form needs to comply with the relevant legal requirements of your particular jurisdiction, and please do not send signed consent form to *BioScience Trends* to respect your patient's and any other individual's privacy. Please instead describe the information clearly in the Methods (patient consent) section of your manuscript while retaining copies of the signed forms in the event they should be needed. Authors should also state that the study conformed to the provisions of the Declaration of Helsinki (as revised in 2013, *https://wma.net/what-we-do/medical-ethics/declaration-of-helsinki*). When reporting experiments on animals, authors should indicate whether the institutional and national guide for the care and use of laboratory animals was followed.

Reporting Clinical Trials: The ICMJE (*https:// icmje.org/recommendations/browse/publishing-and-editorial-issues/clinical-trial-registration.html*) defines a clinical trial as any research project that prospectively assigns people or a group of people to an intervention, with or without concurrent comparison or control groups, to study the relationship between a health-related intervention and a health outcome. Registration of clinical trials in a public trial registry at or before the time of first patient enrollment is a condition of consideration for publication in *BioScience Trends*, and the trial registration number will be published at the end of the Abstract. The registry must be independent of for-profit interest and publicly accessible. Reports of trials must conform to CONSORT 2010 guidelines (*https://consort-statement.org/consort-2010*). Articles reporting the results of randomized trials must include the CONSORT flow diagram showing the progress of patients throughout the trial.

Conflict of Interest: All authors are required to disclose any actual or potential conflict of interest including financial interests or relationships with other people or organizations that might raise questions of bias

in the work reported. If no conflict of interest exists for each author, please state "There is no conflict of interest to disclose".

Submission Declaration: When a manuscript is considered for submission to *BioScience Trends*, the authors should confirm that 1) no part of this manuscript is currently under consideration for publication elsewhere; 2) this manuscript does not contain the same information in whole or in part as manuscripts that have been published, accepted, or are under review elsewhere, except in the form of an abstract, a letter to the editor, or part of a published lecture or academic thesis; 3) authorization for publication has been obtained from the authors' employer or institution; and 4) all contributing authors have agreed to submit this manuscript.

Initial Editorial Check: Immediately after submission, the journal's managing editor will perform an initial check of the manuscript. A suitable academic editor will be notified of the submission and invited to check the manuscript and recommend reviewers. Academic editors will check for plagiarism and duplicate publication at this stage. The journal has a formal recusal process in place to help manage potential conflicts of interest of editors. In the event that an editor has a conflict of interest with a submitted manuscript or with the authors, the manuscript, review, and editorial decisions are managed by another designated editor without a conflict of interest related to the manuscript.

Peer Review: *BioScience Trends* operates a single-anonymized review process, which means that reviewers know the names of the authors, but the authors do not know who reviewed their manuscript. All articles are evaluated objectively based on academic content. External peer review of research articles is performed by at least two reviewers, and sometimes the opinions of more reviewers are sought. Peer reviewers are selected based on their expertise and ability to provide quality, constructive, and fair reviews. For research manuscripts, the editors may, in addition, seek the opinion of a statistical reviewer. Every reviewer is expected to evaluate the manuscript in a timely, transparent, and ethical manner, following the COPE guidelines (*https://publicationethics.org/files/cope-ethical-guidelines-peer-reviewers-v2_0.pdf*). We ask authors for sufficient revisions (with a second round of peer review, when necessary) before a final decision is made. Consideration for publication is based on the article's originality, novelty, and scientific soundness, and the appropriateness of its analysis.

Suggested Reviewers: A list of up to 3 reviewers who are qualified to assess the scientific merit of the study is welcomed. Reviewer information including names, affiliations, addresses, and e-mail should be provided at the same time the manuscript is submitted online. Please do not suggest reviewers with known conflicts of interest, including participants or anyone with a stake in the proposed research; anyone from the same institution; former students, advisors, or research collaborators (within the last three years); or close personal contacts. Please note that the Editor-in-Chief may accept one or more of the proposed reviewers or may request a review by other qualified persons.

Language Editing: Manuscripts prepared by authors whose native language is not English should have their work proofread by a native English speaker before submission. If not, this might delay the publication of your manuscript in *BioScience Trends*.

The Editing Support Organization can provide English proofreading, Japanese-English translation, and Chinese-English translation services to authors who want to publish in *BioScience Trends* and need assistance before submitting a manuscript. Authors can visit this organization directly at *https://www.iacmhr.com/iac-eso/support.php?lang=en*. IAC-ESO was established to facilitate manuscript preparation by researchers whose native language is not English and to help edit works intended for international academic journals.

Copyright and Reuse: Before a manuscript is accepted for publication in *BioScience Trends*, authors will be asked to sign a transfer of copyright agreement, which recognizes the common interest that both the journal and author(s) have in the protection of copyright. We accept that some authors (*e.g.*, government employees in some countries) are unable to transfer copyright. A JOURNAL PUBLISHING AGREEMENT (JPA) form will be e-mailed to the authors by the Editorial Office and must be returned by the authors by mail, fax, or as a scan. Only forms with a hand-written signature from the corresponding author are accepted. This copyright will ensure the widest possible dissemination of information. Please note that the manuscript will not proceed to the next step in publication until the JPA Form is received. In addition, if excerpts from other copyrighted works are included, the author(s) must obtain written permission from the copyright owners and credit the source(s) in the article.

4. Cover Letter

The manuscript must be accompanied by a cover letter prepared by the corresponding author on behalf of all authors. The letter should indicate the basic findings of the work and their significance. The letter should also include a statement affirming that all authors concur with the submission and that the material submitted for publication has not been published previously or is not under consideration for publication elsewhere. The cover letter should be submitted in PDF format. For an example of Cover Letter, please visit: *https://www.biosciencetrends.com/downcentre* (Download Centre).

5. Submission Checklist

The Submission Checklist should be submitted when submitting a manuscript through the Online Submission System. Please visit Download Centre (*https://www.biosciencetrends.com/downcentre*) and download the Submission Checklist file. We recommend that authors use this checklist when preparing your manuscript to check that all the necessary information is included in your article (if applicable), especially with regard to Ethics Statements.

6. Manuscript Preparation

Manuscripts are suggested to be prepared in accordance with the "Recommendations for the Conduct, Reporting, Editing, and Publication of Scholarly Work in Medical Journals", as presented at *https://www.ICMJE.org*.

Manuscripts should be written in clear, grammatically correct English and submitted as a Microsoft Word file in a single-column format. Manuscripts must be paginated and typed in 12-point Times New Roman font with 24-point line spacing. Please do not embed figures in the text. Abbreviations should be used as little as possible and should be explained at first mention unless the term is a well-known abbreviation (*e.g.* DNA). Single words should not be abbreviated.

Title page: The title page must include 1) the title of the paper (Please note the title should be short, informative, and contain the major key words); 2) full name(s) and affiliation(s) of the author(s), 3) abbreviated names of the author(s), 4) full name, mailing address, telephone/fax numbers, and e-mail address of the corresponding author; 5) author contribution statements to specify the individual contributions of all authors to this manuscript, and 6) conflicts of interest (if you have an actual or potential conflict of interest to disclose, it must be included as a footnote on the title page of the manuscript; if no conflict of interest exists for each author, please state "There is no conflict of interest to disclose").

Abstract: The abstract should briefly state the purpose of the study, methods, main findings, and conclusions. For articles that are Original Articles, Brief Reports, Reviews, or Policy Forum articles, a one-paragraph abstract consisting of no more than 250 words must be included in the manuscript. For Communications, Editorials, News, or Letters, a brief summary of main content in 150 words or fewer should be included in the manuscript. For articles reporting clinical trials, the trial registration number should be stated at the end of the Abstract. Abbreviations must be kept to a minimum and non-standard

abbreviations explained in brackets at first mention. References should be avoided in the abstract. Three to six key words or phrases that do not occur in the title should be included in the Abstract page.

Introduction: The introduction should provide sufficient background information to make the article intelligible to readers in other disciplines and sufficient context clarifying the significance of the experimental findings

Materials/Patients and Methods: The description should be brief but with sufficient detail to enable others to reproduce the experiments. Procedures that have been published previously should not be described in detail but appropriate references should simply be cited. Only new and significant modifications of previously published procedures require complete description. Names of products and manufacturers with their locations (city and state/country) should be given and sources of animals and cell lines should always be indicated. All clinical investigations must have been conducted in accordance Materials/ Patients and Methods.

Results: The description of the experimental results should be succinct but in sufficient detail to allow the experiments to be analyzed and interpreted by an independent reader. If necessary, subheadings may be used for an orderly presentation. All Figures and Tables should be referred to in the text in order, including those in the Supplementary Data.

Discussion: The data should be interpreted concisely without repeating material already presented in the Results section. Speculation is permissible, but it must be well-founded, and discussion of the wider implications of the findings is encouraged. Conclusions derived from the study should be included in this section.

Acknowledgments: All funding sources (including grant identification) should be credited in the Acknowledgments section. Authors should also describe the role of the study sponsor(s), if any, in study design; in the collection, analysis, and interpretation of data; in the writing of the report; and in the decision to submit the paper for publication. If the funding source had no such involvement, the authors should so state.

In addition, people who contributed to the work but who do not meet the criteria for authors should be listed along with their contributions.

References: References should be numbered in the order in which they appear in the text. Citing of unpublished results, personal communications, conference abstracts, and theses in the reference list is not recommended but these sources may be mentioned in the text. In the reference list, cite the names of all authors when there are fifteen or fewer authors; if there are sixteen or more authors, list the first three followed by *et al*. Names of journals should be abbreviated in the style used in PubMed. Authors are responsible for the accuracy of the references. The EndNote Style of *BioScience Trends* could be downloaded at **EndNote** (*https://ircabssagroup.com/examples/ BioScience_Trends.ens*).

Examples are given below:

Example 1 (Sample journal reference):

Inagaki Y, Tang W, Zhang L, Du GH, Xu WF, Kokudo N. Novel aminopeptidase N (APN/CD13) inhibitor 24F can suppress invasion of hepatocellular carcinoma cells as well as angiogenesis. Biosci Trends. 2010; 4:56-60.

Example 2 (Sample journal reference with more than 15 authors):

Darby S, Hill D, Auvinen A, *et al*. Radon in homes and risk of lung cancer: Collaborative analysis of individual data from 13 European case-control studies. BMJ. 2005; 330:223.

Example 3 (Sample book reference):

Shalev AY. Post-traumatic stress disorder: Diagnosis, history and life course. In: Post-traumatic Stress Disorder, Diagnosis, Management and Treatment (Nutt DJ, Davidson JR, Zohar J, eds.). Martin Dunitz, London, UK, 2000; pp. 1-15.

Example 4 (Sample web page reference):

World Health Organization. The World Health Report 2008 – primary health care: Now more than ever. *http://www.who.int/whr/2008/whr08_ en.pdf* (accessed September 23, 2022).

Tables: All tables should be prepared in Microsoft Word or Excel and should be arranged at the end of the manuscript after the References section. Please note that tables should not in image format. All tables should have a concise title and should be numbered consecutively with Arabic numerals. If necessary, additional information should be given below the table.

Figure Legend: The figure legend should be typed on a separate page of the main manuscript and should include a short title and explanation. The legend should be concise but comprehensive and should be understood without referring to the text. Symbols used in figures must be explained. Any individually labeled figure parts or panels (A, B, *etc*.) should be specifically described by part name within the legend.

Figure Preparation: All figures should be clear and cited in numerical order in the text. Figures must fit a one- or two-column format on the journal page: 8.3 cm (3.3 in.) wide for a single column, 17.3 cm (6.8 in.) wide for a double column; maximum height: 24.0 cm (9.5 in.). Please make sure that the symbols and numbers appeared in the figures should be clear. Please make sure that artwork files are in an acceptable format (TIFF or JPEG) at minimum resolution (600 dpi for illustrations, graphs, and annotated artwork, and 300 dpi for micrographs and photographs). Please provide all figures as separate files. Please note that low-resolution images are one of the leading causes of article resubmission and schedule delays.

Units and Symbols: Units and symbols conforming to the International System of Units (SI) should be used for physicochemical quantities. Solidus notation (*e.g.* mg/kg, mg/mL, mol/mm^2/min) should be used. Please refer to the SI Guide *www.bipm.org/en/si/* for standard units.

Supplemental data: Supplemental data might be useful for supporting and enhancing your scientific research and *BioScience Trends* accepts the submission of these materials which will be only published online alongside the electronic version of your article. Supplemental files (figures, tables, and other text materials) should be prepared according to the above guidelines, numbered in Arabic numerals (*e.g.*, Figure S1, Figure S2, and Table S1, Table S2) and referred to in the text. All figures and tables should have titles and legends. All figure legends, tables and supplemental text materials should be placed at the end of the paper. Please note all of these supplemental data should be provided at the time of initial submission and note that the editors reserve the right to limit the size and length of Supplemental Data.

5. Submission Checklist

The Submission Checklist will be useful during the final checking of a manuscript prior to sending it to *BioScience Trends* for review. Please visit Download Centre and download the Submission Checklist file.

6. Online Submission

Manuscripts should be submitted to *BioScience Trends* online at *https://www.biosciencetrends.com/login*. Receipt of your manuscripts submitted online will be acknowledged by an e-mail from Editorial Office containing a reference number, which should be used in all future communications. If for any reason you are unable to submit a file online, please contact the Editorial Office by e-mail at *office@ biosciencetrends.com*

8. Accepted Manuscripts

Page Charge: Page charges will be levied on all manuscripts accepted for publication in *BioScience Trends* (Original Articles / Brief Reports / Reviews / Policy Forum / Communications: $140 per page for black white pages, $340 per page for color pages; News / Letters: a total cost of $600). Under exceptional circumstances, the author(s) may apply to the editorial office for a waiver of the publication charges by stating the reason in the Cover Letter when the manuscript online.

Misconduct: *BioScience Trends* takes seriously all allegations of potential misconduct and adhere to the ICMJE Guideline (*https://icmje.org/recommendations*) and COPE Guideline (*https://publicationethics.org/files/Code_of_conduct_for_journal_editors.pdf*). In cases of suspected research or publication misconduct, it may be necessary for the Editor or Publisher to contact and share submission details with third parties including authors' institutions and ethics committees. The corrections, retractions, or editorial expressions of concern will be performed in line with above guidelines.

(As of December 2022)

BioScience Trends
Editorial and Head Office
Pearl City Koishikawa 603,
2-4-5 Kasuga, Bunkyo-ku,
Tokyo 112-0003, Japan.
E-mail: office@biosciencetrends.com